

AN ABSTRACT OF THE THESIS OF

Jeffrey Jay Lienau for the degree of Master of Science in Mechanical Engineering presented on April 4, 1990.

Title: Laminar Microchannel Cooling of Integrated  
Circuits. **Redacted for privacy**

Abstract approved: \_\_\_\_\_  
Milton B. Larson

Liquid cooled, laminar microchannel heat sinks were earlier proposed by Tuckerman for cooling high heat generating integrated circuits and high power microwave generation systems using photoconductive switches. A method of computationally analyzing the heat sinks is presented which produces the desired temperature and velocity distributions within the heat sinks. The problem was solved in two different ways. First, computational techniques were developed to investigate the problem assuming fully developed temperature and velocity profiles. Second, the hydro-thermal code TEMPEST was used to solve the developing problem. A comparison was made between the results of this study and Landrum's integral analysis. Other analytical comparisons were made.

A parametric study was performed which considers the effect of geometric parameters on the solution. From this parametric study, trends were observed which allowed optimization of the geometric parameters of the design. The optimization involved a specified pressure drop across the heat sink. The optimized design was one which had the lowest peak silicon temperature with a given pressure drop across the heat sink. For every given

pressure drop across the heat sink, there was an optimal design. Optimized heat transfer performance characterized by nondimensional peak silicon temperature may be related to the pressure drop across the heat sink so the cooling effect can be compared to its cost in terms of pumping power.

An evaluation of the fully developed momentum and energy assumptions was presented. The developing solution was solved for cases both near the optimized design and for cases which deviated substantially from the optimized design. The fully developed momentum assumption provided accurate velocity profiles in all cases considered. The hydrodynamic entry length can be neglected in most cases. The accuracy of the fully developed energy assumption varied considerably with geometric parameters. The fully developed energy solution did not accurately represent the developing solution for microchannels with small fin width to channel width ratios and large channel aspect ratios. For microchannels with large fin width to channel width ratios and small channel aspect ratios, the fully developed solution accurately represented the developing solution. The fully developed assumption provided accurate temperature profiles in cases at or near the optimum design as determined by the methods in this report.

The effects of variable fluid specific heat and thermal conductivity were considered by comparing the temperature and velocity profiles to constant property cases. The assumption of constant fluid properties provided a conservative estimate of the peak silicon temperature. This suggested using the constant property assumption in order to provide a margin of safety and to simplify the computation.

Laminar Microchannel Cooling  
of  
Integrated Circuits

by

Jeffrey Jay Lienau

A THESIS

submitted to

Oregon State University

in partial fulfillment of  
the requirements for the  
degree of

MASTER OF SCIENCE

COMPLETED April 4, 1990

COMMENCEMENT June 1990

APPROVED:

Redacted for privacy

---

Professor of Mechanical Engineering in charge of major

Redacted for privacy

---

Department Head of Mechanical Engineering

Redacted for privacy

---

Dean of Graduate School

Date thesis is presented April 4, 1990

Students Name: Jeffrey Jay Lienau

**ACKNOWLEDGEMENT**

I would like to acknowledge certain people for their contributions to this project; Dr. Larson for his endless guidance and for helping me to always be truthful to my work and myself, everyone in the thermal fluids group at Lawrence Livermore National Laboratory for their tremendous support and encouragement throughout this project, Charlie Landrum for his most appropriate sense of humor and words of wisdom, and finally, Bill Comfort for always keeping my best interests in mind and for being my friend.

I feel that through my work with these people I have not only grown professionally but have grown personally as well.

## TABLE OF CONTENTS

ii

INTRODUCTION	1
PROBLEM GEOMETRY	5
NOMENCLATURE	6
GREEK SYMBOLS	9
REVIEW OF LITERATURE	12
CHAPTER 1	22
FULLY DEVELOPED LAMINAR MICROCHANNEL COOLING	
1.1 INTRODUCTION	22
1.2 MOTIVATION	23
1.3 PROBLEM DESCRIPTION	24
1.4 GOVERNING EQUATIONS	24
1.5 COMPUTATIONAL TECHNIQUES	27
1.6 GRID DISCRETIZATION	28
1.7 IMPORTANT PRELIMINARY CONSIDERATIONS before running the parametric study	37
1.8 TYPICAL SOLUTION INFORMATION	38
1.9 THE PARAMETRIC STUDY	46
1.10 THE OPTIMIZATION PROCEDURE	50
1.11 REYNOLDS NUMBER OPTIMIZATION	66
1.12 CONCLUDING COMMENTS REGARDING THE STUDY	67

## TABLE OF CONTENTS (continued)

CHAPTER 2	69
DEVELOPING LAMINAR MICROCHANNEL COOLING	
2.1 INTRODUCTION	69
2.2 MOTIVATION	70
2.3 PROBLEM DESCRIPTION	70
2.4 ESTIMATES OF ENTRY LENGTHS	71
2.5 GOVERNING EQUATIONS	74
2.6 VERIFICATION OF THE COMPUTER CODE	76
2.7 RAMIFICATIONS OF THE FULLY DEVELOPED ASSUMPTION	77
2.8 FINDINGS REGARDING THE DEVELOPING SOLUTION	78
2.9 CONCLUDING COMMENTS	102
 CHAPTER 3	 103
SUMMARY AND FUTURE WORK	
3.1 SUMMARY OF CHAPTER 1 Fully Developed Laminar Microchannel Cooling	103
3.2 SUMMARY OF CHAPTER 2 Developing Laminar Microchannel Cooling	106
3.3 RECOMMENDATIONS FOR FUTURE WORK	108
 BIBLIOGRAPHY	 110

## TABLE OF CONTENTS (continued)

APPENDIX A	112
General and Specific Logic of the Computer Code	
1 GENERAL LOGIC	112
2 SPECIFIC LOGIC	116
POINT SUCCESSIVE OVER RELAXATION P.S.O.R.	117
Flowchart for Computer Code: 2DREYN.FOR	121
Source Code listing: 2DREYN.FOR	128
APPENDIX B	163
Separation of Variables Comparison	
1 SEPARATION OF VARIABLES SOLUTION	163
2 RESULTS	164
Source Code listing: EXTHES.FOR	166
Computer Output	170
APPENDIX C	178
Infinite Channel comparisons for Discretization Information	
1 THE INFINITE CHANNEL	178
2 RESULTS	179
APPENDIX D	181
Integral Analysis Manipulations	
1 MINIMUM IN FIN BASE TEMPERATURE VS. $w_w/w_c$	181
2 MINIMUM IN FIN BASE TEMPERATURE WITH ASPECT RATIO	182

## TABLE OF CONTENTS (continued)

APPENDIX E	184
Derivation of Equations	
1 FLUID FLOW REGION. Momentum Equations.	187
2 ENERGY EQUATIONS.	186
3 APPLICATION OF BULK ENERGY BALANCE	188
APPENDIX F	189
Preliminary Calculations	
1 AVERAGE KINEMATIC VISCOSITY	189
2 AVERAGE VELOCITY AND REYNOLDS NUMBER	190
APPENDIX G	192
Output from 2DREYN.FOR	
1 VELOCITY AND TEMPERATURE OUTPUT	192
2 CALCULATED INFORMATION	195
APPENDIX H	206
Spreadsheet for Parametric Study	

## LIST OF FIGURES

<u>Figure</u>	<u>Page</u>
1 Schematic of the compact heat sink incorporated into an IC chip. (reprinted from Tuckerman [1])	5
2 Components of thermal resistance in convectively cooled integrated circuits. (Reprinted from Tuckerman [1])	13
3 Local Nusselt number for laminar flow between parallel plates with uniform heat flux, as a function of nondimensional length $L^* = L / (D_{hydr} RePr)$ .	18
 <b>CHAPTER 1</b>	
1.1 Computational domain for fully developed microchannel problem.	25
1.2 Microchannel for velocity distribution.	29
1.3 Analytical and numerical velocity distributions plotted horizontally at centerline for a 10 celled discretization.	31
1.4 Analytical and numerical velocity distributions plotted vertically at the centerline for a 10 celled discretization.	32
1.5 Infinite channel for analytical and numerical discretization comparisons.	34
1.6 Percent difference between analytical and numerical solutions of centerline temperature for the infinite channel.	35
1.7 Velocity profile in optimized microchannel geometry with $W_c = 60 \mu\text{m}$ , $W_w / W_c = 30 \mu\text{m}$ and $\alpha = 14.5$ where $Y_c = (y - \frac{1}{2}W_w) / \frac{1}{2}W_c$ .	39
1.8 Temperature distribution within the optimized microchannel with $W_c = 60 \mu\text{m}$ , $W_w / W_c = 1$ and $\alpha = 14.5$ where $Y_c = (y - \frac{1}{2}W_w) / \frac{1}{2}W_c$ .	40

## LIST OF FIGURES (continued)

<u>Figure</u>	<u>Page</u>
1.9 Comparison of numerically derived Nusselt number with Tuckerman's constant. $\beta = 5$ , $W_c = 60 \text{ m}$ and $W_w/W_c = .5$	44
1.9a Nusselt number calculated using the bulk fluid temperature vs. $Z/H$ . $W_c = 60 \text{ m}$ , $\beta = 5$ and $W_w/W_c = .5$	45
1.9b Nusselt number vs. $Z/H$ for $W_w/W_c = .5$ , $\beta = 10$ , $W_c = 60 \text{ m}$ . (Thin fin problem)	46
1.10 Integral analysis comparison to numerical solution for a 60 micrometer channel with a 30 micrometer fin.	48
1.10a Temperature vs. aspect ratio $\beta$ for $W_c = 60 \text{ m}$ , $W_w = 30 \text{ m}$ , $Re = 500$ , $q'' = 1000 \text{ w/cm}^2$ .	49
1.10b Scale illustration of computational geometry to show how $\beta$ varies with $Z/H$ and $W_w/W_c$ .	51
1.10c Nondimensional hot spot $y_0$ vs. $\beta$ for $\beta = 10$ , $W_c = 60 \text{ m}$ and $W_w$ varies.	52
1.10d Nondimensional hot spot $y_0$ vs. $\beta$ for $W_c = 60 \text{ m}$ , $W_w = 30 \text{ m}$ and varying $Z/H$ .	53
1.11 Pressure drop across a 1.4 cm heat sink versus channel width $W_c$ , for $\beta = 10$ , $W_w/W_c = .5$ and $Re = 500$ (constant). The mass flow rate is varied.	55

## LIST OF FIGURES (continued)

<u>Figure</u>	<u>Page</u>
1.12 Pressure drop across a 1.4 cm long channel vs. $W_c$ for a mass flowrate of .005 kg/s (constant), $W=1$ cm, $H=600$ micrometers.	55
1.13 Pressure drop across a 1.4 cm chip vs. aspect ratio $\alpha$ for $W_c=60$ $\mu\text{m}$ , $W_w=30$ $\mu\text{m}$ . $Re=500$ (constant)	56
1.14 Nondimensional solid temperature $\Omega$ versus channel width for $\alpha=10$ , $\beta=1$ and $W_w/W_c=.5$ .	58
1.15 Nondimensional peak temperature $\Omega$ vs $W_w/W_c$ for $\alpha=10$ and $Re=500$ .	61
1.16 Nondimensional peak temperature $\Omega$ vs. aspect ratio $\alpha$ for $W_w/W_c=.5$ and $Re=500$ .	63
1.17 Optimized nondimensional temperature $\Omega$ vs. Reynolds number for a heat sink pressure drop of 9.4 psi.	67
<b>CHAPTER 2</b>	
2.1 y-z plane for 3 dimensional computational solution. The x direction runs perpendicular to the plane.	73
2.2 Exit fin temperature profiles comparing fully developed and developing solutions for $W_c=60$ $\mu\text{m}$ , $\alpha=10$ and $W_w=42$ $\mu\text{m}$ .	78
2.3 Exit fin temperature profiles for fully developed constant properties vs. developing variable properties comparison.	80

## LIST OF FIGURES (continued)

<u>Figure</u>	<u>Page</u>
2.4 Exit channel temperature profiles comparing fully developed-developing constant and variable properties solutions. Same geometry as in Figure 2.2.	81
2.5 Nondimensional velocity profile $u/\bar{u}$ plotted vertically for variable and constant properties.	82
2.6 Nondimensional velocity profiles in the flow direction. This plot is for a cell near the bottom centerline at $Z_0/H=.1$ .	83
2.7 Nondimensional fin base temperature gradient, bulk temperature gradient and 120% of the bulk temperature gradient in the flow direction for $\alpha=5$ , $W_w/W_c=1$ , $\beta=8.5$ .	86
2.8 Nondimensional fin base temperature gradient in the axial direction for $\alpha=15$ , $W_w/W_c=.25$ and $\beta=.19$ .	87
2.9 Summary of the comparison of wall and bulk fluid temperature gradients showing $x$ (thermal) as a % of flow distance (L).	89
2.10 Graphical summary of the comparison of fluid and bulk fluid temperature gradients similar to Figure 2.9.	90
2.11 Heat flux off the face of the fin versus $z$ for the fully developed, constant and variable properties developing solutions. ( $\alpha=11.8$ , $W_w/W_c=1$ , $W_c=60 \mu\text{m}$ , $\beta=1.6$ , $Re=500$ )	91
2.12 Nondimensional heat flux near the base of the fin versus axial distance. Also shown is the fully developed value. ( $\alpha=11.8$ , $W_w/W_c=1$ , $W_c=60 \mu\text{m}$ , $\beta=1.6$ , $Re=500$ )	92

## LIST OF FIGURES (continued)

<u>Figure</u>	<u>Page</u>
2.13 Nondimensional temperature $\phi$ in the axial direction for ( $Z_0/H=.1$ ) at the centerline, wall and half way between wall and centerline.	94
2.14 Nondimensional temperature $\phi$ vs. $y$ at $z/H=.1$ for four different axial positions.	95
2.15 Exit fin temperature distribution for fully developed and developing solutions for $\alpha=5$ , $W_w/W_c=1$ and $\beta=8.5$ .	96
2.16 Exit fin temperature distributions for fully developed and developing solutions for $\alpha=15$ , $W_w/W_c=.25$ and $\beta=.19$ .	98
2.17 Percentage difference between fully developed and developing estimates of the peak silicon temperature.	99
2.18 Exit fin temperature profile for the optimized 30 $\mu\text{m}$ 100 $\mu\text{m}$ microchannel. $\beta=.667$ , $W_w/W_c=1$ and $\alpha=18.3$	100
2.19 Exit fin temperature profile for the optimized 90 $\mu\text{m}$ microchannel. $\beta=1.4$ , $W_w/W_c=1$ and $\alpha=12.9$	101
 <b>APPENDIX A</b>	
A1 Microchannel modeling showing the different computational regions and the Von Neumann boundary condition.	115
A2 Five point connector stencil.	120

## LIST OF FIGURES (continued)

<u>Figure</u>		<u>Page</u>
<b>APPENDIX B</b>		
B1	Fluid flow region showing the symmetric computational area and the geometric constants used in the analytical solution.	165
<b>APPENDIX C</b>		
C1	Infinite channel geometry for analytical and numerical discretization comparisons.	182
<b>APPENDIX E</b>		
E1	Computational domain for derivation of the fully developed momentum and energy equations.	187
<b>APPENDIX F</b>		
F1	Kinematic viscosity for water versus temperature and linearizing approximation. {Data taken from Bejan [15]}	192

## LIST OF TABLES

<u>Table</u>		<u>Page</u>
1.1	Nondimensional peak temperature for horizontal discretization verification.	36
1.2	Nondimensional peak temperature for vertical discretization verification.	37
B1	Percent difference between analytical and numerical solutions to the momentum equation.	165
C1	Percent difference between analytical and numerical solutions of the temperature and velocity within an infinite parallel plate heated channel.	180

## PREFACE

This work was initiated as a project at the University of California's Lawrence Livermore National Laboratory. Dr. D. Tuckerman of LLNL initially introduced the concept of liquid flowing in microchannels to cool integrated circuits in a PhD thesis [1] and performed some interesting experimental and analytical evaluations. Lawrence Livermore National Laboratory desired further numerical evaluation of the laminar microchannel cooling process which resulted in this work. Dr. C. Landrum initially presented an integral analysis of the fully developed laminar microchannel cooling process [private communication] which provided a first order approximation of the solution. The present work contains a more exact numerical method of solution whose results were compared to the results of Landrum's integral analysis.

A solution algorithm and a finite difference computer code have been developed to solve the laminar, fully developed, constant properties microchannel cooling problem. The theory and the basic framework for the computer code were attributed to Dr. D. Trent of Battelle Pacific North West Laboratories.

The solution to the laminar microchannel cooling problem and the investigations surrounding it were considered to be an important preliminary step to the solution of the subcooled boiling microchannel cooling problem. Dr. C. Landrum of LLNL and Dr. M. Hoffman of UC Davis have interest in solving the subcooled boiling microchannel problem.

# LAMINAR MICROCHANNEL COOLING OF INTEGRATED CIRCUITS

## INTRODUCTION

Recent predictions in the electronics industry have suggested that thermal effects will limit future transistor speed improvements [2]<sup>1</sup>. Also, high power microwave generation systems using photoconductive switches will require high heat removal rates [3]. Many different designs have been proposed in an attempt to remove the large heat flux produced by these electronic devices. See for instance Tuckerman [1] or Incropera [6]. Tuckerman originally proposed the laminar microchannels as capable of removing large values of heat flux (1000 W/cm<sup>2</sup>) and performed interesting analytical and experimental investigations of the devices [1].

The subject of the present thesis was the specific issue of removing the bulk heat effect from densely packed arrays of integrated circuits by the use of a laminar microchannel heat sink. The fluid mechanics and heat transfer within the microchannels were numerically simulated and investigated for optimum performance.

Two distinct broad primary objectives for this work formed the basis for the breakdown into the first two chapters. The final chapter was then a summary of the important findings of this work. The first objective was to solve the problem assuming fully developed momentum and energy profiles. The second objective was

---

<sup>1</sup> The references will be given in blocks [#], where # indicates the reference number from the Bibliography.

to evaluate the feasibility of the fully developed assumptions. This was done by numerically solving the problem without the fully developed assumptions and comparing the results to the results predicted by the solution obtained using the fully developed assumptions.

The desired effect of any of the cooling devices is to provide the best heat removal rate away from the microelectronics and provide for the lowest operating temperature of the microelectronics. Also, the pumping power required to cool the heat sink should be minimized. The pumping power is proportional to the flow rate times the pressure drop through the heat sink. In the microchannel heat sinks, the liquid flow rates are not normally considered an important design issue. Therefore, the major concern is the pressure drop across the heat sink which is an input design variable.

The primary objective of this work was to perform a parametric study of the geometric properties of the solution to identify an optimization procedure for the design. The optimization procedure provided the geometry with the lowest peak silicon temperature for a given heat flux and pressure drop through the heat sink. The peak temperature relationship was nondimensionalized so that the heat flux was not a design issue. The optimization procedure can be repeated at different pressure drop values across the heat sink. A relation between optimized peak temperature and pressure drop across the heat sink can be observed. This will allow the designer to choose the best possible design based upon an input pressure drop specification.

The optimization procedure is presented in chapter 1 along with the work using the fully developed assumptions. There were two reasons for this. First of all, the optimization procedure was originally derived from trends observed while running constant property, laminar, fully developed cases. Secondly, the optimized cases were the ones for which it was most important to evaluate the fully developed assumption in chapter two. For this reason, the optimization procedure preceded the evaluation of the fully developed assumption. The fully developed assumption was better for some of the parametric cases than for others. In general it was found that the fully developed assumption was good for cases with small channel aspect ratios and large fin width to channel width ratios. The fully developed assumption was poor for cases with large channel aspect ratios and small fin width to channel width ratios.

The important topic of this work was the optimization procedure itself and for this reason it was summarized in the third chapter. The optimization procedure can be used with a solution method that considers either the developing or the fully developed cases. In fact, the optimization procedure can even be used for cases solved computationally which consider variable properties or even for cases run experimentally. In general, the fewer assumptions made in the solution, the more the optimized design will reflect the actual optimized microchannel heat sinks as they are applied in practice.

It was intended to make assumptions which allowed simplification of interpretation but that also produced a

predictable deviation from the actual solution. It was imperative that any assumptions would produce a conservative effect, (i.e. over-estimating the peak temperature as opposed to under-estimating it.) All the assumptions made in the solution were discussed and their corresponding result was predicted.

Laminar microchannel heat sinks are just one of many different methods of approaching the general problem which is to remove the large heat flux generated by the electronic devices predicted in references [2] and [3]. Incropera has prepared a summary of some alternative approaches [6].

Because an optimization procedure for the microchannel heat sinks has been established in this thesis, the best performance of the laminar microchannel heat sinks can be predicted. The performance of other alternative approaches of cooling the integrated circuits can be compared to the optimized laminar microchannel performance. It was not the intent of this work to compare the laminar heat sinks to alternative designs.

This work was performed with the idea that the laminar microchannel cooling problem must be solved before the problem of subcooled boiling in the microchannels could be investigated. It is therefore evident that this work is the first step in the solution to a larger problem.

### PROBLEM GEOMETRY

Consider the schematic of the compact heat sink of Figure 1 with fluid flowing in the microchannels. The substrate contained a planar heat source (the circuits) which supplied a spatially uniform flux  $q''=q/LW$ . The back surface contained deep rectangular channels which carried the coolant. The coolant was assumed to be an incompressible Newtonian fluid of constant density and viscosity. The use of many separate ducts, rather than a single coolant flow over the entire back of the substrate, allowed an increase in the heat transfer surface area by a factor  $\sigma=np/W$ .

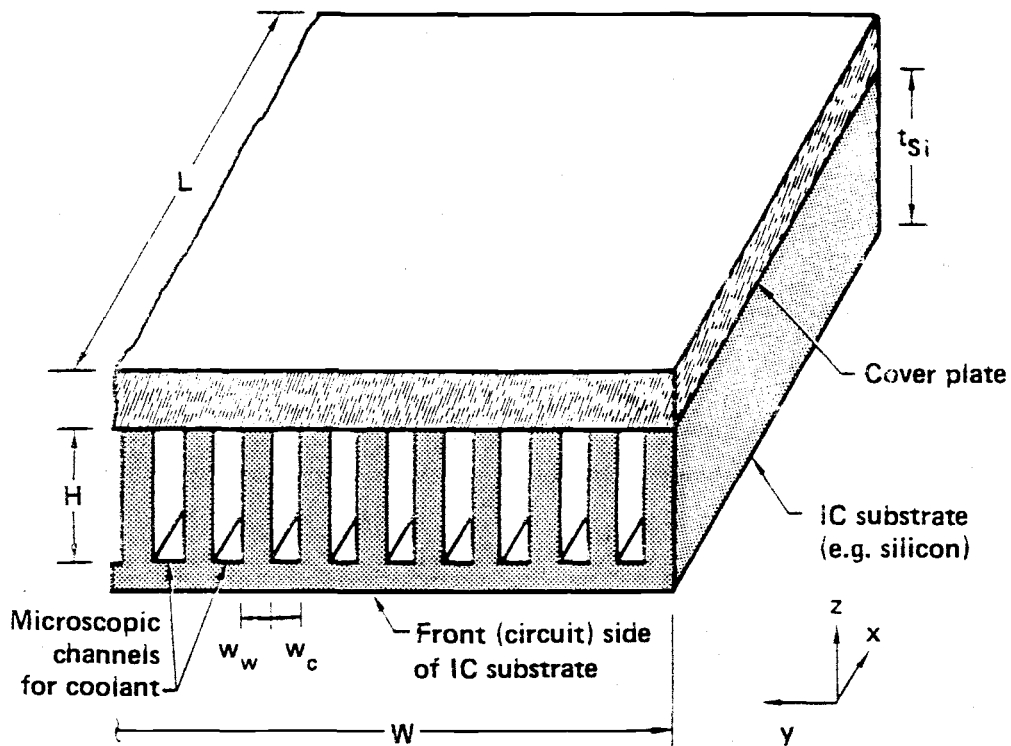


Figure 1 Schematic of the compact heat sink incorporated into an IC chip. (reprinted from Tuckerman [1])

## NOMENCLATURE

$A_{\text{sub}}$	= Substrate area <sup>1</sup> [ $(\mu\text{m})^2$ ]
$C$	= Specific heat of the fluid [kJ/kgK]
$D_{\text{hydr}}$	= Hydraulic diameter = 4(Area/Perimeter) = $2(W_w W_c)/(W_w + W_c)$ [ $\mu\text{m}$ ]
$f$	= Total height of heat sink = $s + H$ [ $\mu\text{m}$ ]
$f(z)$	= Nondimensional temperature distribution for comparison to the integral analysis, see equation (1.8)
$F$	= Volumetric flowrate [ $\text{cm}^3/\text{s}$ ]
$g(z)$	= Nondimensional heat flux for comparison to the integral analysis, see equation (1.9)
$h_T(x, z)$	= Heat transfer coefficient calculated using the bulk fluid temperature [ $\text{W}/(\text{m}^2 \text{K})$ ]  = $\frac{-k(\partial T/\partial y _{\text{wall}})}{T_{\text{wall}}(x, z) - T_{\text{bulk}}(x)}$
$h_{\theta}(x, z)$	= Heat transfer coefficient calculated using the local average fluid temperature $\theta_c$ at height $z$ [ $\text{W}/(\text{m}^2 \text{K})$ ]  = $\frac{-k(\partial T/\partial y _{\text{wall}})}{T_{\text{wall}}(x, z) - \theta_c(x, z)}$
$H$	= Height of the flow channel [ $\mu\text{m}$ ]
$H_o$	= Optimal channel height [ $\mu\text{m}$ ]
$j_y$	= Heat flux into the coolant from fin (in $y$ direction) [ $\text{W}/\text{m}^2$ ]

---

<sup>1</sup> Units will be placed in brackets [] in this section.

$j_z$	= heat flux up fins (in z direction) [W/m <sup>2</sup> ]
$k$	= Fluid conductivity [W/(mK)]
$k_w$	= Solid conductivity [W/(mK)]
$L$	= Length of the heat sink [ $\mu\text{m}$ ]
$n$	= Number of microchannels in the heat sink = $W/(W_w+W_c)$
$Nu_{T,D}(x,z)$	= Nusselt number evaluated at the fin face using the bulk fluid temperature $T_{\text{bulk}}$ = $h_T(x,z)(D_{\text{hydr}})/k$
$Nu_{\theta,D}(x,z)$	= Nusselt number evaluated at the fin face using the local average temperature $\theta_c$ = $h_{\theta}(x,z)(D_{\text{hydr}})/k$
$p$	= Total perimeter of microchannel = $2(W_c+H)$ [ $\mu\text{m}$ ]
$Pr$	= Prandtl number of the fluid
$q''$	= Heat flux through the base [W/cm <sup>2</sup> ]
$q$	= Total heat flow into the heat sink [W]
$q_m$	= Total heat flow into one microchannel [W]
$Re$	= Reynolds number based upon hydraulic diameter
$s$	= Substrate thickness [ $\mu\text{m}$ ]
$t_g$	= Thickness of the energy generation region [ $\mu\text{m}$ ]
$t_{si}$	= Thickness of the heat sink [ $\mu\text{m}$ ]
$t_{IC}$	= Integrated circuit substrate thickness [ $\mu\text{m}$ ]
$T(x,y,z)$	= Temperature of point $x,y,z$ [ $^{\circ}\text{C}$ ]

- $T_{\text{bulk}}(x)$  = Bulk Temperature as a function of  $x$  [ $^{\circ}\text{C}$ ]  

$$= \frac{\int_0^H \int_0^{W_c} u(y,z) T(y,z) dy dz}{\int_0^H \int_0^{W_c} u(y,z) dy dz}$$
- $T_w(x, z)$  = Wall Temperature [ $^{\circ}\text{C}$ ] (Not constant across the fin but is assumed constant across the fin in some discussions)
- $u(x, y, z)$  =  $x$  component of the spacial velocity fluid at point  $x, y, z$  [m/s] (For fully developed assumption use  $u(y, z)$ )
- $\underline{u}$  = Average fluid Velocity in  $x$  direction [m/s].  

$$= \frac{1}{W_c} \int_0^{W_c} u(y) dy$$
- $u_o$  = Peak fluid velocity [m/s]  
 $= u(\sim L, \frac{1}{2}(W_w + W_c), t_g + s + \frac{1}{2}H)$
- $v(x, y, z)$  =  $z$  component of the spacial fluid velocity [m/s]
- $w(x, y, z)$  =  $y$  component of the spacial fluid velocity [m/s]
- $W$  = Width of the heat sink [ $\mu\text{m}$ ]
- $W_c$  = Width of the flow channel [ $\mu\text{m}$ ]
- $W_w$  = Width of the fin [ $\mu\text{m}$ ]
- $(W_w/W_c)_o$  = Optimized Fin width to channel width Ratio
- $x$  = Distance in the flow (axial) direction [ $\mu\text{m}$ ]

- $x(\text{hydrodynamic})$  = The hydrodynamic entry length [cm]  
 $x(\text{thermal})$  = The thermal entry length [cm]  
 $\Delta x$  = Computational cell width in the  $x$  [ $\mu\text{m}$ ]  
 direction (For developing solution only)  
 $y$  = Horizontal distance across the channel  
 and fin. [ $\mu\text{m}$ ]  
 $\Delta y$  = Computational cell width in the  $y$   
 direction [ $\mu\text{m}$ ]  
 $Y_0$  = Nondimensional Fin Base Temperature  
 based on the bulk fluid temperature (This  
 is defined to compare to Landrums  
 results)  
 $= -k(T_{\text{bulk}} - T(L, \frac{1}{2}W_w, s)) / (q''H(1 + W_c/W_w))$   
 $Y_c$  = Fraction of distance across microchannel  
 $= (y - \frac{1}{2}W_w) / \frac{1}{2}W_c$   
 $z$  = Vertical distance up the substrate,  
 channel and fin [ $\mu\text{m}$ ]  
 $\Delta z$  = Computational cell height in the  $z$   
 direction [ $\mu\text{m}$ ]  
 $z_0$  = Reference height up the fin where the  
 local average temperature in  $z$  is  
 evaluated [ $\mu\text{m}$ ]  
 See section 1b of the **REVIEW OF  
 LITERATURE** section of this thesis for a  
 more precise definition of this  
 parameter.

#### GREEK SYMBOLS

- $\alpha$  = Aspect ratio of the channel =  $H/W_c$   
 $\alpha_f$  = Fluid thermal diffusivity [ $\text{cm}^2/\text{s}$ ]  
 $\alpha_o$  = Optimal channel aspect ratio =  $H_o/W_c$

- $\beta$  = Geometric parameter for solution  
 =  $(W_w/W_c)(k_w/k)(1/\alpha^2)$   
 See Figure 1.10b for an illustration of this parameter.
- $\beta_p$  = Characteristic heat penetration length up a fin [ $\mu\text{m}$ ] ( $\beta_p^2 = W_w W_c (k_w/k \text{Nu}_{\theta, x})$ )
- $\partial$  = Partial derivative symbol (i.e.  $\partial T/\partial x$ )
- $\Delta$  = Change in a quantity. (i.e.  $\Delta z$ )
- $\Omega$  = Nondimensional Peak solid temperature (based upon the inlet temperature, used to relate the different peak temperatures from different cases)  
 =  $\frac{-(\text{flux across bottom in flow direction})}{(\text{incoming flux perpendicular to flow})}$   
 =  $\frac{-k((T_{\text{inlet}}(0,0,t_g) - T_{\text{exit}}(L,0,t_g))/L)}{q''}$
- $\phi(x,y,z)$  = Nondimensional fluid temperature using the local average temperature in  $z$  (i.e.  $\theta_c(x,z_0)$ )  
 =  $\frac{T_{\text{wall}}(x,z) - T(x,y,z)}{T_{\text{wall}}(x,z) - \theta_c(x,y,z)}$
- $\Phi(x,y,z)$  = Nondimensional Temperature defined using  $T_{\text{bulk}}(x,z)$ .  
 =  $\frac{T_{\text{wall}}(x,z) - T(x,y,z)}{T_{\text{wall}}(x,z) - T_{\text{bulk}}(x)}$
- $\pi$  = Pi  $\approx 3.141593$
- $\rho$  = Fluid Density [ $\text{kg}/\text{m}^3$ ]
- $\sigma$  = Heat Transfer Surface Area Multiplication Factor for the heat sink  
 =  $np/W$

- $\Sigma$  = Summation symbol
- $\theta$  = Overall Resistance [ $^{\circ}\text{C}/\text{W}$ ]
- $\theta_{\text{bulk}}$  = Bulk thermal resistance due to conduction in through the semiconductor [ $^{\circ}\text{C}/\text{W}$ ]  
 $= t_{\text{IC}}/kA_{\text{sub}}$ .
- $\theta_{\text{cal}}$  = "Caloric" thermal resistance due to heating of the fluid as it absorbs energy passing through the heat sink [ $^{\circ}\text{C}/\text{W}$ ]  
 $= 1/\rho CF$
- $\theta_{\text{conv}}$  = Convective thermal resistance between the heat sink and the coolant fluid [ $^{\circ}\text{C}/\text{W}$ ]  
 $= D_{\text{hydr}}/(LWkNu_L)$
- $\theta_{\text{spread}}$  = Spreading resistance from the individual heat generating devices in the semiconductor substrate [ $^{\circ}\text{C}/\text{W}$ ]
- $\theta_{\text{int}}$  = Resistance associated with the IC/heat sink interface {if any} [ $^{\circ}\text{C}/\text{W}$ ]
- $\theta_c(x, z_0)$  = Local average temperature which is similar to the bulk temperature but is a function of  $z_0$  ( $z_0$  is the local value of  $z$ ).
- $$= \frac{\int_0^{Wc} u(y, z_0) T(y, z_0) dy |_{z=z_0}}{\int_0^{Wc} u(y, z_0) dy |_{z=z_0}}$$
- $\mu$  = fluid kinematic viscosity (assumed constant) [ $\text{kg}/(\text{m}^*\text{s})$ ]

## REVIEW OF LITERATURE

This section was intended to review only information which pertained to the topic of microchannel cooling of integrated circuits. Reference for specific technical issues was made throughout the thesis.

- 1) Dr. David B. Tuckerman PhD Thesis "Heat Transfer Microstructures for Integrated Circuits". February 1984 [1]

This document inspired the investigation which resulted in this thesis. It contained the original idea of laminar microchannel cooling.

### 1a) Components of thermal resistance

Tuckerman [1] identified five components of thermal resistance associated with the laminar microchannel heat sinks. These were: 1) The spreading resistance of the heat from the "point" source ( $\theta_{\text{spread}}$ ); 2) the bulk resistance through the chip itself ( $\theta_{\text{bulk}}$ ); 3) the interfacial resistance between the integrated circuit and the heat sink ( $\theta_{\text{interface}}$ ) 4) the convective resistance between the heat sink and the fluid ( $\theta_{\text{conv}}$ ); and 5) the bulk "caloric" resistance due to heating the fluid as it absorbs energy passing through the heat sink ( $\theta_{\text{cal}}$ ). Figure 2 was reprinted from Tuckerman for explanation of these five components.

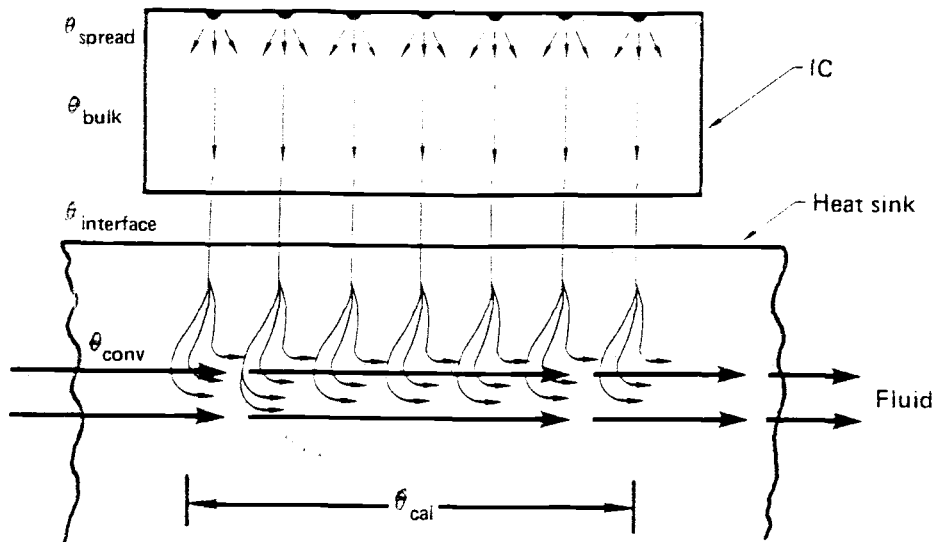


**Figure 2**  
Components of thermal resistance in convectively cooled integrated circuits. (Reprinted from Tuckerman [1])

R. C. Joy and E. S. Schlig discussed the spreading resistance in reference [2] and Tuckerman discussed the bulk, interfacial, convective and "caloric" resistance in reference [1].

This thesis dealt with only the effects within the heat sink, namely, the convective and the bulk "caloric" resistances.

#### 1b) General investigation

Tuckerman formulated an argument for the laminar microchannels with high aspect ratios ( $\sim 10$ ). This was important because it was consistent with the finding of

this thesis that the optimal laminar design has a high aspect ratio.

For a preliminary investigation, Tuckerman assumed that the solid was all at one temperature. (i.e. The solid had infinite thermal conductivity) This was done to provide an order of magnitude estimate of the solution. The local convective heat transfer coefficient  $h_x$  was then defined as

$$h_x = q / [nLp(T_w(x) - T_{bulk}(x))].$$

Energy conservation yields;

$$(1) \quad \frac{T_w(x) - T_{bulk}(0)}{q} = \frac{x}{\rho CFL} + \frac{1}{\sigma LWk} \cdot \frac{D_{hydr}}{Nu_x}.$$

The first term on the right of equation (1) was called the bulk "caloric" effect by Tuckerman and the second term was the convective effect. The maximum wall temperature occurred at the exit of the heat sink and can be found by setting  $x=L$  in equation (1). Writing (1) in terms of resistance and setting  $x=L$  yields

$$\theta = (T_w(L) - T_{bulk}(0)) / q = 1 / \rho CF + D_{hydr} / (\sigma LWk Nu_L) = \theta_{cal} + \theta_{conv}.$$

In order to minimize  $\theta_{conv}$ , the quantity  $D_{hydr} / Nu_L$  must be minimized. Traditionally this has been achieved by using high aspect ratio ducts to increase surface area (making  $\sigma$  large) and by designing to achieve turbulent flow (making  $Nu_L$  large).

Tuckerman proposed to achieve low convective thermal resistance primarily by minimizing  $D_{hydr}$ , rather

than maximizing  $Nu_L$ . Thus, the designs involved laminar flow. The only important lower limit on duct size was set by the coolant viscosity. For a given pumping pressure or pumping power, the mass flow rate decreased rapidly as  $D_{hydr}$  was reduced. This increased  $\theta_{cal}$ . By assuming a practical limit on the available pressure or power, Tuckerman calculated an optimum duct size,  $D_{hydr}$ , which minimized the overall resistance,  $\theta$ . As was shown in Tuckerman's thesis, the optimized geometry had a thermal resistance which, for the short channel length of interest ( $\approx 1$  cm), was comparable to that which was achieved with turbulent flow.

Tuckerman's laminar designs are much more compact (typically by a factor of 20) than conventional turbulent flow heat sinks [9], for a given operating pressure or pumping power. Since volume is at a premium in high speed computer systems, the microscopic laminar flow heat exchangers are necessarily the preferred approach for cooling dense arrays of integrated circuits.

#### 1c) Tuckerman's main assumption

Tuckerman derived an analytical solution to the energy conservation equation for the microchannel geometry. The solution used heat flux as its argument.

The heat flux at the base of the fin is defined by the gradient of the wall temperature;

$$(2) \quad j_z(x,z) = k_w \partial T_{wall}(x,z) / \partial z.$$

Tuckerman neglected the heat transferred from the "prime surface" at the bottoms of the channels. This assumption was not made in the present thesis. Also,

Tuckerman didn't consider the conduction in the substrate below the channels.

The heat flux  $j_y$  from the fin surface into the coolant was determined from energy conservation in the fin

$$(3) \quad 2j_y(x, z) = W_w (\partial j_z / \partial z).$$

The flux,  $j_y$ , was driven by the temperature gradient  $\partial T / \partial y$  between the wall and the coolant. For the high aspect-ratio channels with  $\alpha$  on the order of ten, the heat transfer at a point on the wall was sensitive only to the fluid temperature in the vicinity of that point. Tuckerman defined the local average coolant temperature  $\theta_c$  at a certain value of height by averaging across the channel width as

$$(4) \quad \theta_c(x, z_0) = \text{Local average temperature which is similar to the bulk temperature but is a function of } z \text{ (} z_0 \text{ is the local value of } z \text{.)}$$

$$\theta_c(x, z_0) = \frac{\int_0^{W_c} u(y, z_0) T(y, z_0) dy \big|_{z=z_0}}{\int_0^{W_c} u(y) dy}$$

Tuckerman used this definition in order to express the heat flux in terms of a local heat transfer coefficient  $h_x$  (assumed to be uniform along the height of the fin and in the axial direction),

$$(5) \quad j_y(x, z) = h_\theta [T_w(x, z) - \theta_c(x, z)].$$

Tuckerman's analytical temperature solution was

$$(6) \quad T_{\text{wall}}(x, z) = \frac{q''(W_w + W_c) \beta_p \cosh((H-z)/\beta_p)}{k_w W_w \sinh(H/\beta_p)} + T_{\text{bulk}}(x)$$

where  $\beta_p^2 = W_w W_c (k_w / k \text{Nu}_{\theta, x})$  and

$$T_{\text{bulk}}(x) = L(W_w + W_c) q'' / C_u W_c H = q'' / \rho C F.$$

The important point is that Tuckerman has assumed a uniform heat transfer coefficient in equation (5) in order to obtain the solution. This corresponded to a constant Nusselt number. The validity of the uniform heat transfer coefficient assumption was evaluated in subsection 1.8.3.2 of the present thesis.

1d) Tuckerman's Nusselt number.

The precise value of  $\text{Nu}_L$  depends upon the channel geometry and how fully developed the thermal boundary layer is at the channel exit. Tuckerman assumed that, owing to the very narrow channel size, the flow will be laminar ( $\text{Re} < 2100$ ); then the following general asymptotic forms for  $\text{Nu}_{\theta, L}$  result [1]:

$$\text{Nu}_{\theta, L} \sim (L^*)^{-1/3} \quad \text{for } L^* \ll 0.02$$

$$\text{Nu}_{\theta, L} \sim \text{Nu}_{\theta, \infty}, \quad \text{a constant, for } L^* \gg 0.02$$

In the former case, the thermal boundary layer is developing; in the latter case it is fully developed. Figure 3 shows a plot of  $\text{Nu}_{\theta, L}$  vs.  $L^* = L / (D_{\text{hydr}} \text{RePr})$  for

the case of uniform heat flux into parallel planes (calculated from the published eigenvalues of Cess and Shaffer [14]).

Tuckerman used the asymptotic value of  $Nu_{\theta, L} = 8.235$ .

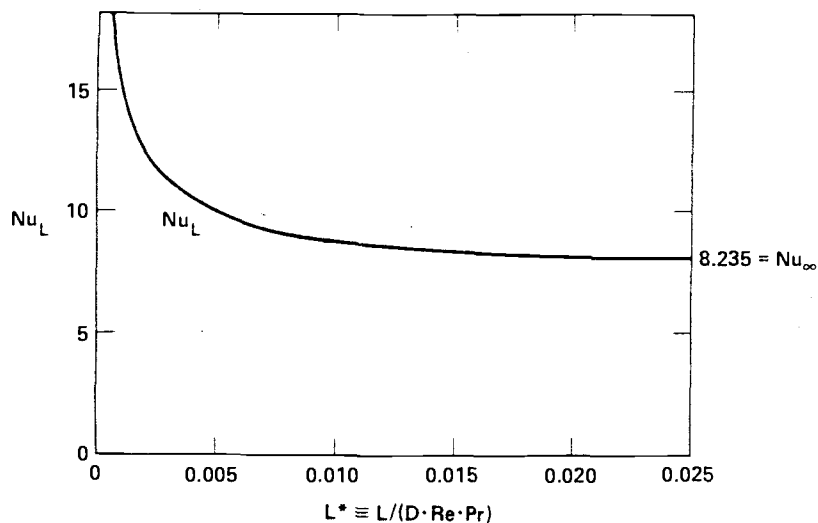


Figure 3. Local Nusselt number for laminar flow between parallel plates with uniform heat flux, as a function of nondimensional length  $L^* = L / (D_{hydr} Re Pr)$ .

1e) One of Tuckerman's Experimental findings.

It was desired to use values for the parameters which have actually been obtained by Tuckerman in experiment. One of Tuckerman's designs (81F9 End fed Etched on page 81 Table 3-5) was chosen for this purpose. The critical dimensions were  $L=1.4$  cm,  $W=2.0$  cm,  $W_C=50$   $\mu\text{m}$ ,  $W_W+W_C=100$   $\mu\text{m}$ ,  $H=302$   $\mu\text{m}$ ,  $t_{Si}=458$   $\mu\text{m}$ ,  $\Delta P=31$  psi,  $F=8.6$   $\text{cm}^3/\text{sec}$ ,  $q''=790$   $\text{W}/\text{cm}^2$ ,  $R=.09$   $^{\circ}\text{Ccm}^2/\text{W}=1/\theta$ .

1f) Tuckerman's fully developed statement.

Tuckerman made the argument that the best designs for thermal performance operated in the thermally fully developed regime. For this reason, the work of chapter 2 was presented to verify this hypothesis.

Tuckerman also stated, "The result that the boundary layer becomes fully developed is not an accident, but is in fact a direct consequence of the optimization of the sum  $\theta = \theta_{\text{conv}} + \theta_{\text{cal}}$ . The optimum design occurs when  $\theta_{\text{cal}}$  is beginning to be comparable to  $\theta_{\text{conv}}$  at the downstream end. That is, the temperature rise associated with coolant heating is comparable to the temperature drop across the channel cross section. It is clear that this condition implies a fully developed temperature profile. More mathematically, one can calculate the ratio  $\theta_{\text{cal}}/\theta_{\text{conv}} = 4\text{Nu}L/(D_{\text{hydr}}\text{RePr})$  for high aspect ratio structures. Thus having  $\theta_{\text{cal}}$  comparable to  $\theta_{\text{conv}}$  implies that  $L^* = (L/D_{\text{hydr}}\text{RePr}) \approx \text{Nu}/4$ , which for laminar flow implies nearly fully developed temperature profiles since  $\text{Nu} \gg 1$ ."

2) S. C. Lau, L. E. Ong, and J. C. Han, "Conjugate heat transfer in channels with internal Longitudinal Fins" [5].

An interesting study has been conducted at Texas A and M University dealing with a similar microchannel cooling problem. The main difference between their work and this work is that their work dealt mainly with low aspect ratio designs ( $\alpha < 4$ ). Their study also dealt with fins that did not reach to the top of the channel and treated fins that do reach to the top of the channel as a

special case. A specific optimization procedure was not discussed.

One important topic in their work is the definition of a nondimensional overall heat transfer per unit pumping power,  $Q_p$ , which is used to evaluate the performance of all of the designs.

### 3) Dr. C. S. Landrum's integral analysis of the laminar microchannel heat sinks. [private communication]

Dr. Landrum assumed no heat transfer through the prime surface at the base of the channels and didn't consider conduction in the substrate below the microchannels. He considered the axial velocity to be uniform along the height of the channel.

The integral analysis assumed that the nondimensional fin temperature distribution  $f(z)$  and the nondimensional heat flux off the face of the fin  $g(z)$  were both unity at all points along the fin. These are defined as;

$$(7) f(z) = \frac{T(x, 0, 0) - T(x, 0, z)}{(q''H/k_w)(1+W_w/W_c)(z/H)(1-z/2H)}$$

$$(8) g(z) = \frac{-k_w(\partial T/\partial y)|_{y=Ww/2}}{(\frac{1}{2}(W_w+W_c)/H)q''}$$

where  $z$  is measured from the fin base.

This assumption was evaluated in Figure 1.10 of section 1.8.3.3.

Equation (9) was predicted for the difference between exit fin base temperature and inlet fluid temperature.

$$(9) \quad T_{\text{fin,base}} - T_{\text{inlet}} = \frac{2(k_w/k)(q''L/k_w)(1+x) + (q''\alpha W_c)(1 + 51k_w/140k \alpha^2 x)(1+x)}{\text{Re}(1+\alpha)\text{Pr} \quad 3k_w \quad x}$$

Where  $x$  is equal to  $W_w/W_c$ .

Equation (9) was used in appendix D to derive equations (1.12) and (1.13) which yield the optimal fin width to channel width ratio and the optimal aspect ratio respectively.

Landrum predicted the nondimensional fin base temperature,  $y_0$ , as a function of the geometric parameter  $\beta$  with the equation

$$(10) \quad y_0 = (1/3)[1 + 0.3\beta].$$

This prediction was displayed in Figure 1.10c and Figure 1.10d of section 1.8.3.3.

## CHAPTER 1 FULLY DEVELOPED LAMINAR MICROCHANNEL COOLING

### 1.1 INTRODUCTION

This work numerically simulated the microchannel heat sinks with the assumption of fully developed momentum and energy solutions. This meant that the velocity profiles did not change in the axial direction and the temperature profiles were linear in the axial direction. A computer code was written which calculates temperature and velocity information within the heat sink.

The assumption of fully developed momentum and energy solutions has been made by Tuckerman [1], Sparrow [4], Lau [5] and Landrum [private communication]. It was felt that the fully developed momentum assumption was very good; while the fully developed energy assumption needed computational verification. This verification was a subject of chapter 2 of this thesis.

In any numerical work it is important to insure that the discretization is fine enough that a representative solution is obtained. For this reason, much effort was applied to this end. First of all, the computational momentum solution was compared to an analytical separation of variables solution. Secondly, the analytical solution to the heat transfer and fluid mechanics in an infinite parallel plate channel was compared to its' numerical formulation for gridding information across the channel. Finally, a comparison of the computational solution using very fine, fine and

coarse discretizations of the same problem was presented. This served to evaluate the discretization.

The results of this chapter were nondimensionalized for generality. Certain results were left dimensional for specific purposes. For example, the pressure drop across a given length of heat sink was specified as an input design variable and was left dimensional for determination. Also, Figure 1.10a was left dimensional to show the relatively low coolant temperatures obtained with the extremely high heat flux of  $1000 \text{ W/cm}^2$ .

One purpose of this work was to provide a procedure which can be used to optimize the design for a given pressure drop across the heat sink. For this reason, an array of pressure drops forming a complete matrix of optimized solutions was not pursued. It was not within the resources available at the time to do this and would only need to be done if an actual design were contemplated. This work provides the basic "roadmap" for performing a complete design analysis if it needs to be done. In addition, the computational techniques were developed in the form of a computer code which is available to perform the analysis.

## 1.2 MOTIVATION

The motivation for using the fully developed assumption is that it simplified the momentum and energy equations so they became a coupled set of elliptic partial differential equations. This reduced the problem from a three dimensional problem to a two dimensional one which resulted in large computational and algorithmic savings.

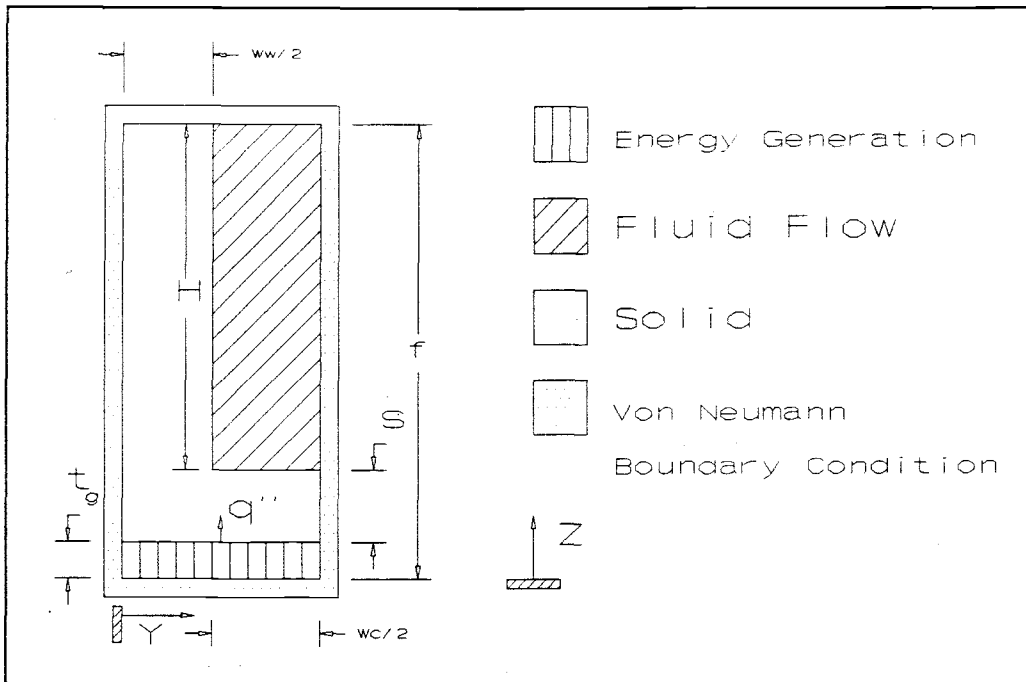
### 1.3 PROBLEM DESCRIPTION

Figure 1 on page 6 shows the general geometry of the silicon microchannel heat sinks. For computational purposes, it was decided to model the smallest repeating unit of this geometry and take advantage of symmetry. The computational domain of the two dimensional microchannel problem is presented in Figure 1.1 which corresponds to the way the problem was simulated numerically.

Comparing the computational domain of Figure 1.1 and the actual geometry of Figure 1 it can be seen that in the actual case there is a silicon cover plate which can transfer heat from the top of the fin into the top of the fluid region. It was chosen not to simulate this effect. The heat transfer from the cover plate to the fluid was small compared to the heat transfer from the face of the fin due to the greater fin surface area (large aspect ratio channels) and the larger temperature difference between the fin and the fluid. Finally, neglecting the heat transfer from the cover plate into the fluid provided a conservative assumption because a source of convective energy transfer has been neglected.

### 1.4 GOVERNING EQUATIONS

The governing equations for the fluid mechanics and convective and conductive heat transfer in the three respective regions identified in Figure 1.1 are given below. These equations result from scale analysis and from the assumption of fully developed momentum and energy conditions. The derivation of these simplified equations from the more generalized equations is given in



**Figure 1.1**  
Computational domain for fully developed microchannel problem.

appendix E entitled "Derivation of equations".

1.4.1 Fluid Flow Region. Viscous dominated Momentum Equation.

$$(1.1) \quad \frac{\partial^2 u}{\partial y^2} + \frac{\partial^2 u}{\partial z^2} = \frac{1}{\mu} \frac{dP}{dx} \quad (\text{fully developed momentum assumption})$$

Boundary Conditions: (No slip)

$$u(\frac{1}{2}W_w, z) = u(y, s) = u(y, f) = 0 \quad (\frac{1}{2}W_w \leq y \leq \frac{1}{2}(W_w + W_c))$$

$$\frac{\partial u}{\partial y}(\frac{1}{2}(W_w + W_c), z) = 0 \quad (s + t_g \leq z \leq f) \quad (\text{symmetry})$$

1.4.2 Energy Generation Region. Energy Equation.

$$(1.2) \quad \frac{\partial^2 T}{\partial y^2} + \frac{\partial^2 T}{\partial z^2} = \frac{q'''}{\alpha_f}$$

Boundary Conditions:

$$\frac{\partial T(0, z)}{\partial y} = \frac{\partial T(\frac{1}{2}(W_w + W_c), z)}{\partial y} = \frac{\partial T(y, 0)}{\partial z} = 0$$

$$(0 < y < \frac{1}{2}(W_w + W_c)), (0 < z < t_g)$$

(Von Neumann boundary conditions resulting from adiabatic and symmetry conditions)

#### 1.4.3 Solid Conduction Region. Energy Equation

$$(1.3) \quad \frac{\partial^2 T}{\partial y^2} + \frac{\partial^2 T}{\partial z^2} = 0$$

Boundary Conditions:

$$\frac{\partial T(0, z)}{\partial y} = \frac{\partial T(\frac{1}{2}(W_w + W_c), z)}{\partial y} = \frac{\partial T(y, f)}{\partial z} = 0$$

$$(0 < y < \frac{1}{2}(W_w + W_c)), (t_g < z < f)$$

(Von Neumann boundary conditions resulting from adiabatic and symmetry conditions)

#### 1.4.4 Fluid Flow Region. Energy Equation

$$(1.4) \quad \frac{\partial^2 T}{\partial y^2} + \frac{\partial^2 T}{\partial z^2} = \frac{u}{\alpha_f} \frac{\partial T}{\partial x} \approx \frac{u}{\alpha_f} T_{\text{bulk}} \quad (\text{fully developed energy assumption})$$

Boundary Conditions:

$$\frac{\partial T(\frac{1}{2}(W_w + W_c), z)}{\partial y} = \frac{\partial T(y, f)}{\partial z} = 0$$

$$(\frac{1}{2}W_w < y < \frac{1}{2}(W_w + W_c)), (s + t_g < z < f)$$

(Von Neumann boundary conditions resulting from symmetry and adiabatic conditions)

## 1.5 COMPUTATIONAL TECHNIQUES

### 1.5.1 Separation of Variables solution code.

A solution to the momentum equation (equation 1.1), was found in Carslaw and Jaeger [8]. A computer code was written which summed terms of a series and computed the solution at all the points of a given discretization. The solution was compared to the finite difference solution for grid discretization verification in 1.6. Appendix B provides the separation of variables solution, the logic and the solution algorithm for the computer code.

### 1.5.2 Finite Difference Heat Transfer Code

In order to solve the above system of elliptic partial differential equations (equations 1.1-1.4) in their respective domains, a finite difference, steady state heat transfer computer code was written in FORTRAN. The discretization of the region in Figure 1.1 was taken as input to the computer code. First the momentum equation (equation 1.1) was solved in the fluid flow region, then the energy equations (equations 1.2-1.4) were solved in all regions. The code used the optimized point successive over-relaxation (PSOR) algorithm for both the momentum and energy solutions.

The general and specific logic of the computer code is given in appendix A along with a flowchart and source code listing. Appendix A also contains the bulk energy balance analysis to find the change in bulk temperature in the flow direction.

## 1.6 GRID DISCRETIZATION

Proper discretizations must be determined for both the momentum and energy equations and the finer discretization must be used. The discretizations for the momentum and energy equations were discussed separately in sections 1.5.1 and 1.5.2 respectively.

In order to simplify the analysis and provide greater ease in the interpretation of results, it was decided to use constant cell width in both the height and width directions. The discretization must be fine enough to represent the largest gradients. Constant cell width implies that the discretization will be uniformly fine everywhere; so some areas will be discretized finer than necessary. It was felt that the extra effort required to interpret the results with the variable cell spacing warranted using the constant cell spacing and fine discretization. It was found after running a few cases that this was a reasonable a priori assumption.

1.6.1 Comparison of numerical results with the separation of variables solution of the momentum equation.

The separation of variables method was used to solve the viscous momentum equation analytically using the code of 1.5.1. The analytical and numerical solutions were compared to determine proper grid discretization in both the height and width directions for the flow channel.

The channel considered had a fifty micrometer width with an aspect ratio of eight. The first discretization

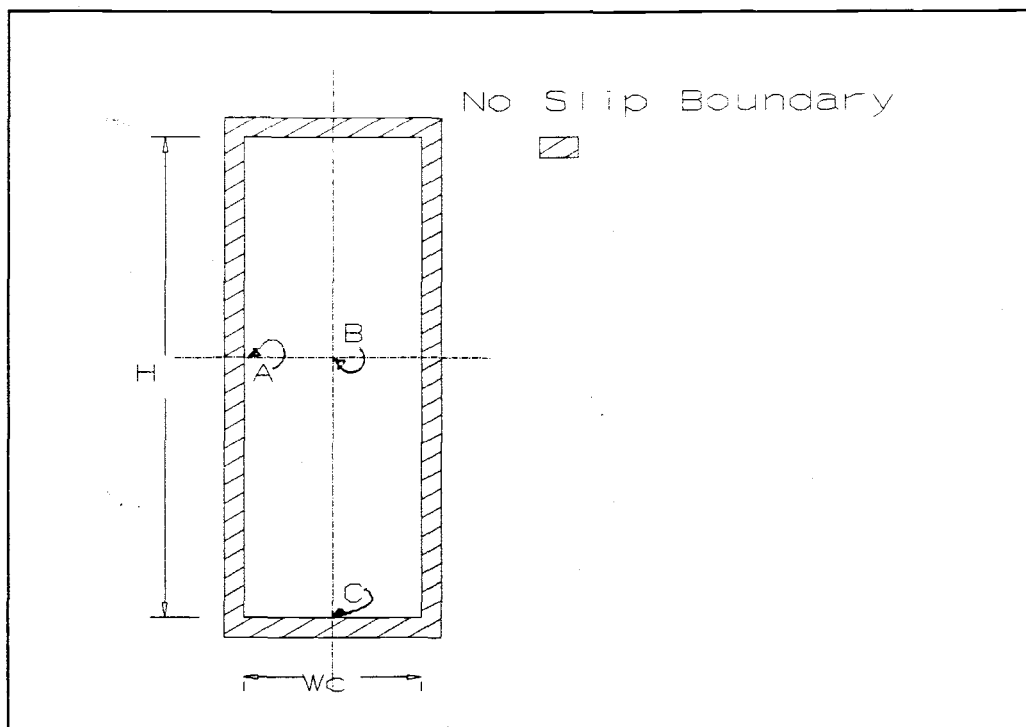


**Figure 1.2**  
Microchannel for velocity distribution.

involved ten cells for the half width and ten cells for the half height (twenty cells in the height direction). Referring to the geometry of Figure 1.2, the analytical and numerical velocity values differed by 2.56% at point A, .25% at point B and 12.84% at point C. The second discretization involved twenty cells for the half width and 20 cells for the half height (forty cells in the height direction). The analytical and numerical velocity values differed by .71% at point A, .49% at point B and 9.5% at point C.

The largest discrepancies occurred near the no slip surfaces as expected. The most important value for the problem solution was the value at point A in Figure 1.2

because most of the convective heat transfer occurred off the face of the fin. The discrepancy at point C was not very important because the aspect ratio of the channels was generally quite high (always over five). The convective heat transfer through the base of the channel was usually a small proportion of the total. Because the analytical and numerical velocities compared well with a discretization of twenty cells in the width ( $y$ ) direction, it was decided to use this for the momentum equation solutions. Also, a value of thirty to forty cells in the height direction was chosen for the momentum solution in the fluid region in the height direction.

In order to show graphically the deviation of the analytical and numerical velocities, graphs of the velocity were plotted for both horizontal and vertical centerline profiles for the channel of Figure 1.2. Figure 1.3 displays the velocity as a function of the distance from the fin face obtained by analytical and numerical methods for a 10 celled discretization. All values agree within 3%. Figure 1.4 shows the velocity as a function of the distance from the base material by both techniques. The discrepancy in the value nearest the wall was approximately 13% deviation. These plots were made for the distribution with 10 cells in each direction. These were plotted because it was difficult to see any discrepancy on the graphs of the solutions with 20 cells in each direction. The curves for a 20 celled discretization were much closer than that shown for the 10 celled case.

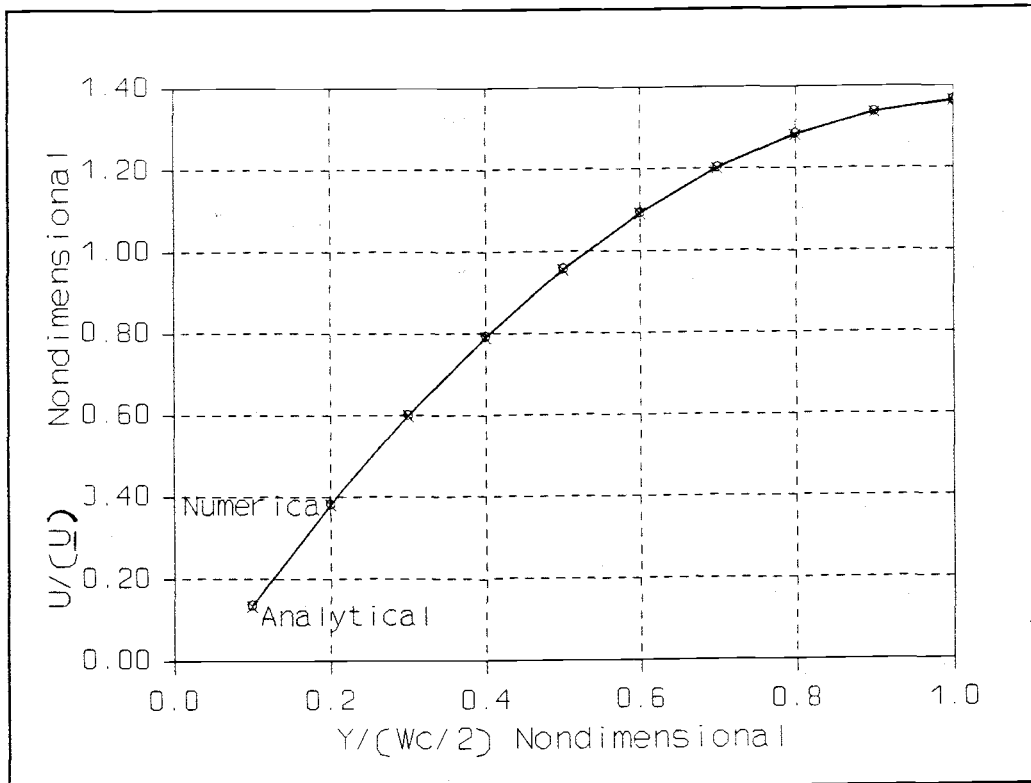


**Figure 1.3**  
Analytical and numerical velocity distributions plotted horizontally at channel horizontal centerline for a 10 celled discretization.

1.6.2 Comparison of numerical results with the solution of the energy and momentum equations for grid discretization information.

Because an analytical solution was not available for the energy equation, two other discretization evaluations were presented. First, the comparisons using the analytical solution for the flow and heat transfer within an infinite parallel plate channel are discussed in 1.6.2.1. This problem was chosen because it had very strong similarity to the high aspect ratio microchannel problem. Finally, the comparisons using

different discretizations of the same microchannel problem are presented in 1.6.2.2..

1.6.2.1 Comparisons using the Solution for the flow and heat transfer within an infinite parallel plate channel.

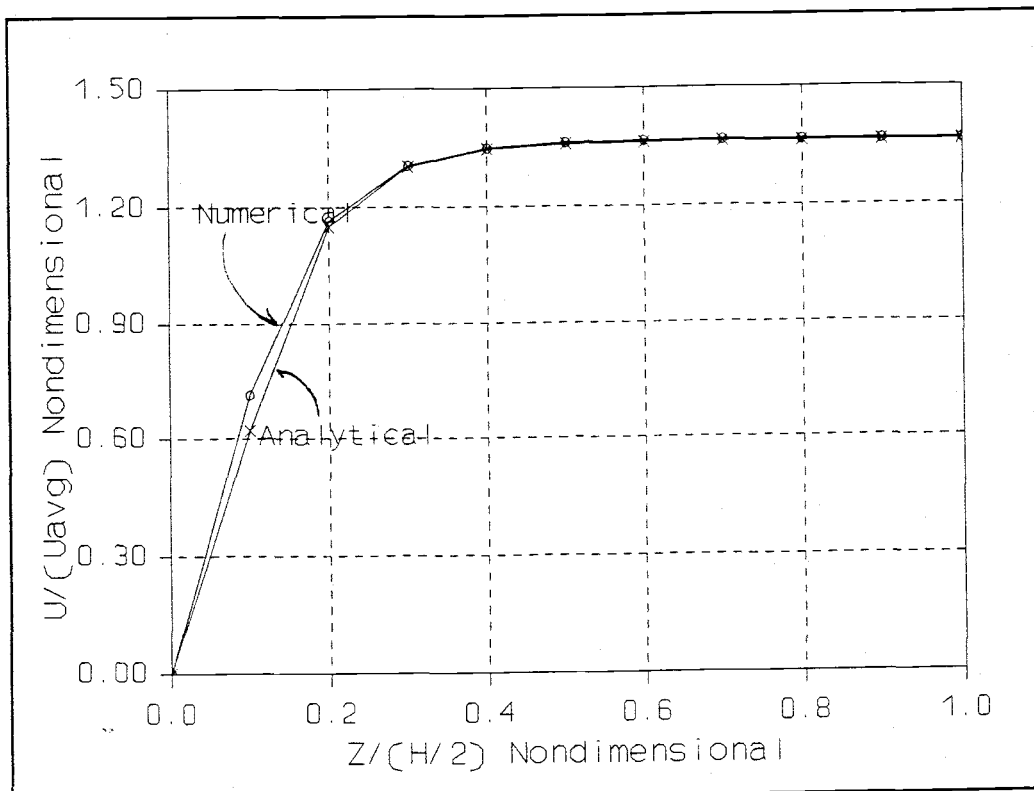


**Figure 1.4**  
Analytical and numerical velocity distributions plotted vertically at the channel horizontal centerline for a 10 celled discretization.

This section references the important findings from the analytical and numerical comparisons of the solution for the flow and heat transfer within an infinite parallel plate channel. Appendix C contains more detailed information.

Figure 1.5 depicts the heated parallel plate channel. The flow is into the plane and the channel extends infinitely in the vertical direction. The code described in section 1.5.2 was used to solve numerically the problem in Figure 1.5 and also gave results from the analytical calculation. The geometry in Figure 1.5 resembles the geometry in the microchannel heat sinks if all the heat is assumed to conduct up the fin and if the heat flux is assumed uniform off the face of the fin. These assumptions are simplistic but are not altogether unreasonable.

The discretization across the half channel and the effect of the discretization on the centerline temperature were studied. Figure 1.6 is a graph of the percent difference between the analytical and numerically derived solutions to the problem in Figure 1.5. The problem was solved for various discretizations across the channel (5, 10, 20 and 40 cells).

The percent difference was calculated by

$$(1.5) \quad \% \text{difference} = \frac{(T_{\text{analy}} - T_{\text{num}})}{(T_{\text{wall}} - T_{\text{analy}})} \times (100).$$

From the figure, a value of discretization across the channel of 20 cells results in favorable comparison (within .1%) between the analytical and numerical values. If a value less than 20 is chosen, inaccuracies may

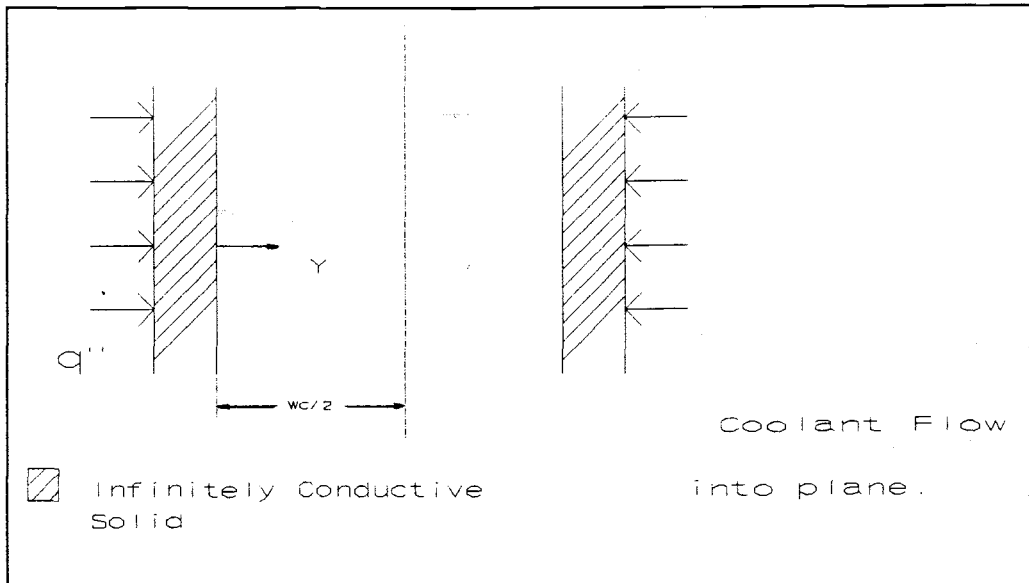


**Figure 1.5**  
Infinite channel for analytical and numerical discretization comparisons.

result and if a value greater than 20 is chosen, the computational costs are not justified by the gain in solution accuracy.

#### 1.6.2.2 Comparisons between fine and coarse discretizations of one microchannel geometry.

The preceding grid verification studies suggested that the value of 20 cells across the half fluid channel and 20 cells in the height direction provide adequate discretizations of the problem. In order to further verify this, the same microchannel geometry was run with considerably fewer and considerably more than twenty cells and a comparison of the solutions was made. The variable used for comparison was the nondimensional peak silicon temperature,  $\Omega$ , defined in the nomenclature section. For the horizontal discretization across the

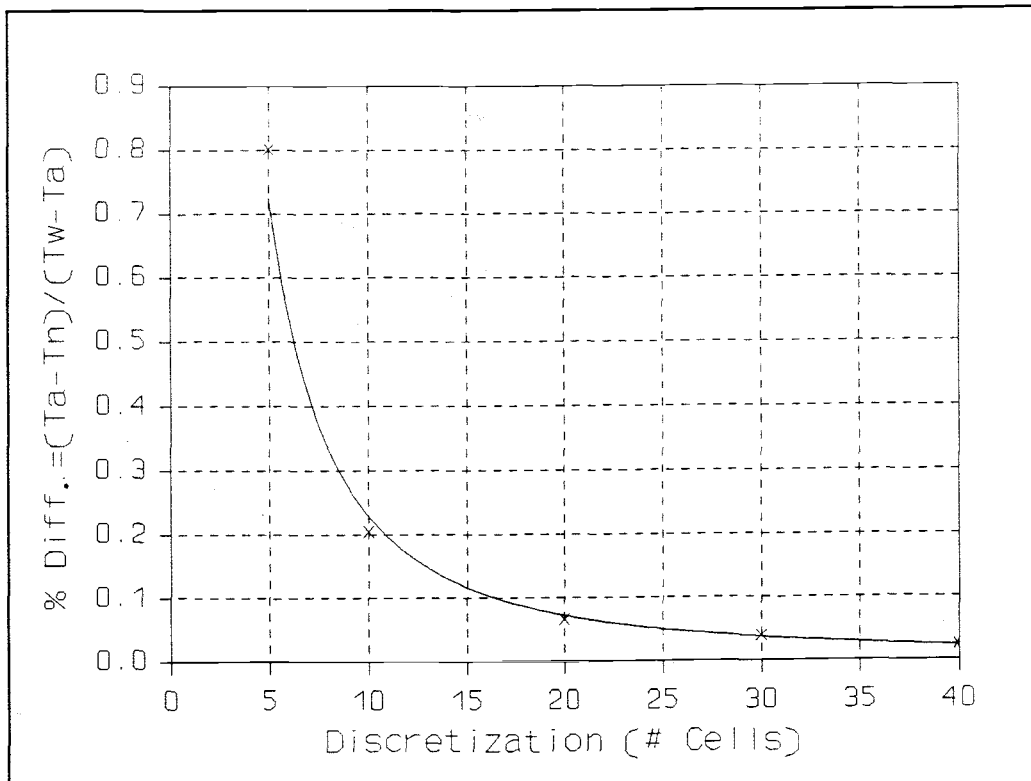


**Figure 1.6**  
Percent difference between analytical and numerical solutions of centerline temperature for the infinite channel.

channel, a microchannel with a  $60 \mu\text{m}$  channel width,  $600 \mu\text{m}$  channel height,  $60 \mu\text{m}$  fin width and a  $100 \mu\text{m}$  substrate was considered. The value of  $\Omega$  was found using discretizations of 7, 21 and 63 cells across the fluid flow region (i.e. half the channel width). The results are summarized in table 1.1 below.

<u>Discretization across the flow channel</u>	<u><math>\Omega</math></u>
7	.10758
21	.10765
63	.10346

**Table 1.1** Nondimensional temperature for horizontal discretization verification.

These results suggest that the nondimensional peak solid temperature is quite insensitive to discretization in the y direction. In fact changing from 21 to 63 cells across the channel only changed the nondimensional peak temperature by 4%. This was not enough discrepancy to warrant using more than 21 cells. The entire temperature field was not changed much by the horizontal discretization when more than 20 cells were used across the channel. This suggests that 20 cells across the channel width provides a good discretization for this problem in general.

For the discretization in the vertical direction up the channel centerline, a microchannel with a 60  $\mu\text{m}$  width, 600  $\mu\text{m}$  channel height, 60  $\mu\text{m}$  fin width and a 120  $\mu\text{m}$  substrate was considered. The value of  $\Omega$  was found using 10, 30 and 90 cells in the vertical direction up the fluid channel centerline. The results are summarized in Table 1.2 below.

<u>Discretization up the channel centerline</u>	<u><math>\Omega</math></u>
10	.10326
30	.10616
90	.10805

Table 1.2 Nondimensional peak temperature for vertical discretization verification.

These results indicate that a discretization of 30 cells in the vertical direction up the channel centerline provided a good discretization for the problem. In fact, changing from 30 to 90 cells only changed the nondimensional temperature by 2% which was insignificant. In fact 30 cells was probably a finer discretization than was needed but since the computational resources were

available, this was chosen to be the discretization in the vertical direction.

### 1.6.3 Summary of Grid discretization section.

Using the separation of variables solution for the momentum equation, it was determined that 20 cells horizontally across the flow channel and 20 cells vertically up the channel centerline provided an adequate discretization. Using the analytical and numerical comparisons for the 1 dimensional solution to the temperature in an infinite parallel plate channel, 20 cells horizontally across the flow channel and 20 cells vertically up the channel centerline were found to provide an adequate discretization. Finally, running the same microchannel geometry with fine and coarse discretization, it was determined that 20 cells horizontally across the flow channel and 30 cells vertically up the channel centerline provided an adequate discretization. This discretization was used for nearly all of the parametric cases considered.

## 1.7 IMPORTANT PRELIMINARY CONSIDERATIONS before running the parametric study

Before commencing on the work, a few preliminary considerations were important. They will be outlined in this section.

Since constant properties were used in the solution, it was necessary to determine an average value for the kinematic viscosity of water between 30°C and 90°C. The value calculated was  $.55(10^{-6})$  m<sup>2</sup>/s which was used exclusively throughout the computations. The

details behind the determination of this value are contained in appendix F.

The Reynolds number is accepted as being representative of the flow conditions for incompressible fluids. It was necessary to ensure that all cases run were in the laminar range. The algorithm of the solution was designed so that the Reynolds number could be specified. The optimization procedure developed in this chapter involved optimization of the geometric variables at one Reynolds number, then the optimization was repeated at different Reynolds numbers and the overall optimum is then found. In order to begin the optimization, an initial Reynolds number was needed. This was chosen from Tuckerman's experimental conditions. It was found that one of Tuckerman's samples had an average velocity of 2.85 m/s and a corresponding Reynolds number of approximately 500. These values are calculated in appendix F.

### 1.8 TYPICAL SOLUTION INFORMATION

Typical output data were the velocity field within the microchannel and the temperature distribution in the liquid and in the solid. The most important temperature was the temperature at the base of the heat sink which was adjacent to the microelectronics.

The code described in section 1.5.1 produced an output file with the complete velocity and temperature arrays at the exit to the heat sink of Figure 1. An output file is included in appendix G along with an explanation of all information contained. The results were presented graphically in this text.

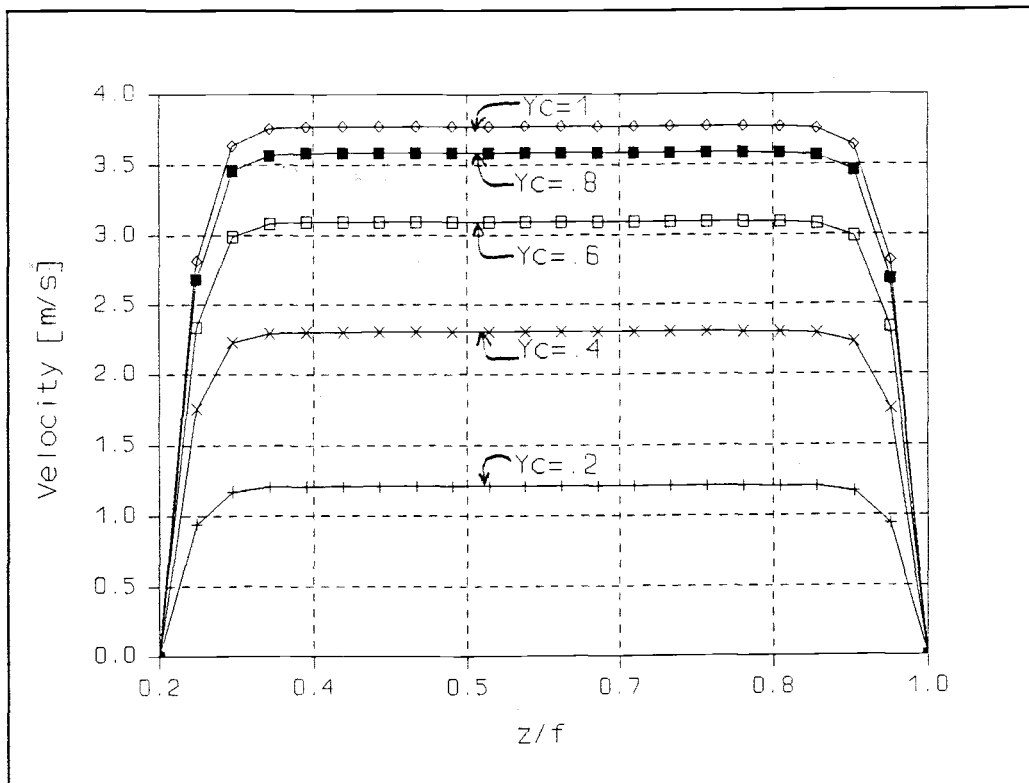


**Figure 1.7**  
Velocity profiles in the optimized microchannel with  $W_C=60 \mu\text{m}$ ,  $W_W/W_C=30 \mu\text{m}$  and  $\alpha=14.5$   $Y_c=(y-\frac{1}{2}W_W)/\frac{1}{2}W_C$ .

### 1.8.1 Velocity Solution

Velocity profiles are plotted in Figure 1.7 versus  $z/h$  with  $Y_c=(y-\frac{1}{2}W_W)/\frac{1}{2}W_C$  as a parameter.  $Y_c$  is the fractional distance across the channel. The velocity gradient in the horizontal direction is zero at the channel centerline because of the symmetry boundary condition. Also, the velocity on all the no-slip surfaces is zero. The velocity distribution displays the general form of a parabolic distribution across the channel as expected.

### 1.8.2 Temperature Solution

Temperature profiles are plotted in Figure 1.8 versus  $z/f$  with  $Yc$  as a parameter. There are drastic differences between the temperature gradient in solid and fluid regions. This is expected due to the large ratio of silicon to water thermal conductivity. Silicon has approximately two hundred and twenty four times the thermal conductivity of water.

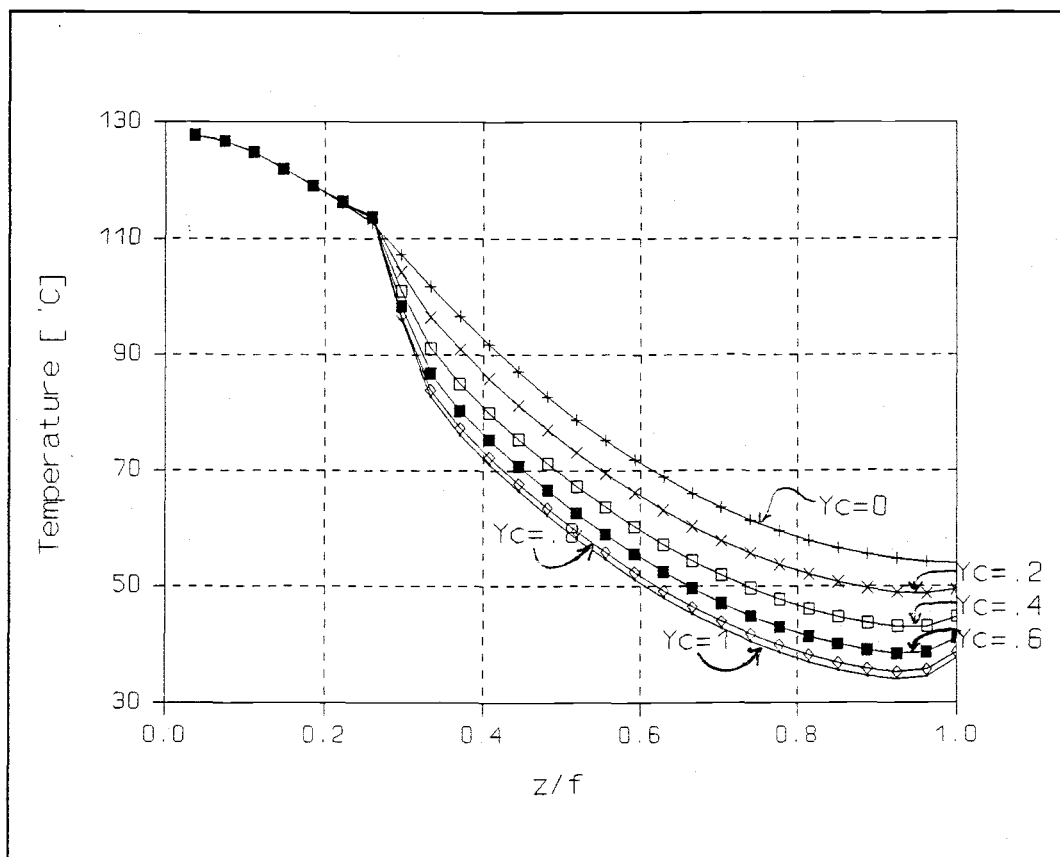


**Figure 1.8**  
Temperature Distribution for the optimized microchannel with  $W_c=60 \mu\text{m}$ ,  $W_w/W_c=1$  and  $\alpha=14.5$ .  $Yc=(y-\frac{1}{2}W_w)/\frac{1}{2}W_c$ .

A temperature gradient appears to exist in the  $z$  direction near the top center of the channel. Numerically the very top of the channel is an adiabatic surface and the temperature gradient is forced to zero. However in the cells next to the top, a temperature gradient exists. The minimum in fluid temperature with height occurs near the top of the channel and not at the very top of the channel. The velocity at the very top of the channel is low because of the no slip boundary. The velocity further down the microchannel is higher which pushes cold fluid into the plane faster and lowers the temperature. This causes the minimum to occur near the top of the channel and not at the very top of the channel.

A positive temperature gradient exists across the channel in the direction parallel to the top adiabatic boundary which can be seen by observing the spacing of the contours. This is necessary to satisfy energy conservation.

#### 1.8.3.1 Evaluation of the Nusselt number assumed by Tuckerman

Tuckerman assumed a constant value for the Nusselt number which corresponds to a uniform heat transfer coefficient on the face of the fin. Figure 1.9 presents the Nusselt number plotted versus the height up the fin ( $Z/H$ ). The Nusselt number is calculated using equation 1.6 below.

$$(1.6) \quad Nu_{\theta}(z) = \frac{-D_{hydr}(\partial T/\partial y|_{wall})}{T_{wall}(x,z) - \theta_c(x,z)}$$

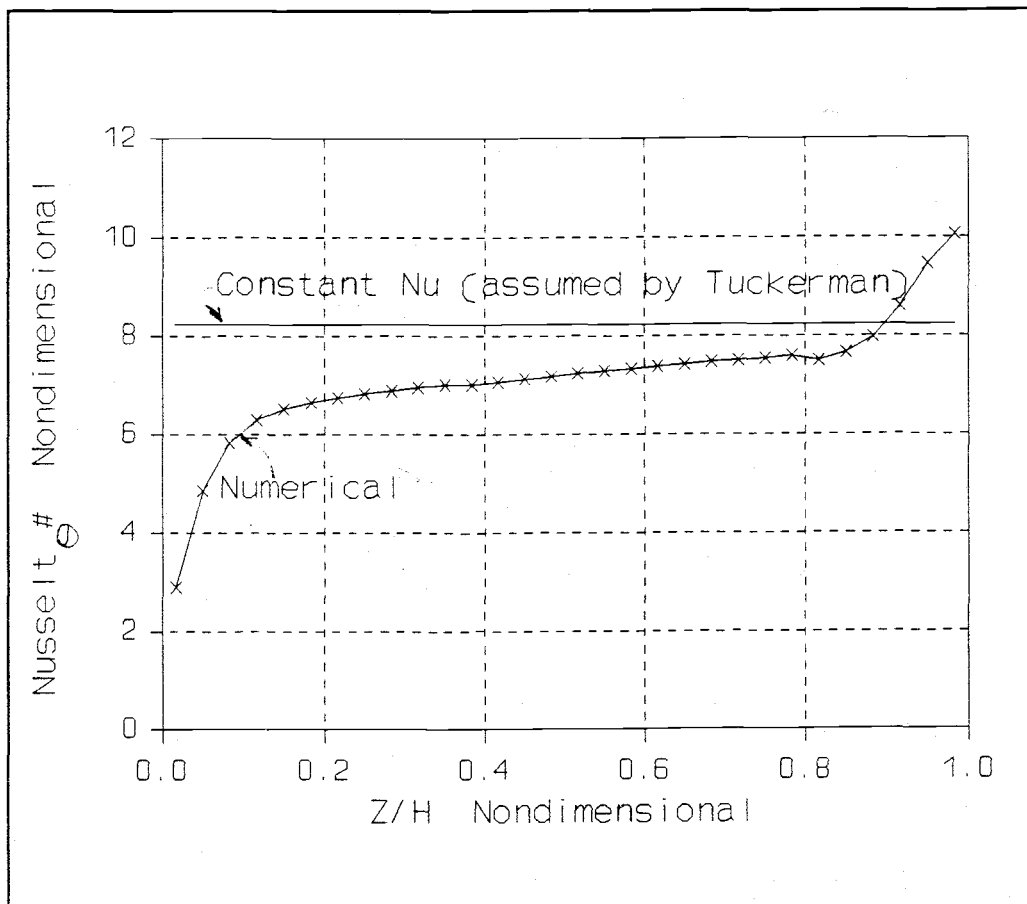


**Figure 1.9**  
Comparison of numerically derived Nusselt number with Tuckerman's constant. [ $\alpha=5$ ,  $W_c=60 \mu\text{m}$ ,  $W_w/W_c=.5$ ]

In this equation, the local bulk temperature  $\theta_c$ , which is a function of height,  $z$ , is used. Note that the numerical results predict a Nusselt number which is on average slightly less than Tuckerman's constant Nusselt number. The value near the base of the fin is quite a bit less than the constant value.

The Nusselt number may also be calculated with the bulk temperature,  $T_{\text{bulk}}$ , instead of the local average

temperature  $\theta_c$  in equation (1.6). This yields the more conventional Nusselt number  $Nu_T$  which is defined in the nomenclature section of this thesis. This Nusselt number was not compared to the results predicted by Tuckerman because he didn't calculate it. Figure 1.9a shows the Nusselt number calculated numerically using the bulk temperature for the same geometry as in Figure 1.9. The Nusselt number has a maximum at about 80% of the way up the fin.

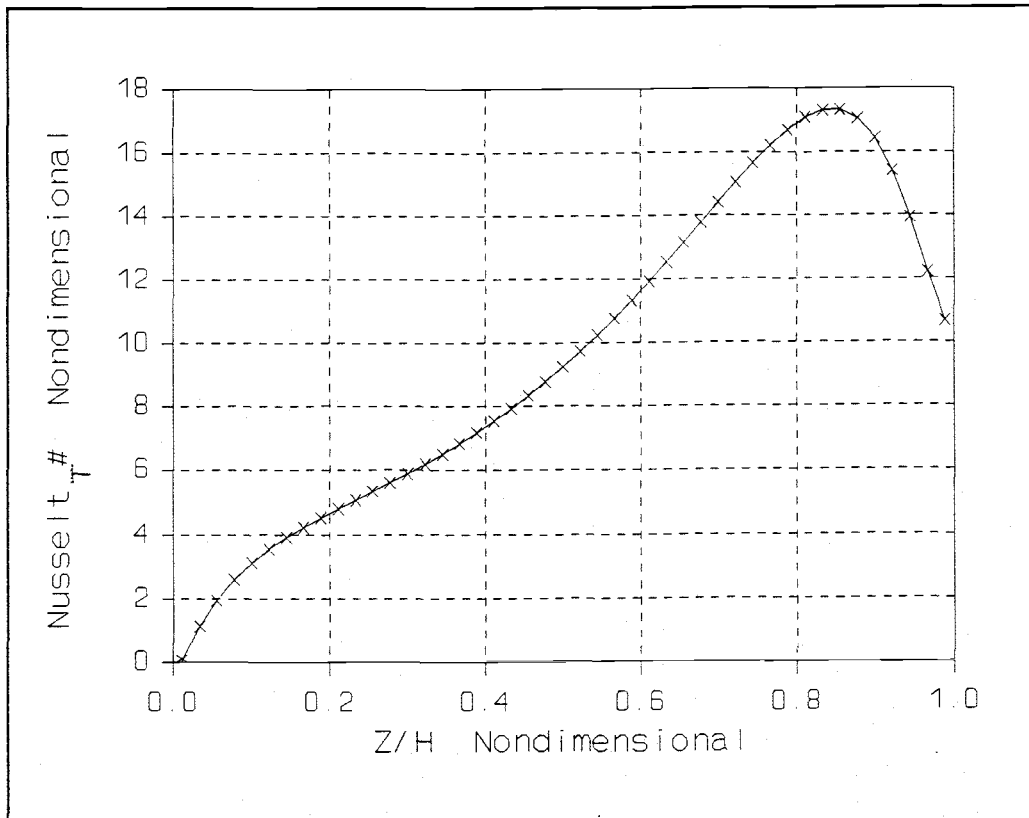


**Figure 1.9a**  
Nusselt number calculated using the bulk fluid temperature vs.  $Z/H$ . [ $W_c=60 \mu\text{m}$ ,  $\alpha=5$ ,  $W_w/W_c=.5$ ]

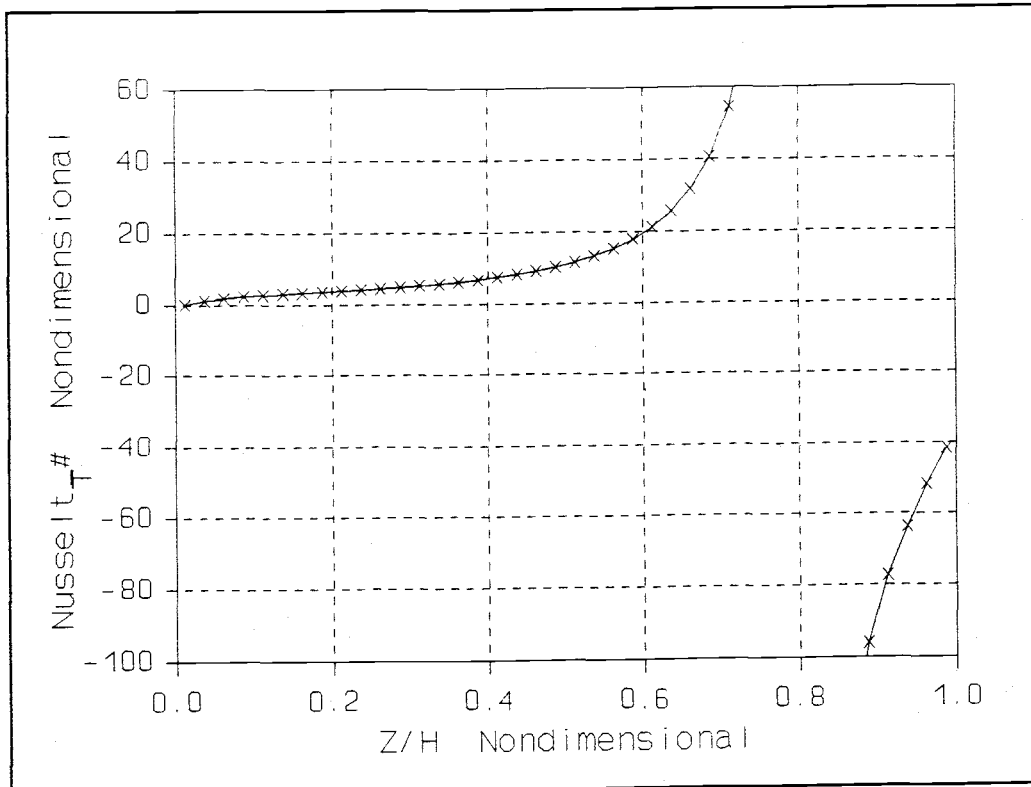


**Figure 1.9b**  
Nusselt number vs.  $Z/H$  for: [ $W_w/W_c=.5$ ,  $\alpha=10$ ,  $W_c=60$   $\mu\text{m}$ .] (Thin fin problem)

Figure 1.9b Shows the Nusselt number calculated numerically for a problem with  $W_w/W_c=.5$ ,  $\alpha=10$  and a  $60 \mu\text{m}$  channel width. This problem is very interesting because it displays a singularity approximately 80% up the channel. The singularity is not due to the heat flux going infinite but is due to the Wall temperature  $T_w$  being equal to the Bulk Temperature  $T_{\text{bulk}}$ . This causes the denominator to approach zero. A physical interpretation of this behavior is that for problems with small fin width to channel width ratios,  $W_w/W_c \approx .5$ , the fins don't have enough cross sectional fin area to

conduct the large heat flux. Thus, the top of the fin remains cooler. In fact, the top of the fin can be at a lower temperature than the bulk temperature as is exhibited in Figure 1.9b. This suggests the use of larger fin widths in order to improve the convective heat transfer near the top of the fin.

The variation of the Nusselt number with  $z/H$  in Figures 1.9a and 1.9b suggest that the Nusselt number defined in terms of the bulk temperature is not helpful in the solution of the high aspect ratio microchannel problem. Tuckerman's definition of  $\theta_c$  results in an improvement as is shown in Figure 1.9a. The assumption of a constant  $Nu_\theta$  still produces erroneous results as is shown in Figure 1.9.

1.8.3.3 Comparison to the results of the integral analysis.

The integral analysis of Dr. C. S. Landrum [private communication] predicted that  $f(z)$  and  $g(z)$  given by equations (7) and (8) were both unity at all points along the fin.

Figure 1.10 presents numerically derived profiles of  $f(z)$  and  $g(z)$  for a 60 micrometer channel with a fin width to channel width ratio of one half and a ten to one aspect ratio. Figure 1.10 reveals that for most of the fin length, the integral analysis and numerical values agree within 10%. The major deviation occurs at the bottom of the fin (to the left in Figure 1.10) and at the top of the fin (to the right in Figure 1.10). The bottom of the fin is where the integral analysis is expected to have the greatest error. It should be noted that the

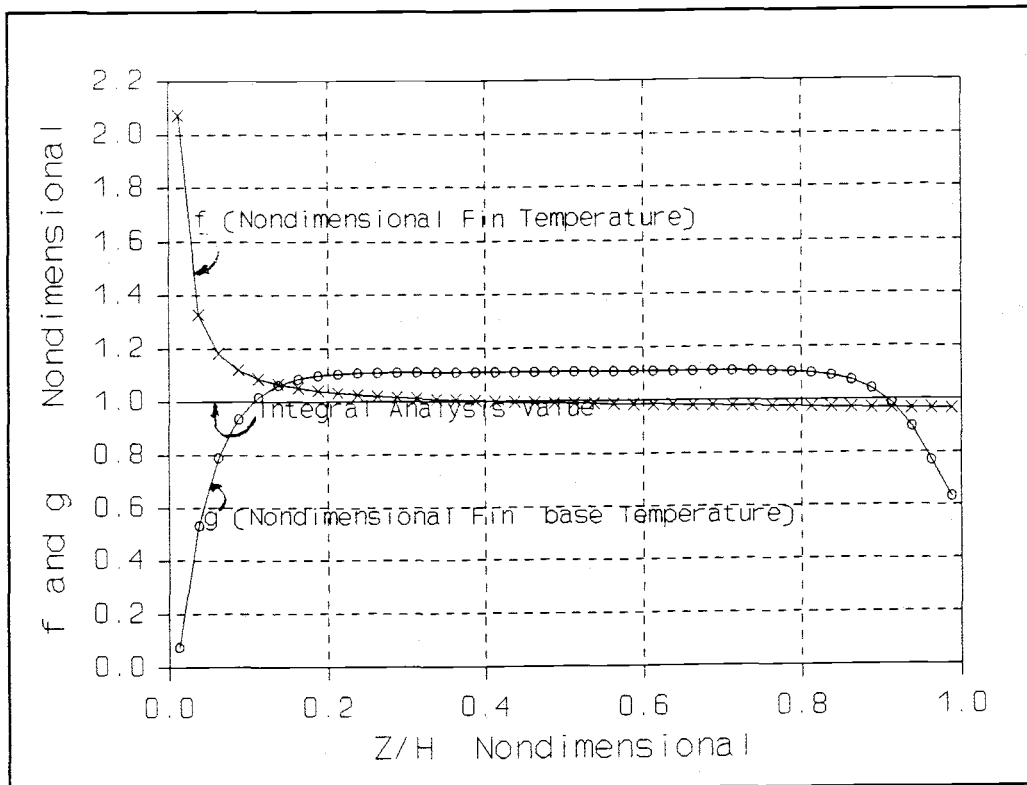


**Figure 1.10**  
Integral analysis comparison to numerical solution for a 60 micrometer channel with a 30 micrometer fin.

integral analysis is a good first order estimation of the solution.

### 1.9 THE PARAMETRIC STUDY

A parametric study was performed on the various geometric cases. The results are presented graphically in the text and numerically in the spreadsheet of appendix H titled "Spreadsheet for the parametric study at RE = 500.". The important results of the parametric study are presented in 1.10 as they are employed to derive the optimization procedure. The results presented in this section will therefore be limited. The first

topic of this section was to present some of the results of the parametric study. The second topic was to present comparisons of the numerical results to the results of the integral analysis of Landrum. The geometric parameters of interest were: 1) The channel aspect ratio, 2) the fin width to channel width ratio and 3) the width of the channel. These parameters were varied independently to observe their effect on the nondimensional peak solid temperature.

#### 1.9.1 Presentation of one parametric result

One important parametric result is the relationship of peak fin temperature to aspect ratio as in Figure 1.10a. The peak fin temperature is the temperature at the base of the fin and is denoted by  $T_{\text{wall}} - T_{\text{inlet}}$  with the inlet temperature being held constant at 25°C. The value of heat flux of 1000 W/cm<sup>2</sup> represents a 20 fold increase over the conventional cooling techniques and the water temperature is just approaching the subcooled boiling regime. This is indeed an outstanding result.

Another striking result of Figure 1.10a is that the graph of peak fin temperature reaches a minimum with aspect ratio. This suggests an optimization as performed in 1.10. Finally, Figure 1.10a is presented in such a way that the "caloric" and convective resistances can be compared by considering the two curves ( $T_{\text{bulk}} - T_{\text{inlet}}$ ) and ( $T_{\text{wall}} - T_{\text{bulk}}$ ) respectively. It can be seen that the first curve ( $T_{\text{bulk}} - T_{\text{inlet}}$ ) continually decreases and the second curve ( $T_{\text{wall}} - T_{\text{bulk}}$ ) reaches a minimum at about

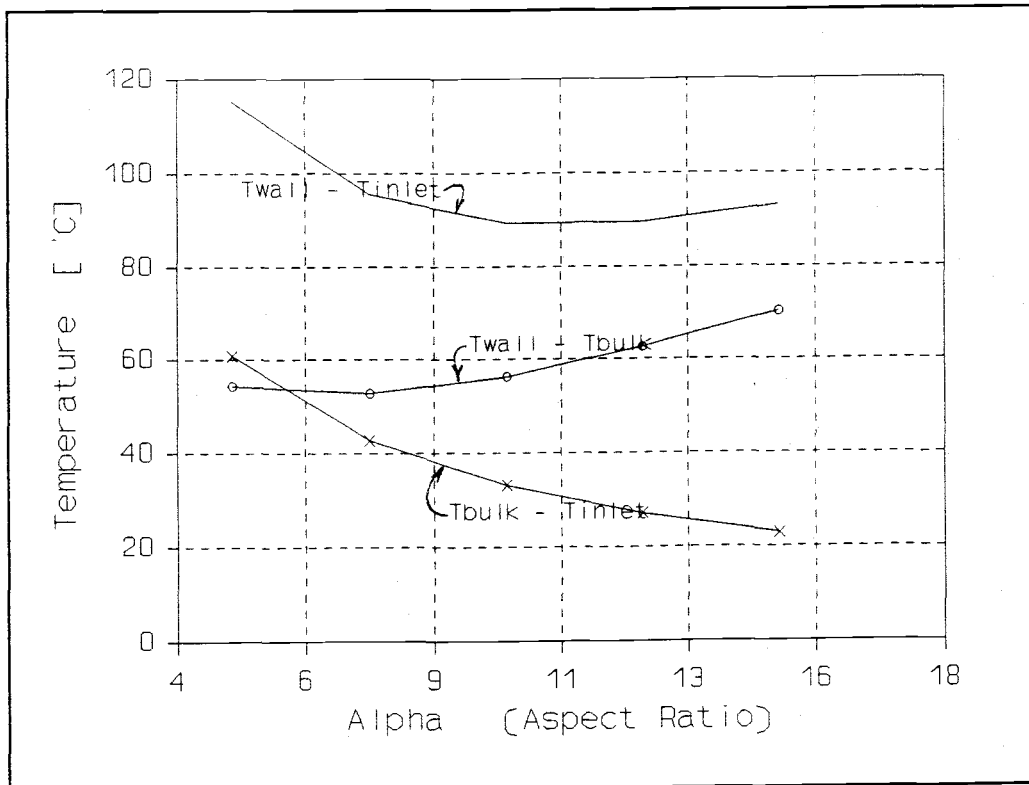


**Figure 1.10a**

Temperature vs. aspect ratio  $\alpha$  for  $W_C=60 \mu\text{m}$ ,  $W_W=30 \mu\text{m}$ ,  $Re=500$  and  $q''=1000 \text{ W/cm}^2$ .

$\alpha=5$ . When these two curves are added, the resulting curve ( $T_{\text{bulk}}-T_{\text{inlet}}$ ) reaches a minimum at an aspect ratio of approximately 11.

#### 1.9.2 Comparison of the solutions with Landrums solution

The integral analysis of Dr. C. Landrum provided a natural comparison to use in the parametric study. The comparison is the nondimensional fin base temperature denoted by  $y_0$  plotted versus the correlating parameter beta ( $\beta=(k_w/k)(W_w/W_c)(1/\alpha^2)$ ).  $\beta$  was first used by

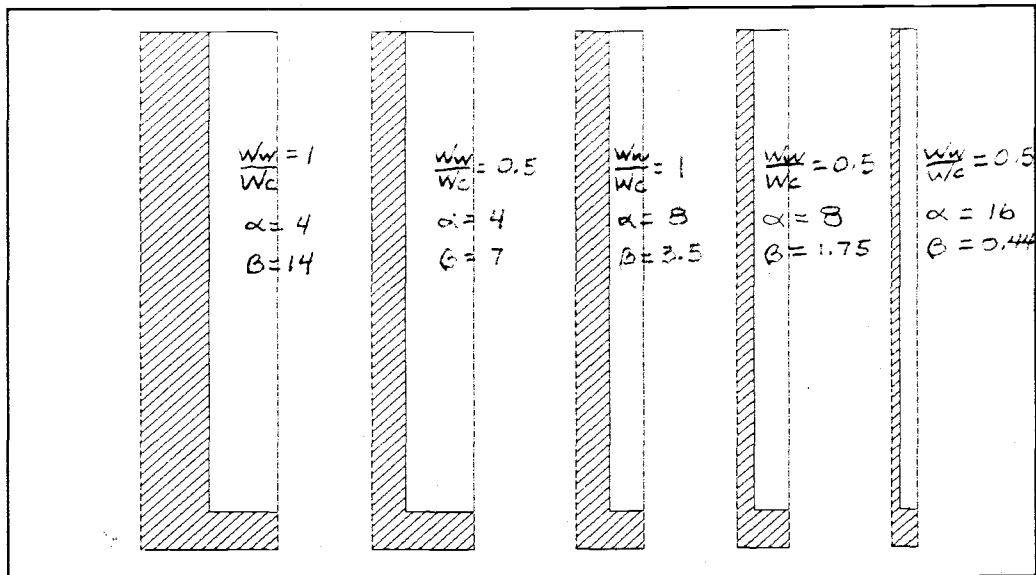


**Figure 1.10b**

Scale illustration of computational geometry to show how  $\beta$  varies with  $\alpha$  and  $W_w/W_c$ .

Landrum to portray with one variable all of the geometric parameters of the problem. Figure 1.10b presents a scale illustration of the computational geometry to show how  $\beta$  varies for different aspect ratios and different fin width to channel width ratios.

Figure 1.10c shows the nondimensional temperature  $y_0$  versus  $\beta$  for varying wall widths. Figure 1.10d shows this correlation for varying aspect ratios. Note that the integral analysis and the numerical cases compare better with smaller  $\beta$  which corresponds to larger aspect ratios and lower  $W_w/W_c$  values. This is reasonable because the integral analysis assumes no vertical variation of velocity which is better with higher aspect ratios. Also, it is interesting to note that both the integral analysis and numerical results predict the

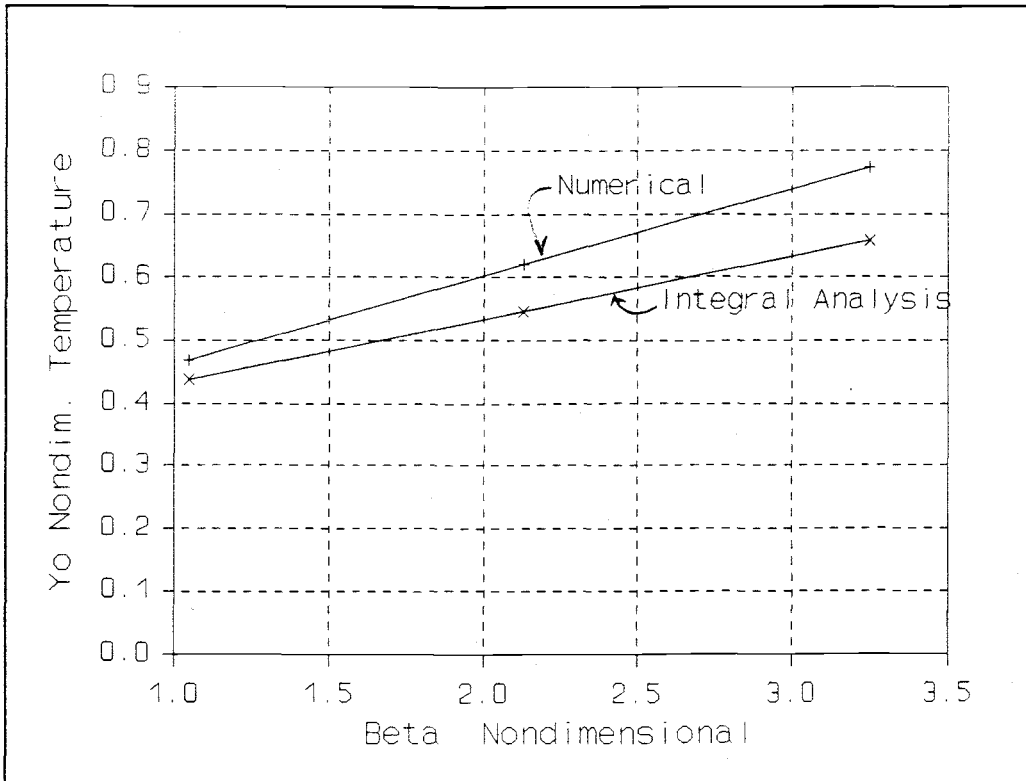


**Figure 1.10c**  
Nondimensional fin base temperature  $y_0$  vs.  $\beta$  for  $\alpha=10$ ,  $W_c=60 \mu\text{m}$  and  $W_w$  varies.

correspondence of  $y_0$  and  $\beta$  to be linear. The slopes are just slightly different due to the "crudeness" of the integral analysis.

### 1.10 THE OPTIMIZATION PROCEDURE

The optimization procedure for the microchannel heat sinks was derived from trends observed in the parametric study. For clarity, the trends are presented along with the optimization procedure. The intent of the optimization is to produce a design which has the minimum possible nondimensional peak substrate temperature  $\Omega$  defined by equation (1.9) for a given pressure drop

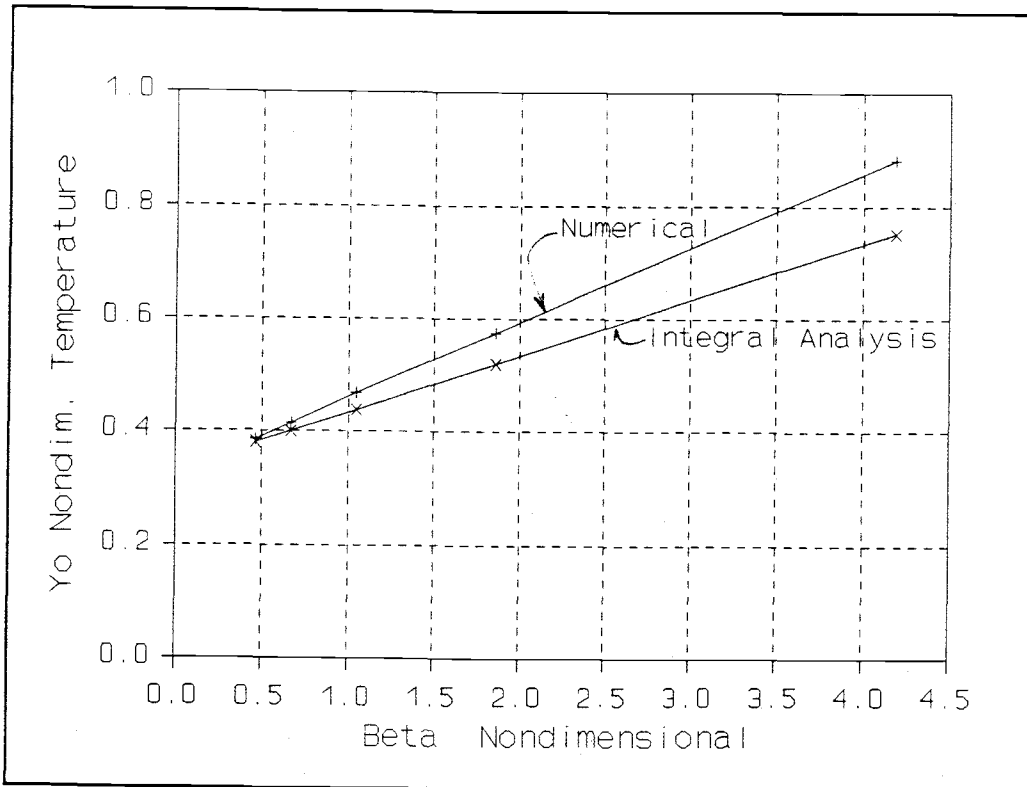


**Figure 1.10d**  
Nondimensional fin base temperature  $y_0$  vs.  $\beta$  for  $W_c=60 \mu\text{m}$ ,  $W_w=30 \mu\text{m}$  and varying  $\alpha$ .

across the heat sink.

(1.9)  $\Omega$  = Nondimensional Peak solid temperature  
(used to relate the different peak temperatures from different geometric cases)

$$= \frac{-(\text{flux across bottom in flow direction})}{(\text{incoming flux perpendicular to flow})}$$

$$= \frac{-k_w((T_{\text{inlet}}(0,0,t_g) - T_{\text{exit}}(L,0,t_g))/L)}{q''}$$

$\Omega$  is actually a nondimensional axial heat flux. However, since all quantities are constant in equation (1.9) except for the exit temperature, it can also be considered a nondimensional exit temperature.

#### 1.10.1 Preliminary Reynolds number Consideration (Fluid Mechanics Consideration)

The original investigation was performed at a constant Reynolds number of five hundred, which simulated the experimental conditions imposed by Tuckerman in section 1c) of the REVIEW OF LITERATURE section. See Appendix F, calculation 2, for the determination of the Reynolds number of five hundred for Tuckerman's sample.

The Reynolds number was held constant to produce a design which was optimized with respect to heat transfer for the one Reynolds number<sup>1</sup>. Then, the Reynolds number was varied and the same optimization was repeated at the various Reynolds numbers. Thus, the design with the minimal nondimensional peak solid temperature could be identified. This is discussed in 1.10. In this manner, optimization could be performed at each fluid mechanics situation separately, then the results from the different fluid mechanics situations could be compared to see which one was truly optimal. The end result is the overall optimized laminar microchannel geometry.

---

<sup>1</sup> If the Reynolds number (velocity) was increased with a fixed microchannel geometry, the temperature would decrease and the pressure drop would increase.

### 1.10.2 Pressure Drop Analysis (Channel Width Determination)

The first trend from the parametric study was suggested by scale analysis and verified computationally.

Consider the fully Developed Momentum equation:

$$(1.10) \quad \frac{\partial^2 u}{\partial y^2} + \frac{\partial^2 u}{\partial z^2} = \frac{1}{\mu} \frac{dP}{dx} \quad (\text{fully developed assumption})$$

Assuming that  $\partial y$  scales as  $W_c$  and  $\partial z$  scales as  $H$  and  $dP/dx$  scales as  $\Delta P/L$  and that the aspect ratio ( $\alpha$ ) is high ( $H \gg W_c$ ) yields the following scale analysis equation

$$(1.11) \quad \Delta P \sim \mu u L / W_c^2 \sim 1 / W_c^2.$$

Scale analysis predicts that the pressure drop will scale in inverse proportion to the square of the channel width. Therefore, it should be expected that the pressure drop is a strong function of channel width and a weak function of channel height. This is what the numerical results attest.

Figure 1.11 shows the relationship between pressure drop across a 1.4 centimeter long heat sink and channel width. Figure 1.11 is for constant Reynolds number which is consistent with the rest of the optimization procedure. The constant Reynolds number restriction tends to complicate interpretation since the average velocity and mass flowrate  $F$  are also changing with channel width. The general trend which is to be observed is the relationship between pressure drop through the heat sink and channel width. An easier result to interpret is if the total mass flowrate through a given width of heat sink (say for instance 1 cm) was

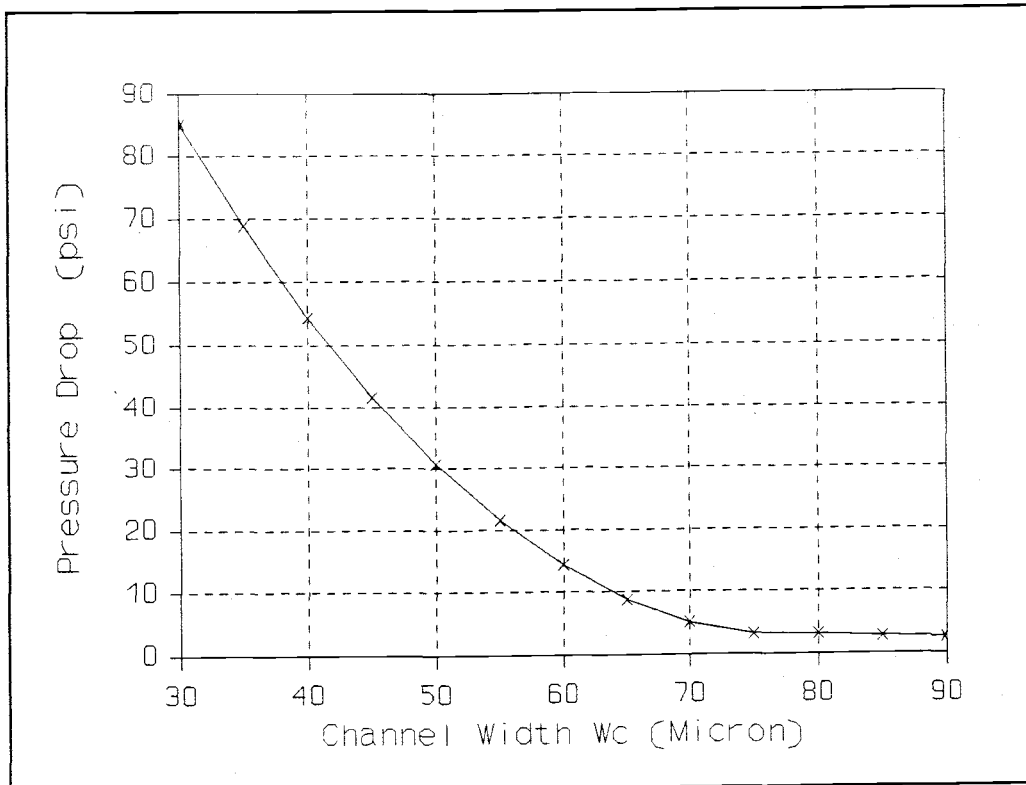


**Figure 1.11**

Pressure drop across a 1.4 cm heat sink versus channel width  $W_c$ , for  $\alpha=10$ ,  $W_w/W_c=0.5$  and  $Re=500$  (constant). The mass flowrate is varied.

held constant and the channel width was varied. This is done in Figure 1.12. Energy conservation suggests that the bulk fluid temperature at the exit of the heat sink is fixed. From either Figure 1.11 for constant Reynolds number or Figure 1.12 for constant mass flowrate through a given width of heat sink it can be observed that the pressure drop across a given length of heat sink increases greatly with decreasing channel width.

Scale analysis of equation 1.11 predicts the pressure drop across the heat sink to be a weak function of channel height (or aspect ratio  $\alpha$ ). This is displayed

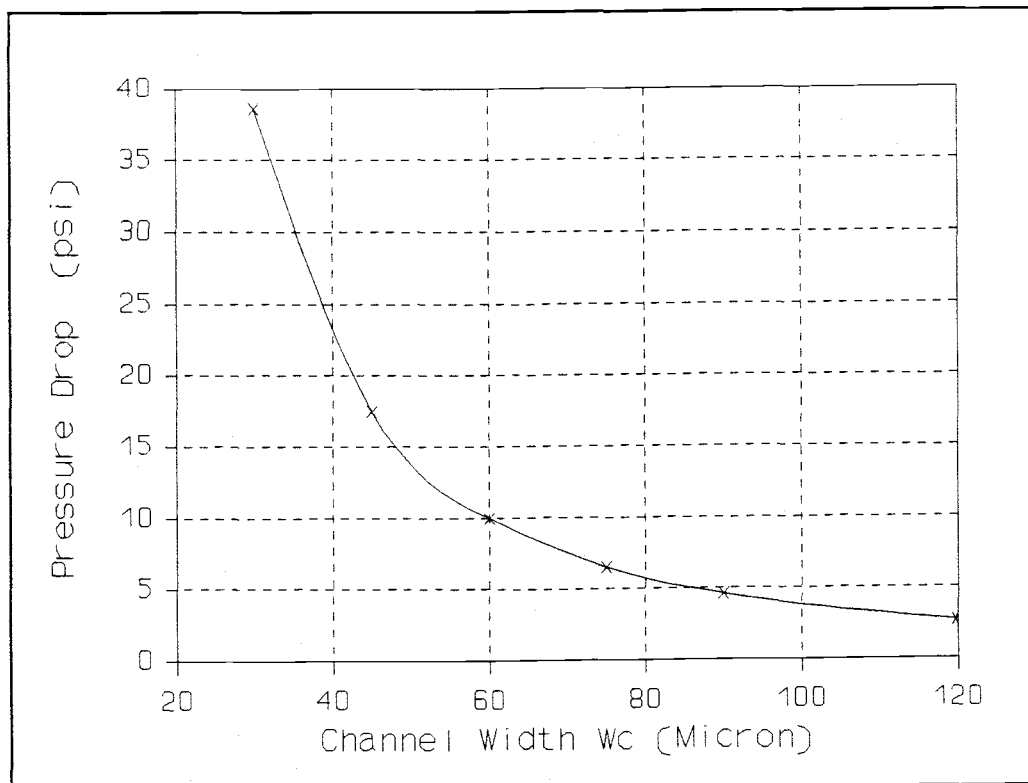


**Figure 1.12**

Pressure drop across a 1.4 cm long channel vs.  $W_c$  for a constant mass flowrate of .005 kg/s (constant),  $W=1$  cm,  $H=600$  micrometers.

in Figure 1.13 which indicates that the value of pressure drop invoked across the channel changes by only 17% when the aspect ratio is varied from 5 to 15. In comparison, Figure 1.11 indicates that the pressure drop changes by about a factor of 20 by changing the channel width from  $30 \mu\text{m}$  to  $90 \mu\text{m}$ . For this reason, the aspect ratio of the channels may be neglected for the purpose of obtaining the initial channel width.

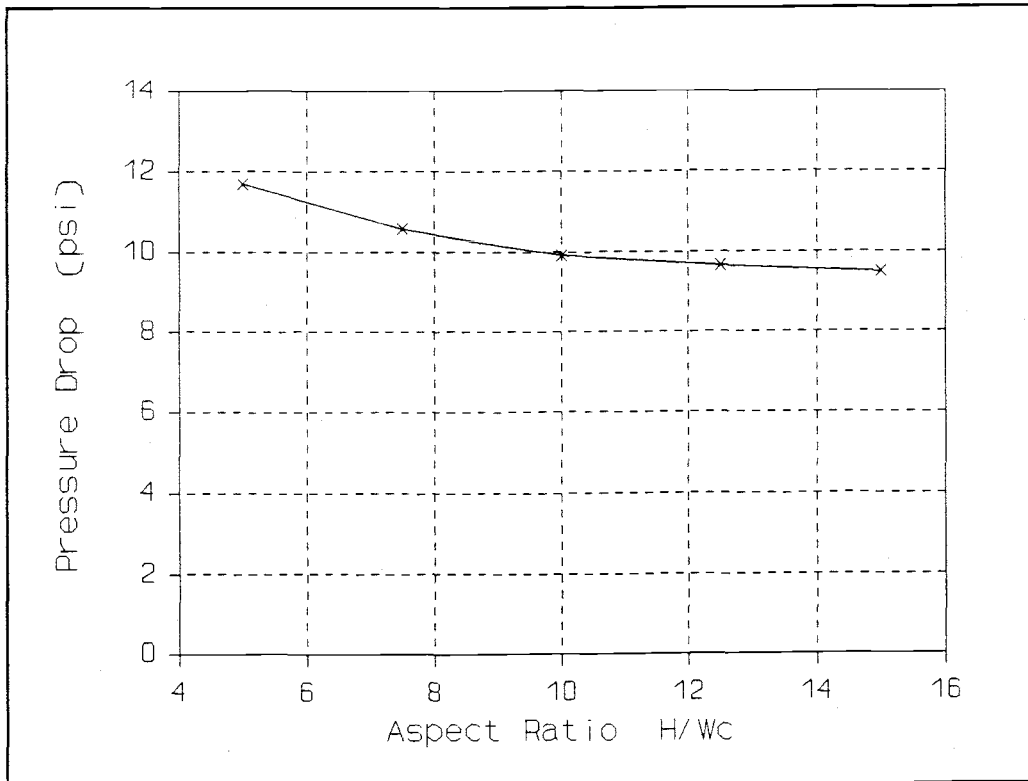


**Figure 1.13**  
Pressure drop across a 1.4 cm heat sink vs. aspect ratio  $\alpha$  for  $W_c=60 \mu\text{m}$ ,  $W_w=30 \mu\text{m}$  and  $Re=500$  (constant).

### 1.10.3 OPTIMIZATION STEP 1 Obtain Channel Width $W_c$

The above trends suggest that the first optimization step is to obtain the channel width,  $W_c$ . This will be for a fixed design Reynolds number and for a design pressure drop which is the primary design variable. This can be obtained by plotting a graph similar to Figure 1.11 and simply choosing the channel width which corresponds to the design pressure drop. An alternative method which is less accurate is to simply use the scale analysis of equation (1.11) to obtain an order of magnitude estimate of  $W_c$ . At this point, the

variation in pressure drop caused by different aspect ratio's,  $\alpha$ , can be neglected since both scale analysis and Figure 1.13 indicate that pressure drop is a weak function of channel height.

Because the pressure drop increases so dramatically with decreasing channel width, it may be advantageous to plot a graph similar to Figure 1.11 before deciding on the design pressure drop and then determining the channel width. For example, it can be seen from Figure 1.11 that the pressure drop curve levels off at about  $W_c = 60 \mu\text{m}$  which corresponds to about 15 psi drop across a 1.4 cm heat sink. If these conditions were acceptable from a design standpoint, this design would be recommended.

The final consideration in choosing the channel width is that from a heat transfer standpoint, it is advantageous to choose the smallest allowable channel width because there is a linear correspondence between channel width and nondimensional peak temperature. Figure 1.14 shows this relationship derived from the numerical methods. This is also predicted by the integral analysis.

To summarize the method of finding the channel width the steps will be listed: 1) Derive a relationship between pressure drop and channel width similar to Figure 1.11; 2) Decide on an acceptable pressure drop across the heat sink; 3) Choose the channel width which corresponds with this pressure drop. (Remember, it is desirable to choose the smallest channel width possible)

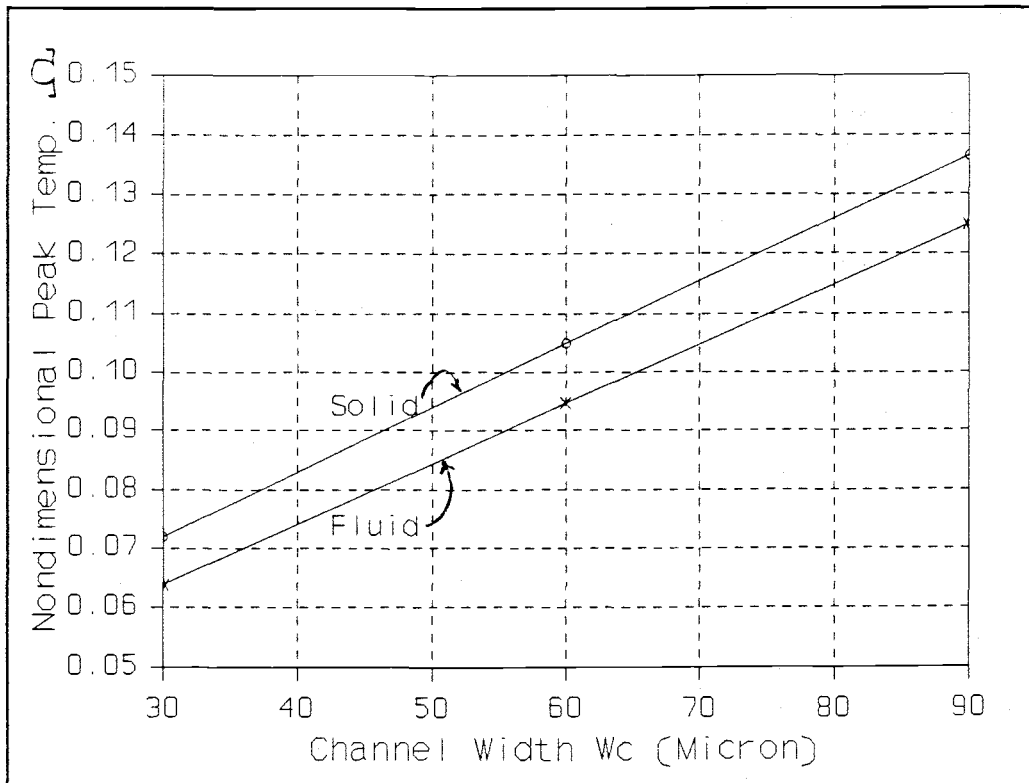


**Figure 1.14**  
Nondimensional temperature  $\Omega$  versus channel width for  $\alpha=10$ ,  $\beta=1$  and  $W_w/W_c=.5$ .

#### 1.10.4 OPTIMIZATION STEP 2 Find optimum $(W_w/W_c)_o$

It was found that the nondimensional peak temperature  $\Omega$  reached a minimum with  $W_w/W_c$ . For the channel width found in step 1, it is desired to determine the optimal fin width to channel width ratio  $(W_w/W_c)_o$ . The ratio  $W_w/W_c$  with the minimum nondimensional peak temperature will be called the optimized fin width to channel width ratio  $(W_w/W_c)_o$ . Similarly, the aspect ratio  $\alpha$  with the minimum

nondimensional peak temperature will be called the optimized aspect ratio  $\alpha_o$ .

A physical argument will be presented to support the statement that the nondimensional peak temperature  $\Omega$  reaches a minimum with  $W_w/W_c$ . Consider a fixed channel width  $W_c$  with a given heat flux across the bottom of the heat sink and varying fin widths. For very thin fin widths, it can be expected that the peak silicon temperature is high because the fin efficiency will be low. For very wide fins, there is more energy flow per microchannel. This is caused by a uniform base heat flux and essentially more base area for each microchannel caused by a larger value of  $\frac{1}{2}(W_w+W_c)$ . These microchannels have essentially the same heat transfer as the microchannels with slightly thinner fins because the solid conductivity is so high. (i.e. there is more than enough cross sectional conduction area) Thus, the peak silicon temperature would be expected to be high with very wide fins. It is expected that with a fin width between these two extremes better heat transfer performance can be found which yields a lower peak silicon temperature. Therefore an optimal fin width should exist.

Equation (1.12), which predicts the optimum  $(W_w/W_c)_o$  value as a function of the other fundamental design variables, was derived from the integral analysis of Dr. C. Landrum. [private communication]. The derivation is given in appendix D.

$$(1.12) \quad (W_w/W_c)_o = [(3\epsilon_1/\epsilon_3) + \epsilon_2]^{-\frac{1}{2}}$$

Where

$$\epsilon_1 = \frac{2(k_w/k)(q''L/k_w)}{\text{Re}(1 + \alpha_o) \text{Pr}} \quad ; \quad \epsilon_2 = \frac{51 k_w l}{140 k \alpha_o^2}$$

$$\epsilon_3 = q''H_o/k_w.$$

The numerical results predicted the relationship between nondimensional peak temperature and fin width to channel width ratio given in Figure 1.15. It can be seen from the curve that indeed a minimum does exist.

The numerical results agreed with Landrum's integral analysis. For a 60  $\mu\text{m}$  channel width and  $\alpha=10$ , the numerical results predicted the minimum peak temperature to occur at  $W_w/W_c=.7$ . Similarly, equation (1.12) from the integral analysis predicted the minimum peak temperature to occur at  $W_w/W_c=.7$ . This was very good correspondence and suggested that the approximations involved in the integral analysis "balanced out" for this parameter.

The value of  $\alpha=10$  is not the optimal aspect ratio so the value of  $W_w/W_c=.7$  is not optimal. It is, however, the value which yields minimum peak temperature for  $\alpha=10$ . Equation (1.12) states that  $(W_w/W_c)_o$  depends on  $\alpha$ . Thus, the optimal aspect ratio and optimal fin to channel width ratio are coupled and must be found concurrently by a trial and error procedure as outlined in section 1.10.6.

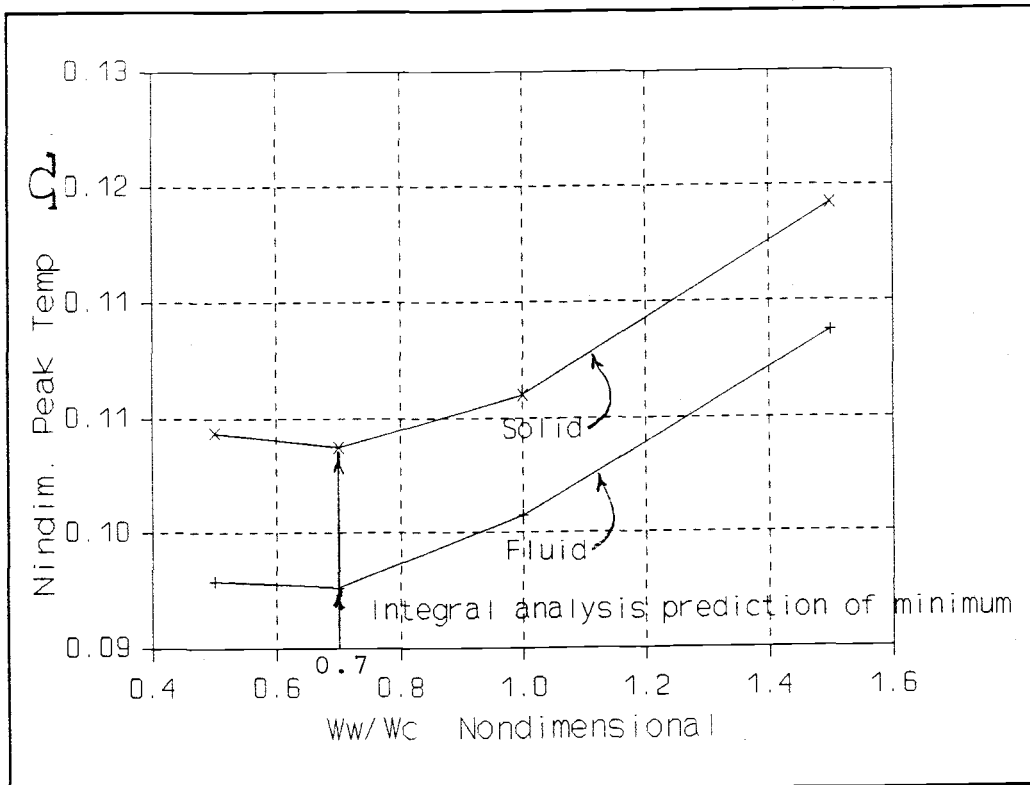


**Figure 1.15**  
Nondimensional peak temperature  $\Omega$  vs  $W_w/W_c$  for  $\alpha=10$  and  $Re=500$ .

### 1.10.5 OPTIMIZATION STEP 3 (find optimum aspect ratio $\alpha_o$ , and $H_o$ )

It was found that the nondimensional peak temperature,  $\Omega$ , reaches a minimum with channel width ratio,  $\alpha$ . For the channel width found in step 1, it was desired to determine the optimal aspect ratio. This was for a given Reynolds number and design pressure drop. Figure 1.10a suggests that this optimal aspect ratio is approximately 11.

A physical argument will be presented to support the statement that the nondimensional peak temperature,  $\Omega$ , reaches a minimum with  $\alpha$ . Consider a given fin width,

channel width and heat flux. If very short fins are used, the cooling effect is poor because there is inadequate fin face area. Increasing the fin height would increase the heat transfer and lower the peak silicon temperature. If very tall fins are used, the cooling effect is also poor because near the top, the temperature gradient between the fin and the coolant is small due to the fact that the fins don't conduct much heat to the top. Most of the energy would leave the fin near the bottom and middle. Therefore at an intermediate aspect ratio, better heat transfer performance is expected, which results in a lower peak silicon temperature. Hence an optimal aspect ratio should exist.

Equation (1.13), which predicts optimal aspect ratio as a function of the other nondimensional parameters of the solution, was derived from the integral analysis of Dr. C. Landrum [private communication].

(1.13)

$$\alpha_o^3 + 2\alpha_o^2 - \alpha_o (W_w/W_c)_o (k_w/k) \Gamma - (51/70) (k_w/k) (W_w/W_c)_o = 0$$

$$\text{Where } \Gamma = (51/140) + \frac{6(L/W_c)}{\text{Re Pr}}$$

The numerically derived results predicted the relationship between nondimensional peak solid temperature,  $\Omega$ , and aspect ratio shown in Figure 1.16. It is important to realize that the curve of Figure 1.16 is plotted for one value of  $W_w/W_c$  and that in general the fin width to channel width ratio affects the optimal aspect ratio. In this manner the optimal aspect ratio and the optimal fin width to channel width ratio are coupled and must be found concurrently by the trial and error procedure presented in section 1.10.6. This is a

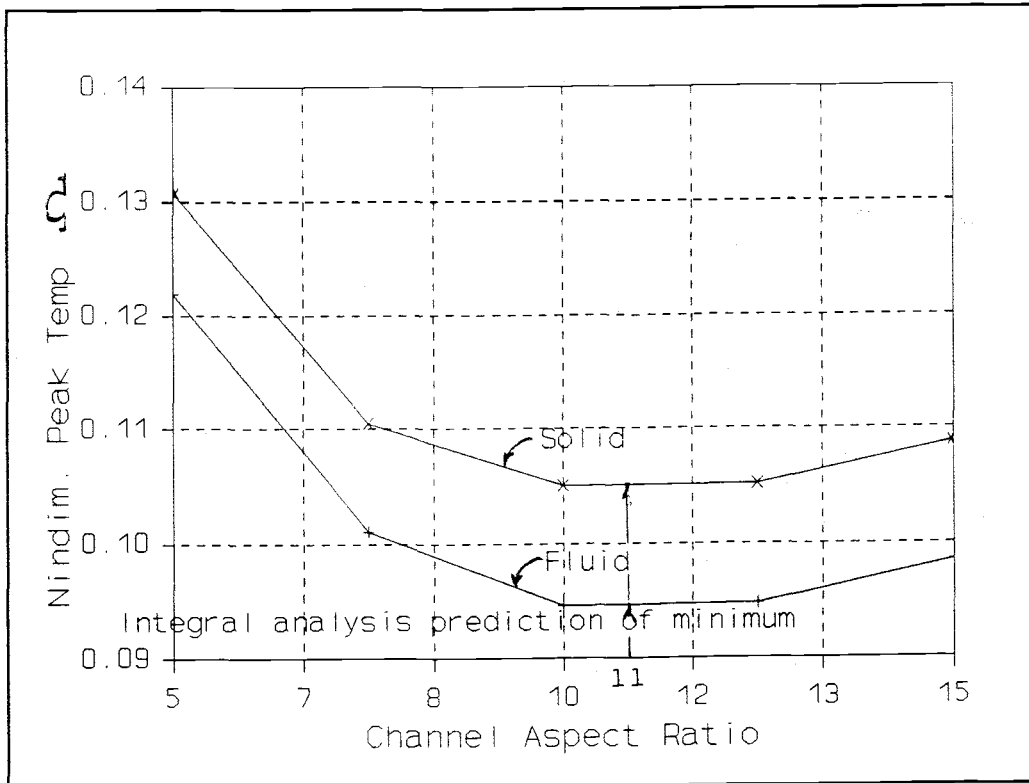


**Figure 1.16**  
Nondimensional peak temperature  $\Omega$  vs. aspect ratio  $\alpha$   
for  $W_w/W_c = 0.5$  and  $Re = 500$ .

consequence of the fact that both the aspect ratio and the fin width to channel width ratio are primary design variables.

#### 1.10.6 TRIAL AND ERROR METHOD TO FIND $\alpha_o$ and

$(W_w/W_c)_o$

Examining equations 1.8 and 1.9 it is evident that each equation contains, as an argument, the result of the other equation. It is clearly stated that the aspect ratio,  $\alpha$ , affects the curve of  $\Omega$  vs.  $W_w/W_c$  in Figure 1.15 and  $W_w/W_c$  affects the curve of  $\Omega$  vs.  $\alpha$  in Figure 1.16.

This suggests that a trial and error procedure must be employed to obtain the optimized solution for  $\alpha_0$  and  $(W_w/W_c)_0$ .

The effort to perform this trial and error procedure can be minimized by using the observation of this author that the optimized value of  $(W_w/W_c)_0$  is nearly unity for all cases of concern.

The procedure then is to first choose a value of  $(W_w/W_c)_0 = 1$  and use equation 1.9 to calculate the first approximation of  $\alpha_0$ . Then use this value of  $\alpha_0$  to calculate the second approximation of  $(W_w/W_c)_0$ . Then use this value to calculate the second approximation of  $\alpha_0$ . Continue this process until a satisfactory solution is obtained (i. e. The variables change very little from iteration to iteration). The result will be an optimized value of  $\alpha_0$  and  $(W_w/W_c)_0$  for the chosen Reynolds number and pressure drop. The Reynolds number restriction will later be removed by optimization with respect to the Reynolds number.

It is recommended to use equations (1.12) and (1.13) to obtain the optimized parameters. In order to verify that the geometry is optimal, plot curves similar to Figure 1.15 and Figure 1.16 by solving the problem numerically and determine the minima. This can be done with either the code by J. Lienau which assumes fully developed momentum and energy solutions, or by a code which considers the developing solution and even possibly variable properties. The key idea is that the fewer

assumptions the model has, the more accurate the solution will be.

#### 1.10.7 OPTIMIZATION STEP 4 (Substrate Thickness)

The substrate thickness,  $s$ , in Figure 1 has not been mentioned in the above optimization procedure because it should cause linear variation in temperature. That is, the temperature drop across the substrate is approximately equal to  $\Delta T_{\text{substrate}} \approx q''s/k_w$  which is linear with  $s$ . This is not exactly linear with  $s$  because slight differences in temperature occur between the substrate material under the fins and under the channels. This is due to about 3% of the heat being convected through the base of the channel. The criteria for the substrate thickness is determined by how uniform the base heat flux must be. Uniform heat flux causes uniform temperature along the base which is near the microelectronics. If extremely uniform temperature is desired, then it is recommended to use large substrate thicknesses. If uniformity is not important, then thinner substrates may be used. In this work substrate thicknesses of approximately  $100 \mu\text{m}$  were used for all of the computational investigations. The numerical cases suggest that if a substrate thickness of at least  $50 \mu\text{m}$  is used, the temperature variation will be less than  $0.01^\circ\text{C}$ . Substrates as small as  $20 \mu\text{m}$  may be used and still provide nearly uniform heat flux because of the extremely high conductivity of the silicon.

It is recommended to run the optimization procedure with a large value of substrate thickness ( $100 \mu\text{m}$  or greater), and examine the temperature profiles along the

width direction. Then decide which value of substrate thickness provides adequately uniform temperature across the base. This will be the substrate thickness to use.

### 1.11 REYNOLDS NUMBER OPTIMIZATION

The preceding optimization procedure has assumed a constant Reynolds number which in essence assumes a similar fluid mechanics situation between the different parametric cases. An optimization procedure has been developed in 1.10 which will produce the geometry for the minimum nondimensional peak solid temperature  $\Omega$  for a given Reynolds number. The objective now is to vary the Reynolds number and perform the preceding optimization at each Reynolds number and the same pressure drop across the heat sink. In this manner the effects of different fluid mechanics and heat transfer are separated. The final design is optimized with respect to both heat transfer and fluid mechanics.

It was originally speculated that the optimization would be reasonably insensitive to the Reynolds number over a moderate range. It was however, a matter which called for computational verification. The optimization procedure of 1.10 was performed for Reynolds numbers of 165, 500, 773, 1135 and 1820. A plot of optimized nondimensional peak solid temperature  $\Omega$  vs. Reynolds number was produced for a pressure drop across the heat sink of 9.4 psi. Figure 1.17 shows that a minimum  $\Omega$  is obtained with Reynolds number. It further shows the desirable feature that this minimum is quite insensitive to Reynolds number over the range from about 500 to 1000. In actual practice, Figure 1.17 may be

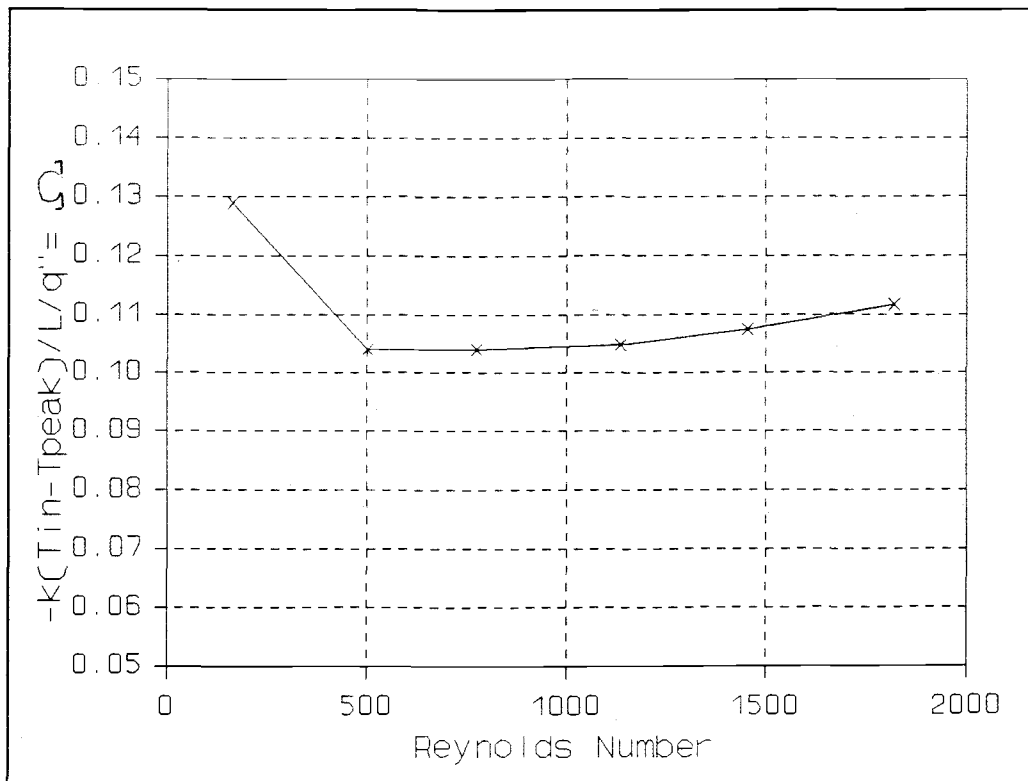


**Figure 1.17**  
Optimized nondimensional temperature  $\Omega$  vs. Reynolds number for a heat sink pressure drop of 9.4 psi.

affected slightly by different values of pressure drop across the heat sink. Due to the breadth of the Reynolds number "plateau" of Figure 1.17, it is recommended that Reynolds numbers between 500 and 1000 be considered optimal in the design of laminar microchannel heat sinks.

#### 1.12 CONCLUDING COMMENTS REGARDING THE STUDY

It was not the intent of this study to perform the optimization over a wide array of pressure drops. Rather, the approach has been to identify the general trends and provide the computational tools by which the

optimal geometry can be chosen given a certain set of constraints. The equations derived from Landrums integral analysis adequately predict the optimal geometry over the entire range of pressure drops of interest. If further verification of the optimization is desired, the numerical simulation may be consulted. For a very precise measure of the temperature distribution, it is recommended to use the numerical simulation. It is comforting that the integral analysis and numerical methods give similar results.

## CHAPTER 2 DEVELOPING LAMINAR MICROCHANNEL COOLING

## 2.1 INTRODUCTION

The initial work with "Heat Transfer Microstructures for Integrated Circuits" presented by Dr. D. Tuckerman [1] suggested that the optimal design may be modelled with the fully developed assumptions.

The validity of the assumptions of fully developed velocity and temperature profiles in laminar microchannel heat sinks were evaluated in this chapter. One approach involved using equations presented in the literature to predict thermal and hydrodynamic entry lengths. In a second approach the results of the two dimensional fully developed analysis were compared to computational analysis of the 3 dimensional developing profiles from the TEMPEST<sup>1</sup> computer code.

It is plausible that the velocity profiles within the microchannels of Figure 2 become fully developed near the beginning of the flow distance which means a small hydrodynamic entrance length. The temperature profiles do not lend themselves to such simple interpretation. From a knowledge of the Prandtl number of the fluid, it is expected that the thermal entry length is greater than the hydrodynamic entry length. These statements were investigated computationally.

The intent of this work is to obtain results concerning the microchannels which are applicable to the real life microchannel cooling problem. The simulation which is closest to the real life process involves the

---

<sup>1</sup> Developed by D. S. Trent and L. L. Eyler of Battelle Pacific Northwest Laboratories. For the Numerical Methods and Input instructions for this computer code see Reference [6].

developing problem considering variable fluid and solid properties. The assumption of constant fluid properties was investigated by considering variable fluid specific heat and thermal conductivity and comparing to the constant property case. The variable solid properties case was not investigated because the temperature variation of solid properties was considerably less than the temperature variation of the fluid properties. Finally, neglecting the temperature variation of solid properties was shown to produce a conservative estimate of the heat transfer in section 2.8.2 of this thesis.

## 2.2 MOTIVATION

The goal of this work was to determine whether the fully developed assumptions can be used to adequately determine the temperature and velocity distribution within the microchannels. The most important issue was to evaluate whether the peak solid temperature was being properly modelled by these assumptions over the range of geometric parameters of interest. If the fully developed assumption proved reliable over the range of parameters of interest in the optimization procedure, it may be suggested to use the fully developed solution for the optimization procedure. If not, the developing solution must be used for the optimization procedure.

Another source of motivation for this work was to gain insight into the behavior of the developing solution for investigation of the subcooled boiling problem.

## 2.3 PROBLEM DESCRIPTION

The three dimensional developing microchannel problem considered the entrance effects in the geometry of Figure 1. The 3 dimensional Navier-Stokes equations

and the energy equation as given in Appendix E were solved computationally with no simplifying assumptions.

The problem discretization for the three dimensional developing problem is essentially the same as the discretization described in 1.3 for the fully developed problem except that it had discretization in the third (axial) direction also. Figure 1.1 shows the two dimensional discretization which is essentially one tier of cells in the three dimensional description. All of the modelling assumptions and the ideas regarding symmetry in 1.3 apply to this problem also.

A discretization of 10 cells in the x direction was originally chosen. This was evaluated by running a simulation with 20 cells in the x direction and comparing the temperatures. The temperatures didn't change by more than 3% between the two simulations. The 10 celled discretization was used because it saved computational resources.

## 2.4 ESTIMATES OF ENTRY LENGTHS

The estimates presented in this section are by nature "crude" because they are derived from problems which are similar to the microchannel problem but which are not identical to the microchannel problem. This should be kept in mind when considering the results of this section.

### 2.4.1 Thermal Entry Length.

Following the analysis presented by Kays [16] for the thermal entry length solution for noncircular cross sections, Kays states that the temperature profile can be considered fully developed when  $x^+ = .1$ , where

$$(2.3) \quad x^+ = 2(x/D_h) \cdot \frac{1}{\text{Re}_{D_h} \text{Pr}}$$

These are the conditions of Tuckerman's experimental sample 81F9, page 81 of reference [1].  $D_{\text{hydr}} = 4A/P(\text{wetted}) \approx 100 \mu\text{m}$ ,  $u = 2.85 \text{ m/s}$ ,  $\text{Pr} = 4.3$  at  $60^\circ\text{C}$  and  $\text{Re} = 500$ . The thermal entry length was calculated as

$$2.3.a \quad X_{\text{thermal}} = .01075 \text{ m} \approx 1.08 \text{ cm}.$$

The thermal entrance effects are much more significant than the hydrodynamic entrance effects. Because the entry length may be the same order of magnitude as the length of the heat sink it is necessary to consider the developing solution. This was the initial observation which prompted the investigation presented in this chapter.

#### 2.4.2 Hydraulic Entrance Length.

Using the assumption of parallel plates and (as a first order approximation) the point when the boundary layers meet to define the entrance length, the similarity solution presented by Bejan [15] yields:

The boundary layer thickness  $\delta$  is

$$(2.1) \quad \delta/x = 4.92 \text{ Re}_x^{-1/2}.$$

Using a boundary layer thickness of  $W_c/2$  yields

$$(2.2) \quad X_{\text{entry}} = .0103 \text{ Re}_{W_c} W_c.$$

Using  $W_c = 60 \mu\text{m}$ ,  $U_o = 2.85 \text{ m/s}$ ,  $\nu = .663 \times 10^{-6} \text{ m}^2/\text{s}$

yields

$$2.2.a \quad X_{\text{entry}} = .016 \text{ cm}.$$

Using the core acceleration effects (see Bejan [15] pp. 69) yields

$$2.2.b \quad X_{\text{entry}} = .010 \text{ cm.}$$

Using Schlichting's matched series solution (see Bejan [15] pp. 70) yields

$$2.2.c \quad X_{\text{entry}} = .3 \text{ cm.}$$

All of the above methods of calculating the hydrodynamic entrance length (though they do not agree very well) suggested that it is small in relation to the 1-2 cm length of the heat sink. This suggested using the assumption of fully developed hydrodynamics as was done in chapter 1.

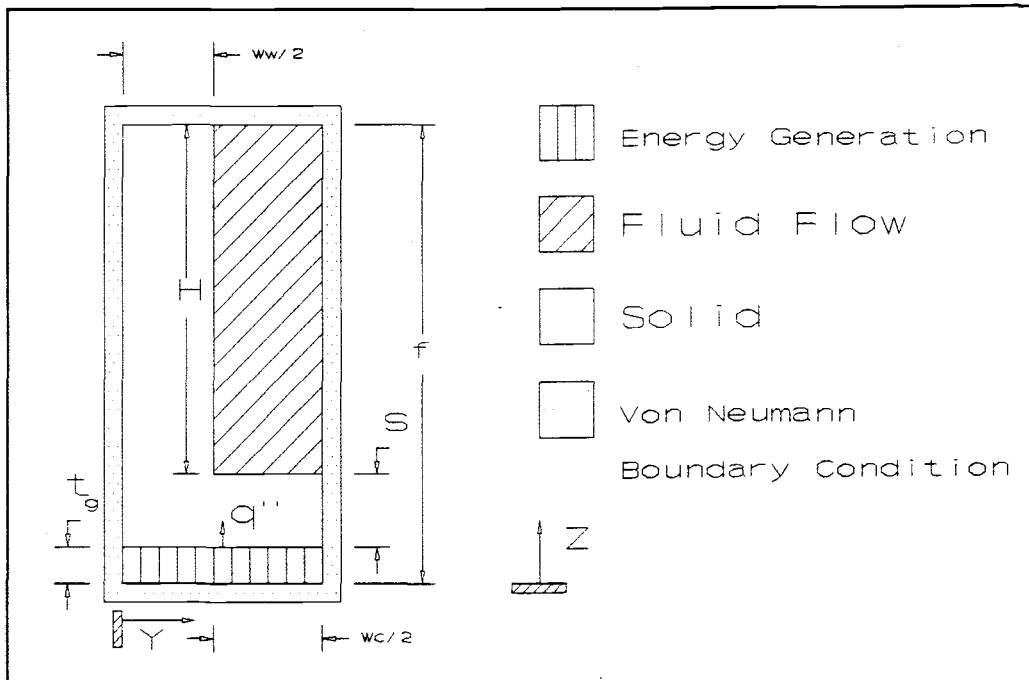


**Figure 2.1**  
y-z plane for 3 dimensional computational solution.  
The x direction runs perpendicular to the plane.

## 2.5 GOVERNING EQUATIONS

The governing equations are given for the fluid mechanics and for the convective and conductive heat transfer for the three regions identified in Figure 2.1. These equations are given in full form as they are found in Bejan [15].

### 2.5.1 Fluid Flow Region. Momentum Equations.

#### 2.5.1.1 X Momentum

$$(2.4a) \quad \rho \left( u \frac{\partial u}{\partial x} + v \frac{\partial u}{\partial y} + w \frac{\partial u}{\partial z} \right) = -\frac{\partial P}{\partial x} + \mu \left( \frac{\partial^2 u}{\partial x^2} + \frac{\partial^2 u}{\partial y^2} + \frac{\partial^2 u}{\partial z^2} \right)$$

Boundary Conditions:

$$u(W_w/2, z) = u(y, s) = u(y, f) = 0 \quad (\text{no slip})$$

$$\frac{\partial u}{\partial y} \left( \frac{1}{2}(W_w + W_c), z \right) = 0 \quad (\text{symmetry})$$

$$\left( \frac{1}{2}W_w \leq y \leq \frac{1}{2}(W_w + W_c) \right), \quad (s + t_g \leq z \leq f)$$

#### 2.5.1.2 Y Momentum

$$(2.4b) \quad \rho \left( u \frac{\partial v}{\partial x} + v \frac{\partial v}{\partial y} + w \frac{\partial v}{\partial z} \right) = -\frac{\partial P}{\partial y} + \mu \left( \frac{\partial^2 v}{\partial x^2} + \frac{\partial^2 v}{\partial y^2} + \frac{\partial^2 v}{\partial z^2} \right)$$

Boundary Conditions:

$$v(W_w/2, z) = v(y, s) = v(y, f) = 0 \quad (\text{no slip})$$

$$\frac{\partial v}{\partial y} \left( \frac{1}{2}(W_w + W_c), z \right) = 0 \quad (\text{symmetry})$$

$$\left( \frac{1}{2}W_w \leq y \leq \frac{1}{2}(W_w + W_c) \right), \quad (s + t_g \leq z \leq f)$$

## 2.5.1.3 Z Momentum

$$(2.4c) \quad \rho(u \frac{\partial w}{\partial x} + v \frac{\partial w}{\partial y} + w \frac{\partial w}{\partial z}) = -\frac{\partial P}{\partial z} + \mu(\frac{\partial^2 w}{\partial x^2} + \frac{\partial^2 w}{\partial y^2} + \frac{\partial^2 w}{\partial z^2}) + \rho g$$

Boundary Conditions:

$$w(W_w/2, z) = w(y, s) = w(y, f) = 0 \quad (\text{no slip})$$

$$\frac{\partial w}{\partial y}(\frac{1}{2}(W_w + W_c), z) = 0 \quad (\text{symmetry})$$

$$(\frac{1}{2}W_w \leq y \leq \frac{1}{2}(W_w + W_c)), \quad (s + t_g \leq z \leq f)$$

## 2.5.2.1 Energy Equation. Energy Generation Region.

$$(2.5) \quad \alpha_f(\frac{\partial^2 T}{\partial x^2} + \frac{\partial^2 T}{\partial y^2} + \frac{\partial^2 T}{\partial z^2}) = q'''$$

Boundary Conditions: Von Neumann

$$\frac{\partial T}{\partial y}(0, z) = \frac{\partial T}{\partial y}(\frac{1}{2}(W_w + W_c), z) = \frac{\partial T}{\partial z}(y, 0) = 0$$

$$(0 \leq y \leq \frac{1}{2}(W_w + W_c)), \quad (0 \leq z \leq t_g)$$

## 2.5.2.2 Energy Equation. Conduction Region.

$$(2.6) \quad \alpha_f(\frac{\partial^2 T}{\partial x^2} + \frac{\partial^2 T}{\partial y^2} + \frac{\partial^2 T}{\partial z^2}) = 0$$

Boundary Conditions: Von Neumann

$$\frac{\partial T}{\partial y}(0, z) = \frac{\partial T}{\partial y}(\frac{1}{2}(W_w + W_c), z) = \frac{\partial T}{\partial z}(y, f + t_g) = 0$$

$$(0 \leq y \leq \frac{1}{2}(W_w + W_c)), \quad (\text{for } y=0, \quad t_g \leq z \leq f + t_g)$$

$$(\text{for } y = \frac{1}{2}(W_w + W_c), \quad t_g \leq z \leq s + t_g)$$

## 2.5.2.3 Energy Equation. Fluid Flow Region.

$$(2.7) \quad \rho(u \frac{\partial T}{\partial x} + v \frac{\partial T}{\partial y} + w \frac{\partial T}{\partial z}) = \alpha_f (\frac{\partial^2 T}{\partial x^2} + \frac{\partial^2 T}{\partial y^2} + \frac{\partial^2 T}{\partial z^2})$$

Boundary Conditions: Von Neumann

$$\frac{\partial T}{\partial y}(\frac{1}{2}(W_w + W_c), z) = \frac{\partial T}{\partial z}(y, f + t_g) = 0$$

$$(\frac{1}{2}W_w \leq y \leq \frac{1}{2}(W_w + W_c)), (s + t_g \leq z \leq f + t_g)$$

## 2.6 VERIFICATION OF THE COMPUTER CODE

Dr. D. Trent suggested using TEMPEST for this problem. The code verification results for TEMPEST in reference [20] contain three examples similar to the microchannel problem. These problems are: a) flow within a square channel, b) channel flow with variable viscosity and c) combined free and forced convection pipe flow (Morton's Problem). The problem with flow in a square channel investigates developing velocity profiles and compares the computational results to experimental results. The channel flow problem investigates the velocity profiles considering temperature dependent fluid viscosity with a linear temperature profile. The results are compared to an analytical solution. The forced convection problem investigates the velocity profiles in a pipe with constant wall heat flux. The results are compared to an analytical solution. TEMPEST was observed to perform extremely well for these three problems which have similarities to the microchannel problem.

Another source of verification was derived from comparing the results from the two dimensional fully developed problem run by 2DREYN and the results from the three dimensional developing problem run by TEMPEST. In

general the temperature distributions at exit and the velocity distributions agree which lends verification to 2DREYN. The degree to which these distributions agree for varying geometry of the heat sink is the subject of this chapter and is a question of the physics of the problem.

## 2.7 RAMIFICATIONS OF THE FULLY DEVELOPED ASSUMPTION

### 2.7.1 Energy Equation.

The fully developed thermal assumption implies that the axial temperature gradient in equation (2.7),  $\partial T / \partial x$ , is equal to the bulk fluid temperature gradient  $dT_{\text{bulk}} / dx$ . In order to evaluate this assumption, it is necessary to calculate  $\partial T / \partial x$  at different locations in the fluid channel for the developing solution and compare this value to the bulk temperature gradient which is found by an energy balance.

Scale analysis and the fully developed assumptions are the only assumptions made to simplify the equation set of 2.4 to the equation set of 1.5. For the scale analysis developments see appendix F.

### 2.7.2 Momentum equation.

The fully developed momentum assumption implies that the velocity profile does not change in the axial direction. This means that all of the x derivatives in equation 2.4 vanish. The distance that fluid moves into the channel before reaching its' fully developed velocity is a measure of the verity of this assumption. The closer to the beginning that this occurs, the better the fully developed momentum assumption is.

## 2.8 FINDINGS REGARDING THE DEVELOPING SOLUTION

### 2.8.1 Temperature Comparisons for Constant Property Developing-Fully developed solutions.

The primary concern is whether the temperature distribution at the exit of the heat sink predicted by the fully developed solution adequately represents the temperature distribution predicted by the developing solution.

Figure 2.2 shows the fully developed and developing solutions for a microchannel with  $W_w/W_c = .7$ ,  $\alpha = 10$  and  $W_c = 60 \mu\text{m}$  for  $q_w'' = 1000 \text{ W/cm}^2$  and  $Re = 500$ . The

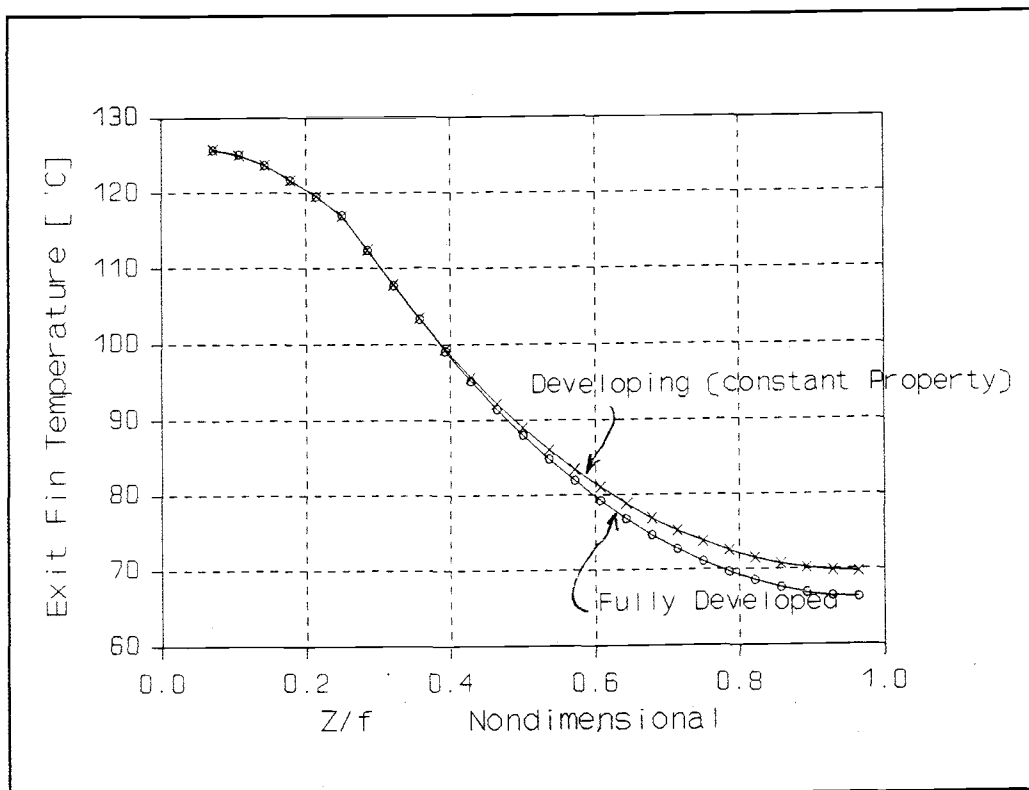
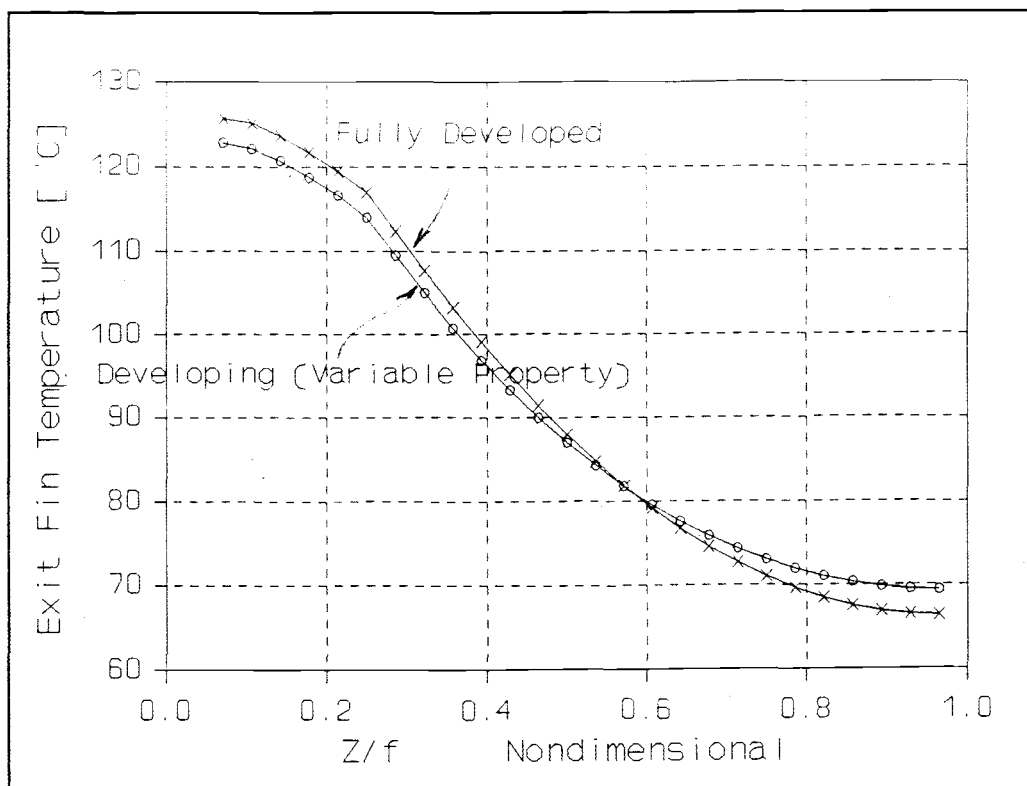


Figure 2.2  
Exit fin temperature profiles comparing fully developed and developing solutions for  $W_c = 60 \mu\text{m}$ ,  $\alpha = 10$  and  $W_w = 42 \mu\text{m}$ .

results are left dimensional to show the temperatures which are reached for an optimized case. The important result is that the two temperature distributions are nearly identical in the substrate and base of the fin and deviate by only 3°C near the top of the fin. This suggests that the fully developed assumption provides a good estimate of the peak temperature. The first value plotted is the peak solid temperature which is the value of the exit fin temperature at the smallest value of  $z/f$ .

#### 2.8.2 Temperature comparisons for variable properties, developing solutions.

Perhaps the most important result is whether the Fully Developed Assumption provides an adequate estimate of the actual fin and substrate temperature profile. The location which is most important is the base of the substrate because this is where the microelectronic elements are. The simulation most representative of the actual conditions is the developing, variable properties solution which considers variable fluid kinematic viscosity and thermal conductivity. The only assumption for this case is that the properties of the solid are constant. This assumption will be discussed briefly here. From reference [17], the thermal conductivity of intrinsic silicon is seen to increase with decreasing temperature below 100°C. Thus at the inlet of the heat sink where the silicon is cooler, the thermal conductivity would be higher which would cause better conduction and essentially decrease the entry length. Thus, assuming constant solid conductivity evaluated at an average temperature tends to provide a conservative estimate and is therefore desirable.



**Figure 2.3**

Exit fin temperature profiles for fully developed constant properties vs. developing variable properties comparison.

Figure 2.3 compares the fully developed, constant properties fin temperature solution to the developing, variable properties solution. The effect of variable properties is to decrease the temperature in the silicon substrate region and near the base of the fin. This is desirable because it indicates that using constant fluid properties provides a conservative estimate. This is favorable because it builds in an automatic margin of safety in the substrate near the microelectronics where the temperature is most critical. Figure 2.3 also reveals that near the top of the fin, the fully developed assumption underestimates the temperature by 3°. The

temperatures at the top of the fin are of less concern since they are farthest away from the microelectronics.

Another interesting comparison is the temperature distribution up the centerline of the channel which is given in Figure 2.4. The constant properties case is again conservative with higher substrate temperature than the variable properties case. A slight increase in temperature at the top of the channel can be clearly seen because of the effect discussed in section 1.8.2.

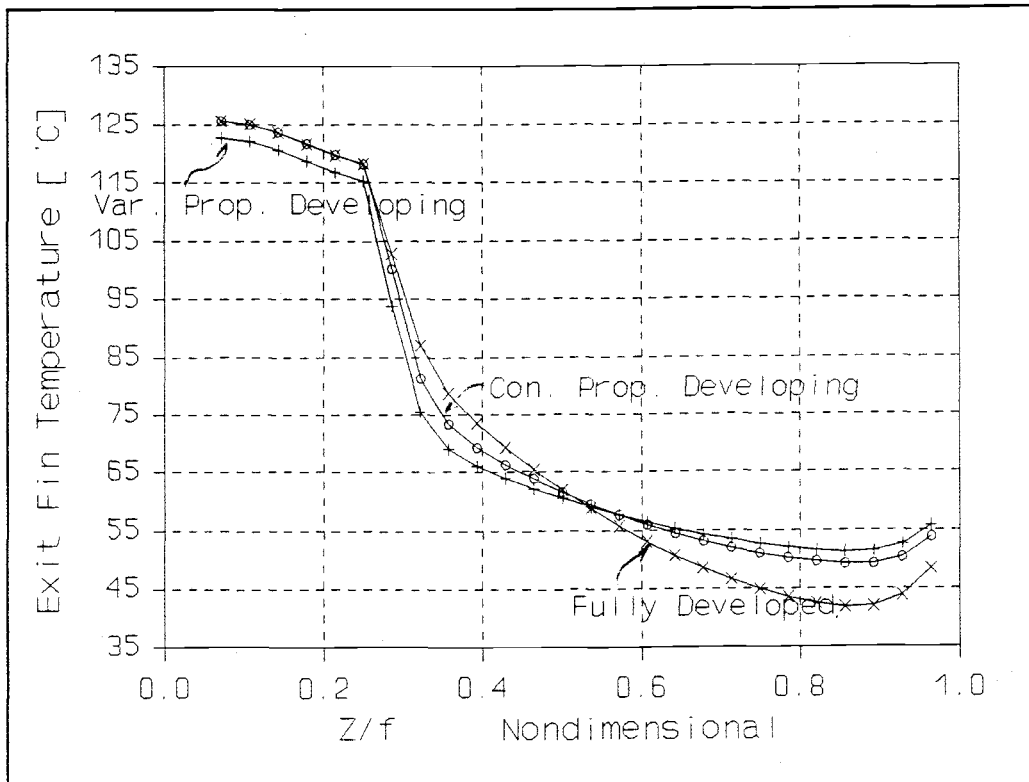


**Figure 2.4**  
Exit channel temperature profiles comparing fully developed and developing, constant and variable properties solutions. Geometry same as Figure 2.2.

### 2.8.3 Variable-Constant Property Velocity Comparison.

In general variable fluid properties cause the velocity to depart considerably from the constant property case. This is because the fluid viscosity is such a strong function of temperature. Figure 2.5 shows the x component of the nondimensional velocity profiles

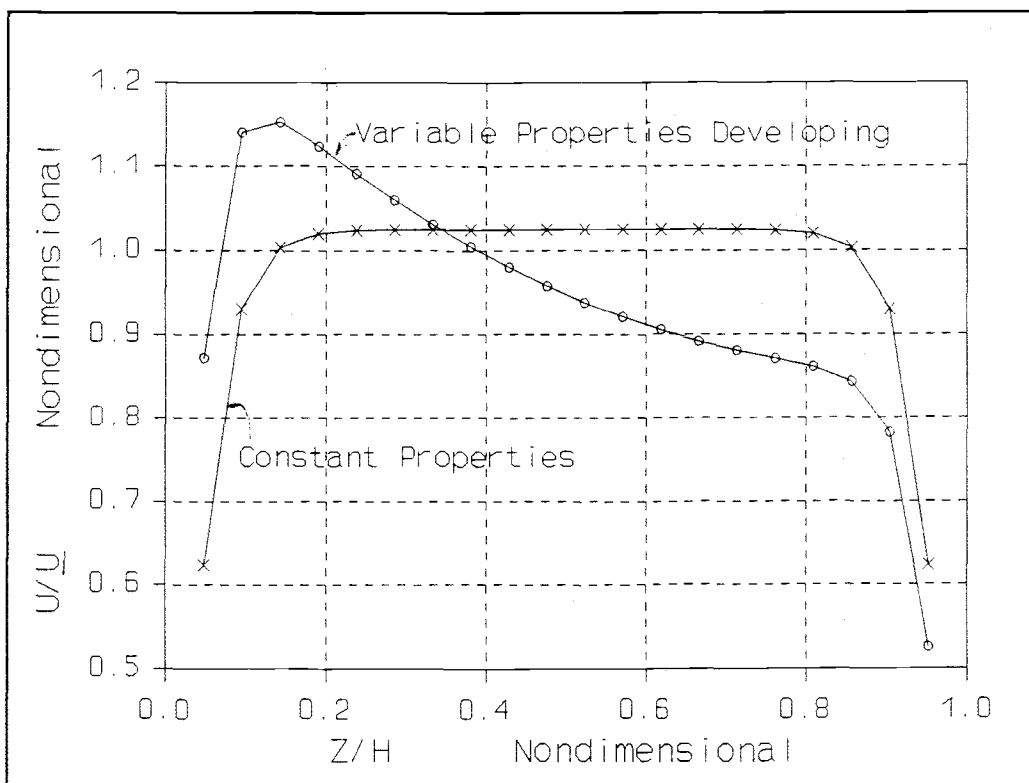


**Figure 2.5**  
Nondimensional velocity Profile  $u/\bar{u}$  plotted vertically for variable and constant properties.

plotted as a function of vertical distance up the channel centerline for both constant and variable viscosity at the exit to the microchannel. The behavior in Figure 2.5 is expected from the temperature distribution. At the bottom of the microchannel the fluid is at a higher temperature which means the viscosity is lower and the velocity is expected to be higher with the same pressure gradient. Similarly, at the top of the microchannel the fluid is cooler, has a higher viscosity and the velocity is expected to be lower.

Variable properties cause the velocity profile to develop more slowly. Figure 2.6 shows the nondimensional velocity profiles in the flow direction for cases with

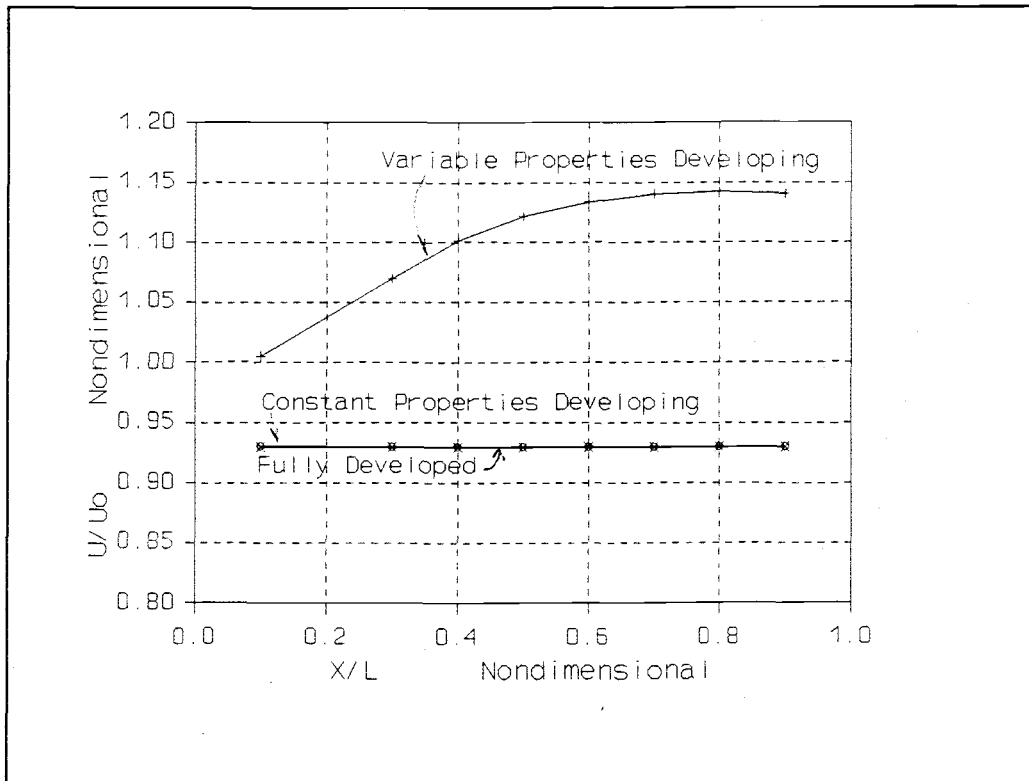


**Figure 2.6**  
Nondimensional velocity profiles in the flow direction. This plot is for a cell near the bottom centerline at  $Z_0/H=0.1$ .

constant and variable properties for a cell near the bottom of the channel at  $z/H=0.1$ . The value of these axial profiles at exit was indicated by the second point ( $z/H=.1$ ) in the vertically plotted exit nondimensional velocity profile of Figure 2.5. Also contained on the graph is the velocity predicted by assuming constant properties fully developed behavior and developing behavior. The constant properties developing and fully developed velocities agree within 97% in the first computational cell in the flow direction so the curves essentially lay right on top of each other. From this observation and from similar observations in every microchannel geometry considered, it can be stated that for constant properties solutions the fully developed momentum assumption is justified.

The variable properties solution takes nearly 80% of the flow distance to reach its' fully developed value. This is also justified physically. Near the entrance of the microchannel, the fluid is cool and at nearly uniform temperature. As it progresses along, the temperature increases and the viscosity decreases which allows it to move faster.

The result of variable fluid properties is that the base temperature is lowered as shown in Figure 2.3 and Figure 2.4. Because differences are not large and because using the constant properties solution provides an automatic margin of safety by overpredicting the peak temperature, the use of constant properties seems desirable.

#### 2.8.4 Wall-Bulk Fluid Temperature Gradient Comparisons.

As discussed in 2.7, the temperature solution

becomes fully developed when the axial temperature gradient becomes equal to the bulk temperature gradient. The bulk temperature gradient is constant along the flow distance and is found by a simple energy balance. To solve the fully developed problem, the bulk temperature gradient is substituted everywhere throughout the region for the partial derivative of temperature ( $\partial T/\partial x$ ) as in equation (1.4).

In order to evaluate the accuracy of using the fully developed assumption,  $\partial T/\partial x$  is compared throughout the region to  $dT_{\text{bulk}}/dx$ . The thermal behavior is considered fully developed when  $\partial T/\partial x$  and  $dT_{\text{bulk}}/dx$  agree within 20%. Determining fully developed behavior is more involved than at first appears because at every point within the fin, substrate and channel this comparison could be made. Also, the behavior is very dependent upon the geometric parameters of the solution. Therefore many different comparisons were made for different points within the cross section and for different geometric parameters. For reasons of brevity, the information will be presented in condensed form. Two different examples of the graphical temperature gradient comparisons will be presented. The rest of the information will be summarized.

Figure 2.7 is a graph of fin base temperature gradient and bulk fluid temperature gradient in the axial direction for a microchannel with a small aspect ratio ( $\alpha=5$ ), a large fin to channel width ratio ( $W_w/W_c=1$ ,  $\beta=8.5$ ),  $q''=1000 \text{ W/cm}^2$  and  $Re=500$ . The bulk temperature gradient and 120% of the bulk temperature gradient are plotted to help show where fully developed behavior begins. Four other plots similar to Figure 2.7 for

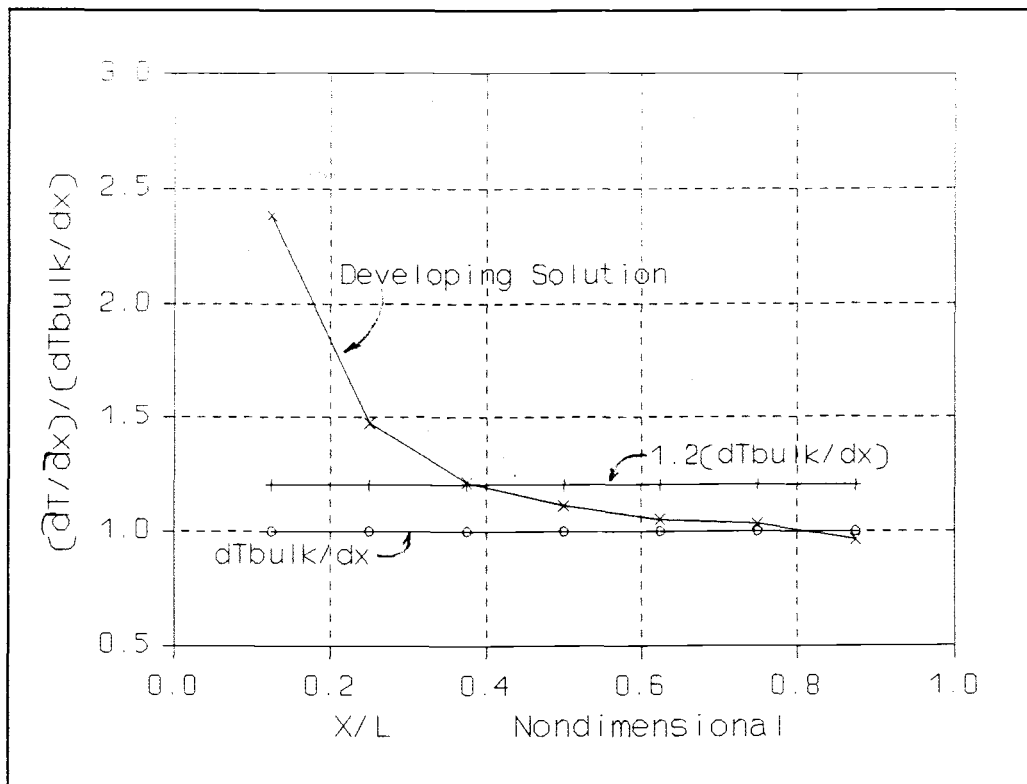


**Figure 2.7**

Nondimensional fin base temperature gradient, bulk temperature gradient and 120% of the bulk temperature gradient in the flow direction for  $\alpha=5$ ,  $W_w/W_c=1$ ,  $\beta=8.5$ .

different points up the fin and four plots up the channel centerline were prepared and show very similar behavior. These are included in the summary of Figure 2.9. The plots near the middle of the fin show better agreement to fully developed behavior than those at the extremes. Because of agreement between the axial and bulk temperature gradients, the fully developed energy assumption is justified for this microchannel geometry which involves a small aspect ratio and a large fin to channel width ratio.

Figure 2.8 is a plot of the fin base temperature gradient and the bulk fluid temperature gradient for a microchannel with a large aspect ratio  $\alpha=15$  and a very

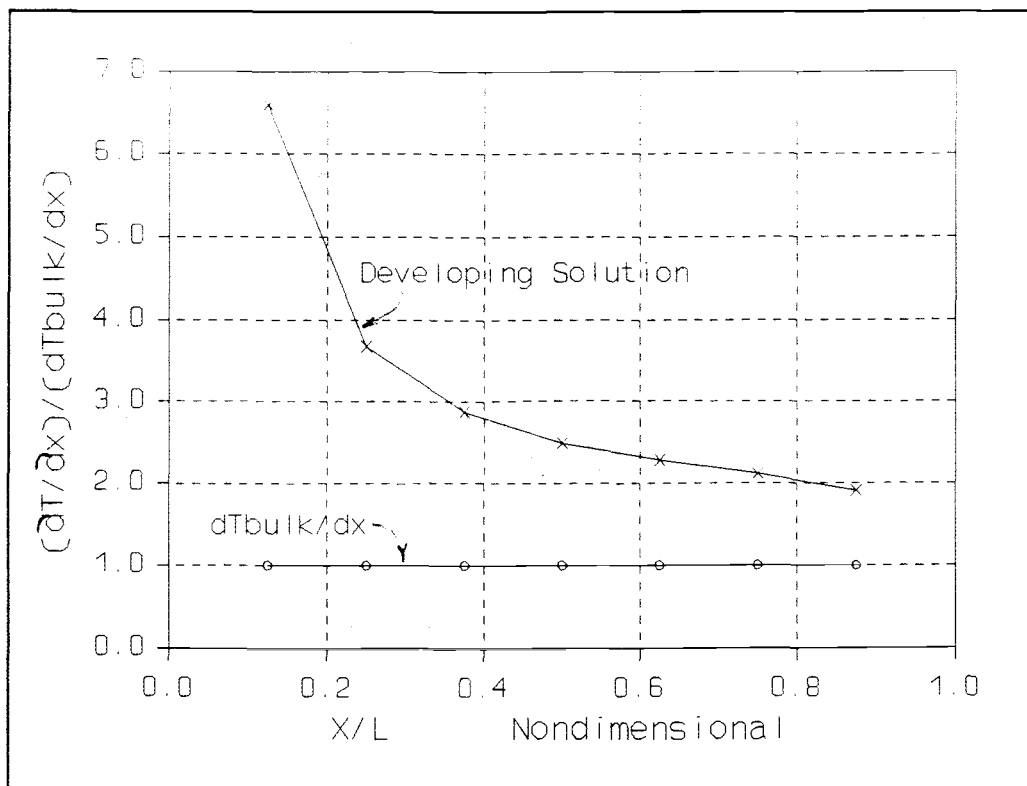


**Figure 2.8**  
Nondimensional fin base temperature gradient in the axial direction for  $\alpha=15$ ,  $W_w/W_c=.25$  and  $\beta=.19$ .

small fin width to channel width ratio ( $W_w/W_c=.25$ ,  $\beta=.19$ ). It can immediately be seen from this plot that the fin base temperature gradient is much steeper than the bulk temperature gradient throughout the entire flow length. Therefore the fully developed energy assumption does not apply in this case and would lead to erroneous results.

The two cases which have been chosen are extreme cases ( $\beta=.19$  and  $\beta=8.5$ ) to exemplify the trend. Figure 2.7 shows that the temperature gradient reaches the fully developed value at about 40% of the flow distance. The temperature gradient of Figure 2.8 does not reach fully developed behavior in the flow distance.

The percentage of the total flow distance where fully developed behavior begins is what is most interesting from all of the plots. A graphical summary of this percentage has been prepared which uses the natural logarithm of  $\beta$  to represent the geometric aspect of the solution. Along the abscissa is the percentage of the flow distance required for the axial temperature gradient and bulk temperature to agree within 20%. This is labeled  $100*(x(\text{thermal})/L)$  where  $x(\text{thermal})$  is the thermal entry length. Plots are presented for four different values of height up the fin. The summary of Figure 2.9 is for the temperature profiles plotted down the centerline of the fin. The method used to obtain the percentages is quite crude as is shown by Figure 2.7. Exponential functions are fit to the data to show the general trend. It is expected that the uncertainty is approximately 10% for these values.

Figure 2.9 reveals that the fully developed assumption is in general better for larger values of Beta than for smaller values of Beta. The smaller values of Beta correspond to large aspect ratio channels ( $\sim 15$ ) and very small fin to channel width ratios ( $\sim .25$ ). Thus, in general it can be stated that the fully developed assumption is better for small aspect ratio, large fin width to channel width ratio microchannels than for large aspect ratio, small fin width to channel width ratio microchannels.

A similar plot has been prepared for different points up the channel centerline in Figure 2.10. The fully developed assumption is much better at  $z_0/H=.33$  than at the top or bottom because at this value of height, the fluid temperature is nearly equal to the bulk

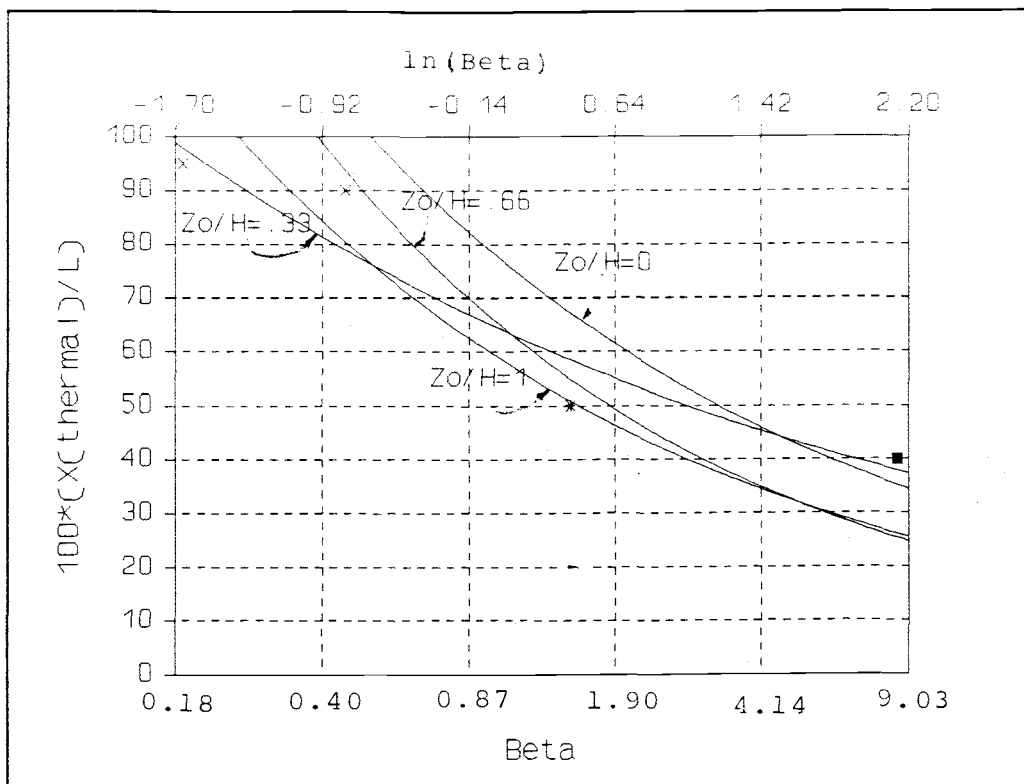


**Figure 2.9**

Summary of the comparison between the wall and bulk fluid temperature gradient showing  $x(\text{thermal})$  as % of flow distance ( $L$ ).

fluid temperature. The important result is that the fully developed assumption is again better for larger values of beta than for smaller values.

2.8.5 Comparison of Heat Flux values between Fully Developed and Developing solutions.

The heat flux into the fluid does not compare well when considering the results from the fully developed and developing solutions. Figure 2.11 is a graph of the ratio of heat flux off the face of the fin to heat flux through the base of the heat sink for an optimized  $60 \mu\text{m}$  channel width. ( $\alpha=11.8$ ,  $W_w/W_c=1$  and  $\beta=1.6$ ). The heat

flux was calculated by considering the negative of the temperature gradient in the fluid times the fluid conductivity. The fully developed heat flux is nearly uniform along the height of the fin and the developing heat flux is higher near the bottom and lower near the top. The important result is that the fully developed solution does not adequately determine the actual heat flux off the fin at the exit plane.

The small value of the ratio of heat flux off the face of the fin to heat flux through the base in Figure 2.11 is due to the large surface area amplification factor  $\sigma$  of the heat sinks.

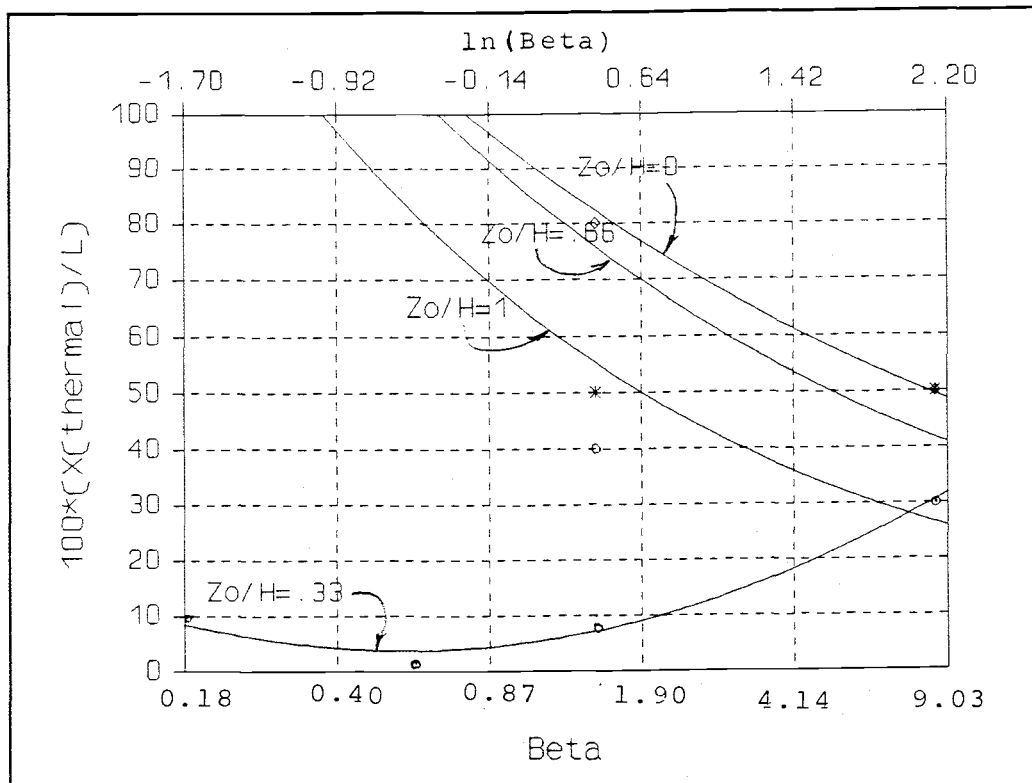


**Figure 2.10**  
Graphical summary of the comparison between fluid and bulk fluid temperature gradients similar to Figure 2.9.

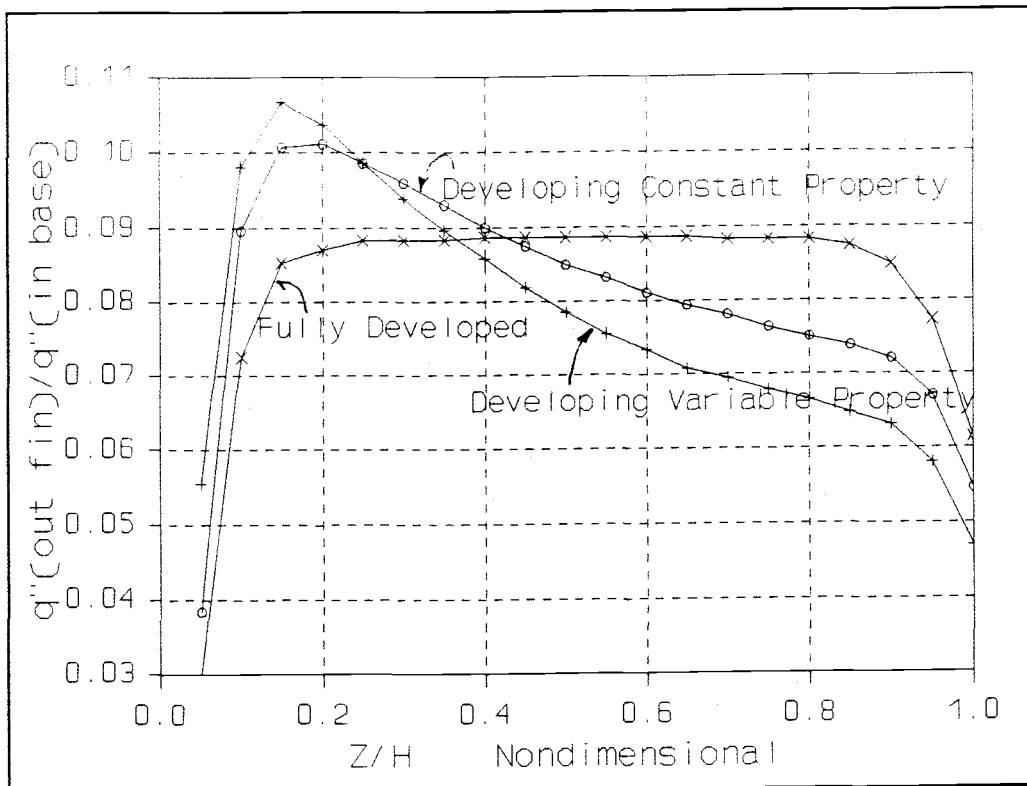


Figure 2.11

Heat flux off the face of the fin versus  $z$  for the fully developed, constant and variable properties developing solutions.  $\{\alpha=11.8, W_w/W_c=1, W_c=60 [\mu\text{m}], \beta=1.6, \text{Re}=500\}$

This is why the microchannels are such effective cooling devices.

The heat flux profile slowly approaches the fully developed value in the axial direction but does not come close to reaching it in the length of microchannels. Figure 2.12 is a profile of the constant property heat flux in the axial direction at the base of the fin for the geometry of Figure 2.11. The important result is that the heat flux does not approach the fully developed value in the channel lengths which are representative.

From the above findings, it is not recommended to assume fully developed behavior for obtaining heat flux

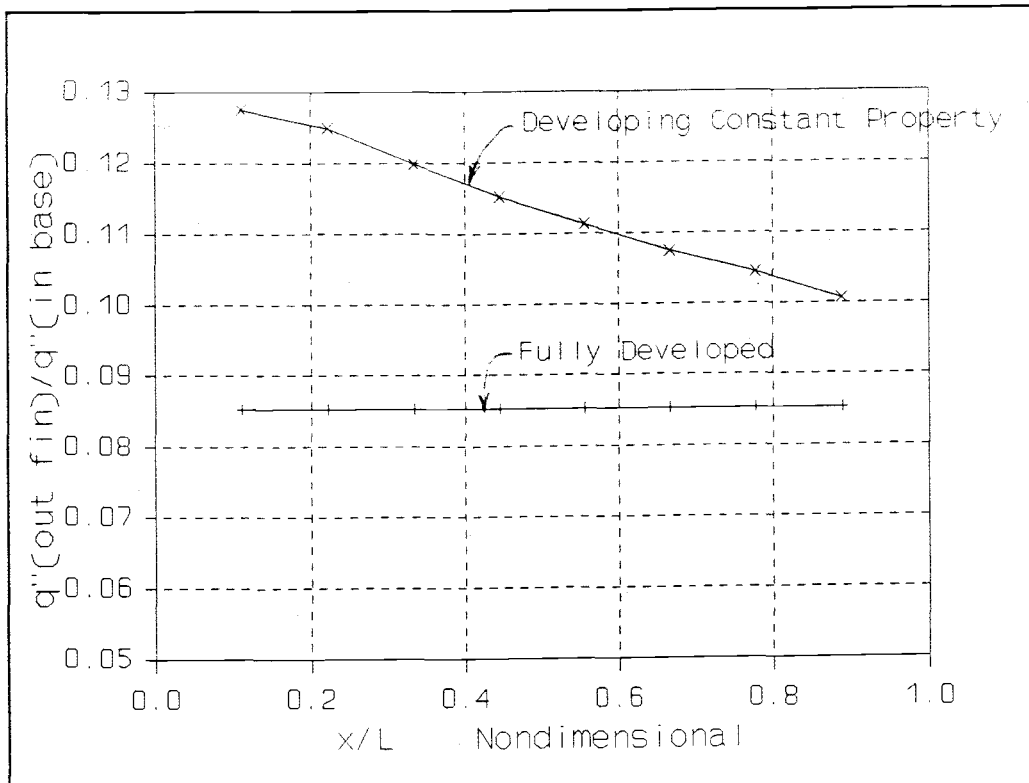


**Figure 2.12**

Nondimensional heat flux near the base of the fin vs. axial distance. Also shown is the fully developed value. ( $\alpha=11.8$ ,  $W_w/W_c=1$ ,  $W_c=60 \mu\text{m}$ ,  $\beta=1.6$  and  $Re=600$ )

values in the microchannels. The heat flux is important when considering subcooled boiling within the microchannels. For this reason, it is recommended to consider variable properties developing solutions when solving the subcooled boiling problem.

#### 2.8.6 Nondimensional Fluid Temperature Profiles.

Nondimensional fluid temperature profiles have been used by Kays [16] to analyze developing-fully developed behavior. Kays considered fluid flowing in a pipe with a heated wall (either uniform heat flux or isothermal).

Kays stated that the energy solution is fully developed when the nondimensional fluid temperature does not change in the flow direction. A similar analysis has been prepared for the microchannels. The main difference between the microchannel problem and Kays pipe problem is that when fully developed conditions are met, Kays pipe problem is one dimensional (a function of radial distance only) whereas the microchannel problem is truly two dimensional (a function of  $y$  and  $z$ ). Kays uses the bulk fluid temperature to calculate his nondimensional fluid temperature  $\phi$ . Because of the two dimensionality of the microchannel problem, a special local average temperature  $\theta_c(x, z_0)$  is defined which is a velocity averaged temperature at a certain value of height  $z_0$ . This is used in place of the bulk temperature to calculate the nondimensional fluid temperature  $\phi$ . In the fully developed regime, this causes every value of  $z_0$  to have only horizontal ( $y$ ) nondimensional fluid temperature variation. This allows an argument similar to Kays fully developed argument.

Figure 2.13 is a plot of nondimensional fluid temperature  $\phi$  in the axial direction<sup>1</sup> near the bottom of the channel next to the wall, at the centerline of the channel and half way between the wall and channel centerline. (i.e.  $y \approx \frac{1}{2}W_w$ ,  $\frac{1}{2}(W_w + W_c)$  and  $\frac{1}{2}(W_w + \frac{1}{2}W_c)$  corresponding to  $y_c = .05$ ,  $.5$  and  $1$  respectively) The thermal entry lengths at the three different locations

---

<sup>1</sup> The geometry of this microchannel is  $\alpha=10$ ,  $\beta=1.5$ ,  $W_c=60$  [ $\mu\text{m}$ ] and  $W_w/W_c=0.7$ . The plot is for  $z/H=0.1$ .

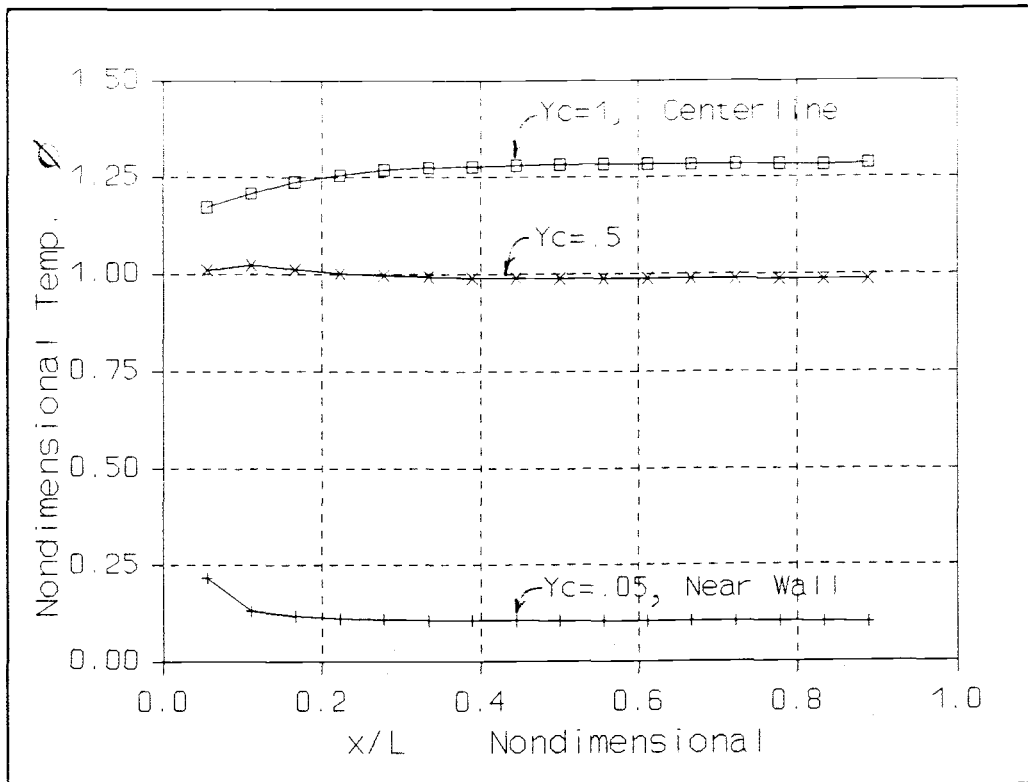


**Figure 2.13**  
 Nondimensional temperature,  $\phi$  vs.  $x/L$  for  $z_0/H=0.1$  at the centerline, wall and half way between wall and  $\phi$ , across the channel can be clearly seen. As expected, the entry length is longest near the channel centerline because it is furthest away from the heating of the fin. The centerline profile takes approximately 40% of the flow distance to develop. This is very similar to the result found by considering the dimensional temperature gradient. The nondimensional fluid temperature profiles more readily show the thermal entry length than the dimensional temperature profiles.

Figure 2.14 represents the argument presented by Kays concerning only radial variation of nondimensional fluid temperature in fully developed conditions.  $\phi$  is plotted near the bottom centerline and at four different axial positions. The curve at the first axial position,

$x/L=.125$ , is different from the other three. All other axial positions have nearly the same profiles. Thus, fully developed behavior is exhibited beyond  $x/L=.375$ .

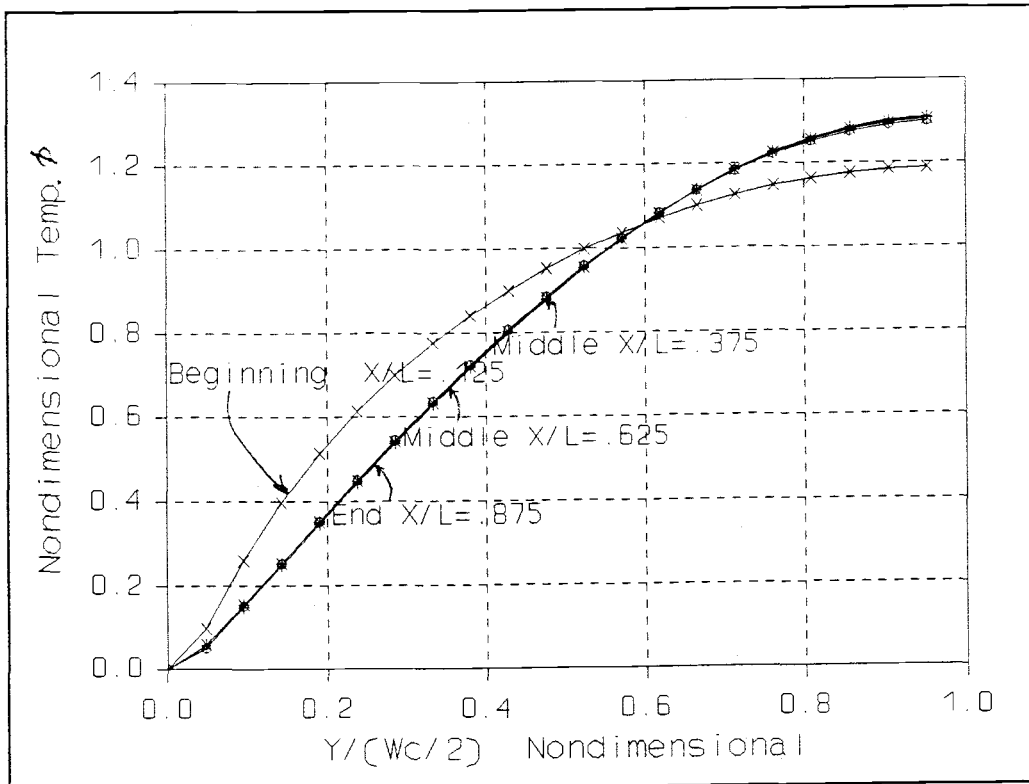


**Figure 2.14**  
Nondimensional temperature  $\phi$  vs.  $y$  at  $z/H=.1$  for four different axial positions.

Nondimensional fluid temperature profiles are an expedient way to analyze fully developed behavior for the laminar microchannels. Many other nondimensional fluid temperature profiles were prepared and are presented in reference [18].

#### 2.8.7 Exit Fin Temperature Comparisons for Different Geometries.

The fully developed assumption provides the exit fin temperature profiles closest to those of the developing solution for cases with wide fins and small aspect ratio channels. The fully developed solution is

best for  $\beta$  greater than about 1 and  $W_w/W_c$  greater than .7. Figure 2.15 provides the exit fin temperature profiles calculated from both the developing and fully developed solutions for a small aspect ratio of 5, wide fin ( $W_w/W_c=1$ ) microchannel. It can be seen that the temperature distributions are within 1% for the entire distribution.

The fully developed assumption provides the worst approximation of the developing solution for very thin fins with high aspect ratio channels. The fully developed assumption is bad for  $\beta$  less than .5 and  $W_w/W_c$  less than .35. Figure 2.16 provides the exit fin

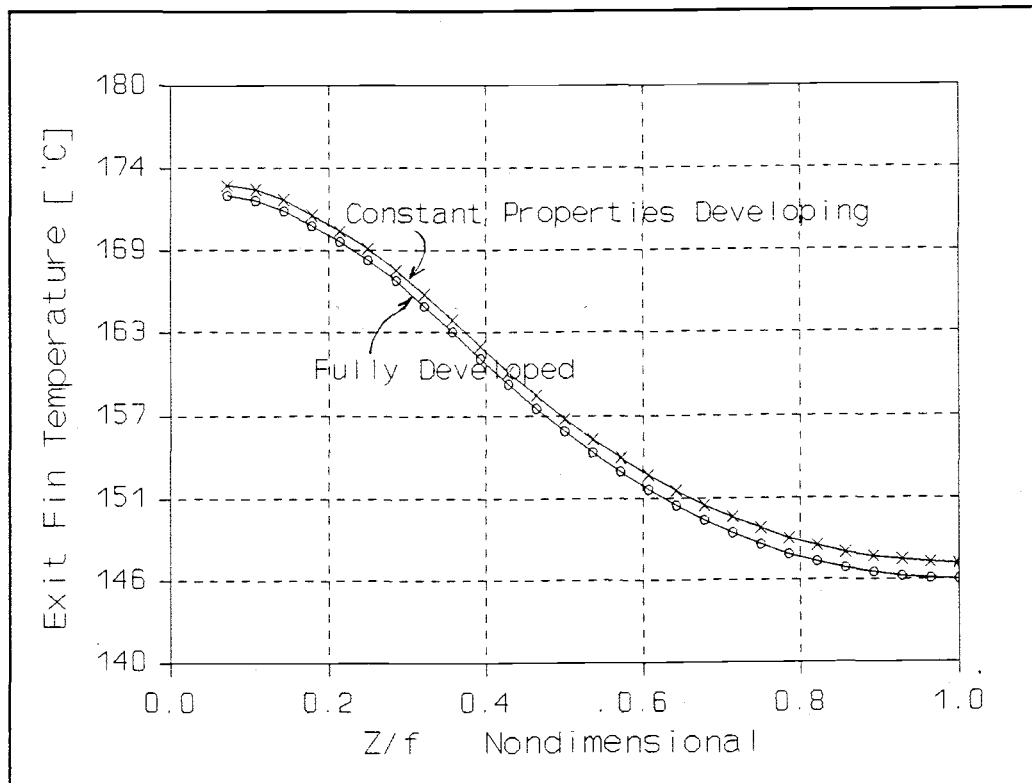


**Figure 2.15**  
Exit fin temperature distribution for fully developed and developing solutions for  $\alpha=5$ ,  $W_w/W_c=1$  and  $\beta=8.5$ .

temperature profiles for the developing and fully developed solutions for a high aspect ratio of 15, thin fin width ( $W_w/W_c=.25$ ) microchannel. The temperature distributions deviate substantially. The largest deviation occurs at the base. Fortunately, the fully developed solution overestimates the solution. The usefulness of a fully developed numerical simulation with this much discrepancy is questionable because the base temperature could be guessed within  $25^{\circ}\text{C}$  for all practical purposes. For thin fin large aspect ratio channels, simulations should use the developing solution.

With the small aspect ratio, large fin width problems the fins have more conduction area and less distance to conduct which causes nearly uniform convection into the fluid. Thus, the thermal boundary layer grows essentially across the microchannel and causes a small thermal entry length and justifies the fully developed assumption. This is because the channel width is small compared to its height. For the large aspect ratio, small fin width problems the fins have very little conduction area and must carry the heat far up the fin. In turn the heat transfer is large at the bottom of the fin and small at the top. The thermal boundary layer grows essentially in the height direction and causes a very large thermal entry length for the large aspect ratio problems. This is vastly different from the prediction of the fully developed assumption. In turn, when the assumption is made that everywhere the temperature gradient in the flow direction is equal to the bulk temperature gradient, the result is meaningless and yields solutions which vary quite a bit from the actual developing solution.

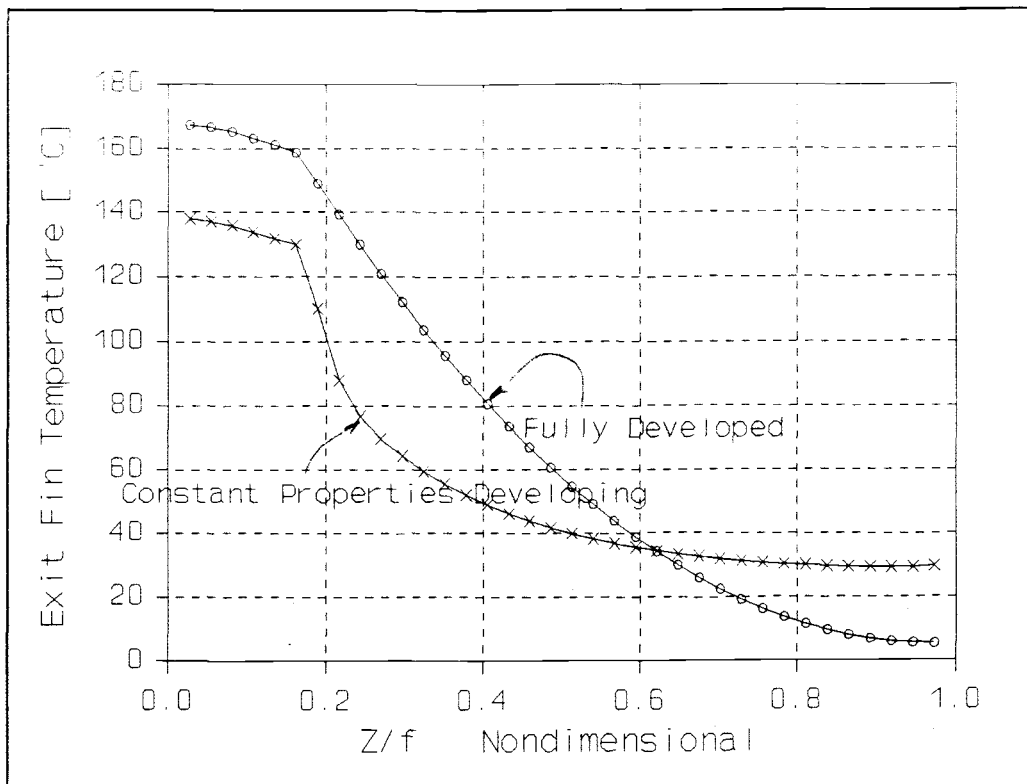


**Figure 2.16**

Exit fin temperature distributions for fully developed and developing solutions for  $\alpha=15$ ,  $W_w/W_c=.25$  and  $\beta=.19$ .

Figure 2.17 shows the percentage difference between the fully developed and developing solution estimates of the peak silicon temperature plotted versus beta. From the graph the fully developed assumption is better for large  $\beta$  than for small  $\beta$ .

By example, it has been shown that the fully developed assumption is good for some parametric cases and poor for others. The important design issue is whether or not the fully developed assumption is valid for the optimized microchannels. The optimization was performed for four different pressure drops resulting in 30, 45, 60 and 90  $\mu\text{m}$  channel widths. The fin exit temperature graphs are presented for the two extreme

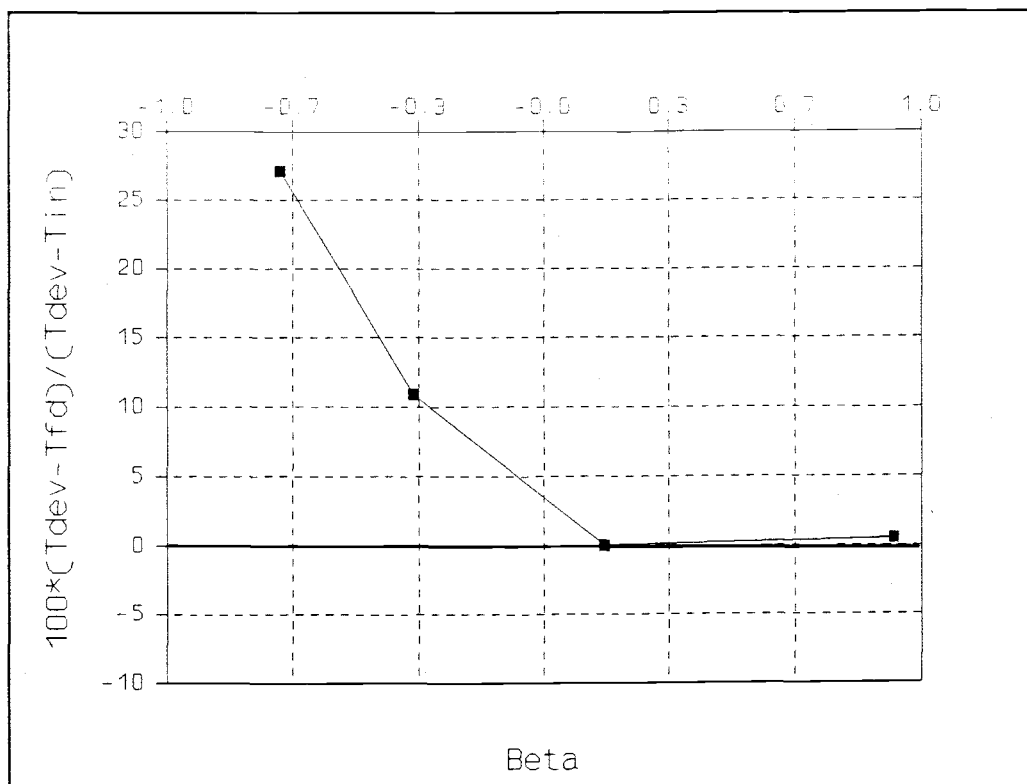


**Figure 2.17**

Percentage difference between fully developed and developing estimates of the peak silicon temperature.

cases to show the trend. (30 and 90  $\mu\text{m}$  channels in Figure 2.18 and Figure 2.19 respectively).

For the optimal geometry of Figure 2.18 it can be seen that the fully developed assumption provides an extremely good representation of the developing solution temperature profile. The best correspondence is at the base and the worst is near the top of the fin where they differ by  $3^\circ$ . Note the very low value of base temperature which is due to the high velocity fluid and large pressure drop for this very thin microchannel.

For the optimal geometry of Figure 2.19 it can be seen that the fully developed solution provides a good representation of the developing solution temperature

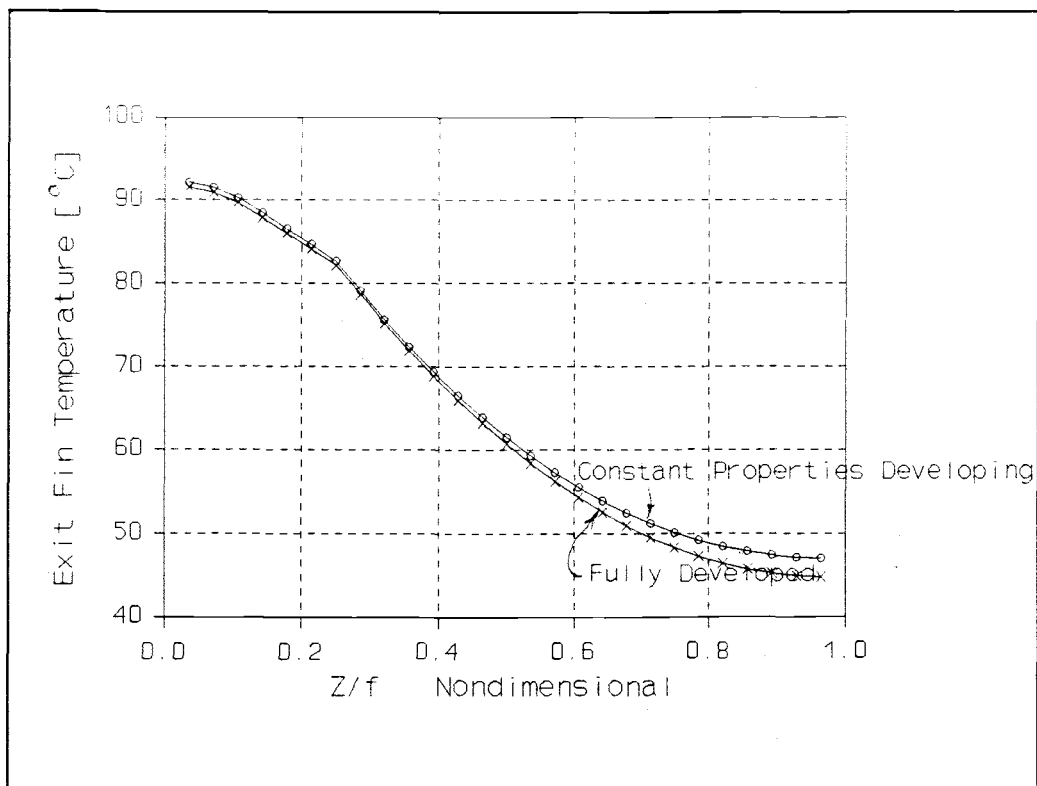


**Figure 2.18**  
Exit fin temperature profile for the optimized 30  $\mu\text{m}$  microchannel. [ $\beta=0.667$ ,  $W_w/W_c=1$  and  $\alpha=18.3$ ]

profile. The difference is approximately the same at the top and bottom and is not more than about  $5^\circ\text{C}$  in either case. Note the high temperature values for this microchannel which are due to relatively slow moving fluid and a small pressure drop.

The other pressure drops corresponding to  $W_c=45$  and  $60 \mu\text{m}$  show similar behavior. In each case, the fully developed solution provides a very good estimate of the developing solution exit fin temperature profile.

It has been shown that for the optimal geometry over a large range of pressure drops, the fully developed solution provides a very good estimate of the exit fin temperature distribution. A physical justification is

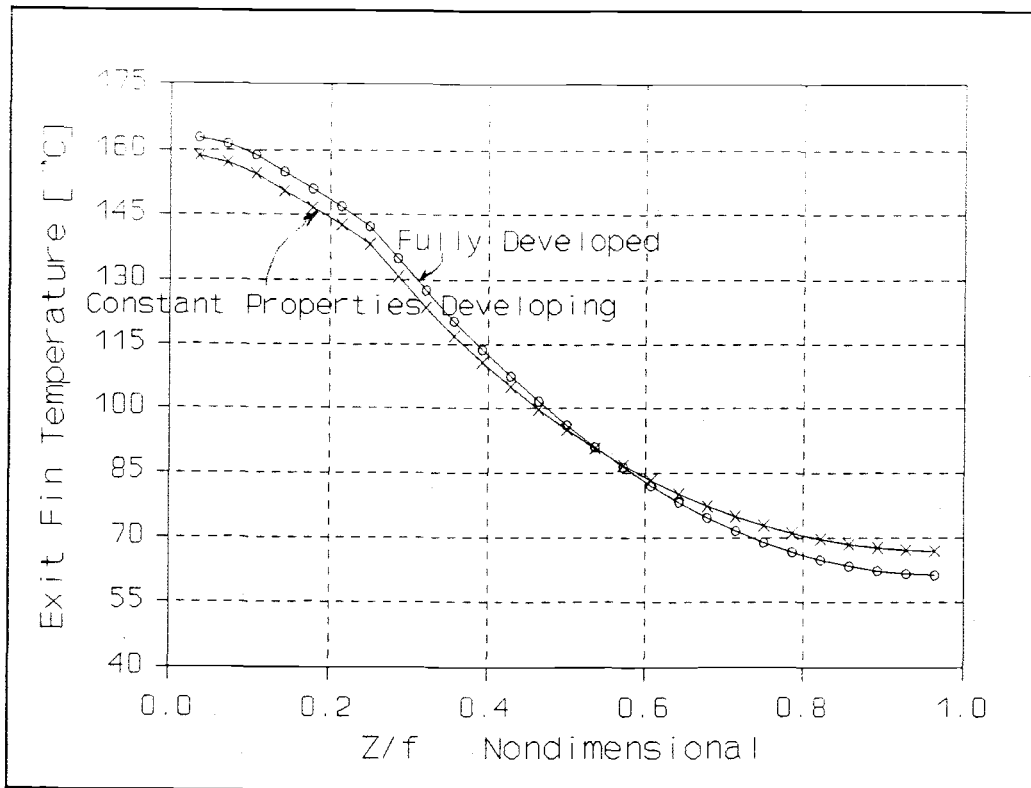


**Figure 2.19**

Exit fin temperature profile for the optimized 90  $\mu\text{m}$  microchannel. [ $\beta=1.4$ ,  $W_w/W_c=1$  and  $\alpha=12.9$ ]

given for this. First of all, the optimization procedure of chapter 1 gives quite consistently a  $W_w/W_c$  value of about 1. This is quite a high value because the conductivity of the solid is much higher than that of the fluid. It provides enough cross-sectional fin area for good conduction all the way to the top of the fin. Thus, the temperature profiles develop quite rapidly as they are essentially developing across the microchannel. Thus, for optimized geometry at nearly any pressure drop, the fully developed assumption is justified.

## 2.9 CONCLUDING COMMENTS

The fully developed energy and momentum assumptions have been analyzed for various microchannel parametric cases. The method was to first use equations from the literature to predict entry lengths then analyze the assumption numerically. It was found that the momentum entry length agreed very well with the equations prediction. It was found to be about 0.01 cm for the 60 micrometer channel with  $\alpha=10$  and  $W_w/W_c=.7$  which is less than 1% of the flow distance. The fully developed momentum assumption was very good for all microchannel cases.

The thermal entry length was found to vary drastically with geometric parameters. The equations predicted 1 cm for the thermal entry length for the above microchannel which is similar to the numerical prediction. The feasibility of using the fully developed assumption also varies at different locations in the channel cross section.

The significant finding of this chapter was that for cases at or near the optimized geometry, the fully developed assumption adequately simulated the actual behavior.

## CHAPTER 3 SUMMARY AND FUTURE WORK

3.1 SUMMARY OF CHAPTER 1 Fully Developed Laminar  
Microchannel Cooling

## 3.1.1 General Considerations.

The laminar microchannels presented by Tuckerman have been computationally analyzed. A computer code was developed to solve for the velocity and temperature profiles within the microchannels using the fully developed assumption. The fully developed assumptions permit large computational savings and reduce the three dimensional microchannel problem to a two dimensional planar problem. This problem is a cross-section of the flow geometry as in Figure 1.1 of chapter 1.

In order to assure that a proper numerical solution was obtained, analysis of the discretization was performed. First of all, the numerical momentum solution was compared to an analytical separation of variables solution. Secondly, the analytical solution to the heat transfer and fluid mechanics in an infinite parallel plate channel was compared to it's numerical formulation for gridding information across the channel. Finally, a comparison of the solution run with very fine, fine and coarse discretizations of the same problem was presented which served to evaluate the discretization.

It may be stated that the desired effect of any of the cooling devices is to provide the best heat removal rate away from the microelectronics and provide for the lowest operating temperature of the microelectronics. Also, for mechanical consideration, the power required to cool the heat sinks should be as low as possible. These considerations were the impetus for the development of the optimization procedure for the microchannel heat

linearly with channel width. (Figure 1.14) The channel width can be chosen based solely on the pressure drop and without regard for the channel height since the pressure drop is a very weak function of the channel height.

(Figure 1.13)

From the channel width obtained, an aspect ratio can be chosen which yields a minimum peak silicon temperature. (Figure 1.15) Equation 1.8 derived from Landrum's integral analysis gives a good estimate of this optimal aspect ratio. Then, numerical solutions may be run and the results plotted to find the minimum temperature and thereby obtain the optimal aspect ratio. From the channel width and aspect ratio obtained, the optimal value of fin to channel width ratio may be found. ( $W_w/W_c$ ). (Figure 1.16) Equation 1.9 gives a good estimate of this optimal fin to channel width ratio. Equations 1.8 and 1.9 must be solved iteratively to obtain the optimal solution and the numerical solution may be run to verify that indeed a true optimal design has been found. A substrate thickness of 50 microns or less can be chosen according to the guidelines of 1.11.7. The optimization procedure completely specifies the microchannel geometry.

The intent of this study was to identify the general trends (the "roadmap") and provide the computational tools by which the optimal geometry can be found for a given pressure gradient and wall flux. In actual application, it is a small matter to follow these computational prescriptions to determine the optimal solution. Then the optimal laminar microchannel solution can be compared to other possible strategies of cooling the electronic components and the best possible choice

may be made.

### 3.2 SUMMARY OF CHAPTER 2 Developing Microchannel Cooling

An investigation of the fully developed momentum and energy assumptions was presented for the laminar microchannel heat sinks. Equations were used which predict thermal and hydrodynamic entry lengths. Then the solutions were investigated numerically. The TEMPEST computer code developed at Battelle Pacific Northwest Laboratories was used to solve the developing microchannel cooling problem. Also, a comparison between constant properties and variable properties solutions was presented.

The fully developed constant properties momentum assumption was found to be extremely good. The velocity profiles became fully developed within about 10% of the flow distance. For the variable properties comparisons, the velocity profiles differ considerably from the constant property profiles. Considering velocity in the flow direction plotted with respect to height up the channel, the constant property velocity profile is quite flat whereas the variable property profile is high near the bottom and low near the top as in Figure 2.4. The temperature comparisons reveal that for variable property solutions, the variable properties temperature profile is lower in the solid and slightly higher in the fluid near the top of the channel but the profiles don't differ by much. (Figure 2.3) It is comforting to see that the constant properties assumption slightly overestimates the peak silicon temperature and therefore provides a built-in margin of safety for this temperature, which is really the variable of interest.

For the optimal cases, the graph of wall temperature in the flow direction obtains nearly the same slope as the bulk temperature which suggests fully developed behavior. This behavior is not constant along the fin height and in most cases is the best near the top of the fin and the worst at the bottom. (i.e. fully developed behavior is observed in the smallest axial distance at the top of the fin). The fully developed assumption is the best in cases with large fin width to channel width ratios and small channel aspect ratios (large  $\beta$ ). The fully developed assumption is the worst in cases with small fin to channel width ratios and large channel aspect ratios (small  $\beta$ ). (Figure 2.8) It must be understood that the fully developed thermal assumption is only approximately correct and that one should understand its implications before using it.

It should be noted that the fully developed assumption should not be used to obtain the proper heat flux from the fin. This may be important in an analysis where the microchannel performance is extended into the subcooled boiling region. Also, if it is desired to obtain very precise values of temperature within the channels, the fully developed assumption may not be good.

The normal definition of nondimensional fluid temperature doesn't seem to apply to this problem since the fully developed problem is truly two dimensional. For this reason, a special bulk temperature which is a function of height up the fin is defined. Using this new definition, results are presented which suggest that the fully developed assumption is good for cases near the optimal geometry. The temperature behavior in the solid at the exit conditions for the developing solution is very similar to the results from the fully developed

assumptions for cases near the optimal geometry. This is an important fact because it implies that the fully developed optimization procedure of chapter 1 may be used to design actual laminar microchannels.

### 3.3 RECOMMENDATIONS FOR FUTURE WORK

The following are recommendations for future work to enhance the mechanical engineering aspect of integrated circuit cooling technology.

- 1) Perform the optimization described in chapter 1 of this thesis for a range of different pressure drops and present the results in a nondimensionalized manner.
- 2) Solve the problem encountered when the heat flux is raised high enough such that subcooled boiling results within the microchannels.
- 3) Solve the problem encountered when different materials are considered for the solid and the fluid. Consider the thermal conductivities of the solid and fluid to be the same order of magnitude as would occur when considering the flow of a liquid metal.
- 4) Numerically solve the turbulent macrochannel described in Tuckerman's thesis. Compare the results to those for the laminar microchannels.
- 5) The limiting factor for the heat transfer in the microchannels in this thesis appears to be the area of heat transfer at the base of the fins. Consider tapered fins which are wider at the base and thinner at the top. Numerically solve this problem and compare the results to

the rectangular microchannels.

6) Numerically solve the rectangular pin fin problem in 3 dimensions presented in Tuckerman's thesis. Compare the results to those for the laminar microchannels.

## BIBLIOGRAPHY

- [1] D. B. Tuckerman, "Heat-Transfer Microstructures for Integrated Circuits", UCRL-53515 for Lawrence Livermore National Laboratory, February 1984
- [2] R. C. Joy and E. S. Schlig, "Thermal Properties of Very fast Transistors", IEEE Transactions on electron devices, Vol. ED-17, #8 August 1970, pp 586-594.
- [3] M. D. Pocha, "Fundamental Limitations and Trade-Offs for high power microwave generation with Photoconductors", UCID-21458, Rev. 1 for Lawrence Livermore National Laboratory, October 4, 1988.
- [4] E. M. Sparrow, B. R. Baliga, and S. V. Patankar, "Forced Convection Heat Transfer from a Shrouded Fin Array with and without Tip Clearances," ASME Journal of Heat Transfer, Vol. 100, Nov. 1978, pp. 572-279.
- [5] S. C. Lau, L. E. Ong, and J. C. Han, "Conjugate Heat Transfer in Channels with Internal Longitudinal Fins", Journal of Thermophysics, Vol. 3, #3, July 1989 pp. 303-308.
- [6] F. P. Incropera, "Convection Heat Transfer in Electronic Equipment Cooling", ASME Journal of Heat Transfer, November 1988, Vol. 110, pp. 1097-1111.
- [7] C. R. Wylie, L. C. Barret, "Advanced Engineering Mathematics", Fifth Edition, McGraw-Hill Book Co, 1982, pp. 490-503.
- [8] Carslaw and Jaegar, "Conduction of Heat in Solids", Second Edition, Oxford University Press (at the Clarendon), 1959, pp. 171.
- [9] A. L. London, "Heat Transfer Conditions in High Power Klystron Tubes," Tech. report 87-800-112, Varian Associates, October 1970.
- [10] "PREPARATION OF THE THESIS 1983 Guidelines, directions and requirements for the mechanics of thesis preparation at OREGON STATE UNIVERSITY"
- [11] W. M. Kays and M. E. Crawford, "Convective Heat and Mass Transfer", 2nd edition, McGraw-Hill, New York, 1980, ISBN 0-07-033457-0. See in particular chapters 6 and 8 on laminar flow in tubes.

- [12] D. B. Tuckerman and R. F. W. Pease, "Optimized convective cooling using micromachined structures," IEEE Electron Device Letters, Vol. EDL-2, #5, May 1981, pp. 126-129.
- [13] R.W. Keyes, "Heat Transfer in Forced Convection Through Fins," Tech. report RC9895, IBM Thomas J. Watson Research Center, March 1983 (Unpublished)
- [14] R. D. Cess and E. C. Shaffer, "Heat Transfer to Laminar Flow between Parallel Plates with a Prescribed Wall Flux," Applied Scientific Research, Vol. 8A, 1958, pp. 339-344.
- [15] A. Bejan, "Convection Heat Transfer", Wiley Interscience Publications, John Wiley and Sons, July 1984, pp. 48.
- [16] W. M. Kays, "Convective Heat and Mass Transfer", McGraw-Hill series in Mechanical Engineering, 1966, pp. 129-130.
- [17] C. Y. Ho, R. W. Powell and P. E. Liley, "J. Phys. Chem. Re. Data," 1974, pp. I-588, Supplement 1.
- [18] J. J. Lienau, "Microchannel Heat Sinks: 3 Dimensional Developing Analysis", LLNL (Private issue), NTED Thermal Fluids Group, Sept 1989.
- [19] J. J. Lienau, "Microchannel Heat Sinks: 2 Dimensional Fully Developed Analysis", LLNL (Private issue), NTED Thermal Fluids Group, August 1989.
- [20] L. L. Eyler, D. S. Trent, M. J. Budden, "TEMPEST, A THREE DIMENSIONAL TIME DEPENDENT COMPUTER PROGRAM FOR HYDROTHERMAL ANALYSIS: VOL II, Assessment and Verification Results", PNL-4348 vol. II, UC-79T, September 1983, pp. 4.15-4.17, pp. 4.21-2.22, pp. 4.29-4.30.
- [21] L. L. Eyler, D. S. Trent, M. J. Budden, "TEMPEST, A THREE DIMENSIONAL TIME DEPENDENT COMPUTER PROGRAM FOR HYDROTHERMAL ANALYSIS: VOL I, Numerical Methods and Input Instructions for TEMPEST", PNL-4348 vol. I Rev. 2, UC-505, Code Version N, Mod 31, January 1989.

## APPENDICES

## APPENDIX A

### General and Specific Logic of the Computer Code

#### 1 GENERAL LOGIC:

The general logic of the finite difference computer code<sup>1</sup> for solving the system of elliptic partial differential equations presented in section 1.5 will be presented in this section. General logic implies the method by which the microchannel problem was analyzed and does not include the specific logic of the computer code (source code or flow chart listing). This specific logic will be covered in 2 of this appendix.

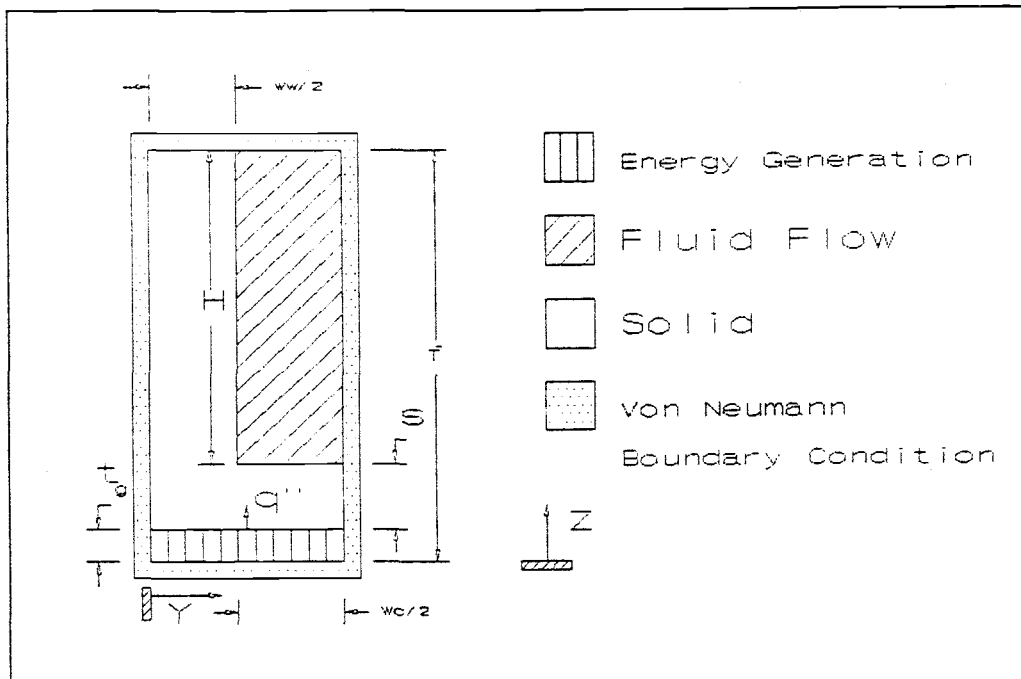
##### 1.1 Modeling Information.

Figure A1 presents the computational regions of the microchannel problem along with the boundary conditions. The computer code is designed to first solve the fully developed momentum equation (equation 1.1) in the fluid flow region using the method of point successive over relaxation. Then, it solves the energy equation (equations 1.2, 1.3 and 1.4) in each of their respective domains. Solving for the temperature involves using the velocity solution in the convective term in equation 1.4 which represents the fluid flow region.

The computer code treats the different materials using material types which can have specified property values. The materials properties for the water and silicon were entered into a special material property library subroutine. (Subroutine PROPLIB) The computer code also deals with the Von Neumann (no flux) boundary

---

<sup>1</sup> The computer code was written in FORTRAN and was named 2DREYN.FOR.



**Figure A1**  
Microchannel Modeling showing the different computational regions and the Von Neumann boundary condition.

conditions with material types in the materials property library. A special material called a Neumann material is defined which has a very small conductivity<sup>1</sup>.

The computer code uses the heat generation term in order to work with the different forms of the energy equation presented in equations 1.2, 1.3 and 1.4. It simply places an energy generation value for the region of equation 1.2 which represents the energy generation region. It uses zero for the heat generation of equation 1.3 which represents conduction and uses the appropriate convective term as a heat generation term in equation 1.4

<sup>1</sup> Neumann materials in this computer code have a value of thermal conductivity of ten to the minus thirtieth power. This number is sufficiently small and prevents "divide by zero" errors.

which represents the fluid flow region. The heat generation array is then built properly and the temperature solution is found using the method of point successive relaxation described in 2 of this appendix.

### 1.2 Bulk Energy Balance for Numerical Solution.

Since the entire thermal region is surrounded by Von Neumann Boundary Conditions and no temperature at any point is fixed (i.e. Dirichlet condition), the numerical solution has the unique feature of being indeterminate. That is, that only differences in temperature between two points calculated will be meaningful. Therefore a bulk energy balance must be applied across the heat sink to determine the change in bulk temperature and use this as the constraint to set the temperature field. That is, we know what the bulk temperature at the exit should be by the energy balance and we can also calculate what the bulk fluid temperature of the numerical solution is<sup>1</sup>. The difference between these two temperatures will be the proper temperature to add to the entire numerical solution so that it represents the actual temperature field at the exit of the heat sink.

In order to illustrate the bulk energy balance, see Figure 2 in the nomenclature section of this thesis. The heat flux value is  $q''$  and is applied to an area of  $\frac{1}{2}(W_w + W_c)L$  per microchannel. The average fluid velocity is  $U_0$  and is flowing in a channel of area  $(H)(\frac{1}{2}W_c)$ . The specific heat of the fluid is  $C_p$  and fluid density . Thus the energy balance yields:

---

<sup>1</sup> The bulk temperature calculated by the numerical solution will be incorrect and the value which is predicted really has no significance.

$$(1) \quad \frac{1}{2} \rho H W_c U_o C_p (T_{\text{bulk,exit}} - T_{\text{bulk,inlet}}) = \frac{1}{2} (W_w + W_c) L q''$$

Solving equation (1) for the bulk fluid temperature at exit yields:

$$(2) \quad T_{\text{bulk,exit}} = T_{\text{bulk,inlet}} + \frac{L(W_w + W_c) q''}{\rho H W_c U_o C_p}$$

This is the equation the computer code uses to calculate the actual bulk temperature at the exit to the heat sink. It uses the temperature field calculated numerically to calculate the fields bulk fluid temperature using equation (3) below.

$$(3) \quad T_{\text{bulk,exit,numerical}} = \frac{\int_0^H \int_0^{W_c} u(y,z) T(y,z) dy dz}{\int_0^H \int_0^{W_c} u(y,z) dy dz}$$

Thus, the temperature which must be added to every point (cell) in the numerically calculated temperature field so it will represent the temperature field at the exit of the heat sink is  $T_{\text{add}}$  defined as:

$$(4) \quad T_{\text{add}} = T_{\text{bulk,exit}} - T_{\text{bulk,exit,numerical}}$$

The computer code calculates this  $T_{\text{add}}$  and adds it to the temperature at every cell then prints out the temperature array.

## 2 SPECIFIC LOGIC:

The specific logic of the computer code involves first of all a discussion of the technique of Point Successive Over Relaxation (PSOR) which is the algorithm used to solve the momentum and energy equations. Secondly, a flowchart of the computer code is presented and finally a source code listing of the computer code is presented. The discussion of the technique of PSOR was taken from the lecture notes of Dr. D. S. Trent for ME 573 in February of 1989. The flowchart was developed by J. J. Lienau and the computer code was written in part by Dr. D. S. Trent and in part by J. J. Lienau. Dr. Trent provided the "shell" of the computer code to the class which didn't contain any of the solution logic or any of the logic in subroutine SSTATE which is the subroutine which solves the microchannel problem. All of the other logic was supplied by J. J. Lienau.

All of the algorithm was taken from the ME 573 lecture notes by Donald S. Trent of Oregon State University. [February 1989.]

The finite volume connectors  $C_{i,j}$  define how the total flux of a scalar variable  $\Phi$  ( $\phi$ ) across each cell boundary is related to the corresponding gradient of  $\phi$  that exist for each cell in the computational grid system. In this diffusion process, the connectors relate the flux between adjacent computational cells. Figure A1 below illustrates these connections for a 2d rectangular grid system.

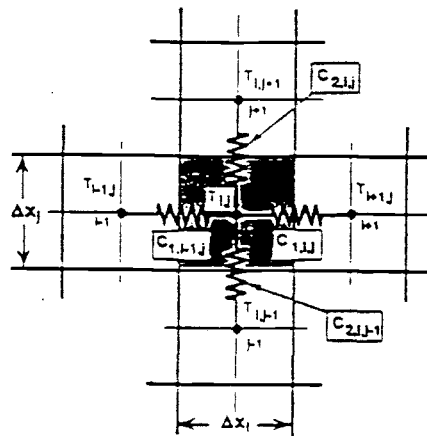


Figure A1 Five point connector stencil.

Now, to apply the energy (conservation) equation to the finite volume computational cell  $i,j$  for steady state transport of heat, it is written in flux form as:

$$(J_{\phi 1,1} - J_{\phi 1,i-1}) + (J_{\phi 2,j} - J_{\phi 2,j-1}) = -\sqrt{g_{i,j}} S_{\phi i,j} \quad (1)$$

$S_{\phi ij}$  is the heat generation or source term,  $J_{\phi}$  is the heat flux.

The symbol  $\sqrt{g_{i,j}}$  in Eq. 1) is the Jacobian or cell volume at cell  $i,j$ .

Now, defining the overall transport coefficient  $H$  and the flux ( $J$ ) in terms of this yields:

$$J_{\phi 1,i} = H_{\phi 1,i} A_{1,i} (\phi_{i+1,j} - \phi_{i,j})$$

and

$$J_{\phi 2,j} = H_{\phi 2,j} A_{2,j} (\phi_{i,j+1} - \phi_{i,j}) .$$

(2)

where:

where

$$H_{\phi 1,i} = \frac{2}{\left\{ \frac{\Delta x_i}{\Gamma_{\phi,i}} + \frac{\Delta x_{i+1}}{\Gamma_{\phi,i+1}} + \frac{2}{h_{\phi,i}} \right\}}$$

and

$$H_{\phi 2,j} = \frac{2}{\left\{ \frac{\Delta x_j}{\Gamma_{\phi,j}} + \frac{\Delta x_{j+1}}{\Gamma_{\phi,j+1}} + \frac{2}{h_{\phi,j}} \right\}}$$

(3)

where  $\Gamma\phi$  is the diffusion coefficients.

The connections are then written as:

$$C_{1,i} = H_{\phi 1,i} A_{1,i}$$

and

$$C_{2,j} = H_{\phi 2,j} A_{2,j} .$$

(4)

The conservation law can then be applied to 1) and like terms can be collected to yield:

$$C_{1,i} \phi_{i+1} + C_{1,i-1} \phi_{i-1} + C_{2,j} \phi_{j+1} + C_{2,j-1} \phi_{j-1} - [C_{1,i} + C_{1,i-1} + C_{2,j} + C_{2,j-1}] \phi_{i,j}$$

$$= -\sqrt{g_{i,j}} S_{\phi,i,j}$$

(5)

Where S is the source term (heat generation or removal in the velocity region) and phi is the scalar variable (temperature in this case) and J is the heat flux from one cell to the other.

Now to implement the method of Point Successive over relaxation to the above differencing scheme we introduce the concept of the over relaxation factor omega (w).

$$\phi_{ij}^{n+1} = w\phi_{ij}^{n+1} + \{1 - w\} \phi_{ij}^n \quad (6)$$

where n is the iteration level.

Now defining Dp as the sum of the connectors:

$$Dp = C_{1,i} + C_{1,i-1} + C_{2,j} + C_{2,j-1} \quad (7)$$

and rewriting the above equation in terms of omega and the current iteration level for every temperature yields:

$$\phi_{ij}^{n+1} = \frac{\omega [C_{1,i} \phi_{i+1}^n + C_{1,i-1} \phi_{i-1}^{n+1} + C_{2,j} \phi_{j+1}^n + C_{2,j-1} \phi_{j-1}^{n+1} + \sqrt{g_{ij}} S\phi_{ij}]}{Dp} + (1 - w) \phi_{ij}^n \quad (8)$$

Now, the actual solution progresses in terms of delta phi (incremental) quantities defined by:

$$\delta \phi_{ij}^{n+1} = \phi_{ij}^{n+1} - \phi_{ij}^{n+1} - \phi_{ij}^n \quad (9)$$

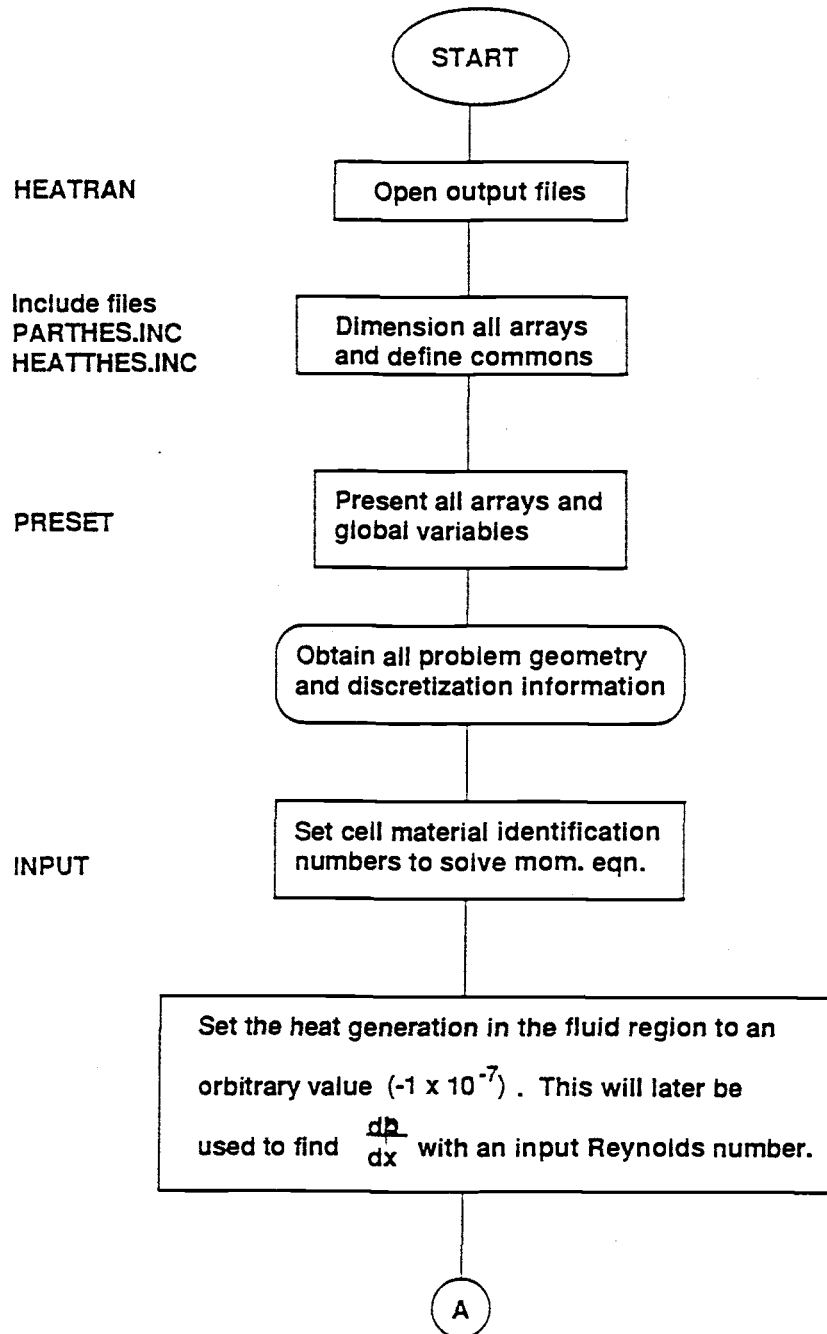
Now implementing the incremental logic into the above equation yields the following difference equation for delta phi which is actually what we solve for.

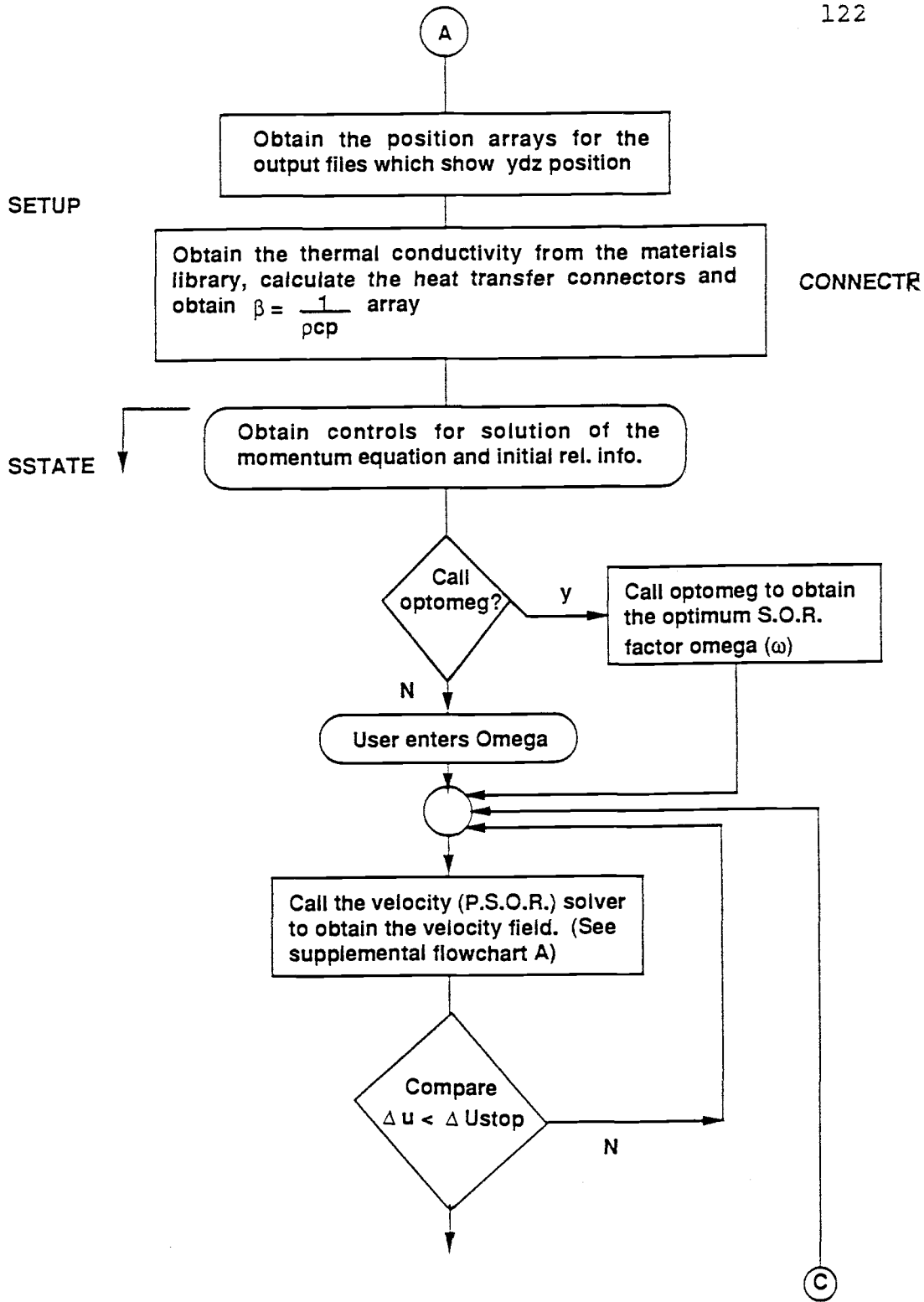
$$\delta \phi_{ij}^{n+1} = \frac{W [C_{1,i} \phi_{i+1}^n + C_{1,i-1} \delta \phi_{i-1}^{n+1} + C_{2,j} \delta \phi_j^n + C_{2,j-1} \delta \phi_{j-1}^{n+1} + \sqrt{g_{ij}} S\phi_{ij}]}{Dp} \quad (10)$$

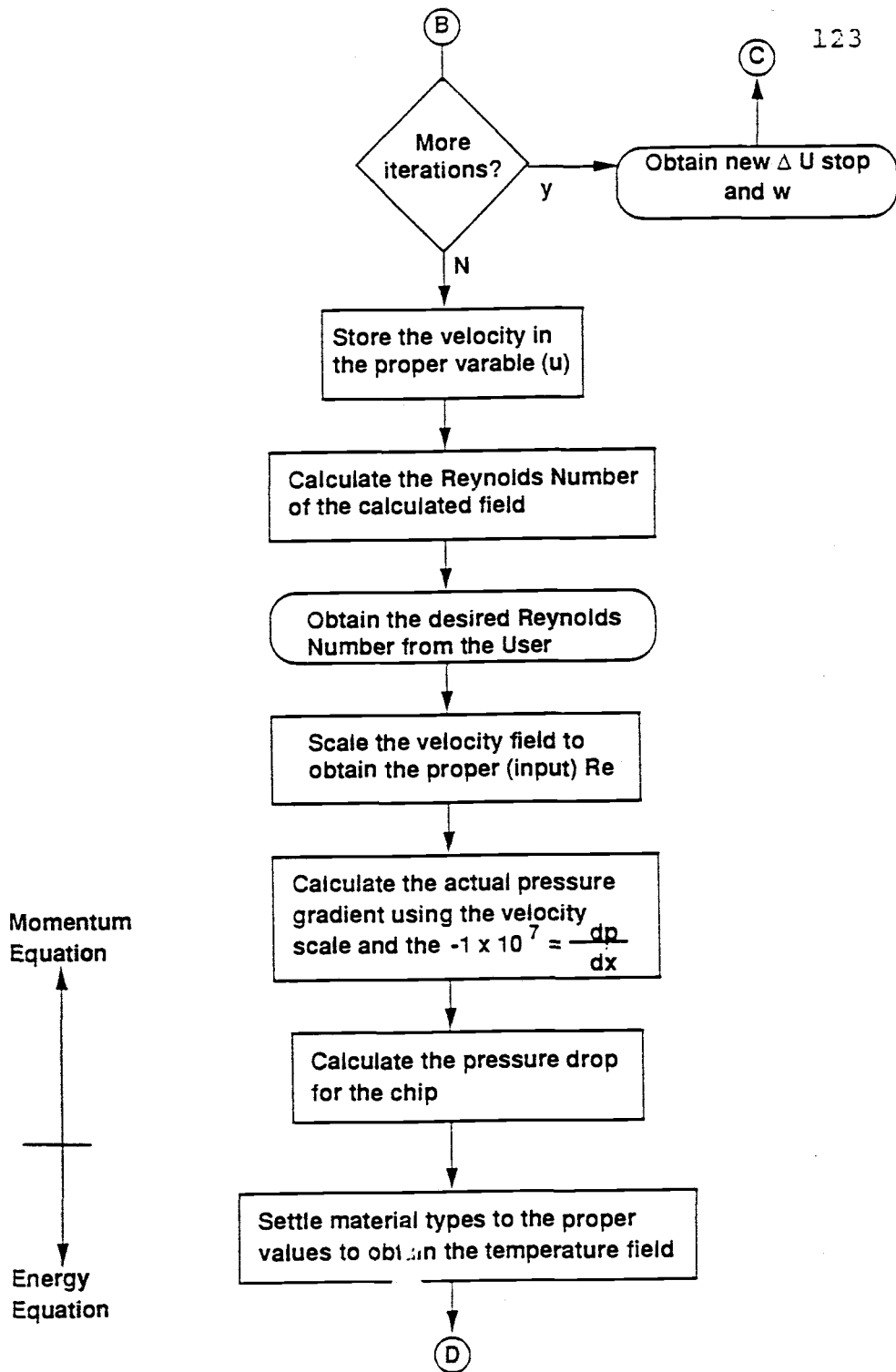
After we obtain the delta phi solution, we increment to the new value of temperature using:

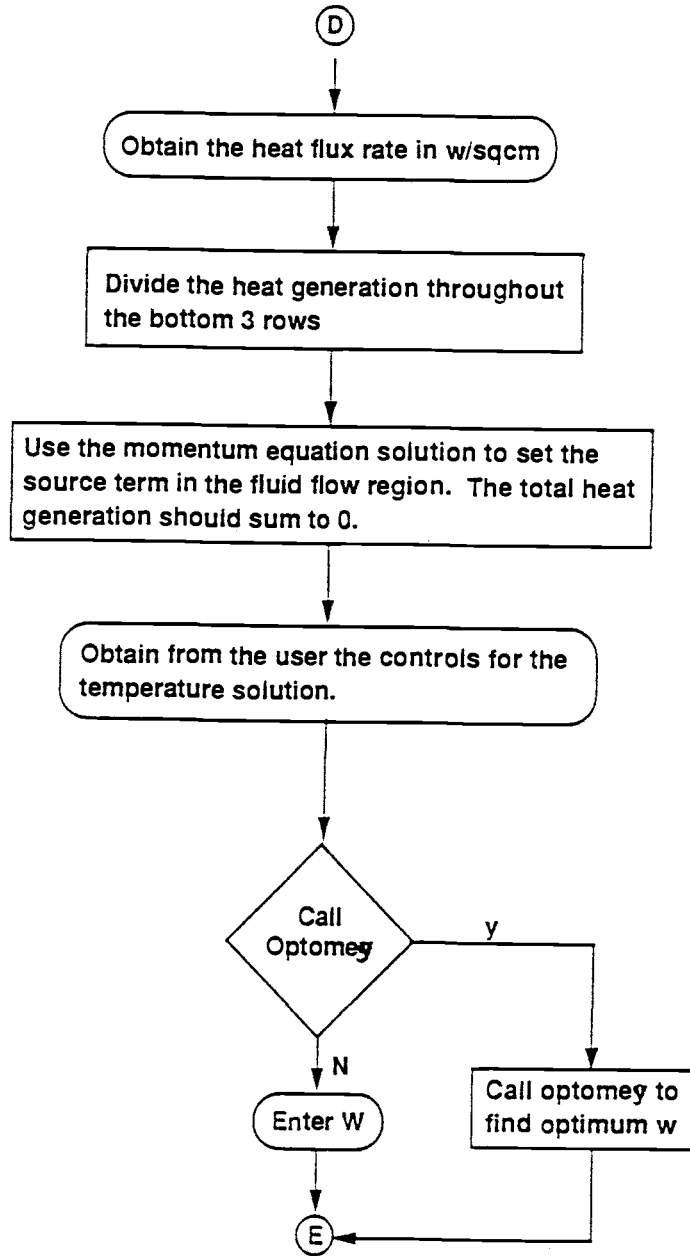
$$\phi_{ij}^{n+1} = \phi_{ij}^n + \delta \phi_{ij}^{n+1} \quad (11)$$

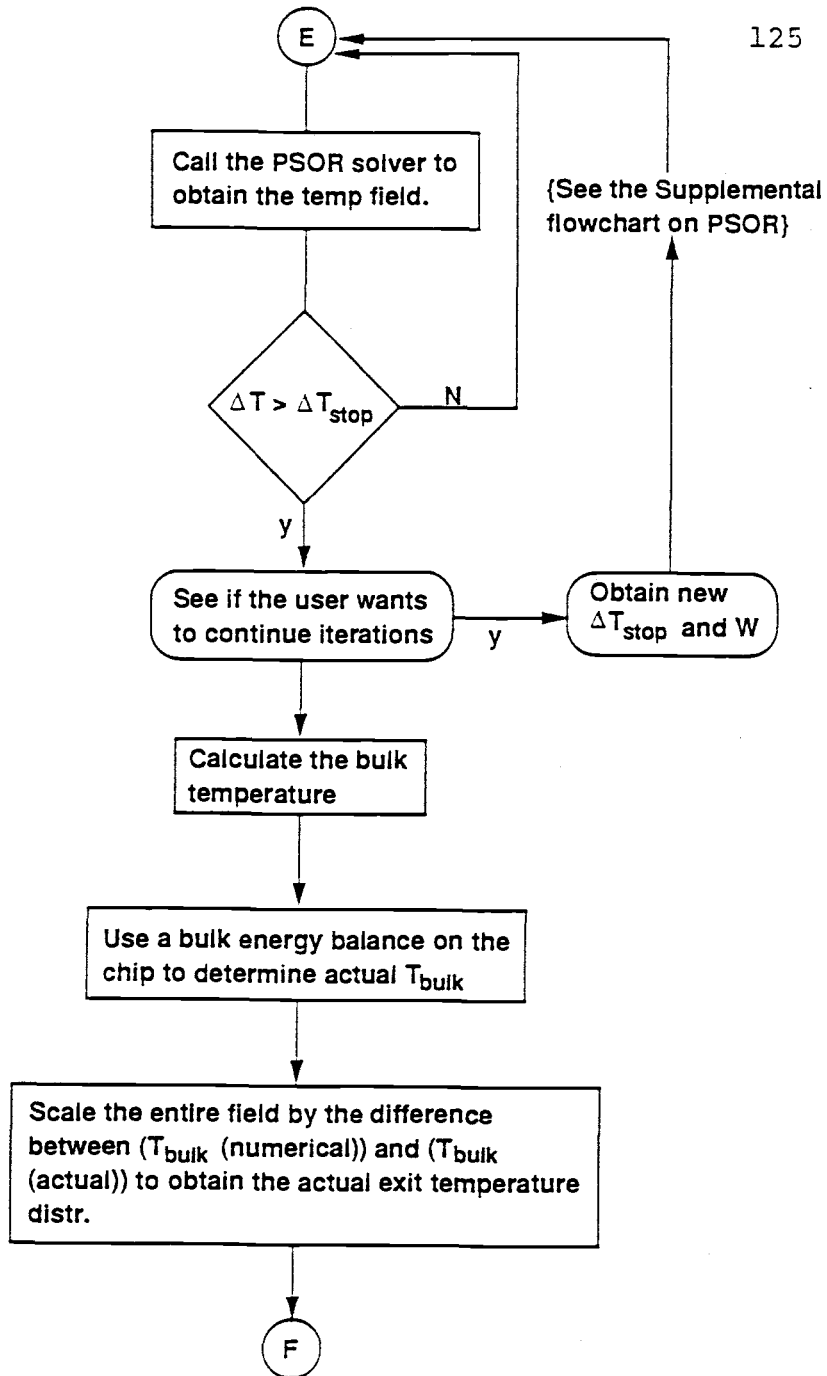
This is how the code actually calculates the temperature and velocity fields using the Point Successive Over Relaxation method. The nice thing about P.S.O.R. is that we have a numerical algorithm which will find the optimum S.O.R factor ( $w$ ) which can speed up computation dramatically. The algorithm will not be discussed here but if it is desired, I will write it up on request.

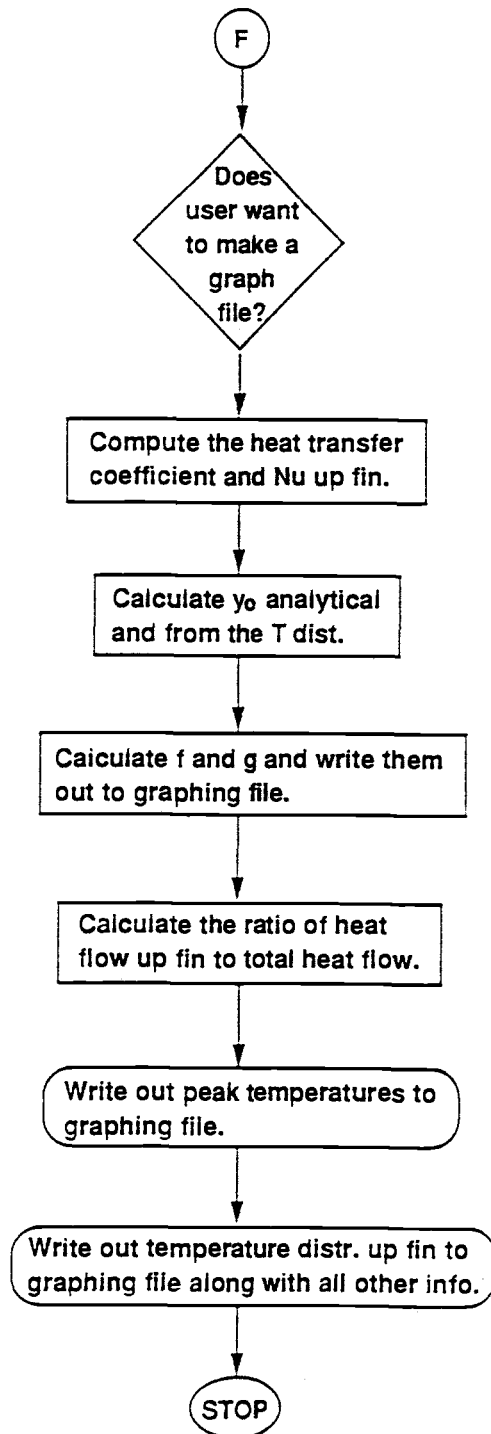




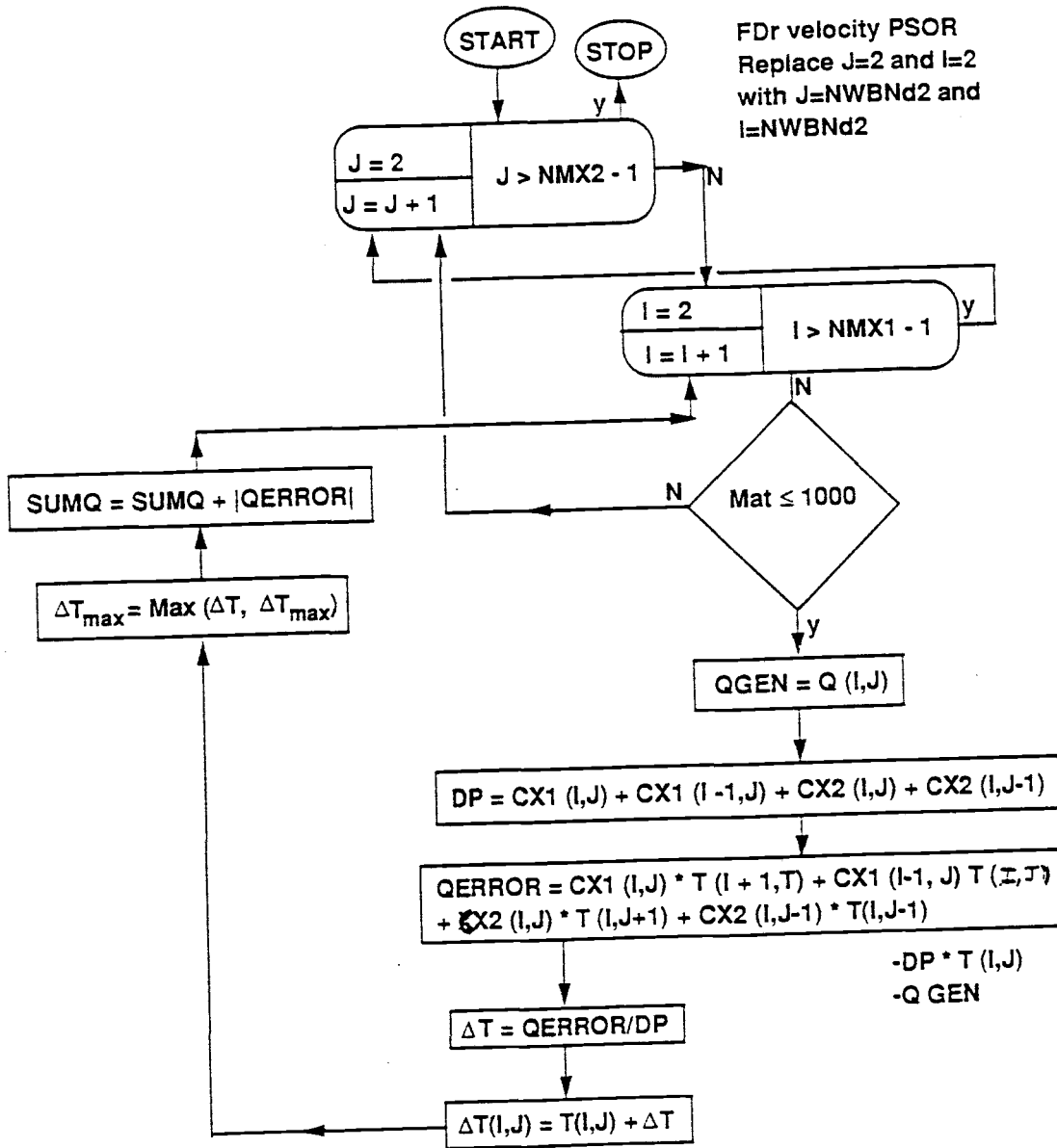








Supplemental Flowchart A. (P.S.O.R.)



```

C** ME 573 NUMERICAL METHODS FOR ENGINEERING ANALYSIS DST/3/6/89

C**
PROGRAM HEATRAN
C** THIS IS THE MAIN DRIVER PROGRAM
INCLUDE PARTHES.INC
INCLUDE HEATTHES.INC

C** OPEN A LOGICAL UNIT FOR AN INPUT FILE (INP IS A PARAMETER)
C OPEN(UNIT=INP,FILE='INPUT',STATUS='OLD',FORM='FORMATTED')

C** OPEN A LOGICAL UNIT FOR THE PRINTER (LOUT IS A PARAMETER)
OPEN(UNIT=LOUT,FILE='2DOUT',STATUS='NEW',FORM='FORMATTED')

C** OPEN A LOGICAL UNIT FOR PLOTTING (NPOUT IS A PARAMETER)
OPEN(UNIT=NPOUT,FILE='2DPLOT',STATUS='NEW',FORM='FORMATTED')

C** OPEN A LOGICAL UNIT FOR GRAPHICS (NGRAPH IS A PARAMETER)
OPEN(UNIT=NGRAPH,FILE='2DGRAPH',STATUS='NEW',FORM='FORMATTED')

WRITE(*,1000)
WRITE(*,1001)
WRITE(LOUT,1000)
WRITE(LOUT,1001)

CALL PRESET
CALL INPUT
CALL SETUP
IF(CONTROL(1)) CALL SSTATE
IF(CONTROL(2)) CALL TRANSIENT
STOP

1000 FORMAT(///10X,
1'ME 573 NUMERICAL METHODS FOR ENGINEERING ANALYSIS 2/10/89')
1001 FORMAT(//18X,'TRANSPORT EQUATION SOLUTION ALGORITHM TESTER'//)
END

C*****

SUBROUTINE PRESET

INCLUDE PARTHES.INC
INCLUDE HEATTHES.INC
C** PRESET ARRAYS ( LETS DEFINE A COMPLETE SET FOR FLEXIBILTY)
DO 10 J = 1,MAX2
DO 10 I = 1,MAX1
T(I,J) = 0. ! CURRENT TEMPERATURE
ETA (I,J) = 0. ! DELTA SOLUTION
BETA(I,J) = 0. ! TRANSIENT COEFFICIENT
DPHI(I,J) = 0. ! UTILITY ARRAY
CX1(I,J) = SMALL ! CONNECTORS - X1 DIRECTION
CX2(I,J) = SMALL ! CONNECTORS - X2 DIRECTION
C HC1(I,J) = BIG ! FILM/CONTACT COEFF - X1 DIR
C HC2(I,J) = BIG ! FILM/CONTACT COEFF - X2 DIR
DX1(I,J) = 0. ! CELL WIDTH - X1 DIRECTION
DX2(I,J) = 0. ! CELL WIDTH - X2 DIRECTION
AR1(I,J) = SMALL ! CELL INTERFACE AREA - X1 DIR
AR2(I,J) = SMALL ! CELL INTERFACE AREA - X2 DIR
CAY(I,J) = SMALL ! THERMAL CONDUCTIVITY
Q(I,J) = SMALL ! This is the Dp/Dx driving force

```

```

                                ! SHOULD BE 1.827E7 PA/M
      CV(I,J)   = 0.              ! VOLUME
      U(I,J)   = 0.              ! VELOCITY
      MAT(I,J)  = 1003           ! CELL MATERIAL ID NUMBER
10  CONTINUE
      PREF     = 1.01E+5        ! REFERENCE PRESS, PASCALS (GAS)
      DT       = 0.              ! TIME STEP, SECONDS
      TYME     = 0.              ! SIMULATION TIME, SECONDS

      DO 20    I = 1,10
      CONTROL(I) = .FALSE.      ! PROGRAM CONTROL: LOGICAL
20  CONTINUE

C** MATERIAL BOUNDARY CONDITION ID NUMBERS
C** LISTED BELOW ARE THE FICTICIOUS BOUNDARY MATERIAL ID NUMBERS:
C**      ID = 1000 : CAY = 1    - MODEL MATERIAL
C**      ID = 1001 : CAY = SMALL - THE VON NEUMANN CONDITION
C**      ID = 1002 : CAY = BIG  - THE DIRICHLET CONDITION
C**      ID = 1003 : CAY = SMALL - NULL CELL

C** INITIALIZE CONSTANTS

      PI      = 4.0*DATAN(1.0D0) ! CONVENIENT AND ACCURATE WAY TO SET PI

      LEVEL   = 1000000
      ITMAX   = 1000             ! MAXIMUM NUMBER OF TEMP ITERATIONS
      ITMAXT  = 100             ! MAXIMUM NUMBER OF ITERATIONS (TRANS)
      TCRIT   = 0.001          ! ITERATION CONVERGENCE CRITERION
      OMEGA   = 1.700          ! OVER-RELAXATION FACTOR
      TINIT   = 0.              ! INITIAL TEMPERATURE
      QMAX    = .1              ! HEAT BALANCE ERROR
      F       = .5              ! IMPLICIT FACTOR
      NWBND1  = 21              ! WATER BOUNDARY RIGHT LOCATION
      NWBND2  = 17              ! WATER BOUNDARY LEFT LOCATION
      RETURN
      END

C*****

      SUBROUTINE INPUT

      INCLUDE PARTHES.INC
      INCLUDE HEATTHES.INC
      CHARACTER * 1 ANS
C** SET DATA

      ANS      = 'y'
      WRITE(*,*) 'PROGRAM CONTROLS'
      WRITE(*,*) '      STEADY STATE SOLUTION (YES OR NO )'
C      READ (*,*) ANS
      CONTROL(1) = .FALSE.
      IF(ANS.EQ.'Y'.OR.ANS.EQ.'y') CONTROL(1) = .TRUE.
C      ANS      = ' '
C      WRITE(*,*) '      TRANSIENT SOLUTION (YES OR NO )'
C      READ (*,*) ANS
C      CONTROL(2) = .FALSE.
C      IF(ANS.EQ.'Y'.OR.ANS.EQ.'y') CONTROL(2) = .TRUE.

      NMAX1    = 42              ! NUMBER OF CELLS IN X1 DIRECTION
      NMAX2    = 58              ! NUMBER OF CELLS IN X2 DIRECTION
      IJ       = NMAX1*NMAX2    ! TOTAL ARRAY SIZE

```

```

MONIT(1)      = 12           ! MONITOR POINT 1:I INDEX
MONIT(2)      = 10           ! MONITOR POINT 1:J INDEX
MONIT(3)      = 21           ! MONITOR POINT 2:I INDEX
MONIT(4)      = 22           ! MONITOR POINT 2:J INDEX
MONIT(5)      = 11           ! MONITOR POINT 3:I INDEX
MONIT(6)      = 5            ! MONITOR POINT 3:J INDEX
MONIT(7)      = 5            ! MONITOR POINT 4:I INDEX
MONIT(8)      = 12           ! MONITOR POINT 4:J INDEX

C    TB1S      = 0.           ! SSTATE BOUNDARY CONDITION
C    TB1F      = 0.           ! SSTATE BOUNDARY CONDITION
C    TB2S      = 0.           ! SSTATE BOUNDARY CONDITION
C    TB2F      = 0.           ! SSTATE BOUNDARY CONDITION

C    ASPECT    = 1.           ! ASPECT RATIO

C    10 WRITE(*,*) ' NEW APSECT RATIO (YES OR NO): CURRENT VALUE =', ASPECT
C      READ(*,*) ANS
C      IF(ANS.EQ.'Y'.OR.ANS.EQ.'y') THEN
C        WRITE(*,*) ' TYPE IN ASPECT RATIO'
C        READ(*,*) ASPECT
C      ENDIF
C**  ENTER THE NUMBER OF CELLS IN EACH COORDINATE DIRECTION
      ANS      = ' '
      WRITE(*,*) 'THE NUMBER OF CELLS IN THE 1 (Y) DIR. IS:',NMAX1
      WRITE(*,*) 'THE NUMBER OF CELLS IN THE 2 (Z) DIR. IS:',NMAX2
      WRITE(*,*) 'DO YOU WANT TO CHANGE EITHER OF THESE? (Y/CR)'
      READ(*,1025) ANS
      IF(ANS.EQ.'Y'.OR.ANS.EQ.'y') THEN
      WRITE(*,*) 'ENTER NMAX1 (MAX IN Y DIRECTION) [LESS THAN 42]'
      READ(*,*) NMAX1
      WRITE(*,*) 'ENTER NMAX2 (MAX IN Z DIRECTION) [LESS THAN 72]'
      READ(*,*) NMAX2
      ENDIF

C**  SET THE DX1 AND DX2 ARRAYS ( OTHOGONAL METRIC:SQRT OF Gi_j)
      ADX1     = 1.25D-6
      ANS      = ' '
      WRITE(*,*) 'DX1 =: ',ADX1,' METERS'
      WRITE(*,*) 'DO YOU WANT TO CHANGE THIS? (Y/CR)'
      READ(*,1025) ANS
      IF(ANS.EQ.'Y'.OR.ANS.EQ.'y') READ(*,*) ADX1

      ADX2     = 1.D-5
      ANS      = ' '
      WRITE(*,*) 'DX2 =: ',ADX2,' METERS'
      WRITE(*,*) 'DO YOU WANT TO CHANGE THIS? (Y/CR)'
      READ(*,1025) ANS
      IF(ANS.EQ.'Y'.OR.ANS.EQ.'y') READ(*,*) ADX2

      DX3      = .014D0
      ANS      = ' '
      WRITE(*,*) 'DX3 =: ',DX3,' METERS'
      WRITE(*,*) 'DO YOU WANT TO CHANGE THIS? (Y/CR)'
      READ(*,1025) ANS
      IF(ANS.EQ.'Y'.OR.ANS.EQ.'y') READ(*,*) DX3

DO 110 J = 1,NMAX2

```

```

DO 110 I = 1,NMAX1
  DX1(I,J) = ADX1
  DX2(I,J) = ADX2
110 CONTINUE
                                !WIDTH OF COMPUTATIONAL CELL m
                                !HEIGHT OF COMPUTATIONAL CELL m

C** SET THE AREA ARRAYS: AR1 AND AR2
DO 120 J = 1,NMAX2
DO 120 I = 1,NMAX1
  AR1(I,J) = DX2(I,J)*DX3
  AR2(I,J) = DX1(I,J)*DX3
120 CONTINUE

C** SET THE CELL VOLUMES ( THE ORTHOGONAL JACOBIAN)
DO 130 J = 1,NMAX2
DO 130 I = 1,NMAX1
  CV(I,J) = DX1(I,J)*DX2(I,J)*DX3
130 CONTINUE

C** OBTAIN THE INFORMATION OF WHICH REGION IS SOLID AND WHICH IS FLUID
ANS = ' '
WRITE(*,*) 'THE WATER BOUNDARY IN THE 1 DIRECTION IS AT:',NWBND1
WRITE(*,*) 'THE WATER BOUNDARY IN THE 2 DIRECTION IS AT:',NWBND2
WRITE(*,*)
WRITE(*,*) 'DO YOU WANT TO CHANGE THESE?'
READ(*,1025) ANS
IF(ANS.EQ.'Y'.OR.ANS.EQ.'y') THEN
  WRITE(*,*) 'ENTER NWBND1 : '
  READ(*,*) NWBND1
  WRITE(*,*) 'ENTER NWBND2 : '
  READ(*,*) NWBND2
ENDIF

C** SET THE CELL MATERIAL IDENTIFICATION NUMBERS ( FOR THE LIBRARY)
DO 140 J = 1,NMAX2
DO 140 I = 1,NMAX1

  MAT(I,J) = 2 ! Silicon identification number

C** ALL BOUNDARY CONDITIONS ARE SET TO VON NEUMANN ON THE OUTSIDE OF THE
C** FOR THE HEAT TRANSFER COMPUTATION.
C IF(I.EQ.1) MAT(I,J) = 1001
C IF(I.EQ.NMAX1) MAT(I,J) = 1001
C IF(J.EQ.1) MAT(I,J) = 1001
C IF(J.EQ.NMAX2) MAT(I,J) = 1001

C** THE BOUNDARY CONDITIONS ARE SET TO THE FOLLOWING FOR THE FLUID MECHAN
C** COMPUTATION

IF(I.EQ.NWBND1) MAT(I,J) = 1002 !DIRICHLET B.C.(NO SLIP) L.H.S
IF(I.EQ.NMAX1) MAT(I,J) = 1001 !VON NEUMANN B.C. (SYMMETRY) S
IF(J.EQ.NWBND2) MAT(I,J) = 1002 !DIRICHLET B.C. (NO SLIP) BOT
IF(J.EQ.NMAX2) MAT(I,J) = 1002 !DIRICHLET B.C. (NO SLIP) TOP

IF(I.GT.NWBND1.AND.I.LT.NMAX1.AND.J.GT.NWBND2.AND.J.LT.NMAX2)
1 MAT(I,J) = 8 !WATER FOR MOMENTUM SOLN.
140 CONTINUE

C** LET'S SET THE HEAT GENERATION IN THE FLUID REGION FOR THE MOM. SOLN.
C** FOR THIS CODE WE USE A VALUE OF -1.D7 AS A CONSTANT AND THEN SCALE BY

```

```

C** THIS TO OBTAIN A REYNOLDS NUMBER OF 2000
C      WRITE(*,*) 'ENTER dp/dx MOMENTUM DRIVING FORCE (SHOULD BE -) '
C      READ(*,*) QGEN

      QGEN      = -1.D7

      DO 150 I=NWBND1+1,NMAX1-1
        DO 150 J=NWBND2+1,NMAX2-1
          Q(I,J) = QGEN*CV(I,J)
150    CONTINUE

1025  FORMAT(A1)
      RETURN
      END

C*****

      SUBROUTINE SETUP

      INCLUDE PARTHES.INC
      INCLUDE HEATTHES.INC
C**   ARRAYS FOR OUTPUT FORMATS

      NIX(1)   = 1
      X1(1)    = -.5*DX1(1,1)
      DO 110 I = 2,NMAX1
        X1(I)  = X1(I-1) +.5*(DX1(I-1,1) + DX1(I,1))
        NIX(I) = I
110    CONTINUE

      X2(1)    = -.5*DX2(1,1)
      DO 120 J = 2,NMAX2
        X2(J)  = X2(J-1) +.5*(DX2(1,J-1) + DX2(1,J))
120    CONTINUE

      CALL CONNECTOR(1)          ! CALCULATE THE THERMAL CONDUCTIVITY
      CALL CONNECTOR(2)          ! CALCULATE THE CONNECTORS
      CALL CONNECTOR(3)          ! CALCULATE BETA
      RETURN
      END

C*****

      SUBROUTINE SSTATE

      INCLUDE PARTHES.INC
      INCLUDE HEATTHES.INC

      CHARACTER *1  ANS
      CHARACTER *10 METHOD

C**   DIMENSIONING FOR THE GRID FILE
      PARAMETER (NWATZ = 50)
      DIMENSION HWAT(NWATZ), FN(NWATZ), G(NWATZ), ANU(NWATZ)

      YZERO = 0.DO
      BBETA = 0.DO
      HTRAT = 0.DO

      WRITE(NGRAPH,4000) NWBND1,NWBND2,NMAX1,NMAX2,DX1(NWBND1,NWBND2),

```

```

1DX2 (NWBND1,NWBND2)
C   WRITE(*,4000) NWBND1,NWBND2,NMAX1,NMAX2,DX1(NWBND1,NWBND2),
C   1DX2(NWBND1,NWBND2)

C**   *****

      LSKIP = 1           ! PRINT ONLY LSKIP ITER STEPS
      ITERS = 0          ! ITERATION COUNTER

50 CONTINUE

      METHOD = 'PSOR'

C** INTERACTIVE SESSION FOR VELOCITY SOLUTION*****

      ANS = ' '
      WRITE(*,*) ' ARE YOU A "SMART" USER ? (CR = YEP !)'
      READ(*,1025) ANS
      IF(ANS.EQ.'N'.OR.ANS.EQ.'n') GO TO 105

      WRITE(*,*) ' '
      ANS = ' '
      WRITE(*,*) 'THE CURRENT SETTING OF LSKIP IS: ',LSKIP
      WRITE(*,*) 'DO YOU WANT TO CHANGE THIS (Y/CR)'
      READ(*,1025) ANS
      IF(ANS.EQ.'Y'.OR.ANS.EQ.'y') THEN
      WRITE(*,*) ' TYPE LSKIP: CURRENT SETTING IS ', LSKIP,' TIME STEPS'
      READ (*,*) LSKIP
      ENDIF

      ANS = ' '
      WRITE(*,*) 'THE U-CRITERION IS: ',TCRIT
      WRITE(*,*) 'DO YOU WANT TO CHANGE THIS (Y/CR)'
      READ(*,1025) ANS
      IF(ANS.EQ.'Y'.OR.ANS.EQ.'y') THEN
      WRITE(*,*) ' TYPE U-CRITERION: CURRENT SETTING ', TCRIT
      READ (*,*) TCRIT
      ENDIF

      ANS = ' '
      WRITE(*,*) 'THE Q-CRITERION IS: ',QMAX
      WRITE(*,*) 'DO YOU WANT TO CHANGE THIS (Y/CR)'
      READ(*,1025) ANS
      IF(ANS.EQ.'Y'.OR.ANS.EQ.'y') THEN
      WRITE(*,*) ' TYPE Q-CRITERION: CURRENT SETTING ', QMAX, ' WATTS'
      READ (*,*) QMAX
      ENDIF
      GO TO 108
105 CONTINUE

      WRITE(*,*) ' IF YOU WANT TO PRINT ONLY EVERY LSKIP LINES THEN,'
      WRITE(*,*) ' TYPE IN THE VALUE OF LSKIP (LIKE 5, 10, 22, ETC)'
      WRITE(*,*) ' OTHERWISE, DEFAULT (HIT CARRAIGE RETURN) '
      WRITE(*,*) ' '
      WRITE(*,*) ' CURRENT SETTING IS PRINT EVERY ', LSKIP,' TIME STEPS'
      READ (*,*) LSKIP

      WRITE(*,*) ' TYPE IN DELTA-U CONVERGENCE CRITERIA: CURRENT ',TCRIT

```

```

READ (*,*) TCRIT

WRITE(*,*) ' TYPE Q-ERROR CRITERION: CURRENT SET = ',QMAX, ' WATTS'
READ (*,*) QMAX

108 CONTINUE

ANS = ' '
WRITE(*,*) 'DO YOU WANT TO CALL OPTOMEG (Y) OR ENTER OMEGA?'
READ(*,1025) ANS
IF(ANS.EQ.'Y'.OR.ANS.EQ.'y') THEN
  CALL OPTOMEG(LSKIP)
  GO TO 115
ENDIF

OMEGA = 1.75D0
ANS = ' '
WRITE(*,*) 'THE CURRENT SETTING FOR OMEGA IS: ',OMEGA
WRITE(*,*) 'DO YOU WANT TO CHANGE THIS? (Y/CR)'
READ(*,1025) ANS
IF(ANS.EQ.'Y'.OR.ANS.EQ.'y') THEN
  WRITE(*,*) ' TYPE IN SOR FACTOR (OMEGA): CURRENT VALUE ', OMEGA
110 READ(*,*) OMEGA
  IF(OMEGA.LE.0..OR.OMEGA.GT.2.)THEN
    WRITE(*,*) ' OMEGA = ',OMEGA,' OUT OF RANGE - TRY AGAIN'
    GO TO 110
  ENDIF
ENDIF

115 ANS = ' '
WRITE(*,*) 'THE INITIAL VELOCITY IS:',TINIT
WRITE(*,*) 'DO YOU WANT TO CHANGE THIS? (Y/CR)'
READ(*,1025) ANS
IF(ANS.EQ.'Y'.OR.ANS.EQ.'y') THEN
  WRITE(*,*) ' TYPE IN INITIAL VELOCITY: CURRENT ' ,TINIT
  READ (*,*) TINIT
ENDIF

ANS = ' '
WRITE(*,*) ' REVIEW ? - CR MEANS NO'           ! LOOK AT THE STUFF
ANS = ' '
READ(*,1025) ANS
IF(ANS.EQ.'Y'.OR.ANS.EQ.'y') THEN
  WRITE(*,*) ' CONVERGENCE CRITERION, UCRIT = ',TCRIT,' M/S'
  WRITE(*,*) ' CONVERGENCE CRITERION, QMAX = ', QMAX,' WATTS'
  WRITE(*,*) ' INITIAL VELOCITY      , UINIT = ',TINIT,' M/S'
  WRITE(*,*) ' SOR FACTOR,           OMEGA = ', OMEGA
  WRITE(*,*) ' LINE SKIPPING,        LSKIP = ', LSKIP
ENDIF

ANS = ' '
WRITE(*,*) ' START OVER ? - CR MEANS NO'
ANS = ' '
READ(*,1025) ANS
IF(ANS.EQ.'Y'.OR.ANS.EQ.'y') GO TO 50

120 CONTINUE

```

C\*\* LETS WRITE OUT SOME STUFF HERE !

```

WRITE(LOUT,1003) METHOD,NMAX1,NMAX2,DX1(1,1),DX2(1,1),OMEGA,ITMAX,
1 TCRIT,QMAX,TINIT
WRITE(*,1001) MONIT
WRITE(LOUT,1001) MONIT

130 CONTINUE
C** SET INITIAL VELOCITIES IN COMPUTATIONAL REGION
DO 150 J = 2,NMAX2-1
DO 150 I = 2,NMAX1-1
IF(MAT(I,J).LE.1000) T(I,J) = TINIT
TOLD(I,J)= T(I,J)
150 CONTINUE

200 CONTINUE ! OR MORE ITERATIONS

IF(OMEGA.LT.SMALL) THEN
WRITE(*,*) ' OMEGA NOT SET CORRECTLY - - TRY AGAIN !'
WRITE(*,*) ' THE VALUE IS: OMEGA = ', OMEGA
GO TO 50
ENDIF

DO 600 M = 1,ITMAX
ITERS = ITERS +1

C** LET'S OBTAIN THE VELOCITY SOLUTION USING THE VPSOR SOLVER

CALL VPSOR(QERROR,SUMR,OMEGA,TUMAX)

IF(MOD(ITERS,LSKIP).EQ.0) THEN
C** PRINT INTERIM (MONITOR) RESULTS TO HARD COPY DEVICE AND SCREEN

WRITE(LOUT,1002) ITERS,TUMAX,T(MONIT(1),MONIT(2)),
1 T(MONIT(3),MONIT(3)),T(MONIT(5),MONIT(6)),T(MONIT(7),MONIT(8))
WRITE(*,1002) ITERS,TUMAX,T(MONIT(1),MONIT(2)),
1 T(MONIT(3),MONIT(3)),T(MONIT(5),MONIT(6)),T(MONIT(7),MONIT(8))
ENDIF

C** CHECK CHANGE IN TEMP FOR THIS ITERATION
IF(TUMAX.LE.TCRIT) THEN
CALL QELAST(QERROR)
GO TO 650 ! IF TEMP CHANGE CRITERA AND QERROR OK, BAIL OUT
ENDIF

600 CONTINUE

650 CONTINUE

ANS = ' '
WRITE(*,*) ' TYPE CR FOR HT TX.- Y TO CONTINUE WITH ITERATIONS'
READ(*,1025) ANS

IF(ANS.EQ.'Y'.OR.ANS.EQ.'y') THEN
WRITE(*,*) 'NEW UCRIT ?' ! CHANGE DELTA-T CONVERGENCE
READ(*,*) TCRIT
WRITE(*,*) 'NEW OMEGA ?' ! CHANGE OMEGA
READ(*,*) OMEGA
GO TO 200 ! ITMAX MORE ITERATIONS
ENDIF

```

```

C** STORE THE VELOCITY FIELD IN THE PROPER U VARIABLE

      DO 700 I=NWBND1+1,NMAX1
        DO 700 J=NWBND2+1,NMAX2-1
          U(I,J) = T(I,J)
          T(I,J) = 0.DO
700 CONTINUE

C** FIND MAX AND MIN ALONG WITH I,J LOCATIONS
C   CALL ASMAX(NMAX1,NMAX2,MAT,U,IMAX,JMAX,TMAX)
C   CALL ASMIN(NMAX1,NMAX2,MAT,U,IMIN,JMIN,TMIN)

C   WRITE(*,1004)   ITERS,OMEGA,TUMAX,QERROR,0.DO,IMAX,JMAX,0.DO,
C   1              IMIN,JMIN
C   WRITE(LOUT,1004) ITERS,OMEGA,TUMAX,QERROR,0.DO,IMAX,JMAX,0.DO,
C   1              IMIN,JMIN

C** WRITE OUT MATERIALS MAP
C   CALL IWRITER (   MAT,'MATERIALS MAP FOR MOMENTUM SOLN      ')
C**   COULD WRITE OUT ANY OTHER INTEGER ARRAY WITH "IWRITER"

      ANS      = ' '
      WRITE(*,*) ' TYPE Q TO QUIT - CR TO CONTINUE WITH HEAT TRANS SOLN'
      READ(*,1025) ANS
      IF(ANS.EQ.'Q'.OR.ANS.EQ.'q') GO TO 10000

              CALL AVGVEL(UAVG)                                !CALL THE avg vel. sub.

C** CALCULATE THE REYNOLDS NUMBER BASED UPON THE HYDRAULIC DIAMETER
C** WE FIRST NEED TO FIND THE CHANNEL DIMENSIONS

C** FIND THE HEIGHT OF THE FLOW CHANNEL
      HEIGHT = 0.DO
      I=NMAX1
      DO 800 J=NWBND2+1,NMAX2-1
        HEIGHT = HEIGHT + DX2(I,J)
800 CONTINUE

C** FIND THE WIDTH OF THE FLOW CHANNEL
      WIDTH = 0.DO
      J=NMAX2
      DO 900 I=NWBND1+1,NMAX1-1
        WIDTH = WIDTH + DX1(I,J)
900 CONTINUE

C** MULTIPLY WIDTH BY TWO TO ACCOUNT FOR SYMMETRY
      WIDTH = WIDTH*2.DO

      WRITE(*,901) HEIGHT
      WRITE(LOUT,901) HEIGHT
      WRITE(NGRAPH,901) HEIGHT
901 FORMAT(1X,'THE FLOW CHANNEL HEIGHT IS: ',6P,F8.3,' MICROMETERS')
      WRITE(*,902) WIDTH
      WRITE(LOUT,902) WIDTH
      WRITE(NGRAPH,902) WIDTH
902 FORMAT(1X,'THE FLOW CHANNEL WIDTH (complete) IS:',6P,F8.3,
A' MICROMETERS')

```

```

C** CALCULATE THE HYDRAULIC DIAMETER
    DHYDR = 4.DO*(HEIGHT*WIDTH)/(2.DO*(HEIGHT + WIDTH))

    WRITE(*,903) DHYDR
    WRITE(LOUT,903) DHYDR
    WRITE(NGRAPH,903) DHYDR
    903 FORMAT(1X,'THE HYDRAULIC DIAMETER IS: ',6P,F8.3,' MICROMETERS')

C** HARDWIRE THE KINEMAT VISCOSITY FOR THIS CALCULATION (VALUE AT 60'C)

    AKNVIS = .55D-6

C** CALCULATE THE DESIRED VELOCITY USING A REYNOLDS NUMBER INPUT

    ANS = ' '
    REYN = 500.DO
    WRITE(*,*) 'THE REYNOLDS NUMBER IS: ',REYN
    WRITE(*,*) 'DO YOU WANT TO CHANGE THIS? (Y/CR)'
    READ(*,1025) ANS
    IF(ANS.EQ.'Y'.OR.ANS.EQ.'y') THEN
    WRITE(*,*) 'ENTER THE REYNOLDS NUMBER: '
    READ(*,*) REYN
    ENDIF

    VELDES = (REYN*AKNVIS)/DHYDR

C** CALCULATE THE RATIO TO MULTIPLY THE AVERAGE VELOCITY BY

    VELRAT = VELDES/UAVG

C** MULTIPLY THE ENTIRE VELOCITY FIELD AND PRESSURE GRAD. BY THIS RATIO
    DO 950 I=1,NMAX1
    DO 950 J=1,NMAX2
    U(I,J) = U(I,J)*VELRAT
    950 CONTINUE

C** WRITE OUT VELOCITY ARRAY
    CALL AWRITER (1,ITERS,U,'STEADY STATE VELOCITY')
C** COULD WRITE OUT ANY OTHER REAL ARRAY WITH "AWRITER"

C** MULTIPLY THE PRESSURE GRADIENT BY THIS RATIO TO GET IT

    PGRAD = -1.D7*VELRAT

    WRITE(*,*) ' THE PRESSURE GRADIENT IS: ',PGRAD,' PA/M'
    WRITE(LOUT,*) ' THE PRESSURE GRADIENT IS: ',PGRAD,' PA/M'
    WRITE(NGRAPH,*) ' THE PRESSURE GRADIENT IS: ',PGRAD,' PA/M'

C** CALCULATE THE PRESSURE DROP ACROSS THE CHIP IN PSI

    PDROP = DX3*PGRAD*.000145038D0
    WRITE(*,1030) DX3,PDROP
    WRITE(LOUT,1030) DX3,PDROP
    WRITE(NGRAPH,1030) DX3,PDROP

    1030 FORMAT(1X,'PRESSURE DROP ACROSS A ',2P,F6.3,' CM CHIP IS: '
    A,0P,F12.3,' PSI')

```

```

WRITE(*,*) ' '
WRITE(LOUT,*) ' '
139

WRITE(*,1031) REYN
WRITE(LOUT,1031) REYN
WRITE(NGRAPH,1031) REYN
1031 FORMAT(1X,'THE REYNOLDS NUMBER IS: ',F10.2,' [UNITLESS]')

CALL AVGVEL(UAVG) !CALL THE avg vel. sub.
WRITE(*,1032) UAVG
WRITE(LOUT,1032) UAVG
WRITE(NGRAPH,1032) UAVG
1032 FORMAT(1X,'THE AVERAGE VELOCITY IS: ',F8.4,' [METERS/SEC]')

C** WRITE OUT TEMPERATURE (velocity) ARRAY ( FOR PLOTTING )
C**
CALL PREPLOT
ANS = ' '
WRITE(*,*) 'DUMP TEMPERATURE (velocity) ARRAY INTO PLOT FILE ?'
WRITE(*,*) ' ( Y=YES, OTHER = NO ) '
READ(*,1025) ANS
IF(ANS.EQ.'Y'.OR.ANS.EQ.'y') THEN
WRITE(*,*) 'ENTER PLOT FILE SPECIFICATIONS ?'
READ '(A)',LABEL
CALL APLOT(U,LABEL,'STEADY STATE velocity ' )
ENDIF

C** NOW FOR THE STEADY STATE HEAT TRANSFER SOLUTION *****
C*****

C** WE MUST SET THE CONNECTORS PROPERLY TO HANDLE HEAT TRANSFER NOW
C** ALL BOUNDARIES ARE SET TO THE VON NEUMANN BOUNDARY CONDITION

DO 2100 I=1,NMAX1
DO 2100 J=1,NMAX2

C** FOR SILICON
MAT(I,J) = 2

C** FOR THE BOUNDARIES
IF(I.EQ.1) MAT(I,J) = 1001
IF(I.EQ.NMAX1) MAT(I,J) = 1001
IF(J.EQ.1) MAT(I,J) = 1001
IF(J.EQ.NMAX2) MAT(I,J) = 1001

C** SET THE WATER MATERIAL NUMBER OF 1 FOR THE FLUID REGION
IF(I.GT.NWBND1.AND.I.LT.NMAX1.AND.J.GT.NWBND2.AND.J.LT.NMAX2)
1 MAT(I,J) = 1

2100 CONTINUE

C** NOW TO OBTAIN THE PROPER CONNECTORS *****

CALL CONNECTOR(1)
CALL CONNECTOR(2)
CALL CONNECTOR(3)

```

```

C** NOW WE MUST BUILD THE HEAT GENERATION ARRAY FOR THE SOLUTION
C** WE MUST OBTAIN FROM THE USER THE HEAT GENERATION RATE

    QWALL      = 1000
    WRITE(*,*) 'THE ENERGY GENERATION WALL FLUX IS [W/CM^2]',QWALL
    WRITE(*,*) 'DO YOU WANT TO CHANGE THIS (Y/N)'
    READ(*,1025) ANS
    IF(ANS.EQ.'Y'.OR.ANS.EQ.'y') THEN
        WRITE(*,*) 'ENTER THE HEAT GENERATION RATE FOR THE ENERGY EQN.'
        WRITE(*,*) 'ENTER THIS IN W/CM^2'
        READ(*,*) QWALL
    ENDIF

    WRITE(LOUT,2101) QWALL
    WRITE(NGRAPH,2101) QWALL
2101 FORMAT(1X,'THE ENERGY GENERATION WALL FLUX IS: ',F10.3,
    A' [W/CM^2]')

C** CONVERT FROM W/CM^2 TO W/M^2

    QWALL = QWALL*10000.DO

C** NOW TO FIND THE FLUX AT THE WALL USING THE FIRST 3 ROWS AS HEAT GEN.
    SUMVOL    = 0.DO
    DO 2025 I=2,NMAX1-1
        DO 2025 J=2,4
            SUMVOL = SUMVOL+CV(I,J)
2025    CONTINUE

C** FIND THE AREA OF HEAT TRANSFER FOR Q AT THE WALL
    SUMAR     = 0.DO
    J=4
    DO 2030 I=2,NMAX1-1
        SUMAR = SUMAR + AR2(I,J)
2030    CONTINUE

C** FIND THE TOTAL HEAT GENERATION WITHIN THE SOLID REGION

    QUTOT    = QWALL*SUMAR

C** FIND THE VOLUMETRIC HEAT GENERATION WITHIN THE SOLID REGION

    QGEN     = QUTOT/SUMVOL

C** FIND THE FACIAL AREA OF FLOW
    SUMFAR   = 0.DO
    DO 2040 I=NWBND1+1,NMAX1-1
        DO 2040 J=NWBND2+1,NMAX2-1
            SUMFAR = SUMFAR + DX1(I,J)*DX2(I,J)
2040    CONTINUE

C** CLEAR THE HEAT GENERATION ARRAY
    DO 2045 I=1,NMAX1
        DO 2045 J=1,NMAX2
            Q(I,J) = 0.DO
2045    CONTINUE

C** DX3 IS THE DELTA X IN THE 3 DIRECTION (same as in subroutine input)
C** TFVOL IS THE TOTAL VOLUME OF THE FLOW CELLS

```

C\*\* this simply divides the heat volumetrically throughout the flow region  
 C\*\* it also uses the solution for the momentum equation to divide the heat  
 C\*\* flow up within the flow field.

```
DO 2000 I=2,NMAX1-1
  DO 2000 J=2,NMAX2-1
```

```
C** FOR THE ENERGY GENERATION REGION
  IF(I.GT.1.AND.I.LT.NMAX1.AND.J.GT.1.AND.J.LT.5)
  1 Q(I,J) = -QGEN*CV(I,J)
```

```
C** FOR THE FLUID FLOW REGION
  IF(I.GT.NWBND1.AND.I.LT.NMAX1.AND.J.GT.NWBND2.AND.J.LT.NMAX2)
  1 Q(I,J) = (U(I,J)/UAVG)*((DX1(I,J)*DX2(I,J))/SUMFAR)*QUTOT
```

```
2000 CONTINUE
```

C\*\* SEE IF THE HEAT GENERATION IS ZERO.

```
SUMHT = 0.DO
DO 2047 I=2,NMAX1-1
  DO 2047 J=2,NMAX2-1
    SUMHT = SUMHT + Q(I,J)
2047 CONTINUE
```

```
WRITE(*,2048) SUMHT
WRITE(LOUT,2048) SUMHT
WRITE(NGRAPH,2048) SUMHT
2048 FORMAT(1X,'THE SUM OF THE HEAT GENERATION IS: ',E12.3,' [WATTS]')
```

C\*\* SEE IF THE USER WANTS TO DUMP THE UTILITY ARRAYS

```
ANS = ' '
WRITE(*,*) 'DO YOU WANT TO DUMP THE HEAT GEN. ARRAY? (Y/CR)'
READ(*,1025) ANS
IF(ANS.EQ.'Y'.OR.ANS.EQ.'y')
  1 CALL AWRITER(1,1,Q,'HEAT GENERATION ARRAY [WATTS]')
```

```
ANS = ' '
WRITE(*,*) 'DO YOU WANT TO DUMP THE CONNECTOR ARRAYS? (Y/CR)'
READ(*,1025) ANS
IF(ANS.EQ.'Y'.OR.ANS.EQ.'y') THEN
  CALL AWRITER(1,1,CX1,'Y DIRECTION CONNECTOR ARRAY')
  CALL AWRITER(1,1,CX2,'Z DIRECTION CONNECTOR ARRAY')
ENDIF
```

C\*\* NOW TO BEGIN THE SOLUTION FOR THE TEMPERATURE PROFILE

```
LSKIP = 1 ! PRINT ONLY LSKIP ITER STEPS
ITERS = 0 ! ITERATION COUNTER
2050 CONTINUE
```

```
METHOD = 'PSOR'
```

C\*\* INTERACTIVE SESSION FOR TEMPERATURE SOLUTION\*\*\*\*\*

```
ANS = ' '
WRITE(*,*) ' ARE YOU A "SMART" USER ? (CR = YEP !)'
READ(*,1025) ANS
IF(ANS.EQ.'N'.OR.ANS.EQ.'n') GO TO 2105
```

```
ANS = ' '
WRITE(*,*) ' '
LSKIP = 5
WRITE(*,*) 'LSKIP = :',LSKIP
WRITE(*,*) 'DO YOU WANT TO CHANGE THIS? (Y/CR)'
READ(*,1025) ANS
IF(ANS.EQ.'Y'.OR.ANS.EQ.'y') THEN
WRITE(*,*) ' TYPE LSKIP: CURRENT SETTING IS ', LSKIP,' TIME STEPS'
READ (*,*) LSKIP
ENDIF
```

```
ANS = ' '
TCRIT = .01D0
WRITE(*,*) 'THE T-CRITERION IS: ',TCRIT
WRITE(*,*) 'DO YOU WANT TO CHANGE THIS? (Y/CR)'
READ(*,1025) ANS
IF(ANS.EQ.'Y'.OR.ANS.EQ.'y') THEN
WRITE(*,*) ' TYPE T-CRITERION: CURRENT SETTING ', TCRIT
READ (*,*) TCRIT
ENDIF
```

```
ANS = ' '
WRITE(*,*) 'THE Q-CRITERION IS: ',QMAX
WRITE(*,*) 'DO YOU WANT TO CHANGE THIS? (Y/CR)'
READ(*,1025) ANS
IF(ANS.EQ.'Y'.OR.ANS.EQ.'y') THEN
WRITE(*,*) ' TYPE Q-CRITERION: CURRENT SETTING ', QMAX, ' WATTS'
READ (*,*) QMAX
ENDIF
GO TO 2108
```

2105 CONTINUE

```
WRITE(*,*) ' IF YOU WANT TO PRINT ONLY EVERY LSKIP LINES THEN,'
WRITE(*,*) ' TYPE IN THE VALUE OF LSKIP (LIKE 5, 10, 22, ETC)'
WRITE(*,*) ' OTHERWISE, DEFAULT (HIT CARRAIGE RETURN) '
WRITE(*,*) ' '
WRITE(*,*) ' CURRENT SETTING IS PRINT EVERY ', LSKIP,' TIME STEPS'
READ (*,*) LSKIP
```

```
WRITE(*,*) ' TYPE IN DELTA-T CONVERGENCE CRITERIA: CURRENT ',TCRIT
READ (*,*) TCRIT
```

```
WRITE(*,*) ' TYPE Q-ERROR CRITERION: CURRENT SET = ',QMAX, ' WATTS'
READ (*,*) QMAX
```

2108 CONTINUE

```
ANS = ' '
WRITE(*,*) 'DO YOU WANT TO CALL OPTOMEG (Y) OR ENTER OMEGA?'
READ(*,1025) ANS
IF(ANS.EQ.'Y'.OR.ANS.EQ.'y') THEN
CALL OPTOMEG(LSKIP)
```

GO TO 2115  
ENDIF

142

```
ANS      = ' '
WRITE(*,*) 'OMEGA IS: ',OMEGA
WRITE(*,*) 'DO YOU WANT TO CHANGE THIS? (Y/CR) '
READ(*,1025) ANS
IF(ANS.EQ.'Y'.OR.ANS.EQ.'y') THEN
2110 WRITE(*,*) ' TYPE IN SOR FACTOR (OMEGA): CURRENT VALUE ', OMEGA
    READ(*,*) OMEGA
        IF(OMEGA.LE.0..OR.OMEGA.GT.2.)THEN
            WRITE(*,*) ' OMEGA = ',OMEGA,' OUT OF RANGE - TRY AGAIN'
            GO TO 2110
        ENDIF
    ENDIF
ENDIF
```

```
2115 ANS      = ' '
    TINIT    = 25.0
    WRITE(*,*) 'THE INITIAL TEMPERATURE IS: ',TINIT
    WRITE(*,*) 'DO YOU WANT TO CHANGE THIS? (Y/CR) '
    READ(*,1025) ANS
    IF(ANS.EQ.'Y'.OR.ANS.EQ.'y') THEN
        WRITE(*,*) ' TYPE IN INITIAL TEMPERATURE: CURRENT ' ,TINIT
        READ (*,*) TINIT
    ENDIF
```

```
WRITE(*,*) ' REVIEW ? - CR MEANS NO'           ! LOOK AT THE STUFF
ANS      = ' '
READ(*,1025) ANS
IF(ANS.EQ.'Y'.OR.ANS.EQ.'y') THEN
WRITE(*,*) ' CONVERGENCE CRITERION, TCRIT = ',TCRIT,' DEGREES C'
WRITE(*,*) ' CONVERGENCE CRITERION, QMAX = ', QMAX,' WATTS'
WRITE(*,*) ' INITIAL TEMPERATURE, TINIT = ',TINIT,' DEGREES C'
WRITE(*,*) ' SOR FACTOR, OMEGA = ', OMEGA
WRITE(*,*) ' LINE SKIPPING, LSKIP = ', LSKIP
ENDIF
```

```
WRITE(*,*) ' START OVER ? - NO MEANS NO'
ANS      = ' '
READ(*,1025) ANS
IF(ANS.EQ.'Y'.OR.ANS.EQ.'y') GO TO 2050
```

2120 CONTINUE

```
C** LETS WRITE OUT SOME STUFF HERE !
WRITE(LOUT,3003) METHOD,NMAX1,NMAX2,DX1(1,1),DX2(1,1),OMEGA,ITMAX,
1 TCRIT,QMAX,TINIT
WRITE(*,3001) MONIT
WRITE(LOUT,3001) MONIT
```

2130 CONTINUE

```
C** SET INITIAL TEMPERATURES IN COMPUTATIONAL REGION
DO 2150 J = 2,NMAX2-1
DO 2150 I = 2,NMAX1-1
    IF(MAT(I,J).LE.1000) T(I,J) = TINIT
    TOLD(I,J)= T(I,J)
```

2150 CONTINUE

2200 CONTINUE

! OR MORE ITERATIONS

```

IF(OMEGA.LT.SMALL) THEN
WRITE(*,*) ' OMEGA NOT SET CORRECTLY - - TRY AGAIN !'
WRITE(*,*) ' THE VALUE IS: OMEGA = ', OMEGA
GO TO 2050
ENDIF

DO 2600 M = 1,ITMAX
ITERS = ITERS +1

C** LET'S OBTAIN THE TEMPERATURE SOLUTION USING THE PSOR SOLVER

CALL PSOR(QERROR,SUMR,OMEGA,TUMAX)

IF(MOD(ITERS,LSKIP).EQ.0) THEN
C** PRINT INTERIM (MONITOR) RESULTS TO HARD COPY DEVICE AND SCREEN

WRITE(LOUT,3002) ITERS,TUMAX,T(MONIT(1),MONIT(2)),
1 T(MONIT(3),MONIT(3)),T(MONIT(5),MONIT(6)),T(MONIT(7),MONIT(8))
WRITE(*,3002) ITERS,TUMAX,T(MONIT(1),MONIT(2)),
1 T(MONIT(3),MONIT(3)),T(MONIT(5),MONIT(6)),T(MONIT(7),MONIT(8))
ENDIF

C** CHECK CHANGE IN TEMP FOR THIS ITERATION
IF(TUMAX.LE.TCRIT) THEN
CALL QELAST(QERROR)
GO TO 2650 ! IF TEMP CHANGE CRITERA AND QERROR OK, BAIL OUT
ENDIF

2600 CONTINUE

2650 CONTINUE

ANS = ' '
WRITE(*,*) ' TYPE CR TO QUIT- Y TO CONTINUE WITH ITERATIONS'
READ(*,1025) ANS

IF(ANS.EQ.'Y'.OR.ANS.EQ.'y') THEN
WRITE(*,*) 'NEW TCRIT ?' ! CHANGE DELTA-T CONVERGENCE
READ(*,*) TCRIT
WRITE(*,*) 'NEW OMEGA ?' ! CHANGE OMEGA
READ(*,*) OMEGA
GO TO 2200 ! ITMAX MORE ITERATIONS
ENDIF

C** SET THE TEMPERATURES ON THE BOUNDARIES FOR PLOTTING PURPOSES
DO 2700 I=1,NMAX1
DO 2700 J=1,NMAX2
IF(I.EQ.1) T(I,J) = T(I+1,J)
IF(I.EQ.NMAX1) T(I,J) = T(I-1,J)
IF(J.EQ.1) T(I,J) = T(I,J+1)
IF(J.EQ.NMAX2) T(I,J) = T(I,J-1)
2700 CONTINUE

C** FIND MAX AND MIN ALONG WITH I,J LOCATIONS
C CALL ASMAX(NMAX1,NMAX2,MAT,T,IMAX,JMAX,TMAX)
C CALL ASMIN(NMAX1,NMAX2,MAT,T,IMIN,JMIN,TMIN)

```

```

C      WRITE(*,3004)   ITERS,OMEGA,TUMAX,QERROR,0.D0,IMAX,JMAX,0.D0,
C      1              IMIN,JMIN
C      WRITE(LOUT,3004) ITERS,OMEGA,TUMAX,QERROR,0.D0,IMAX,JMAX,0.D0,
C      1              IMIN,JMIN

C**   WRITE OUT MATERIALS MAP
      CALL IWRITER ( MAT,'MATERIALS MAP FOR TEMPERATURE SOLN      ')
C**   COULD WRITE OUT ANY OTHER INTEGER ARRAY WITH "IWRITER"

C**   LET'S FIND THE AVERAGE (mean) BULK TEMPERATURE IN THE FLUID REGION

      SUM      = 0.0
      DO 2750 J=NWBND2+1,NMAX2-1
      DO 2750 I=NWBND1+1,NMAX1-1
          SUM = SUM + (T(I,J))*(U(I,J)/UAVG)
2750 CONTINUE
      TWAVG = SUM/((NMAX1-1-NWBND1)*(NMAX2-1-NWBND2))
C      WRITE(NGRAPH,*) 'THE BULK FLUID TEMPERATURE IS: ',TWAVG

C**   NOW USE THE BULK ENERGY BALANCE TO FIND THE BULK FLUID TEMP. CHANGE
      CP      = 4181          !J/KG*K
      AMDOT = 1000*SUMFAR*UAVG

      TBDIFF = QTOT/(AMDOT*CP)

C**   SCALE THE TEMPERATURE TO OBTAIN THE CORRECT DISTRIBUTION
C**   THIS USES THE BULK ENERGY BALANCE AND ADDS THE TEMPERATURE
C**   DIFFERENCE TO IT.

      TDIFF = TBDIFF + TINIT - TWAVG
      DO 2800 I=1,NMAX1
      DO 2800 J=1,NMAX2
          T(I,J) = T(I,J) + TDIFF
2800 CONTINUE

C**   LET'S FIND THE AVERAGE BULK TEMPERATURE IN THE FLUID REGION

      SUM      = 0.0
      DO 2805 J=NWBND2+1,NMAX2-1
      DO 2805 I=NWBND1+1,NMAX1-1
          SUM = SUM + (T(I,J))*(U(I,J)/UAVG)
2805 CONTINUE
      TWAVG = SUM/((NMAX1-1-NWBND1)*(NMAX2-1-NWBND2))
      WRITE(*,2806) TWAVG
      WRITE(NGRAPH,2806) TWAVG
      WRITE(LOUT,2806) TWAVG
2806 FORMAT(1X,'THE BULK FLUID TEMPERATURE IS: ',F10.3,' [DEGREES C]')

C**   WRITE OUT TEMPERATURE ARRAY
      CALL AWRITER (1,ITERS,T,'STEADY STATE TEMPERATURE      ')
C**   COULD WRITE OUT ANY OTHER REAL ARRAY WITH "AWRITER"

C**   WRITE OUT TEMPERATURE ARRAY ( FOR PLOTTING )
C**
      ANS = ' '
      WRITE(*,*) 'DUMP TEMPERATURE ARRAY INTO PLOT FILE ?'
      WRITE(*,*) ' ( Y=YES, OTHER = NO ) '
      READ(*,1025) ANS
      IF(ANS.EQ.'Y'.OR.ANS.EQ.'y') THEN

```

```

WRITE(*,*) 'ENTER PLOT FILE SPECIFICATIONS ?'
READ '(A)', LABEL
CALL APLOT(T, LABEL, 'STEADY STATE TEMPERATURE ')
ENDIF

C** WRITE OUT IMPORTANT INFORMATION TO THE GRAPHING FILE
C** THIS FILE CAN BE USED IN A QUATTRO SPREADSHEET.

ANS = ' '
WRITE(*,*) ' WANT TO DUMP INFO TO A GRAPH FILE? (NO/CR)'
READ(*,1025) ANS
IF(ANS.NE.'N'.OR.ANS.NE.'n') THEN

C** FOR THE HEAT TRANSFER COEFFICIENT

COND = .66D0
INCR = 1
I=NWBND1+1
DO 2810 J=NWBND2+1,NMAX2-1
  DER = (T(I+1,J)-T(I,J))/((DX1(I,J)+DX1(I+1,J))/2.DO)
  HWAT(INCR) = -COND*DER/(T(I-1,J)-T(WAVG))
  ZEE = 0.DO
  DO 2807 JC=NWBND2+1,J
    ZEE = ZEE + DX2(I,J)
2807 CONTINUE
  ZEE = ZEE - DX2(I,J)/2.DO
  WRITE(NGRAPH,4010) INCR,ZEE,HWAT(INCR)
C   WRITE(*,4010) INCR,ZEE,HWAT(INCR)
  INCR = INCR + 1
2810 CONTINUE

C** CALCULATE THE ANALYTICAL (constant) HEAT TRANSFER COEFFICIENT

HANALY = (140.DO/17.DO)*(COND/DHYDR)
WRITE(*,2811) HANALY
WRITE(LOUT,2811) HANALY
WRITE(NGRAPH,2811) HANALY
2811 FORMAT(1X,'TUCKERMANS (constant) H IS: ',F12.2,' [W/M^2K]')

C** COMPUTE YZERO (THE NONDIMENSIONAL HOT SPOT TEMPERATURE) AND BETA

WRITE(NGRAPH,*) ' '
CONDSI = 148
CONRAT = CONDSI/COND

WRITE(*,*) 'THE CONDUCTIVITY RATIO IS: ',CONRAT
WRITE(*,*) 'DO YOU WANT TO CHANGE THIS? '
READ(*,1025) ANS
IF(ANS.EQ.'Y'.OR.ANS.EQ.'y') THEN
  READ(*,*) CONRAT
ENDIF

COND = CONDSI/CONRAT

WRITE(*,2815) CONRAT
WRITE(LOUT,2815) CONRAT
WRITE(NGRAPH,2815) CONRAT
2815 FORMAT(1X,'THE CONDUCTIVITY RATIO IS: ',F10.3)
WRITE(*,2816) COND
WRITE(LOUT,2816) COND

```

```

WRITE(NGRAPH,2816) COND
2816 FORMAT(1X,'THE CONDUCTIVITY OF WATER IS: ',F7.4,' [W/MK]')

      TYDIFF = T(NWBND1,NWBND2) - TWAVG
      J=2
      WWALL = 0.DO
      DO 2820 I=2,NWBND1-1
      WWALL = WWALL + DX1(I,J)
2820 CONTINUE
      WWALL = 2.DO*WWALL

      WRATIO = WIDTH/WWALL

      YZERO = TYDIFF/((QWALL/CONDSI)*HEIGHT*(1.DO+WRATIO))
      BBETA = (1.DO/WRATIO)*CONRAT*((WIDTH/HEIGHT)**2)

C** ANALYTICAL YZERO
      YZERAN = (1.DO/3.DO)*(1.DO+{.3DO*BBETA})

      WRITE(*,2821) YZERO
      WRITE(LOUT,2821) YZERO
      WRITE(NGRAPH,2821) YZERO
2821 FORMAT(1X,'THE VALUE OF Yo IS: ',F10.5,' [UNITLESS]')

      WRITE(*,2822) YZERAN
      WRITE(LOUT,2822) YZERAN
      WRITE(NGRAPH,2822) YZERAN
2822 FORMAT(1X,'THE INTEGRAL ANALYSIS Yo IS: ',F10.5,' [UNITLESS]')

      WRITE(*,2823) BBETA
      WRITE(LOUT,2823) BBETA
      WRITE(NGRAPH,2823) BBETA
2823 FORMAT(1X,'THE VALUE OF BETA IS: ',F12.4,' [UNITLESS]')

      WRITE(*,*)
      WRITE(NGRAPH,*)

C** FOR THE FUNCTION F (THE NONDIMENSIONAL TEMPERATURE DIST. UP THE FIN)

C      WRITE(*,4015)
C      WRITE(NGRAPH,4015)
      I=NWBND1
      INCR = 1
      DO 2830 J=NWBND2+1,NMAX2-1
      TYDIFF = T(NWBND1,NWBND2) - T(I,J)
      ZEE = 0.DO
      DO 2825 JC=NWBND2+1,J
      ZEE = ZEE + DX2(I,J)
2825 CONTINUE
      ZEE = ZEE - DX2(I,J)/2.DO
      FN(INCR) = TYDIFF/((QWALL/CONDSI)*HEIGHT*(1.DO+WRATIO)
      * (ZEE/HEIGHT)*(1.DO-(ZEE/(2.DO*HEIGHT))))
C      WRITE(*,4020) INCR,ZEE/HEIGHT,FN(INCR)
C      WRITE(NGRAPH,4020) INCR,ZEE/HEIGHT,FN(INCR)
      INCR = INCR + 1
2830 CONTINUE

C** FOR THE FUNCTION G (THE NONDIMENSIONAL HEAT TRANSFER COEFFICIENT

```

```

C      WRITE(*,4025)
C      WRITE(NGRAPH,4025)
      WRITE(NGRAPH,4005)
      WRITE(*,4005)
      I=NWBND1
      INCR = 1
      DO 2840 J=NWBND2+1,NMAX2-1
      DER = (T(I+2,J) - T(I+1,J))/((DX1(I+1,J)+DX1(I+2,J))/2.DO)
      ZEE = 0.DO
      DO 2835 JC = NWBND2+1,J
      ZEE = ZEE + DX2(I,J)
2835  CONTINUE
      ZEE = ZEE - DX2(I,J)/2.DO
      G(INCR) = -COND*DER/(((WWALL+WIDTH)/(2.DO*HEIGHT))*QWALL)
      WRITE(*,4010) INCR,ZEE,ZEE/HEIGHT,HWAT(INCR),FN(INCR),G(INCR)
      WRITE(NGRAPH,4010) INCR,ZEE,ZEE/HEIGHT,HWAT(INCR),FN(INCR)
      A      ,G(INCR)
      INCR = INCR + 1
2840  CONTINUE

C** FOR THE NUSSELT NUMBER
      WRITE(*,4035)
      WRITE(NGRAPH,4035)
      I=NWBND1
      INCR = 1
      DO 2850 J=NWBND2+1,NMAX2-1
      ZEE = 0.DO
      DO 2845 JC = NWBND2+1,J
      ZEE = ZEE + DX2(I,J)
2845  CONTINUE
      ZEE = ZEE - (DX2(I,J)/2.DO)
      ANU(INCR) = HWAT(INCR)*DHYDR/COND
C      ANU(INCR) = BBETA*G(INCR)/(YZERO-(ZEE/HEIGHT))*
C      1      (1.DO-(Z/(2.DO*HEIGHT))*FN(INCR))
      WRITE(*,4040) INCR,ZEE/HEIGHT,ANU(INCR)
      WRITE(NGRAPH,4040) INCR,ZEE/HEIGHT,ANU(INCR)
      INCR = INCR + 1
2850  CONTINUE

C** CALCULATE THE RATIO OF HEAT FLOW UP THE FIN TO THE TOTAL (AVERAGE)
      J=NWBND2
      SUMHT = 0.DO
      DO 2860 I=2,NWBND1
      DER = (T(I,J+1)-T(I,J))/((DX2(I,J+1)+DX2(I,J))/2.DO)
      SUMHT = SUMHT - CONDSI*DER
2860  CONTINUE

      SUMAR = 0.DO
      J=NWBND2
      DO 2866 I=2,NMAX1-1
      SUMAR = SUMAR + AR2(I,J)
2866  CONTINUE

      J=NWBND2
      ARR = 0.DO
      DO 2867 I=2,NWBND1
      ARR = ARR + AR2(I,J)
2867  CONTINUE
      ARRAT = ARR/SUMAR

```

```

HTRAT = (SUMHT/(QWALL*(NWBND1-1)))*ARRAT          148
WRITE(*,2861) HTRAT
WRITE(LOUT,2861) HTRAT
WRITE(NGRAPH,2861) HTRAT
2861 FORMAT(1X,'THE RATIO OF FLUX UP THE FIN TO TOTAL FLUX IS: ',
AF7.5,' [UNITLESS]')

C** WRITE OUT THE PEAK WATER AND SILICON TEMPERATURES
WRITE(*,2862) T(NWBND1+1,NWBND2+1)
WRITE(LOUT,2862) T(NWBND1+1,NWBND2+1)
WRITE(NGRAPH,2862) T(NWBND1+1,NWBND2+1)
2862 FORMAT(1X,'THE PEAK WATER TEMPERATURE IS: ',F9.3,' [DEGREES C]')

WRITE(*,2863) T(NMAX1-1,5)
WRITE(LOUT,2863) T(NMAX1-1,5)
WRITE(NGRAPH,2863) T(NMAX1-1,5)
2863 FORMAT(1X,'THE PEAK SILICON TEMP. IS: ',F9.3,' [DEGREES C]')

C** WRITE OUT THE DIMENSIONAL TEMPERATURE DISTRIBUTION UP THE FIN

WRITE(*,*)
WRITE(NGRAPH,*)

WRITE(*,4045)
WRITE(NGRAPH,4045)
INCR = 1
I=2
DO 2870 J=2,NMAX2-1
ZEE = 0.D0
DO 2865 JC=2,J
ZEE = ZEE + DX2(I,J)
2865 CONTINUE
WRITE(*,4050) INCR,ZEE,T(I,J)
WRITE(NGRAPH,4050) INCR,ZEE,T(I,J)
INCR = INCR + 1
2870 CONTINUE

ENDIF          !ENDIF FOR THE GRAPHING CASE

10000 RETURN

C** OUTPUT FORMATS
1001 FORMAT(/30X,'ITERATION DETAILS'/9X,
1'ITER NO. DELTA-U MONITOR VELOCITY'/
1 31X,4('U(',I3,',',I3,')',2X)/)
1002 FORMAT(8X,I6,F12.4,5F12.2)
1003 FORMAT(/
+ 5X,'SOLUTION METHOD',A10 /
1/5X,'NUMBER OF CELLS IN X1-DIRECTION, NMAX1 - - - ',I5
2/5X,'NUMBER OF CELLS IN X2-DIRECTION, NMAX2 - - - ',I5
3/5X,'WIDTH OF CELLS IN X1-DIRECTION, DX1 - - - ',E10.5
4/5X,'WIDTH OF CELLS IN X2-DIRECTION, DX2 - - - ',E10.5
5/5X,'OVER-RELAXATION FACTOR',OMEGA - - - ',F8.3
6/5X,'MAXIMUM NUMBER ITERATIONS',ITMAX - - - ',I4
7/5X,'DELTA-PHI ERROR CRITERION',TCRIT - - - ',1P,E12.3
8/5X,'HEAT BALANCE ERROR CRITERION',QMAX - - - ',0P,F8.3
9/5X,'INITIAL VELOCITY',TINIT - - - ',1P,E11.4
B)

```

```

1004 FORMAT(//
+25X,'STEADY-STATE SOLUTION SUMMARY '//
1/15X,'TOTAL NUMBER OF ITERATIONS',ITERS - - - -',I5
+/15X,'OVER-RELAXATION FACTOR',OMEGA - - - -',F10.5
2/15X,'MAXIMUM VEL. CHANGE, LAST',DTMAX - - - -',F10.5
4/15X,'SYSTEM HEAT BALANCE ERROR',QERROR - - - -',1P,E12.3
5/15X,'MAXIMUM SYSTEM VELOCITY',UMAX - - - -',F10.5
6/15X,'',LOCATION',U(I,J) - - - T('',I3,'','','',
7I3,'')'
8/15X,'MINIMUM SYSTEM VELOCITY',UMIN - - - -',F10.5
9/15X,'',LOCATION',T(I,J) - - - T('',I3,'','','',
A I3,'')'
B/)

```

```
1025 FORMAT(A1)
```

C\*\* FORMATS FOR HEAT TRANSFER CALCULATION

```

3001 FORMAT(//30X,'ITERATION DETAILS'/9X,
1'ITER NO. DELTA-T',MONITOR TEMPERATURE'/
1 31X,4('T('',I3,'','','',I3,'')',2X)//
3002 FORMAT(8X,I6,F12.4,5F12.2)
3003 FORMAT(//
+ 5X,'SOLUTION METHOD',A10 /
1/5X,'NUMBER OF CELLS IN X1-DIRECTION',NMAX1 - - - -',I5
2/5X,'NUMBER OF CELLS IN X2-DIRECTION',NMAX2 - - - -',I5
3/5X,'WIDTH OF CELLS IN X1-DIRECTION',DX1 - - - -',E10.5
4/5X,'WIDTH OF CELLS IN X2-DIRECTION',DX2 - - - -',E10.5
5/5X,'OVER-RELAXATION FACTOR',OMEGA - - - -',F8.3
6/5X,'MAXIMUM NUMBER ITERATIONS',ITMAX - - - -',I4
7/5X,'DELTA-PHI ERROR CRITERION',TCRIT - - - -',1P,E12.3
8/5X,'HEAT BALANCE ERROR CRITERION',QMAX - - - -',0P,F8.3
9/5X,'INITIAL TEMPERATURE',TINIT - - - -',1P,E11.4
B)

```

```

3004 FORMAT(//
+25X,'STEADY-STATE SOLUTION SUMMARY '//
1/15X,'TOTAL NUMBER OF ITERATIONS',ITERS - - - -',I5
+/15X,'OVER-RELAXATION FACTOR',OMEGA - - - -',F10.5
2/15X,'MAXIMUM TEMP CHANGE, LAST',DTMAX - - - -',F10.5
4/15X,'SYSTEM HEAT BALANCE ERROR',QERROR - - - -',1P,E12.3
5/15X,'MAXIMUM SYSTEM TEMPERATURE',TMAX - - - -',F10.2
6/15X,'',LOCATION',T(I,J) - - - T('',I3,'','','',
7I3,'')'
8/15X,'MINIMUM SYSTEM TEMPERATURE',TMIN - - - -',F10.5
9/15X,'',LOCATION',T(I,J) - - - T('',I3,'','','',
A I3,'')'
B/)

```

C\*\* FORMATS FOR THE GRAPH FILE

```

4000 FORMAT(1X,/' GRAPH FILE FOR TEMPERATURE RESULTS',//
A,' The left water boundary is at:',I5,/
B,' The bottom water boundary is at:',I5,/
C,'The maximum horizontal cells is:',I5,/
D,'The maximum vertical cells is:',I5,/
E,'Delta x horizontal is:',E12.5,/
F,'Delta x vertical is:',E12.5,/
G/)

```

```

C 4005 FORMAT(1X,/' Cell # z[meters] z/h h(z) f(z)
C A g(z) ')

```

```
4005 FORMAT(1X,' Cell # z z/h h(z) f(z)
```

```

A      g(z)',/,',          [meters]          [1]          [W/m*k]
B      [1]          [1]',/,',-----
C-----')

```

```
4010 FORMAT(1X,3X,I3,3X,E10.5,F12.5,2X,F12.3,F12.5,F12.5)
```

```
C 4015 FORMAT(1X,/' # of cell in z dir.      z/h          f(z)')
```

```
C 4020 FORMAT(1X,11X,I3,8X,E12.5,F12.3)
```

```
C 4025 FORMAT(1X,/' # of cell in z dir.      z/h          g(z)')
```

```
C 4030 FORMAT(1X,11X,I3,8X,E12.5,F12.3)
```

```
4035 FORMAT(1X,/' # of cell in z dir.      z/h          NU(z)',/
A,'-----')
```

```
4040 FORMAT(1X,11X,I3,8X,E12.5,F12.3)
```

```
4045 FORMAT(1X,/' Cell #      z[meters]          T(z) [C]',/
A,'-----')
```

```
4050 FORMAT(1X,3X,I3,3X,E12.5,F13.3)
```

END

\*\*\*\*\*

SUBROUTINE TRANSIENT

INCLUDE PARTHES.INC  
INCLUDE HEATHES.INC

RETURN  
END

\*\*\*\*\*

SUBROUTINE CONNECTOR(MODE)

INCLUDE PARTHES.INC  
INCLUDE HEATHES.INC

C\*\* MODE = 1 CALCULATE THE THERMAL CONDUCTIVITY ARRAY  
C\*\* MODE = 2 CALCULATE THE CONNECTOR ARRAYS  
C\*\* MODE = 3 CALCULATE THE BETA ARRAY

GO TO (100,200,300),MODE

100 CONTINUE

CALL PROPLIB ! SET THERMAL CONDUCTIVITY ARRAY, CAY(I,J)  
GO TO 800

200 CONTINUE

C\*\* COMPUTE CONNECTORS, CX1(I,J) AND CX2(I,J)

HX1 = BIG

HX2 = BIG

DO 250 J = 1,NMAX2-1

DO 250 I = 1,NMAX1-1

C HX1 = HC1(I,J)

C HX2 = HC2(I,J)

```

CX1(I,J) = DX1(I,J)/CAY(I,J)+DX1(I+1,J)/CAY(I+1,J) + 2./HX1
CX1(I,J) = 2.D0*AR1(I,J)/CX1(I,J)

CX2(I,J) = DX2(I,J)/CAY(I,J)+DX2(I,J+1)/CAY(I,J+1) + 2./HX2
CX2(I,J) = 2.D0*AR2(I,J)/CX2(I,J)
250 CONTINUE
GO TO 800

300 CONTINUE                                ! COMPUTE BETA ARRAY
DO 350 J = 1,NMAX2-1
DO 350 I = 1,NMAX1-1
BETA(I,J) = BETA(I,J)/CV(I,J)
350 CONTINUE

800 CONTINUE

RETURN
END
C*****

SUBROUTINE JACOBI(SUMQ,TEMAX)

INCLUDE PARTHES.INC
INCLUDE HEATTHES.INC
RETURN
END
C*****

SUBROUTINE OPTOMEG(LSKIP)

C** LSKIP IS THE OUTPUT LINE SKIPPING PARAMETER
C** OMEGR IS THE OPTIMUM SOR FACTOR COMPUTED IN THIS ROUTINE

INCLUDE PARTHES.INC
INCLUDE HEATTHES.INC

C*****Writing By Jeffrey Lienau*****

REAL ALNEW,ALTEST,ALOLD
OMEGA=1.0           !SETS OMEGA EQUAL TO 1 FOR COMPUTATION.
QERROR = 0.         !RESET THE TOTAL ERROR FOR HEAT TRANS.
SUMOLD = 100000.    !SETS THE INITIAL VALUE OF THE sq. SUM.
SUMEPN = 0.         !SQUARE SUMMING VARIABLE
ALOLD = 1.          !OLD VALUE OF LAMBDA
IT = 1              !ITERATIONS COUNTER
WRITE(*,*) 'TYPE IN ASPECT RATIO'
READ(*,*) ASPECT
C*****WRITE THE OUTPUT TO THE LOGICAL UNIT*****

WRITE(*,*) 'OUTPUT FOR OPTIMUM OMEGA SEARCHING ROUTINE'
WRITE(LOUT,*) 'OUTPUT FOR OPTIMUM OMEGA SEARCHING ROUTINE'

WRITE(*,*) 'FOR THE CASE WHERE THE ASPECT RATIO IS: ',ASPECT
WRITE(LOUT,*) 'FOR THE CASE WHERE THE ASPECT RATIO IS: ',ASPECT
WRITE(*,*) ' '
WRITE(LOUT,*) ' '
WRITE(*,11)
WRITE(LOUT,11)

C*****NOW TO SWEEP CALCULATE THE NEW TEMPS SWEEPING BY ROWS*****

```

```

C
10 DO 200 J=2,NMAX2-1 !For the J Sweep
C DO 100 I = 2,NMAX1-1 !For The I Sweep
C
      DP = CX1(I,J) + CX1(I-1,J) + CX2(I,J) + CX2(I,J-1)
      P1 = (CX1(I,J))*(T(I+1,J))
      P2 = (CX1(I-1,J))*(T(I-1,J)) !New Value Of Temp.
      P3 = (CX2(I,J))*(T(I,J+1))
      P4 = (CX2(I,J-1))*(T(I,J-1)) !New Value of Temp.
C
      EPN = Q(I,J) + P1 + P2 + P3 + P4 - DP*T(I,J)
      QERROR = QERROR + ABS(EPN) !SUMMING OVER ALL ERROR
      SUMEPN=SUMEPN + ABS(EPN**2)
C
      T(I,J) = (Q(I,J)+(P1+P2+P3+P4))/DP !Sets New Temp.
      T(I,J) = OMEGA*(T(I,J)) + (1.-OMEGA)*(TOLD(I,J))
100 CONTINUE
200 CALCULATE LAMBDA n+1
C**
      ALNEW = SQRT(SUMEPN/SUMOLD)
C
      ALTEST = (ABS(ALNEW - ALOLD))/ALNEW
      DUM1= 2./(1.+SQRT(ABS(1.-ALNEW)))
C
      IF(MOD(IT,LSKIP).EQ.0) THEN
      WRITE (*,20) IT,ALTEST,DUM1
      WRITE (LOUT,20) IT,ALTEST,DUM1
C
      ENDIF
C
      IF(ALTEST.GE.1.E-5) THEN
      IT = IT +1
      ALOLD = ALNEW
      SUMOLD = SUMEPN
      SUMEPN = 0.0
      GO TO 10
      ENDIF
C**
      NOW TO CALCULATE THE OPTIMUM OMEGA *****
      DUM = 2./(1.+SQRT(ABS(1.-ALNEW)))
C
      OMEGA = DUM
C
      WRITE (*,30) DUM
      WRITE (LOUT,30) DUM
11 FORMAT(1X,'ITERATIONS',10X,'LAMBDA',12X,'OMEGA')
20 FORMAT(1X,I3,15X,F9.6,11X ,F5.3)
30 FORMAT(1X,'THE OPTIMUM OMEGA IS: ',F5.3)
*
* End of writing by Jeffrey Lienau*****
RETURN
END
C*****
SUBROUTINE AVGVEL(UDUM)
INCLUDE PARTHES.INC
INCLUDE HEATHES.INC

```

```

C** SUBROUTINE FOR CALCULATING THE AVERAGE VELOCITY (TEMPERATURE)
C** THIS SUBROUTINE USES TRAPEZOIDAL INTEGRATION OF THE FLOW FIELD

C      DO 200 J=2,NMAX2-1
C      DO 100 I=2,NMAX1-1

C**      TRAPEZOIDAL INTEGRATION TECHNIQUE

C          IF(I.EQ.2.OR.I.EQ.NMAX1-1) SUMY(J) = SUMY(J) + T(I,J)
C          IF(I.NE.2.AND.I.NE.NMAX1-1) SUMY(J) = SUMY(J) + 2.DO*T(I,J)
C100      CONTINUE
C          SUMY(J) = (DX1(NMAX1/2,NMAX2/2)/2.)*SUMY(J)
C          IF(J.EQ.2.OR.J.EQ.NMAX2-1) SUMZ = SUMZ + SUMY(J)
C          IF(J.NE.2.AND.J.NE.NMAX2-1) SUMZ = SUMZ + 2.DO*SUMY(J)
C200      CONTINUE
C          SUMZ = (DX2(NMAX1/2,NMAX2/2)/2.)*SUMZ

C          AREA = ((NMAX2-2)*DX2(NMAX1/2,NMAX2/2)*(NMAX1-2)*DX1(NMAX1/2
C 1          ,NMAX2/2))
C          UDUM = SUMZ/AREA

C          SUM = 0.0
C          SUMAR = 0.0

C**      NUMERICAL INTEGRATION TECHNIQUE
DO 250 J=NWBND2+1,NMAX2-1
DO 250 I=NWBND1+1,NMAX1-1
SUMAR = SUMAR + DX2(I,J)*DX1(I,J)
250 CONTINUE

DO 300 J=NWBND2+1,NMAX2-1
DO 300 I=NWBND1+1,NMAX1-1
SUM = SUM + U(I,J)
300 CONTINUE
UDUM = SUM/((NMAX1-1-NWBND1)*(NMAX2-1-NWBND2))

RETURN
END

C*****
SUBROUTINE PSOR(SUMQ,SUMR,OMEG,TEMAX)
INCLUDE PARTHES.INC
INCLUDE HEATTHES.INC

SUMQ = 0.
SUMR = 0.
TEMAX = 0.
SUMDP = SMALL
OMEGR = OMEG
QGEN = 0.
DO 100 J = 2,NMAX2-1
DO 100 I = 2,NMAX1-1
IF(MAT(I,J).LE.1000) THEN
QGEN = Q(I,J)
DP = CX1(I,J)+CX2(I,J) + CX1(I-1,J)+CX2(I,J-1)

```

```

      QERR = CX1(I,J)*T(I+1,J) + CX1(I-1,J)*T(I-1,J) +
1      CX2(I,J)*T(I,J+1) + CX2(I,J-1)*T(I,J-1) - DP*T(I,J) -
2      QGEN
      DELT = QERR/DP
      TEMAX = MAX(ABS(DELT), TEMAX)
      ABSQE = ABS(QERR)
      SUMDP = SUMDP + DP
      SUMQ = SUMQ + ABSQE
      SUMR = SUMR + QERR
      T(I,J) = OMEGA*DELT + T(I,J)
      ENDIF
100 CONTINUE

```

END

C\*\*\*\*\*

```

SUBROUTINE VPSOR(SUMQ, SUMR, OMEG, TEMAX)
INCLUDE PARTHES.INC
INCLUDE HEATTHES.INC

```

```

SUMQ = 0.
SUMR = 0.
TEMAX = 0.
SUMDP = SMALL
OMEGR = OMEG
QGEN = 0.
DO 100 J = NWBND2+1, NMAX2-1
DO 100 I = NWBND1+1, NMAX1-1
IF(MAT(I,J).LE.1000) THEN
  QGEN = Q(I,J)
  DP = CX1(I,J)+CX2(I,J) + CX1(I-1,J)+CX2(I,J-1)
1  QERR = CX1(I,J)*T(I+1,J) + CX1(I-1,J)*T(I-1,J) +
2  CX2(I,J)*T(I,J+1) + CX2(I,J-1)*T(I,J-1) - DP*T(I,J) -
  QGEN
  DELT = QERR/DP
  TEMAX = MAX(ABS(DELT), TEMAX)
  ABSQE = ABS(QERR)
  SUMDP = SUMDP + DP
  SUMQ = SUMQ + ABSQE
  SUMR = SUMR + QERR
  T(I,J) = OMEGA*DELT + T(I,J)
  ENDIF
100 CONTINUE

```

END

C\*\*\*\*\*

```

SUBROUTINE LSOR(SUMQ, TEMAX)

```

```

INCLUDE PARTHES.INC
INCLUDE HEATTHES.INC
RETURN
END

```

C\*\*\*\*\*

```

SUBROUTINE QELAST(SUMQ)
INCLUDE PARTHES.INC
INCLUDE HEATTHES.INC

```

```

SUMQ      = 0.
QGEN      = 0.

DO 100 J = 2, NMAX2-1
DO 100 I = 2, NMAX1-1
IF (MAT(I,J).LE.1000) THEN
  QGEN     = Q(I,J)
  DP       = CX1(I,J)+CX2(I,J)   + CX1(I-1,J)+CX2(I,J-1)
  QERR     = CX1(I,J)*T(I+1,J) + CX1(I-1,J)*T(I-1,J) +
1          CX2(I,J)*T(I,J+1) + CX2(I,J-1)*T(I,J-1) - DP*T(I,J) -
2          QGEN
  SUMQ     = SUMQ + ABS(QERR)
  END IF
100 CONTINUE

RETURN
END

C*****
SUBROUTINE EXPLICIT(SUMEXP, TUMAX)
  INCLUDE PARTHES.INC
  INCLUDE HEATHTHES.INC
  RETURN
END
C*****
SUBROUTINE TPSOR(FIMP, TUMAX)
  INCLUDE PARTHES.INC
  INCLUDE HEATHTHES.INC
  RETURN
END
C*****
SUBROUTINE TLSOR(FIMP, TUMAX)
  INCLUDE PARTHES.INC
  INCLUDE HEATHTHES.INC
  RETURN
END
C*****
SUBROUTINE ADI(FIMP, TUMAX)
  INCLUDE PARTHES.INC
  INCLUDE HEATHTHES.INC
  RETURN
END
C****
SUBROUTINE SAULEV(TUMAX)

```

```
INCLUDE PARTHES.INC
INCLUDE HEATTHES.INC
```

156

```
C**  SORRY!! NO ONE IS HOME !!
```

```
RETURN
END
```

```
C*****
```

```
  SUBROUTINE LARKIN(TUMAX)
```

```
    INCLUDE PARTHES.INC
    INCLUDE HEATTHES.INC
```

```
C**  SORRY!! NO ONE IS HOME !!
```

```
RETURN
END
```

```
C*****
```

```
  SUBROUTINE TRIDIAG(M,AM,AP,AC,B)
```

```
    INCLUDE PARTHES.INC
    DIMENSION  AM(MAXLINE),AC(MAXLINE),AP(MAXLINE),B(MAXLINE)
```

```
C**  THIS SOLVER NORMALIZES THE DIAGONAL TO 1.0
C**  ELIMINATES NEED FOR DIVISION ON BACK-SUBSTITUTION.
```

```
  AP(1)  = AP(1)/AC(1)
  B(1)   = B (1)/AC(1)
```

```
  DO 100 K = 2,M
    BET  = 1./(AC(K)-AM(K)*AP(K-1))
    AP(K) = AP(K)*BET
    B (K) = (B(K)+AM(K)*B(K-1))*BET
```

```
100 CONTINUE
```

```
C**
```

```
  DO 200 K = M-1,1,-1
    B(K) = B(K) + AP(K)*B(K+1)
```

```
200 CONTINUE
```

```
RETURN
END
```

```
C*****
```

```
  SUBROUTINE PROPLIB
  INCLUDE PARTHES.INC
  INCLUDE HEATTHES.INC
  REAL          *8 KAY,KELVIN
```

```
C**  SUBROUTINE COMPUTES SI THERMAL CONDUCTIVITY
C**  TC - - DEGREES CENTIGRADE
C**  CAY - WATTS/M-DEGREE C ( OR K) ALSO - KAY)
C**  cay is used here for viscosity 658e-6 Pa S
  RP = PREF/8314.          ! PREF IS REFERENCE PRESSURE
```

```
  DO 700 J = 1,NMAX2
  DO 700 I = 1,NMAX1
```

```

TC      = T(I,J)
KELVIN  = TC + 273.15
PFACT   = RP/KELVIN
MATNO   = MAT(I,J)

```

```

IF(MATNO.GT.15) GO TO 500 ! THE FOLLOWING COMPUTED GO TO SET 15 MAT'L

```

```

GO TO (110,120,130,140,150,160,170,180,190,200,210,220,230,240,
1      250), MATNO

```

```

110 CONTINUE                                ! WATER
C* note- I have used the correct specific heat here and the value of the
C* viscosity must be hardwired for the momentum calculation.

```

```

KAY     = .64
RHON    = 1000.
SPHT    = 4184.
AMU     = .047

```

```

GO TO 600
120 CONTINUE                                ! Silicon
KAY     = 148.d0
RHON    = 2333.
SPHT    = 703.
AMU     = 1.

```

```

GO TO 600
130 CONTINUE                                ! LITHIUM
KAY     = 40.15 + 0.0190*TC
RHON    = 515. - 0.101*(TC-200.)
SPHT    = 4186.8
AMU     = KELVIN**(-.7368)*10.**(.4936+109.95/KELVIN)*.01
IF(TC.GT.800.) THEN
AMU     = 10.**(726.07/KELVIN -1.3380)*.001
ENDIF

```

```

GO TO 600
140 CONTINUE                                ! YOUR CHOICE

```

```

GO TO 600
150 CONTINUE                                ! YOUR CHOICE

```

```

GO TO 600
160 CONTINUE                                ! HELIUM
KAY     = 0.00337*(KELVIN)**0.668
RHON    = 4.003*PFACT
SPHT    = 1.24*4168.6
AMU     = 4.7744E-7*KELVIN**.6567

```

```

GO TO 600
170 CONTINUE                                ! ARGON
KAY     = 0.015673 + 4.8226E-5*TC-1.7226E-8*TC*TC+4.0703E-12*TC**3
RHON    = 39.948*PFACT
SPHT    = .12428*4186.8
AMU     = (2.0377+.006254*TC-2.69584E-6*TC**2+6.30257E-10*TC**3)
1      *1.E-5

```

```

GO TO 600
180 CONTINUE                                ! water for

```

```

      KAY = 550E-6
      RHON = 1.
      SPHT = 1.
      AMU = 1.
! momentum soln.
! value in Pa*S

      GO TO 600
190 CONTINUE
! YOUR CHOICE

      GO TO 600
200 CONTINUE
! YOUR CHOICE

      GO TO 600
210 CONTINUE
! YOUR CHOICE

      GO TO 600
220 CONTINUE
! YOUR CHOICE

      GO TO 600
230 CONTINUE
! YOUR CHOICE

      GO TO 600
240 CONTINUE
! YOUR CHOICE

      GO TO 600
250 CONTINUE
! YOUR CHOICE

      GO TO 600
500 CONTINUE
! SPECIAL MATERIALS

      IF (MAT(I,J).EQ.1000) THEN
      KAY = 1.
      RHON = 1.
      SPHT = 1.
      AMU = 1

      ELSEIF (MAT(I,J).EQ.1001) THEN
      KAY = 1.E-30
      RHON = 1.
      SPHT = 1.
      AMU = 1
! VON NEUMANN

      ELSEIF (MAT(I,J).EQ.1002) THEN
      KAY = 1.E+30
      RHON = 1.
      SPHT = 1.
      AMU = 1
! DIRICHLET

      ELSEIF (MAT(I,J).EQ.1003) THEN
      KAY = 1.E-30
      RHON = 1.
      SPHT = 1.
      AMU = 1
! NULL

      ENDIF

600 CAY(I,J) = KAY
      BETA(I,J) = 1./(RHON*SPHT)
      AMU = AMU ! TRYING TO GET RID OF THE COMPILER COMPLAINTS

700 CONTINUE

```

```
RETURN
END
```

```
C*****
```

```

SUBROUTINE ASMIN(NMAX1,NMAX2,MAT,A,II,JJ,AMIN)
C** FIND INDICES LOCATION AND MINIMUM OF A
INCLUDE PARTHES.INC
C REAL *8 A(MAX1,MAX2),AMIN
C DIMENSION MAT(MAX1,MAX2)
C**
C II = 2
C JJ = 2
C AMIN = A(2,2)
C DO 100 J = 2,NMAX2-1
C DO 100 I = 2,NMAX1-1
C IF(MAT(I,J).LE.1000) THEN
C IF(A(I,J).LT.AMIN) THEN
C AMIN = A(I,J)
C JJ = J
C II = I
C ENDIF
C ENDIF
C 100 CONTINUE
RETURN
END
```

```
C*****
```

```

SUBROUTINE ASMAX(NMAX1,NMAX2,MAT,A,II,JJ,AMAX)
C** FIND INDICES LOCATION AND MAXIMUM OF A
INCLUDE PARTHES.INC
C REAL *8 A(MAX1,MAX2),AMAX
C DIMENSION MAT(MAX1,MAX2)
C**
C II = 2
C JJ = 2
C AMAX = A(2,2)
C DO 100 J = 2,NMAX2-1
C DO 100 I = 2,NMAX1-1
C IF(MAT(I,J).LE.1000) THEN
C IF(A(I,J).GT.AMAX) THEN
C AMAX = A(I,J)
C JJ = J
C II = I
C ENDIF
C ENDIF
C 100 CONTINUE
RETURN
END
```

```
C*****
```

```

SUBROUTINE AWRITER (MODE,NSTEP,ARRAY,LABEL)
C** GENERAL REAL ARRAY WRITER
INCLUDE PARTHES.INC
INCLUDE HEATTHES.INC
REAL *8 ARRAY(MAX1,MAX2)
CHARACTER *32 LABEL

C** TRIM THE TRAILING BLANKS FROM LABEL
```

```

DO 10 I = 32,1,-1
IF(LABEL(I:I).GT.' ') GO TO 20
10 CONTINUE
20 CONTINUE

IF(MODE.EQ.1) WRITE(LOUT,1000) LABEL(1:I),NSTEP
IF(MODE.EQ.2) WRITE(LOUT,1005) LABEL(1:I),NSTEP,TYME

N2      = 0
100 CONTINUE
    N1      = N2 + 1
    N2      = N1 + 9
    IF(N2.GT.NMAX1) N2 = NMAX1
    WRITE(LOUT,1001) (NIX(I),I=N1,N2)
    WRITE(LOUT,1002) (X1(I),I=N1,N2)
DO 200 J = 1,NMAX2
    JN      = NMAX2+1-J
    WRITE(LOUT,1003) JN,X2(JN),(ARRAY(I,JN),I=N1,N2)
200 CONTINUE

IF(N2.NE.NMAX1) GO TO 100

RETURN
1000 FORMAT(//30X,A32,' ARRAY OUTPUT FOR ITERATION NUMBER:',I5//)
1001 FORMAT(/14X,'I = ',10(I8,3X))
1002 FORMAT( 9X,' X1 = ',10(E10.4,1X)/)
1003 FORMAT( ' J=',I3,' X2=',E8.3,1P,10E11.3)
1005 FORMAT(//20X,A32,' ARRAY OUTPUT FOR TIME STEP NUMBER:',I5,' TIME
1 = ',F15.4,' SECONDS'//)
END
*****

SUBROUTINE IWRTITER (NARRAY,LABEL)
C** GENERAL INTEGER ARRAY WRITER
INCLUDE PARTHES.INC
INCLUDE HEATHTHES.INC
C INTEGER *4 NARRAY(MAX1,MAX2)
C CHARACTER *32 LABEL
C CHARACTER *4 DUMMY(MAX1),CARRAY(MAX1)
C
CC**
CC** TRIM THE TRAILING BLANKS FROM LABEL
C DO 10 I = 32,1,-1
C IF(LABEL(I:I).GT.' ') GO TO 20
C 10 CONTINUE
C 20 CONTINUE
C
CC**
C N2 = 0
C 100 CONTINUE
C N1 = N2+1
C N2 = N1+39
C IF(N2.GT.NMAX1) N2 = NMAX1
C WRITE(LOUT,1000) LABEL(1:I)
C WRITE(LOUT,1001) (NIX(N),N=N1,N2)
C
C DO 200 J = 1,NMAX2
C JN = NMAX2+1-J
C WRITE(DUMMY,'(I4)') (NARRAY(I,JN),I = 1,NMAX1)
C READ (DUMMY,'(A4)') (CARRAY(I),I = 1,NMAX1)

```

```

C
C      DO 300 I = N1,N2
C          IF(CARRAY(I).EQ.'1000') CARRAY(I) = '  M'
C          IF(CARRAY(I).EQ.'1001') CARRAY(I) = '  V'
C          IF(CARRAY(I).EQ.'1002') CARRAY(I) = '  D'
C          IF(CARRAY(I).EQ.'1003') CARRAY(I) = '  N'
C 300 CONTINUE
C
C      WRITE(LOUT,1002) JN, (CARRAY(I) (2:4), I=N1,N2)
C 200 CONTINUE
C      IF(N2.NE.NMAX1) GO TO 100
C      RETURN

C 1000 FORMAT(/A32//
C      115X,'M = MODEL MATERIAL'//
C      215X,'D = DIRICHLET BOUNDARY'//
C      315X,'V = VON NEUMANN BOUNDARY'//
C      415X,'N = NULL CELL ')
C 1001 FORMAT(/' I = ',5X,40I3/)
C 1002 FORMAT(' J = ',I3,2X,40A3)
C      END

```

```

C*****
C**
C**      SUBROUTINE PREPLOT
C**
C**      PREPARE PLOT FILE
C**
C**      INCLUDE PARTHES.INC
C**      INCLUDE HEATTHES.INC
C**
C**      WRITE(NPOUT,200) NMAX1,NMAX2
C**      WRITE(NPOUT,100) ( X1(I), I = 1,NMAX1 )
C**      WRITE(NPOUT,100) ( X2(J), J = 1,NMAX2 )
C**
C**      RETURN
C**
C**      100 FORMAT(1X,5F15.10)
C**      200 FORMAT(1X,2I10)
C**      END

```

```

C*****
C**
C**      SUBROUTINE APLOT(ARRAY,PFS,LABEL)
C**
C**      SET UP PLOT FILE
C**
C**      INCLUDE PARTHES.INC
C**      INCLUDE HEATTHES.INC
C**
C**      REAL*8 ARRAY(MAX1,MAX2)
C**      CHARACTER*32 LABEL
C**      CHARACTER*80 PFS
C**
C**      WRITE(NPOUT,1000) LABEL
C**      WRITE(NPOUT,1010) PFS
C**      DO 100 J = 1,NMAX2
C**      WRITE(NPOUT,1020) ( ARRAY(I,J), I = 1,NMAX1 )

```

```
100 CONTINUE
```

```
C**
```

```
1000 FORMAT(A32)
```

```
1010 FORMAT(A80)
```

```
1020 FORMAT(1X,3E20.10)
```

```
C**
```

```
RETURN
```

```
END
```

```
C*****
```

## APPENDIX B

## Separation of Variables Comparison

## 1 SEPARATION OF VARIABLES SOLUTION:

An analytical solution was derived for the momentum equation (equation 1.1) which gave the velocity distribution in the laminar microchannels. The solution technique involved the separation of variables method which is discussed in [7]. The solution obtained agreed with Carslaw and Jaeger [8]. The Carslaw and Jaeger solution is for the temperature distribution in a heated rectangular plate but the partial differential equation of energy transfer is exactly the same as the fully developed momentum equation 1.1. Consider the schematic of the fluid flow region given in **Figure B1** which the repeating symmetric momentum solution area and all of the geometric constants of the problem.

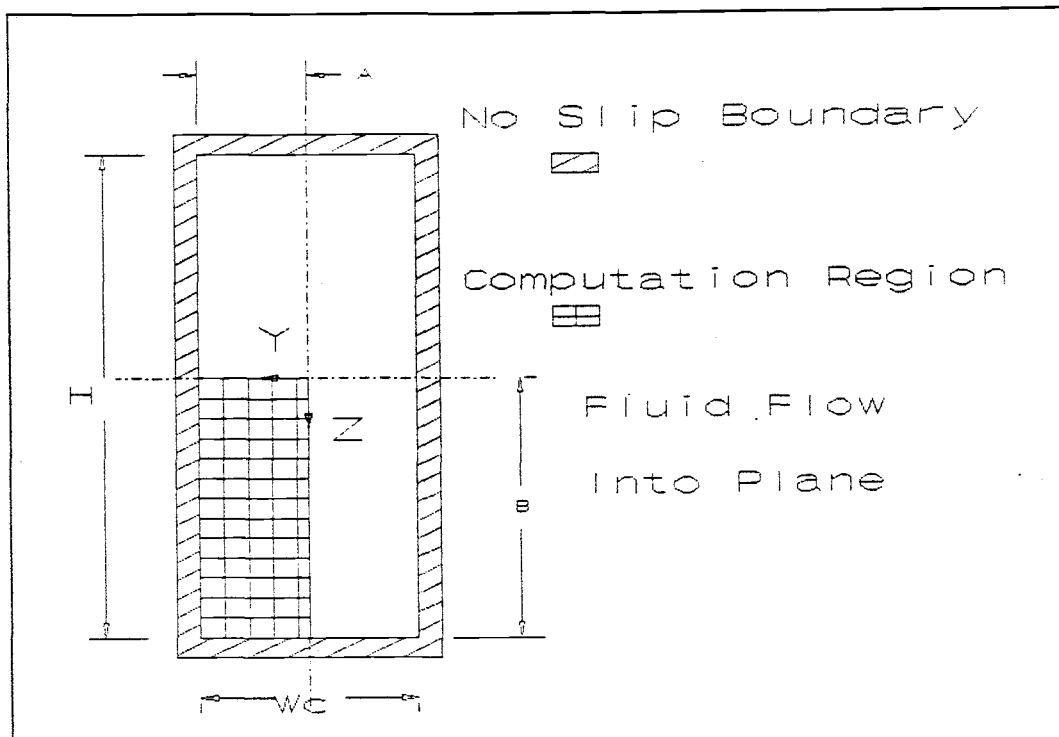


**Figure B1**  
Fluid Flow region showing the symmetric computation area and the geometric constants used in the analytical solution.

The analytical solution for the velocity distribution is:

$$(1) u(x, y, z) =$$

$$\frac{1}{dx} \frac{dP}{2} (A^2 - y^2) - \frac{16A^2}{\pi^5} \sum_{n=0}^{\infty} \frac{(-1)^n \cos((2n+1)\pi y/2A) \cosh((2n+1)\pi z/2A)}{(2n+1)^5 \cosh((2n+1)\pi B/2A)}$$

A computer code was written in FORTRAN which solves the above equation terms and prints out a velocity distribution for a given grid discretization. The computer code is called EXTHES.FOR and the source code is included at the end of this appendix. The computer code uses the first seven terms of the infinite series. A previous calculation revealed that the seventh term was contributing less than .1% to the solution so the eighth term was neglected.

## 2 RESULTS

The velocity distribution was found for a microchannel with an aspect ratio  $\alpha$  of 8, a channel width  $W_c$  of 25  $\mu\text{m}$ , a pressure gradient  $dP/dx$  of 50 MPa/m using fluid of viscosity  $\mu$  of 550  $\mu\text{PaS}$ . The problem was solved using 10 and 20 cells in the  $y$  and  $z$  directions. The finite difference results using the method of point successive relaxation were compared to the analytical solution (1). The output from the analytical solution code and from the finite difference code are presented in this appendix on 14" wide computer paper. In order to help interpret the output, the channel locations ( $y$  and  $z$ ) are printed above and to the left of the arrays. The zero's in the finite difference output correspond to solid cells where there is zero velocity.

The major results will now be summarized using the percent deviation of the numerical and analytical results at various points within the distribution. The points chosen are A, B and C of Figure 1.2 and also the corner which will

be referred to here as point D. Point A corresponds to the first cell next to the the horizontal fin. Point B corresponds to the center point. Point C corresponds to the first cell next to the centerline of the vertical base Table B1 contains the summarized results. The percent deviation is calculated by:

$$(2) \quad \% \text{ deviation} = 100 \text{abs}(u_{\text{numerical}} - u_{\text{analytical}}) / u_{\text{analytical}}$$

	10 cell discretization	20 cell discretization
Point		
A	2.56%	.71%
B	.25%	.49%
C	12.84%	9.50%
D	15.70%	12.14%

**Table B1** Percent Difference between analytical and numerical solutions to the momentum equation.

The most important point to have accurate velocities is at point A next to the vertical fin. This is where most of the convection is occurring. This was the point considered in the determination of the discretization. Twenty cells were chosen across the half channel width because the percentage departure between the analytical and numerical solutions was less than 1% for this discretization.

```

C*****
C*
C*           Jeffrey Jay Lienau
C*
C*           ME 503           THESIS           APRIL 16,1989
C*
C*           This is a program to calculate the exact solution of the
C*           velocity in the microchannel using an analytical solution
C*           found in Carslaw and Jaegar's "Conduction of heat in Solids"*
C*           Second edition. Oxford University Press 1959. pp171 eqn. 6
C*           This equation assumes zero temperature (no slip) on all
C*           boundaries and must then be solved for the half width
C*
C*           The purpose of this program is to provide a means of
C*           checking the velocity distribution in the microchannel
C*           with the analytical solution using the fully developed
C*           flow assumption.
C*
C*****

PROGRAM EXTHES           !EXACT SOLUTION TO THE MOMENTUM EQN.

C** Lets open a logical unit for the printer

OPEN(UNIT=1,FILE='OUTTHES',STATUS='NEW')

C** Dimension the array for the solution::::::::::::::::::

NMAX1   =           25
NMAX2   =           50

DIMENSION V(0:25,0:50),VISCOS(0:25,0:50)
DOUBLE PRECISION Y,DY,Z,DZ,A,B,VISC,PI,SUM,COSHTN,COSHTD
1, SUMTERM,TD,TERM1,COTERM2,COSTN,V,VISCOS

C** Interactive Session for the input data::::::::::::::::::

1 WRITE(*,*) 'Enter the value of the y half width (MICROMETERS)'
  READ(*,*) A
  IF(A.LE.0) GO TO 1
  A           =           A*1E-6

2 WRITE(*,*) 'Enter the value of the z half width (MICROMETERS)'
  READ(*,*) B
  IF(B.LE.0) GO TO 2
  B           =           B*1E-6

3 WRITE(*,*) 'Enter the value of the pressure Drop (PSI)'
  READ(*,*) PDROP
  WRITE(*,*) 'Enter the length of the heat sink (cm)'
  READ(*,*) HLENG
  PGRAD=(PDROP/HLENG)*6.89476D5
  IF(PGRAD.LE.0) GO TO 3

4 WRITE(*,*) 'Enter the value of the Viscosity (PA*S)'
  READ(*,*) visc
  IF(VISC.LE.0) GO TO 4

```

```

5  WRITE(*,*) 'Enter the value of delta y (MICROMETERS)'
   READ(*,*) DY
   IF(DY.LE.0) GO TO 5
   DY      =      DY*1E-6

6  WRITE(*,*) 'Enter the value of delta z (MICROMETERS)'
   READ(*,*) DZ
   IF(DZ.LE.0) GO TO 6
   DZ      =      DZ*1E-6

C**  Lets set up the viscosity as an array so we can vary it.

      DO 10  YC=0,NMAX1
        DO 10  ZC=0,NMAX2
          VISCOS(YC,ZC) =      VISC
10  CONTINUE

C**  CONSTANTS FOR THE PROBLEM::::::::::::::::::::::::::::::::::

PI      =      4.D0*DATAN(1.D0)
NUM1    =      A/DY      !NUMBER OF Y CELLS
NUM2    =      B/DZ      !NUMBER OF Z CELLS
K       =      1.0      !CONSTANT RELATES Y AND Z VIS
SUMVEL  =      0.0      !SUM FOR AVERAGE VELOCITY
SUM     =      0.0      !INITIALIZE SUM
NSUM    =      0        !SUM FOR AVERAGE VELOCITY #

C**  BEGIN CALCULATION::::::::::::::::::::::::::::::::::::::::::

DO 200  Y      =      0.,A,DY  !COUNTER FOR Y DIR.
      NY      =      NINT(Y/DY)

      DO 100  Z      =      0.,B,DZ  !COUNTER FOR Z DIR.
        NZ      =      NINT(Z/DZ)

      TERM1      =(A**2 - ((Y+DY/2.)**2))/(2.*VISCOS(NY,NZ))
      COTERM2    =16.*(A**2)/((VISCOS(NY,NZ))*(PI**3))

C**  SUM FOR THE SECOND TERM

      SUM      =      0.0

      DO 50  N=0,7

        COSTN   =DCOS((2.D0*N+1.D0)*PI*(Y+DY/2.)/(2.D0*A))
        COSHTN  =DCOSH((2.D0*N+1.D0)*PI*K*(Z+DZ/2.)/(2.D0*A))
        IF(COSHTN.LE.1.E-30) GO TO 60
        TD      =      (2.D0*N +1.D0)**3
        COSHTD  =      DCOSH((2.D0*N +1.D0)*PI*K*B/(2.D0*A))
        IF(COSHTD.LE.1.E-30) GO TO 60
        SUMTERM =      (COSTN*COSHTN)/(TD*COSHTD)
        IF(MOD(N,2).NE.0) SUMTERM = -SUMTERM

      SUM      =      SUM + SUMTERM

50  CONTINUE

```

```

C**      CALCULATE THE VELOCITY AT THIS POINT
60      V(NY,NZ) =      PGRAD*(TERM1 - COTERM2*SUM)
100     CONTINUE          !CONTINUE FOR THE Z BOUND
200     CONTINUE          !CONTINUE FOR THE Y BOUND

C**      CALCULATE THE AVERAGE VELOCITY OVER THE FIELD

DO 350  Y      =      0., (A-DY),DY      !COUNTER FOR Y DIR.
        NY     =      NINT(Y/DY)
DO 350  Z      =      0., (B-DZ),DZ      !COUNTER FOR Z DIR.
        NZ     =      NINT(Z/DZ)
        SUMVEL =      SUMVEL + V(NY,NZ)
        NSUM   =      NSUM   + 1
350     CONTINUE
        AVGVEL =      SUMVEL/NSUM

C**      Let's Calculate The Reynold's Number
DHYDR = 4.d0*A*B/(A+B)
RHO   = 1000.
REYN  = RHO*AVGVEL*DHYDR/VISC

C**      LET'S PRINT OUT THE VELOCITY DISTRIBUTION *****
WRITE(*,*) 'VELOCITY DISTRIBUTION FOR MICROCHANNEL-----'
WRITE(1,*) 'VELOCITY DISTRIBUTION FOR MICROCHANNEL-----'

WRITE(*,*)
WRITE(1,*)

WRITE(*,*) 'Pressure gradient is: [Pa/m] ', pgrad
WRITE(1,*) 'Pressure gradient is: [Pa/m] ', pgrad

WRITE(*,*) 'Pressure Drop is: [psi]', PDROP
WRITE(1,*) 'Pressure Drop is: [psi]', PDROP

WRITE(*,*) 'The Length of the Heat sink is: [cm]', HLENG
WRITE(1,*) 'The Length of the Heat sink is: [cm]', HLENG

WRITE(*,*) 'The Reynolds Number is: [1]', REYN
WRITE(1,*) 'The Reynolds Number is: [1]', REYN

WRITE(*,*) 'Viscosity is: [Pa*S] ', VISC
WRITE(1,*) 'Viscosity is: [Pa*S] ', VISC

WRITE(*,*)
WRITE(1,*)

WRITE(*,*) ' One quarter is calculated because of symmetry'
WRITE(1,*) ' One quarter is calculated because of symmetry'

WRITE(*,*) ' The y dir. runs rows and the z dir. runs columns.'
WRITE(1,*) ' The y dir. runs rows and the z dir. runs columns.'

WRITE(*,*) ' Distance is in micrometers and Velocity is in M/S.'
WRITE(1,*) ' Distance is in micrometers and velocity is in M/S.'

WRITE(*,*) 'This program assumes no slip boundaries.'
WRITE(1,*) 'This program assumes no slip boundaries.'

```

```

WRITE(*,*)
WRITE(1,*)

WRITE(*,*) 'The average velocity is: ',AVGVEL
WRITE(1,*) 'The average velocity is: ',AVGVEL

WRITE(*,*)
WRITE(1,*)

WRITE(*,1000) (Y, Y=(A-DY)*1E6,0,-DY*1e6)
WRITE(1,1000) (Y, Y=(A-DY)*1E6,0,-DY*1E6)

WRITE(*,*)
WRITE(1,*)

DO 500 NZ=0,NUM2-1

WRITE(*,1010) NINT(NZ*DZ*1E6), (V(NY,NZ), NY=NUM1-1,0,-1)
WRITE(1,1010) NINT(NZ*DZ*1E6), (V(NY,NZ), NY=NUM1-1,0,-1)

500    CONTINUE

WRITE(*,*)
WRITE(1,*)

WRITE(*,*) '----- FINISHED -----'
WRITE(1,*) '----- FINISHED -----'

C**    OUTPUT FORMATS
C      NUM1=10    !FOR THIS SETUP
1000   FORMAT(1X,3X,10(2X,F5.0))
1010   FORMAT(1X,I3,10(2X,F5.2))

STOP
END

```

C:\F77L\TYPE OUTTHES  
 VELOCITY DISTRIBUTION FOR MICROCHANNEL-----

Pressure gradient is: [Pa/m] 0.500000E+08  
 Viscosity is: [Pa\*S] 0.550000000000000D-003

One quarter is calculated because of symmetry  
 The y dir. runs rows and the x dir. runs columns.  
 Distance is in micrometers and velocity is in M/S.  
 This program assumes no slip boundaries.

The average velocity is: 17.5659

	22.	20.	17.	15.	12.	10.	7.	5.	2.	0.
0	2.77	7.88	12.43	16.41	19.82	22.66	24.93	26.63	27.77	28.34
20	2.77	7.88	12.43	16.41	19.81	22.66	24.93	26.63	27.77	28.34
40	2.77	7.88	12.43	16.41	19.81	22.65	24.93	26.63	27.77	28.34
60	2.77	7.88	12.43	16.40	19.81	22.65	24.92	26.63	27.76	28.33
80	2.77	7.88	12.42	16.39	19.80	22.63	24.90	26.61	27.74	28.31
100	2.76	7.86	12.39	16.35	19.75	22.58	24.84	26.54	27.67	28.24
120	2.74	7.80	12.29	16.22	19.58	22.38	24.62	26.30	27.42	27.98
140	2.67	7.59	11.94	15.74	18.99	21.69	23.85	25.46	26.54	27.08
160	2.42	6.84	10.72	14.08	16.92	19.27	21.13	22.52	23.44	23.90
180	1.50	4.11	6.28	8.07	9.52	10.69	11.59	12.25	12.68	12.90

-----  
 FINISHED  
 -----

TRANSPORT EQUATION SOLUTION ALGORITHM TESTER

```

SOLUTION METHOD          PSOR
NUMBER OF CELLS IN X1-DIRECTION, NMAX1 - - - - 22
NUMBER OF CELLS IN X2-DIRECTION, NMAX2 - - - - 30
WIDTH OF CELLS IN X1-DIRECTION, DX1 - - - - .25000E-05
WIDTH OF CELLS IN X2-DIRECTION, DX2 - - - - .20000E-04
OVER-RELAXATION FACTOR , OMEGA - - - - 1.750
MAXIMUM NUMBER ITERATIONS , ITHAX - - - -1000
DELTA-PHI ERROR CRITERION , TCRIT - - - - 1.000E-03
HEAT BALANCE ERROR CRITERION , QMAX - - - - 0.100
INITIAL VELOCITY , TINIT - - - - 0.0000E+00
    
```

STEADY STATE VELOCITY ARRAY OUTPUT FOR ITERATION NUMBER: 14

```

          I =          1          2          3          4          5          6          7          8          9          10
          X1 = -.1250E-05 0.1250E-05 0.3750E-05 0.6250E-05 0.8750E-05 0.1125E-04 0.1375E-04 0.1625E-04 0.1875E-04 0.2125E-04
J= 30 X2=.570E-03 0.000E+00 0.000E+00 0.000E+00 0.000E+00 0.000E+00 0.000E+00 0.000E+00 0.000E+00 0.000E+00 0.000E+00
J= 29 X2=.550E-03 0.000E+00 0.000E+00 0.000E+00 0.000E+00 0.000E+00 0.000E+00 0.000E+00 0.000E+00 0.000E+00 0.000E+00
J= 28 X2=.530E-03 0.000E+00 0.000E+00 0.000E+00 0.000E+00 0.000E+00 0.000E+00 0.000E+00 0.000E+00 0.000E+00 0.000E+00
J= 27 X2=.510E-03 0.000E+00 0.000E+00 0.000E+00 0.000E+00 0.000E+00 0.000E+00 0.000E+00 0.000E+00 0.000E+00 0.000E+00
J= 26 X2=.490E-03 0.000E+00 0.000E+00 0.000E+00 0.000E+00 0.000E+00 0.000E+00 0.000E+00 0.000E+00 0.000E+00 0.000E+00
J= 25 X2=.470E-03 0.000E+00 0.000E+00 0.000E+00 0.000E+00 0.000E+00 0.000E+00 0.000E+00 0.000E+00 0.000E+00 0.000E+00
J= 24 X2=.450E-03 0.000E+00 0.000E+00 0.000E+00 0.000E+00 0.000E+00 0.000E+00 0.000E+00 0.000E+00 0.000E+00 0.000E+00
J= 23 X2=.430E-03 0.000E+00 0.000E+00 0.000E+00 0.000E+00 0.000E+00 0.000E+00 0.000E+00 0.000E+00 0.000E+00 0.000E+00
J= 22 X2=.410E-03 0.000E+00 0.000E+00 0.000E+00 0.000E+00 0.000E+00 0.000E+00 0.000E+00 0.000E+00 0.000E+00 0.000E+00
J= 21 X2=.390E-03 0.000E+00 0.000E+00 0.000E+00 0.000E+00 0.000E+00 0.000E+00 0.000E+00 0.000E+00 0.000E+00 0.000E+00
J= 20 X2=.370E-03 0.000E+00 0.000E+00 0.000E+00 0.000E+00 0.000E+00 0.000E+00 0.000E+00 0.000E+00 0.000E+00 0.000E+00
J= 19 X2=.350E-03 0.000E+00 0.000E+00 0.000E+00 0.000E+00 0.000E+00 0.000E+00 0.000E+00 0.000E+00 0.000E+00 0.000E+00
J= 18 X2=.330E-03 0.000E+00 0.000E+00 0.000E+00 0.000E+00 0.000E+00 0.000E+00 0.000E+00 0.000E+00 0.000E+00 0.000E+00
J= 17 X2=.310E-03 0.000E+00 0.000E+00 0.000E+00 0.000E+00 0.000E+00 0.000E+00 0.000E+00 0.000E+00 0.000E+00 0.000E+00
J= 16 X2=.290E-03 0.000E+00 0.000E+00 0.000E+00 0.000E+00 0.000E+00 0.000E+00 0.000E+00 0.000E+00 0.000E+00 0.000E+00
J= 15 X2=.270E-03 0.000E+00 0.000E+00 0.000E+00 0.000E+00 0.000E+00 0.000E+00 0.000E+00 0.000E+00 0.000E+00 0.000E+00
J= 14 X2=.250E-03 0.000E+00 0.000E+00 0.000E+00 0.000E+00 0.000E+00 0.000E+00 0.000E+00 0.000E+00 0.000E+00 0.000E+00
J= 13 X2=.230E-03 0.000E+00 0.000E+00 0.000E+00 0.000E+00 0.000E+00 0.000E+00 0.000E+00 0.000E+00 0.000E+00 0.000E+00
J= 12 X2=.210E-03 0.000E+00 0.000E+00 0.000E+00 0.000E+00 0.000E+00 0.000E+00 0.000E+00 0.000E+00 0.000E+00 0.000E+00
J= 11 X2=.190E-03 0.000E+00 0.000E+00 0.000E+00 0.000E+00 0.000E+00 0.000E+00 0.000E+00 0.000E+00 0.000E+00 0.000E+00
J= 10 X2=.170E-03 0.000E+00 0.000E+00 0.000E+00 0.000E+00 0.000E+00 0.000E+00 0.000E+00 0.000E+00 0.000E+00 0.000E+00
J= 9 X2=.150E-03 0.000E+00 0.000E+00 0.000E+00 0.000E+00 0.000E+00 0.000E+00 0.000E+00 0.000E+00 0.000E+00 0.000E+00
J= 8 X2=.130E-03 0.000E+00 0.000E+00 0.000E+00 0.000E+00 0.000E+00 0.000E+00 0.000E+00 0.000E+00 0.000E+00 0.000E+00
J= 7 X2=.110E-03 0.000E+00 0.000E+00 0.000E+00 0.000E+00 0.000E+00 0.000E+00 0.000E+00 0.000E+00 0.000E+00 0.000E+00
J= 6 X2=.900E-04 0.000E+00 0.000E+00 0.000E+00 0.000E+00 0.000E+00 0.000E+00 0.000E+00 0.000E+00 0.000E+00 0.000E+00
J= 5 X2=.700E-04 0.000E+00 0.000E+00 0.000E+00 0.000E+00 0.000E+00 0.000E+00 0.000E+00 0.000E+00 0.000E+00 0.000E+00
J= 4 X2=.500E-04 0.000E+00 0.000E+00 0.000E+00 0.000E+00 0.000E+00 0.000E+00 0.000E+00 0.000E+00 0.000E+00 0.000E+00
J= 3 X2=.300E-04 0.000E+00 0.000E+00 0.000E+00 0.000E+00 0.000E+00 0.000E+00 0.000E+00 0.000E+00 0.000E+00 0.000E+00
J= 2 X2=.100E-04 0.000E+00 0.000E+00 0.000E+00 0.000E+00 0.000E+00 0.000E+00 0.000E+00 0.000E+00 0.000E+00 0.000E+00
J= 1 X2=***** 0.000E+00 0.000E+00 0.000E+00 0.000E+00 0.000E+00 0.000E+00 0.000E+00 0.000E+00 0.000E+00 0.000E+00
          I =          11          12          13          14          15          16          17          18          19          20
          X1 = 0.2375E-04 0.2625E-04 0.2875E-04 0.3125E-04 0.3375E-04 0.3625E-04 0.3875E-04 0.4125E-04 0.4375E-04 0.4625E-04
    
```

J= 26	X2= .500E-03	0.000E+00	2.508E+00	6.965E+00	1.088E+01	1.427E+01	1.714E+01	1.952E+01	2.141E+01	2.282E+01	2.375E+01
J= 27	X2= .510E-03	0.000E+00	2.740E+00	7.653E+00	1.201E+01	1.580E+01	1.905E+01	2.175E+01	2.390E+01	2.551E+01	2.659E+01
J= 26	X2= .490E-03	0.000E+00	2.810E+00	7.862E+00	1.235E+01	1.627E+01	1.963E+01	2.243E+01	2.466E+01	2.634E+01	2.746E+01
J= 25	X2= .470E-03	0.000E+00	2.832E+00	7.927E+00	1.245E+01	1.641E+01	1.981E+01	2.263E+01	2.490E+01	2.659E+01	2.772E+01
J= 24	X2= .450E-03	0.000E+00	2.839E+00	7.947E+00	1.249E+01	1.646E+01	1.986E+01	2.270E+01	2.497E+01	2.667E+01	2.780E+01
J= 23	X2= .430E-03	0.000E+00	2.841E+00	7.954E+00	1.250E+01	1.647E+01	1.988E+01	2.272E+01	2.499E+01	2.670E+01	2.783E+01
J= 22	X2= .410E-03	0.000E+00	2.841E+00	7.955E+00	1.250E+01	1.648E+01	1.989E+01	2.273E+01	2.500E+01	2.670E+01	2.784E+01
J= 21	X2= .390E-03	0.000E+00	2.841E+00	7.956E+00	1.250E+01	1.648E+01	1.989E+01	2.273E+01	2.500E+01	2.671E+01	2.784E+01
J= 20	X2= .370E-03	0.000E+00	2.841E+00	7.956E+00	1.250E+01	1.648E+01	1.989E+01	2.273E+01	2.500E+01	2.671E+01	2.784E+01
J= 19	X2= .350E-03	0.000E+00	2.841E+00	7.956E+00	1.250E+01	1.648E+01	1.989E+01	2.273E+01	2.500E+01	2.671E+01	2.784E+01
J= 18	X2= .330E-03	0.000E+00	2.841E+00	7.955E+00	1.250E+01	1.648E+01	1.989E+01	2.273E+01	2.500E+01	2.670E+01	2.784E+01
J= 17	X2= .310E-03	0.000E+00	2.841E+00	7.955E+00	1.250E+01	1.648E+01	1.989E+01	2.273E+01	2.500E+01	2.670E+01	2.784E+01
J= 16	X2= .290E-03	0.000E+00	2.840E+00	7.953E+00	1.250E+01	1.647E+01	1.988E+01	2.272E+01	2.499E+01	2.669E+01	2.783E+01
J= 15	X2= .270E-03	0.000E+00	2.838E+00	7.947E+00	1.249E+01	1.646E+01	1.986E+01	2.270E+01	2.497E+01	2.667E+01	2.781E+01
J= 14	X2= .250E-03	0.000E+00	2.832E+00	7.927E+00	1.245E+01	1.642E+01	1.981E+01	2.264E+01	2.490E+01	2.659E+01	2.772E+01
J= 13	X2= .230E-03	0.000E+00	2.810E+00	7.863E+00	1.235E+01	1.627E+01	1.963E+01	2.243E+01	2.466E+01	2.634E+01	2.746E+01
J= 12	X2= .210E-03	0.000E+00	2.740E+00	7.654E+00	1.201E+01	1.580E+01	1.905E+01	2.175E+01	2.390E+01	2.551E+01	2.659E+01
J= 11	X2= .190E-03	0.000E+00	2.508E+00	6.966E+00	1.088E+01	1.427E+01	1.714E+01	1.952E+01	2.141E+01	2.282E+01	2.375E+01
J= 10	X2= .170E-03	0.000E+00	1.722E+00	4.638E+00	7.095E+00	9.146E+00	1.083E+01	1.220E+01	1.325E+01	1.403E+01	1.454E+01
J= 9	X2= .150E-03	0.000E+00									
J= 8	X2= .130E-03	0.000E+00									
J= 7	X2= .110E-03	0.000E+00									
J= 6	X2= .900E-04	0.000E+00									
J= 5	X2= .700E-04	0.000E+00									
J= 4	X2= .500E-04	0.000E+00									
J= 3	X2= .300E-04	0.000E+00									
J= 2	X2= .100E-04	0.000E+00									
J= 1	X2= -----	0.000E+00									

I = 21 22  
X1 = 0.4875E-04 0.5125E-04

J= 30	X2= .570E-03	0.000E+00	0.000E+00
J= 29	X2= .550E-03	1.480E+01	0.000E+00
J= 28	X2= .530E-03	2.422E+01	0.000E+00
J= 27	X2= .510E-03	2.712E+01	0.000E+00
J= 26	X2= .490E-03	2.802E+01	0.000E+00
J= 25	X2= .470E-03	2.839E+01	0.000E+00
J= 24	X2= .450E-03	2.837E+01	0.000E+00
J= 23	X2= .430E-03	2.840E+01	0.000E+00
J= 22	X2= .410E-03	2.841E+01	0.000E+00
J= 21	X2= .390E-03	2.841E+01	0.000E+00
J= 20	X2= .370E-03	2.841E+01	0.000E+00
J= 19	X2= .350E-03	2.841E+01	0.000E+00
J= 18	X2= .330E-03	2.841E+01	0.000E+00
J= 17	X2= .310E-03	2.841E+01	0.000E+00
J= 16	X2= .290E-03	2.840E+01	0.000E+00
J= 15	X2= .270E-03	2.837E+01	0.000E+00
J= 14	X2= .250E-03	2.839E+01	0.000E+00
J= 13	X2= .230E-03	2.802E+01	0.000E+00
J= 12	X2= .210E-03	2.712E+01	0.000E+00
J= 11	X2= .190E-03	2.422E+01	0.000E+00
J= 10	X2= .170E-03	1.480E+01	0.000E+00
J= 9	X2= .150E-03	0.000E+00	0.000E+00
J= 8	X2= .130E-03	0.000E+00	0.000E+00
J= 7	X2= .110E-03	0.000E+00	0.000E+00
J= 6	X2= .900E-04	0.000E+00	0.000E+00
J= 5	X2= .700E-04	0.000E+00	0.000E+00
J= 4	X2= .500E-04	0.000E+00	0.000E+00
J= 3	X2= .300E-04	0.000E+00	0.000E+00
J= 2	X2= .100E-04	0.000E+00	0.000E+00
J= 1	X2= -----	0.000E+00	0.000E+00

AVERAGE VELOCITY IS: 20.7799129848849  
THE FLOW CHANNEL HEIGHT IS: 0.6000000000000000D-003  
THE FLOW CHANNEL WIDTH (complete) IS: 0.5000000000000000D-004  
THE HYDRAULIC DIAMETER IS: 0.8888888888888888D-004  
THE AVERAGE REYNOLDS NUMBER IS: 3848.13203423794  
THE ENERGY GEN. WALL FLUX IS: (W/CM^2) 1000.0000000000

Pressure gradient is: [Pa/m] 0.500000E+08  
 Viscosity is: [Pa·S] 0.5000000000000000E-009

One quarter is calculated because of symmetry.  
 The y dir. runs rows and the z dir. runs columns.  
 Distance is in micrometers and velocity is in M/S.  
 This program assumes no slip boundaries.

The average velocity is: 17.4781

	24.	22.	21.	20.	19.	17.	16.	15.	14.	12.	11.	10.	9.	7.	6.	5.	4.	2.	1.	0.
0	1.40	4.10	6.66	9.07	11.35	13.48	15.47	17.31	19.02	20.58	22.00	23.28	24.41	25.41	26.26	26.97	27.54	27.96	28.25	28.39
10	1.40	4.10	6.66	9.07	11.35	13.48	15.47	17.31	19.02	20.68	22.00	23.28	24.41	25.41	26.26	26.97	27.54	27.96	28.25	28.39
20	1.40	4.10	6.66	9.07	11.36	13.48	15.46	17.31	19.02	20.68	22.00	23.28	24.41	25.41	26.26	26.97	27.54	27.96	28.25	28.39
30	1.40	4.10	6.66	9.07	11.36	13.48	15.46	17.31	19.02	20.58	22.00	23.28	24.41	25.41	26.26	26.97	27.54	27.96	28.25	28.39
40	1.40	4.10	6.66	9.07	11.35	13.48	15.46	17.31	19.02	20.68	22.00	23.28	24.41	25.41	26.26	26.97	27.54	27.96	28.25	28.39
50	1.40	4.10	6.66	9.07	11.34	13.46	15.46	17.31	19.01	20.68	22.00	23.28	24.41	25.41	26.26	26.97	27.54	27.96	28.25	28.39
60	1.40	4.10	6.66	9.07	11.34	13.47	15.46	17.31	19.01	20.67	21.99	23.27	24.41	25.40	26.26	26.97	27.53	27.96	28.24	28.39
70	1.40	4.10	6.66	9.07	11.34	13.47	15.46	17.31	19.01	20.57	21.99	23.27	24.40	25.40	26.25	26.96	27.53	27.96	28.24	28.38
80	1.40	4.10	6.66	9.07	11.34	13.47	15.45	17.30	19.00	20.56	21.98	23.26	24.40	25.39	26.24	26.96	27.52	27.94	28.23	28.37
90	1.40	4.10	6.66	9.06	11.34	13.46	15.45	17.29	18.99	20.55	21.97	23.25	24.38	25.37	26.22	26.93	27.50	27.93	28.21	28.36
100	1.40	4.09	6.64	9.06	11.32	13.45	15.43	17.27	18.97	20.53	21.94	23.22	24.35	25.34	26.19	26.90	27.47	27.89	28.17	28.32
110	1.40	4.09	6.63	9.04	11.30	13.42	15.40	17.23	18.93	20.48	21.90	23.17	24.30	25.29	26.13	26.84	27.40	27.83	28.11	28.26
120	1.39	4.07	6.61	9.00	11.25	13.37	15.34	17.17	18.86	20.40	21.81	23.07	24.20	25.18	26.02	26.72	27.29	27.71	27.99	28.13
130	1.38	4.04	6.56	8.94	11.17	13.27	15.22	17.04	18.71	20.24	21.64	22.89	24.00	24.98	25.81	26.51	27.08	27.48	27.76	27.90
140	1.37	3.99	6.48	8.82	11.03	13.09	15.01	16.80	18.44	19.96	21.32	22.56	23.64	24.60	25.42	26.10	26.65	27.06	27.33	27.47
150	1.33	3.90	6.32	8.60	10.75	12.75	14.62	16.36	17.94	19.40	20.73	21.92	22.97	23.89	24.69	25.34	25.87	26.26	26.53	26.66
160	1.27	3.72	6.02	8.19	10.22	12.11	13.87	15.60	17.00	18.37	19.61	20.72	21.71	22.57	23.31	23.92	24.41	24.78	25.02	25.14
170	1.16	3.38	5.46	7.41	9.23	10.92	12.48	13.92	15.23	16.43	17.52	18.49	19.34	20.09	20.73	21.26	21.68	22.00	22.21	22.31
180	0.95	2.74	4.39	5.92	7.33	8.63	9.82	10.90	11.89	12.77	13.57	14.28	14.90	15.44	15.90	16.28	16.59	16.81	16.96	17.04
190	0.60	1.40	2.19	2.89	3.61	4.06	4.56	5.00	5.39	5.74	6.05	6.33	6.67	6.77	6.96	7.09	7.20	7.29	7.34	7.37

----- FINISHED -----

TRANSPORT EQUATION SOLUTION ALGORITHM TESTER

```

SOLUTION METHOD          PSOR
NUMBER OF CELLS IN X1-DIRECTION, NMAX1  - - - - 42
NUMBER OF CELLS IN X2-DIRECTION, NMAX2  - - - - 58
WIDTH OF CELLS IN X1-DIRECTION, DX1    - - - - .12500E-05
WIDTH OF CELLS IN X2-DIRECTION, DX2    - - - - .10000E-04
OVER-RELAXATION FACTOR      , OMEGA   - - - - 1.750
MAXIMUM NUMBER ITERATIONS   , ITMAX  - - - -1000
DELTA-PHI ERROR CRITERION   , TCRIT - - - - 2.000E-02
HEAT BALANCE ERROR CRITERION , QMAX  - - - - 0.100
INITIAL VELOCITY            , TINIT  - - - - 0.0000E+00
    
```

STEADY STATE VELOCITY ARRAY OUTPUT FOR ITERATION NUMBER: 105

	I = 1	2	3	4	5	6	7	8	9	10
X1 =	-.6250E-06	0.6250E-06	0.1875E-05	0.3125E-05	0.4375E-05	0.5625E-05	0.6875E-05	0.8125E-05	0.9375E-05	0.1063E-04
J= 58 X2= .565E-03	0.000E+00									
J= 57 X2= .555E-03	0.000E+00									
J= 56 X2= .545E-03	0.000E+00									
J= 55 X2= .535E-03	0.000E+00									
J= 54 X2= .525E-03	0.000E+00									
J= 53 X2= .515E-03	0.000E+00									
J= 52 X2= .505E-03	0.000E+00									
J= 51 X2= .495E-03	0.000E+00									
I = 21	22	23	24	25	26	27	28	29	30	
X1 =	0.2417E-04	0.2562E-04	0.2687E-04	0.2812E-04	0.2937E-04	0.3062E-04	0.3188E-04	0.3313E-04	0.3438E-04	0.3563E-04
J= 58 X2= .565E-03	0.000E+00									
J= 57 X2= .555E-03	0.000E+00	5.609E-01	1.552E+00	2.430E+00	3.210E+00	3.905E+00	4.524E+00	5.076E+00	5.568E+00	6.006E+00
J= 56 X2= .545E-03	0.000E+00	9.754E-01	2.788E+00	4.468E+00	6.022E+00	7.456E+00	8.776E+00	9.986E+00	1.109E+01	1.210E+01
J= 55 X2= .535E-03	0.000E+00	1.181E+00	3.404E+00	5.490E+00	7.441E+00	9.262E+00	1.095E+01	1.252E+01	1.396E+01	1.529E+01
J= 54 X2= .525E-03	0.000E+00	1.289E+00	3.728E+00	6.027E+00	8.188E+00	1.021E+01	1.210E+01	1.386E+01	1.549E+01	1.698E+01
J= 53 X2= .515E-03	0.000E+00	1.347E+00	3.899E+00	6.311E+00	8.584E+00	1.072E+01	1.272E+01	1.458E+01	1.630E+01	1.789E+01
J= 52 X2= .505E-03	0.000E+00	1.377E+00	3.990E+00	6.363E+00	8.795E+00	1.099E+01	1.304E+01	1.496E+01	1.673E+01	1.837E+01
J= 51 X2= .495E-03	0.000E+00	1.393E+00	4.038E+00	6.542E+00	8.906E+00	1.113E+01	1.321E+01	1.516E+01	1.696E+01	1.863E+01
J= 50 X2= .485E-03	0.000E+00	1.402E+00	4.063E+00	6.584E+00	8.964E+00	1.120E+01	1.330E+01	1.526E+01	1.708E+01	1.876E+01
J= 49 X2= .475E-03	0.000E+00	1.406E+00	4.076E+00	6.606E+00	8.994E+00	1.124E+01	1.335E+01	1.532E+01	1.714E+01	1.883E+01
J= 48 X2= .465E-03	0.000E+00	1.408E+00	4.083E+00	6.617E+00	9.010E+00	1.126E+01	1.337E+01	1.534E+01	1.718E+01	1.887E+01
J= 47 X2= .455E-03	0.000E+00	1.409E+00	4.086E+00	6.622E+00	9.017E+00	1.127E+01	1.339E+01	1.536E+01	1.719E+01	1.888E+01
J= 46 X2= .445E-03	0.000E+00	1.410E+00	4.088E+00	6.625E+00	9.021E+00	1.128E+01	1.339E+01	1.537E+01	1.720E+01	1.889E+01
J= 45 X2= .435E-03	0.000E+00	1.410E+00	4.088E+00	6.626E+00	9.023E+00	1.128E+01	1.339E+01	1.537E+01	1.720E+01	1.890E+01
J= 44 X2= .425E-03	0.000E+00	1.410E+00	4.089E+00	6.627E+00	9.024E+00	1.128E+01	1.340E+01	1.537E+01	1.721E+01	1.890E+01
J= 43 X2= .415E-03	0.000E+00	1.410E+00	4.089E+00	6.627E+00	9.024E+00	1.128E+01	1.340E+01	1.537E+01	1.721E+01	1.890E+01
J= 42 X2= .405E-03	0.000E+00	1.410E+00	4.089E+00	6.627E+00	9.024E+00	1.128E+01	1.340E+01	1.537E+01	1.721E+01	1.890E+01
J= 41 X2= .395E-03	0.000E+00	1.410E+00	4.089E+00	6.627E+00	9.024E+00	1.128E+01	1.340E+01	1.537E+01	1.721E+01	1.890E+01
J= 40 X2= .385E-03	0.000E+00	1.410E+00	4.089E+00	6.627E+00	9.024E+00	1.128E+01	1.340E+01	1.537E+01	1.721E+01	1.890E+01
J= 39 X2= .375E-03	0.000E+00	1.410E+00	4.089E+00	6.627E+00	9.024E+00	1.128E+01	1.340E+01	1.537E+01	1.721E+01	1.890E+01
J= 38 X2= .365E-03	0.000E+00	1.410E+00	4.089E+00	6.627E+00	9.024E+00	1.128E+01	1.340E+01	1.537E+01	1.721E+01	1.890E+01

J= 37 X2= .355E-03	0.000E+00	1.410E+00	4.089E+00	6.627E+00	9.024E+00	1.128E+01	1.340E+01	1.537E+01	1.721E+01	1.890E+01
J= 36 X2= .345E-03	0.000E+00	1.410E+00	4.089E+00	6.627E+00	9.024E+00	1.128E+01	1.340E+01	1.537E+01	1.721E+01	1.890E+01
J= 35 X2= .335E-03	0.000E+00	1.410E+00	4.089E+00	6.627E+00	9.024E+00	1.128E+01	1.340E+01	1.537E+01	1.721E+01	1.890E+01
J= 34 X2= .325E-03	0.000E+00	1.410E+00	4.089E+00	6.627E+00	9.024E+00	1.128E+01	1.340E+01	1.537E+01	1.721E+01	1.890E+01
J= 33 X2= .315E-03	0.000E+00	1.410E+00	4.089E+00	6.627E+00	9.024E+00	1.128E+01	1.340E+01	1.537E+01	1.721E+01	1.890E+01
J= 32 X2= .305E-03	0.000E+00	1.410E+00	4.089E+00	6.627E+00	9.024E+00	1.128E+01	1.340E+01	1.537E+01	1.721E+01	1.890E+01
J= 31 X2= .295E-03	0.000E+00	1.410E+00	4.088E+00	6.626E+00	9.023E+00	1.128E+01	1.339E+01	1.537E+01	1.720E+01	1.890E+01
J= 30 X2= .285E-03	0.000E+00	1.410E+00	4.088E+00	6.625E+00	9.022E+00	1.128E+01	1.339E+01	1.537E+01	1.720E+01	1.890E+01
J= 29 X2= .275E-03	0.000E+00	1.409E+00	4.087E+00	6.624E+00	9.020E+00	1.128E+01	1.339E+01	1.536E+01	1.720E+01	1.889E+01
J= 28 X2= .265E-03	0.000E+00	1.409E+00	4.085E+00	6.621E+00	9.016E+00	1.127E+01	1.338E+01	1.536E+01	1.719E+01	1.888E+01
J= 27 X2= .255E-03	0.000E+00	1.408E+00	4.082E+00	6.615E+00	9.008E+00	1.126E+01	1.337E+01	1.534E+01	1.717E+01	1.886E+01
J= 26 X2= .245E-03	0.000E+00	1.405E+00	4.075E+00	6.604E+00	8.992E+00	1.124E+01	1.335E+01	1.531E+01	1.714E+01	1.882E+01
J= 25 X2= .235E-03	0.000E+00	1.401E+00	4.062E+00	6.582E+00	8.961E+00	1.120E+01	1.330E+01	1.526E+01	1.707E+01	1.875E+01
J= 24 X2= .225E-03	0.000E+00	1.392E+00	4.036E+00	6.539E+00	8.902E+00	1.112E+01	1.321E+01	1.515E+01	1.695E+01	1.862E+01
J= 23 X2= .215E-03	0.000E+00	1.376E+00	3.988E+00	6.459E+00	8.790E+00	1.098E+01	1.303E+01	1.495E+01	1.672E+01	1.836E+01
J= 22 X2= .205E-03	0.000E+00	1.346E+00	3.897E+00	6.307E+00	8.579E+00	1.071E+01	1.271E+01	1.457E+01	1.629E+01	1.788E+01
J= 21 X2= .195E-03	0.000E+00	1.289E+00	3.725E+00	6.022E+00	8.182E+00	1.021E+01	1.210E+01	1.385E+01	1.548E+01	1.697E+01
J= 20 X2= .185E-03	0.000E+00	1.181E+00	3.402E+00	5.486E+00	7.436E+00	9.256E+00	1.095E+01	1.251E+01	1.396E+01	1.528E+01
J= 19 X2= .175E-03	0.000E+00	9.748E-01	2.786E+00	4.465E+00	6.018E+00	7.451E+00	8.770E+00	9.979E+00	1.108E+01	1.209E+01
J= 18 X2= .165E-03	0.000E+00	5.607E-01	1.551E+00	2.429E+00	3.209E+00	3.903E+00	4.522E+00	5.074E+00	5.565E+00	6.003E+00
J= 17 X2= .155E-03	0.000E+00									
J= 16 X2= .145E-03	0.000E+00									
J= 15 X2= .135E-03	0.000E+00									
J= 14 X2= .125E-03	0.000E+00									
J= 13 X2= .115E-03	0.000E+00									
J= 12 X2= .105E-03	0.000E+00									
J= 11 X2= .950E-04	0.000E+00									
J= 10 X2= .850E-04	0.000E+00									
J= 9 X2= .750E-04	0.000E+00									
J= 8 X2= .650E-04	0.000E+00									
J= 7 X2= .550E-04	0.000E+00									
J= 6 X2= .450E-04	0.000E+00									
J= 5 X2= .350E-04	0.000E+00									
J= 4 X2= .250E-04	0.000E+00									
J= 3 X2= .150E-04	0.000E+00									
J= 2 X2= .500E-05	0.000E+00									
J= 1 X2=*****	0.000E+00									

I = 31 32 33 34 35 36 37 38 39 40  
X1 = 0.3688E-04 0.3813E-04 0.3938E-04 0.4063E-04 0.4188E-04 0.4313E-04 0.4438E-04 0.4563E-04 0.4688E-04 0.4813E-04

J= 58 X2= .565E-03	0.000E+00									
J= 57 X2= .555E-03	6.395E+00	6.738E+00	7.039E+00	7.300E+00	7.525E+00	7.714E+00	7.870E+00	7.993E+00	8.085E+00	8.146E+00
J= 56 X2= .545E-03	1.301E+01	1.382E+01	1.455E+01	1.519E+01	1.574E+01	1.621E+01	1.660E+01	1.691E+01	1.714E+01	1.730E+01
J= 55 X2= .535E-03	1.649E+01	1.758E+01	1.856E+01	1.942E+01	2.017E+01	2.081E+01	2.135E+01	2.177E+01	2.209E+01	2.230E+01
J= 54 X2= .525E-03	1.835E+01	1.959E+01	2.070E+01	2.169E+01	2.255E+01	2.329E+01	2.390E+01	2.439E+01	2.476E+01	2.501E+01
J= 53 X2= .515E-03	1.934E+01	2.066E+01	2.185E+01	2.291E+01	2.383E+01	2.462E+01	2.527E+01	2.580E+01	2.620E+01	2.646E+01
J= 52 X2= .505E-03	1.987E+01	2.124E+01	2.246E+01	2.355E+01	2.451E+01	2.533E+01	2.601E+01	2.655E+01	2.696E+01	2.724E+01
J= 51 X2= .495E-03	2.015E+01	2.154E+01	2.279E+01	2.390E+01	2.487E+01	2.570E+01	2.640E+01	2.695E+01	2.737E+01	2.765E+01
J= 50 X2= .485E-03	2.030E+01	2.170E+01	2.296E+01	2.408E+01	2.506E+01	2.590E+01	2.660E+01	2.716E+01	2.759E+01	2.787E+01
J= 49 X2= .475E-03	2.038E+01	2.178E+01	2.305E+01	2.417E+01	2.516E+01	2.600E+01	2.671E+01	2.727E+01	2.770E+01	2.798E+01
J= 48 X2= .465E-03	2.042E+01	2.182E+01	2.309E+01	2.422E+01	2.521E+01	2.606E+01	2.676E+01	2.733E+01	2.776E+01	2.804E+01
J= 47 X2= .455E-03	2.043E+01	2.185E+01	2.312E+01	2.425E+01	2.524E+01	2.608E+01	2.679E+01	2.736E+01	2.779E+01	2.807E+01
J= 46 X2= .445E-03	2.044E+01	2.186E+01	2.313E+01	2.426E+01	2.525E+01	2.610E+01	2.681E+01	2.738E+01	2.781E+01	2.809E+01
J= 45 X2= .435E-03	2.045E+01	2.186E+01	2.313E+01	2.426E+01	2.525E+01	2.610E+01	2.681E+01	2.738E+01	2.781E+01	2.809E+01
J= 44 X2= .425E-03	2.045E+01	2.186E+01	2.314E+01	2.427E+01	2.526E+01	2.611E+01	2.682E+01	2.739E+01	2.782E+01	2.810E+01
J= 43 X2= .415E-03	2.045E+01	2.186E+01	2.314E+01	2.427E+01	2.526E+01	2.611E+01	2.682E+01	2.739E+01	2.782E+01	2.810E+01
J= 42 X2= .405E-03	2.045E+01	2.186E+01	2.314E+01	2.427E+01	2.526E+01	2.611E+01	2.682E+01	2.739E+01	2.782E+01	2.810E+01
J= 41 X2= .395E-03	2.045E+01	2.187E+01	2.314E+01	2.427E+01	2.526E+01	2.611E+01	2.682E+01	2.739E+01	2.782E+01	2.810E+01
J= 40 X2= .385E-03	2.045E+01	2.187E+01	2.314E+01	2.427E+01	2.526E+01	2.611E+01	2.682E+01	2.739E+01	2.782E+01	2.810E+01
J= 39 X2= .375E-03	2.045E+01	2.187E+01	2.314E+01	2.427E+01	2.526E+01	2.611E+01	2.682E+01	2.739E+01	2.782E+01	2.810E+01
J= 38 X2= .365E-03	2.045E+01	2.187E+01	2.314E+01	2.427E+01	2.526E+01	2.611E+01	2.682E+01	2.739E+01	2.782E+01	2.810E+01
J= 37 X2= .355E-03	2.045E+01	2.187E+01	2.314E+01	2.427E+01	2.526E+01	2.611E+01	2.682E+01	2.739E+01	2.782E+01	2.810E+01
J= 36 X2= .345E-03	2.045E+01	2.187E+01	2.314E+01	2.427E+01	2.526E+01	2.611E+01	2.682E+01	2.739E+01	2.782E+01	2.810E+01
J= 35 X2= .335E-03	2.045E+01	2.187E+01	2.314E+01	2.427E+01	2.526E+01	2.611E+01	2.682E+01	2.739E+01	2.782E+01	2.810E+01

J= 34 X2= .352E-03	1.043E+01	2.186E+01	2.319E+01	2.427E+01	2.526E+01	2.611E+01	2.682E+01	2.739E+01	2.781E+01	2.810E+01
J= 33 X2= .312E-03	1.045E+01	2.136E+01	2.311E+01	2.427E+01	2.526E+01	2.611E+01	2.682E+01	2.739E+01	2.781E+01	2.810E+01
J= 32 X2= .272E-03	1.045E+01	2.136E+01	2.311E+01	2.427E+01	2.526E+01	2.611E+01	2.682E+01	2.738E+01	2.781E+01	2.810E+01
J= 31 X2= .232E-03	2.045E+01	2.186E+01	2.313E+01	2.427E+01	2.526E+01	2.611E+01	2.681E+01	2.738E+01	2.781E+01	2.810E+01
J= 30 X2= .192E-03	2.045E+01	2.136E+01	2.313E+01	2.426E+01	2.525E+01	2.610E+01	2.681E+01	2.738E+01	2.781E+01	2.809E+01
J= 29 X2= .152E-03	2.044E+01	2.135E+01	2.313E+01	2.426E+01	2.525E+01	2.609E+01	2.680E+01	2.737E+01	2.780E+01	2.808E+01
J= 28 X2= .112E-03	2.043E+01	2.184E+01	2.311E+01	2.424E+01	2.523E+01	2.608E+01	2.679E+01	2.736E+01	2.778E+01	2.807E+01
J= 27 X2= .072E-03	2.041E+01	2.132E+01	2.309E+01	2.422E+01	2.520E+01	2.605E+01	2.675E+01	2.733E+01	2.775E+01	2.804E+01
J= 26 X2= .032E-03	2.037E+01	2.178E+01	2.304E+01	2.417E+01	2.515E+01	2.600E+01	2.670E+01	2.727E+01	2.769E+01	2.798E+01
J= 25 X2= .235E-03	2.029E+01	2.169E+01	2.295E+01	2.407E+01	2.505E+01	2.589E+01	2.659E+01	2.715E+01	2.758E+01	2.786E+01
J= 24 X2= .225E-03	2.014E+01	2.153E+01	2.278E+01	2.389E+01	2.486E+01	2.569E+01	2.638E+01	2.694E+01	2.736E+01	2.764E+01
J= 23 X2= .215E-03	1.986E+01	2.122E+01	2.245E+01	2.354E+01	2.449E+01	2.531E+01	2.599E+01	2.654E+01	2.695E+01	2.722E+01
J= 22 X2= .205E-03	1.933E+01	2.065E+01	2.184E+01	2.289E+01	2.381E+01	2.460E+01	2.526E+01	2.579E+01	2.613E+01	2.645E+01
J= 21 X2= .195E-03	1.334E+01	1.958E+01	2.069E+01	2.168E+01	2.254E+01	2.327E+01	2.389E+01	2.438E+01	2.475E+01	2.499E+01
J= 20 X2= .185E-03	1.648E+01	1.757E+01	1.854E+01	1.941E+01	2.016E+01	2.080E+01	2.133E+01	2.176E+01	2.208E+01	2.229E+01
J= 19 X2= .175E-03	1.300E+01	1.381E+01	1.454E+01	1.518E+01	1.573E+01	1.620E+01	1.659E+01	1.690E+01	1.713E+01	1.729E+01
J= 18 X2= .165E-03	6.391E+00	6.734E+00	7.035E+00	7.297E+00	7.521E+00	7.711E+00	7.865E+00	7.990E+00	8.091E+00	8.142E+00
J= 17 X2= .155E-03	0.000E+00									
J= 16 X2= .145E-03	0.000E+00									
J= 15 X2= .135E-03	0.000E+00									
J= 14 X2= .125E-03	0.000E+00									
J= 13 X2= .115E-03	0.000E+00									
J= 12 X2= .105E-03	0.000E+00									
J= 11 X2= .950E-04	0.000E+00									
J= 10 X2= .850E-04	0.000E+00									
J= 9 X2= .750E-04	0.000E+00									
J= 8 X2= .650E-04	0.000E+00									
J= 7 X2= .550E-04	0.000E+00									
J= 6 X2= .450E-04	0.000E+00									
J= 5 X2= .350E-04	0.000E+00									
J= 4 X2= .250E-04	0.000E+00									
J= 3 X2= .150E-04	0.000E+00									
J= 2 X2= .500E-05	0.000E+00									
J= 1 X2= *****	0.000E+00									

I =		41	42
X1 =		0.4938E-04	0.5063E-04
J= 58 X2= .565E-03	0.000E+00	0.000E+00	
J= 57 X2= .555E-03	8.177E+00	0.000E+00	
J= 56 X2= .545E-03	1.738E+01	0.000E+00	
J= 55 X2= .535E-03	2.241E+01	0.000E+00	
J= 54 X2= .525E-03	2.513E+01	0.000E+00	
J= 53 X2= .515E-03	2.659E+01	0.000E+00	
J= 52 X2= .505E-03	2.738E+01	0.000E+00	
J= 51 X2= .495E-03	2.779E+01	0.000E+00	
J= 50 X2= .485E-03	2.801E+01	0.000E+00	
J= 49 X2= .475E-03	2.813E+01	0.000E+00	
J= 48 X2= .465E-03	2.819E+01	0.000E+00	
J= 47 X2= .455E-03	2.822E+01	0.000E+00	
J= 46 X2= .445E-03	2.823E+01	0.000E+00	
J= 45 X2= .435E-03	2.824E+01	0.000E+00	
J= 44 X2= .425E-03	2.824E+01	0.000E+00	
J= 43 X2= .415E-03	2.824E+01	0.000E+00	
J= 42 X2= .405E-03	2.825E+01	0.000E+00	
J= 41 X2= .395E-03	2.825E+01	0.000E+00	
J= 40 X2= .385E-03	2.825E+01	0.000E+00	
J= 39 X2= .375E-03	2.825E+01	0.000E+00	
J= 38 X2= .365E-03	2.825E+01	0.000E+00	
J= 37 X2= .355E-03	2.825E+01	0.000E+00	
J= 36 X2= .345E-03	2.825E+01	0.000E+00	
J= 35 X2= .335E-03	2.825E+01	0.000E+00	
J= 34 X2= .325E-03	2.825E+01	0.000E+00	
J= 33 X2= .315E-03	2.825E+01	0.000E+00	
J= 32 X2= .305E-03	2.824E+01	0.000E+00	
J= 31 X2= .295E-03	2.824E+01	0.000E+00	
J= 30 X2= .285E-03	2.824E+01	0.000E+00	
J= 29 X2= .275E-03	2.823E+01	0.000E+00	
J= 28 X2= .265E-03	2.823E+01	0.000E+00	

```

J= 31 X2=-.295E-03 2.824E+01 0.000E+00
J= 30 X2=-.285E-03 2.824E+01 0.000E+00
J= 29 X2=-.275E-03 2.823E+01 0.000E+00
J= 28 X2=-.265E-03 2.821E+01 0.000E+00
J= 27 X2=-.255E-03 2.818E+01 0.000E+00
J= 26 X2=-.245E-03 2.812E+01 0.000E+00
J= 25 X2=-.235E-03 2.800E+01 0.000E+00
J= 24 X2=-.225E-03 2.778E+01 0.000E+00
J= 23 X2=-.215E-03 2.736E+01 0.000E+00
J= 22 X2=-.205E-03 2.658E+01 0.000E+00
J= 21 X2=-.195E-03 2.512E+01 0.000E+00
J= 20 X2=-.185E-03 2.240E+01 0.000E+00
J= 19 X2=-.175E-03 1.737E+01 0.000E+00
J= 18 X2=-.165E-03 8.173E+00 0.000E+00
J= 17 X2=-.155E-03 0.000E+00 0.000E+00
J= 16 X2=-.145E-03 0.000E+00 0.000E+00
J= 15 X2=-.135E-03 0.000E+00 0.000E+00
J= 14 X2=-.125E-03 0.000E+00 0.000E+00
J= 13 X2=-.115E-03 0.000E+00 0.000E+00
J= 12 X2=-.105E-03 0.000E+00 0.000E+00
J= 11 X2=-.950E-04 0.000E+00 0.000E+00
J= 10 X2=-.850E-04 0.000E+00 0.000E+00
J= 9 X2=-.750E-04 0.000E+00 0.000E+00
J= 8 X2=-.650E-04 0.000E+00 0.000E+00
J= 7 X2=-.550E-04 0.000E+00 0.000E+00
J= 6 X2=-.450E-04 0.000E+00 0.000E+00
J= 5 X2=-.350E-04 0.000E+00 0.000E+00
J= 4 X2=-.250E-04 0.000E+00 0.000E+00
J= 3 X2=-.150E-04 0.000E+00 0.000E+00
J= 2 X2=-.500E-05 0.000E+00 0.000E+00
J= 1 X2=***** 0.000E+00 0.000E+00
AVERAGE VELOCITY IS: 18.831577738515
THE FLOW CHANNEL HEIGHT IS: 0.400000000000000D-003
THE FLOW CHANNEL WIDTH (complete) IS: 0.500000000000000D-004
THE HYDRAULIC DIAMETER IS: 0.88888888888889D-004
THE AVERAGE REYNOLDS NUMBER IS: 3487.32921737991
THE ENERGY GEN. WALL FLUX IS: [W/CM^2] 1000.00000000000

```

## APPENDIX C

## Infinite Channel Comparisons for Discretization Information

## 1 THE INFINITE CHANNEL

Dr. C. Landrum provided the analytical solution to the temperature and velocity distributions for flow within an infinite parallel plate channel. This solution was also used by Tuckerman in reference [1]. Since it has such similarity to the microchannel it can be used to obtain discretization information. If the microchannels are considered very tall and the heat flux is constant along the face of the fin the microchannel problem essentially reduces to the infinite channel problem which is one dimensional.

The analytical solution for the temperature and velocity within the infinite channel are as follows:

$$(1) \quad u/u_0 = 3y'(1 - \frac{1}{2}y')$$

$$\text{where:} \quad y' = y/(\frac{1}{2}W_C)$$

$$(2) \quad T-T_w = \frac{q_w' \frac{1}{2}W_C}{k} \{ \frac{1}{2}y'^3 (1 - \frac{1}{2}y') - y' \}$$

$$\text{where:} \quad q_w' = \frac{(W_w + W_C)}{2H} q''$$

$$T_w = \text{Wall Temperature } [^{\circ}\text{C}]$$

All other parameters are as defined in the nomenclature section of the thesis.

The finite difference computer code was set up to solve for the temperature and velocity distribution in the channel of Figure C1. The computer code calculated the velocity and temperature solutions numerically and printed out both the analytical and numerical results at

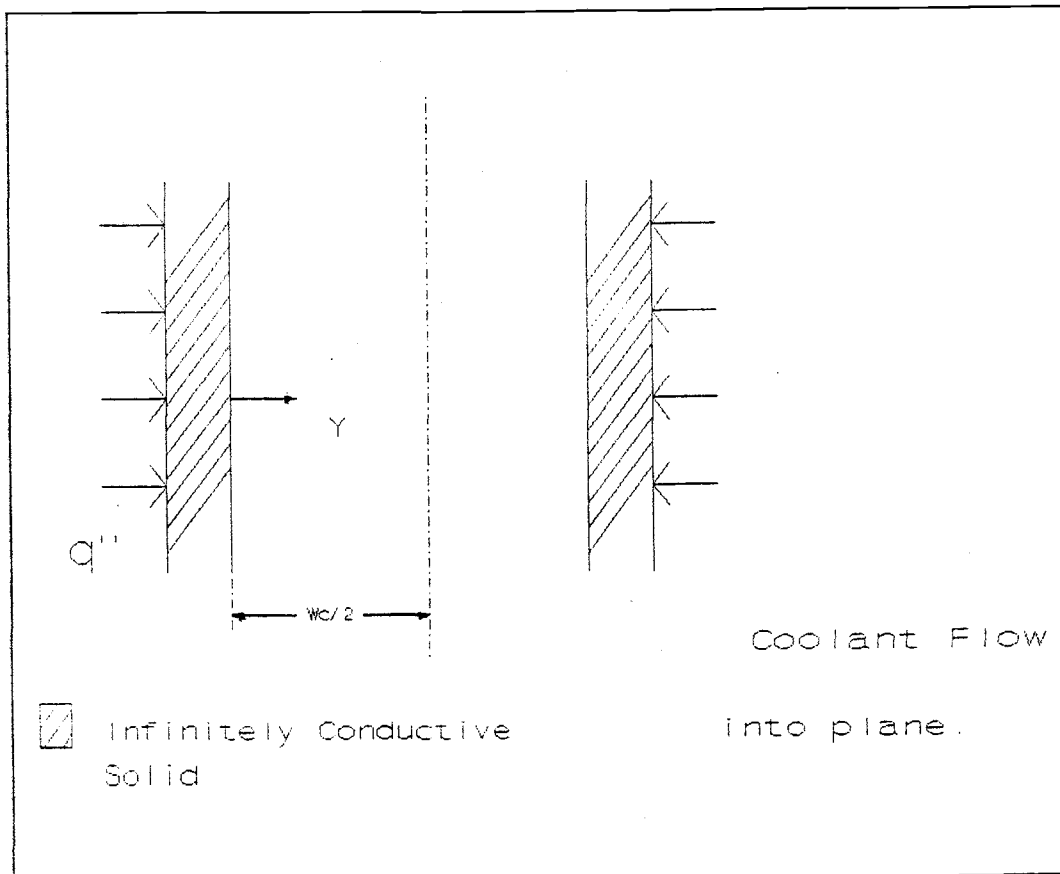


Figure C1  
Infinite channel geometry for analytical and numerical discretization comparisons.

each cell center.

## 2 RESULTS

The infinite channel problem was solved for a value of  $\frac{1}{2}W_c$  of 25  $\mu\text{m}$ . It was solved for discretizations of 5, 10, 20, 30 and 40 cells across the channel. The computer outputs follow and are on 14" wide computer paper. The results are analyzed using the percent deviation between analytical and numerical centerline velocity as defined in equation (2) of appendix b. Table C1 below presents the summary.

% Deviation Discretization	Temperature	Velocity
5	.80%	3.21%
10	.29%	2.06%
20	.10%	1.21%
30	.07%	.76%
40	.05%	.62%

Table C1 Percent Difference between analytical and numerical solutions of the temperature and velocity within an infinite parallel plate heated channel.

The temperature percent difference is calculated by:

$$(3) \text{ \% difference} = 100 \text{abs}(T_{\text{analy}} - T_{\text{numerical}}) / (T_{\text{wall}} - T_{\text{center}})$$

The temperature percent difference for velocity decreases very rapidly with discretization. The value of 20 cells across the half channel provides an acceptable result of approximately 1% deviation. This agrees with the value chosen in appendix b.

It can be seen that the values of percent difference for temperature are very low. The discretization of 20 cells across the channel width was used for nearly all the microchannel problems considered in this work.

## APPENDIX D

## Integral Analysis Manipulations

The integral analysis of Dr. C. Landrum suggested equations which could be used to find important relations for the optimization procedure. These are the equation for the optimal fin to channel width ratio and the equation for the optimal aspect ratio. They will be derived here out of the results presented by Landrum.

1 MINIMUM IN FIN BASE TEMPERATURE VS.  $W_w/W_c$ 

Landrum's Integral analysis gave the following:

$$(1) \quad T_{\text{bulk}} - T_{\text{inlet}} = \Gamma_1(1+x)$$

Where:

$$\Gamma_1 = \frac{2(k_w/k)(q''L/k_w)}{\text{Re}(1+H/W_c)\text{Pr}}$$

and:

$$x = W_w/W_c$$

$$(2) \quad T_{\text{fin,base}} - T_{\text{bulk}} = \frac{\Gamma_2}{3} (1+\Gamma_2 x) \frac{(1+x)}{x}$$

Where:

$$\Gamma_2 = \frac{51 k_w}{140 k} \frac{1}{\alpha^2} \quad \Gamma_3 = \frac{q''H}{k_w}$$

Adding equations (1) and (2) yields:

$$(3) \quad T_{\text{fin,base}} - T_{\text{inlet}} = \frac{\Gamma_1}{3} (1+x) + \frac{\Gamma_2}{3} (1+\Gamma_2 x) \frac{(1+x)}{x}$$

Differentiating and holding all other parameters constant except  $x$  yields:

$$(4) \quad \frac{dT_{fin,base}}{dx} = \Gamma_1 + \Gamma_3 \left( -1 + \frac{\Gamma_2}{x^2} \right)$$

Taking the second derivative to test for concavity yields:

$$(5) \quad \frac{d^2 T_{fin,base}}{dx^2} = \frac{2\Gamma_3}{3} \frac{1}{x^2} > 0 \rightarrow \text{Minimum.}$$

Setting the first derivative to zero to find the minimum yields:

$$(6) \quad x_0 = [3\Gamma_1/\Gamma_3 + \Gamma_2]^{-\frac{1}{2}}$$

This is the equation which will yield the value of  $x=W_w/W_c$  for minimum temperature at the base of the fin with a given pressure drop and a given heat flux. The subscript  $_0$  indicates that it is for the optimal geometry.

## 2 MINIMUM IN FIN BASE TEMPERATURE WITH ASPECT RATIO

Starting with the fin temperature equation above:

$$(3) \quad T_{fin,base} - T_{inlet} = \frac{2(k_w/k)(q''L/k_w)(1+x)}{Re(1+\alpha)Pr} + \frac{(q''\alpha W_c)(1+51k_w/x)(1+x)}{3k_w \cdot 140k \cdot \alpha^2 \cdot x}$$

Taking the derivative with respect to  $\alpha$  yields:

$$(7) \quad \frac{dT_{fin,base}}{d\alpha} = \frac{-2(k_w/k)(q''L/k_w)(1+x)}{Re(1+\alpha^2)Pr} + \frac{W_c q''(1+x)}{3k_w} \left[ \frac{\alpha(-51k_w/x)}{140k \alpha^3} + \frac{(1+51k_w/x)}{140k \alpha^2} \right]$$

If this derivative is zero it will yield an extreme point. We know that the extreme point will be a minimum because of the upwards (positive) concavity of Figure 1.16. Setting the above derivative to zero and simplifying yields:

$$(8) \quad \frac{6(k_w/k)(L/W_c)x}{\text{Re Pr}} = (1+\alpha)^2 \left[ 1 - \frac{51 k_w}{140 k} \frac{1x}{\alpha^2} \right]$$

For large alpha  $\alpha > 5$ ,  $2\alpha \gg 1$  so the 1 in the quadratic  $(1+\alpha)^2$  can be disregarded. Thus, we are making the approximation:

$$(1+\alpha)^2 \approx \alpha^2 + 2\alpha \quad \text{for large } \alpha \quad (\alpha > 5)$$

Making this substitution and simplifying yields:

$$(9) \quad \alpha_o^3 + 2\alpha_o^2 + x_o \alpha_o k_w \left[ \frac{51 + 6(L/W_c)}{k [140 \text{ Re Pr}]} \right] - \frac{51 k_w x_o}{70 k} = 0$$

This is the equation for the optimal aspect ratio  $\alpha_o$  where the subscript  $_o$  indicates that this is the optimal value.

Observing equations (6) and (9) reveals the parameters  $x_o$  and  $\alpha_o$  are coupled. Thus these two equations must be solved iteratively for  $x_o$  and  $\alpha_o$  respectively. The methodology for this is outlined in section 1.11.6.

APPENDIX E  
Derivation of Equations

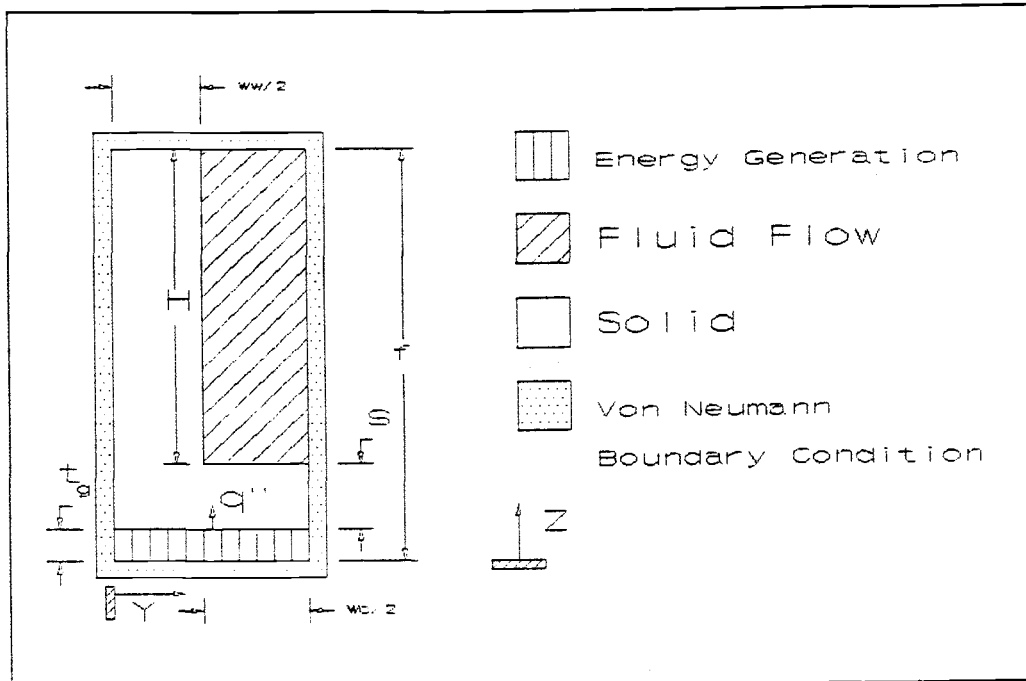


Figure E1  
Computational Domain for derivation of the fully developed momentum and energy equations.

The governing equations are given for the fluid mechanics, convective and conductive heat transfer for the three respective regions identified in Figure E1. These equations are given in complete form as they are found in Bejan [2]. The scale analysis and fully developed assumptions will be applied to these equations to produce the equations presented in 1.5.

### 1 Fluid Flow Region. Momentum Equations.

#### 1.1 X Momentum

$$(1a) \quad \rho(u\frac{\partial u}{\partial x} + v\frac{\partial u}{\partial y} + w\frac{\partial u}{\partial z}) = -\frac{\partial P}{\partial x} + \mu(\frac{\partial^2 u}{\partial x^2} + \frac{\partial^2 u}{\partial y^2} + \frac{\partial^2 u}{\partial z^2})$$

## 1.2 Y Momentum

$$(1b) \quad \rho \left( u \frac{\partial v}{\partial x} + v \frac{\partial v}{\partial y} + w \frac{\partial v}{\partial z} \right) = -\frac{\partial P}{\partial y} + \mu \left( \frac{\partial^2 v}{\partial x^2} + \frac{\partial^2 v}{\partial y^2} + \frac{\partial^2 v}{\partial z^2} \right)$$

## 1.3 Z Momentum

$$(1c) \quad \rho \left( u \frac{\partial w}{\partial x} + v \frac{\partial w}{\partial y} + w \frac{\partial w}{\partial z} \right) = -\frac{\partial P}{\partial z} + \mu \left( \frac{\partial^2 w}{\partial x^2} + \frac{\partial^2 w}{\partial y^2} + \frac{\partial^2 w}{\partial z^2} \right) + g\rho$$

The scaling relations which will be applied for the distances are:

$$\begin{array}{lll} \partial x \sim L & \partial y \sim W_c & \partial z \sim H \\ \partial x^2 \sim L^2 & \partial y^2 \sim W_c^2 & \partial z^2 \sim H^2 \end{array}$$

The scaling relations which will be applied for the velocities are:

$\Delta t$  The time for a fluid molecule to pass through the heat sink. [s]

$$u \sim L/\Delta t \quad v \sim W_c/\Delta t \quad w \sim H/\Delta t$$

Using the above and the fact that a typical microchannel has  $L \sim 1$  [cm],  $W_c \sim 50$  [ $\mu\text{m}$ ] and  $H \sim 500$  [ $\mu\text{m}$ ] yields:

$$\begin{array}{ll} \partial x \gg \partial y & \partial x \gg \partial z \\ \partial x^2 \gg \partial y^2 & \partial x^2 \gg \partial z^2 \\ u \gg v & u \gg w \end{array}$$

Using these scaling relationships in the above equations (1a), (1b) and (1c) and cancelling all terms of inferior order of magnitude (i.e. terms with order of magnitude smaller than other terms) yields:

$$(2a) \quad 0 = \frac{-\partial P}{\partial x} + \mu \left( \frac{\partial^2 u}{\partial y^2} + \frac{\partial^2 u}{\partial z^2} \right)$$

$$(2b) \quad 0 = \frac{-\partial P}{\partial y}$$

$$(2c) \quad 0 = \frac{-\partial P}{\partial z} + \rho g$$

Using the fact that  $g$  is a constant which scales as order 1 yields:  $P_z = g z^{-0}$

Thus, the pressure drop is a function of  $x$  only. This allows the partial derivative in (2a) to be replaced with an ordinary derivative with pressure. The final result is:

$$(3) \quad \frac{1}{\mu} \frac{dP}{dx} = \frac{\partial^2 u}{\partial y^2} + \frac{\partial^2 u}{\partial z^2}$$

This is the fully developed momentum equation (equation 1.1) as it is solved in chapter 1 of this thesis.

## 2 ENERGY EQUATIONS.

### 2.1 Energy Equation. Energy Generation Region.

$$(4) \quad \alpha_f \left( \frac{\partial^2 T}{\partial x^2} + \frac{\partial^2 T}{\partial y^2} + \frac{\partial^2 T}{\partial z^2} \right) = q'''$$

### 2.2 Energy Equation. Conduction Region.

$$(5) \quad \alpha_f \left( \frac{\partial^2 T}{\partial x^2} + \frac{\partial^2 T}{\partial y^2} + \frac{\partial^2 T}{\partial z^2} \right) = 0$$

### 2.3 Energy Equation. Fluid Flow Region.

$$(6) \quad \left( u \frac{\partial T}{\partial x} + v \frac{\partial T}{\partial y} + w \frac{\partial T}{\partial z} \right) = \alpha_f \left( \frac{\partial^2 T}{\partial x^2} + \frac{\partial^2 T}{\partial y^2} + \frac{\partial^2 T}{\partial z^2} \right)$$

Applying the above scaling rules to equations (4), (5) and (6) and cancelling all terms of inferior magnitude yields equations (7), (8) and (9) respectively:

Energy Generation Region.

$$(7) \quad \alpha_f \left( \frac{\partial^2 T}{\partial y^2} + \frac{\partial^2 T}{\partial z^2} \right) = q'''$$

Conduction Region.

$$(8) \quad \alpha_f \left( \frac{\partial^2 T}{\partial y^2} + \frac{\partial^2 T}{\partial z^2} \right) = 0$$

Fluid Flow Region.

$$(9) \quad \left( u \frac{\partial T}{\partial x} + v \frac{\partial T}{\partial y} + w \frac{\partial T}{\partial z} \right) = \alpha_f \left( \frac{\partial^2 T}{\partial y^2} + \frac{\partial^2 T}{\partial z^2} \right)$$

Making the further assumption that  $v \sim 0$  and  $w \sim 0$  transforms equation (9) into:

$$(10) \quad \frac{u}{\alpha_f} \frac{\partial T}{\partial x} = \frac{\partial^2 T}{\partial y^2} + \frac{\partial^2 T}{\partial z^2}$$

Using the fully developed assumption which states that the axial temperature gradient is equal to the bulk fluid temperature gradient yields:

$$(11) \quad \frac{u}{\alpha_f} \frac{dT_{\text{bulk}}}{dx} = \frac{\partial^2 T}{\partial y^2} + \frac{\partial^2 T}{\partial z^2}$$

For reference, all three energy equations will be listed.

Energy Generation Region.

$$(12) \quad \alpha_f \left( \frac{\partial^2 T}{\partial y^2} + \frac{\partial^2 T}{\partial z^2} \right) = q'''$$

Conduction Region.

$$(13) \quad \alpha_f \left( \frac{\partial^2 T}{\partial y^2} + \frac{\partial^2 T}{\partial z^2} \right) = 0$$

Fluid Flow Region.

$$(14) \quad \frac{u}{\alpha_f} \frac{dT_{\text{bulk}}}{dx} = \frac{\partial^2 T}{\partial y^2} + \frac{\partial^2 T}{\partial z^2}$$

### 3 APPLICATION OF BULK ENERGY BALANCE

The bulk energy balance will be applied to the fully developed energy equation in the fluid flow region above in the manner which it was used in the computer code. Recalling the bulk energy balance of appendix A yields an expression for the bulk fluid temperature at the axial distance  $x$ :

$$(15) \quad T_{\text{bulk},x} = T_{\text{bulk},\text{inlet}} + \frac{x(W_w + W_c)q''}{\rho H W_c U_o C_p}$$

Taking the derivative of this expression with respect to  $x$  yields:

$$(16) \quad \frac{dT_{\text{bulk}}}{dx} = \frac{(W_w + W_c)q''}{\rho H W_c U_o C_p}$$

Thus substituting this into equation (11) yields:

$$(17) \quad \frac{\partial^2 T}{\partial y^2} + \frac{\partial^2 T}{\partial z^2} = \frac{(u(y,z)) (W_w + W_c) q''}{U_o \alpha_f \rho H W_c C_p}$$

## APPENDIX F

## Preliminary Calculations

## 1 AVERAGE KINEMATIC VISCOSITY:

It was necessary to determine an average value of kinematic viscosity of water between 30° and 90°. Assume that the kinematic viscosity behaves linearly between 30° and 90° as in Figure F1. The linear segment yields the following:

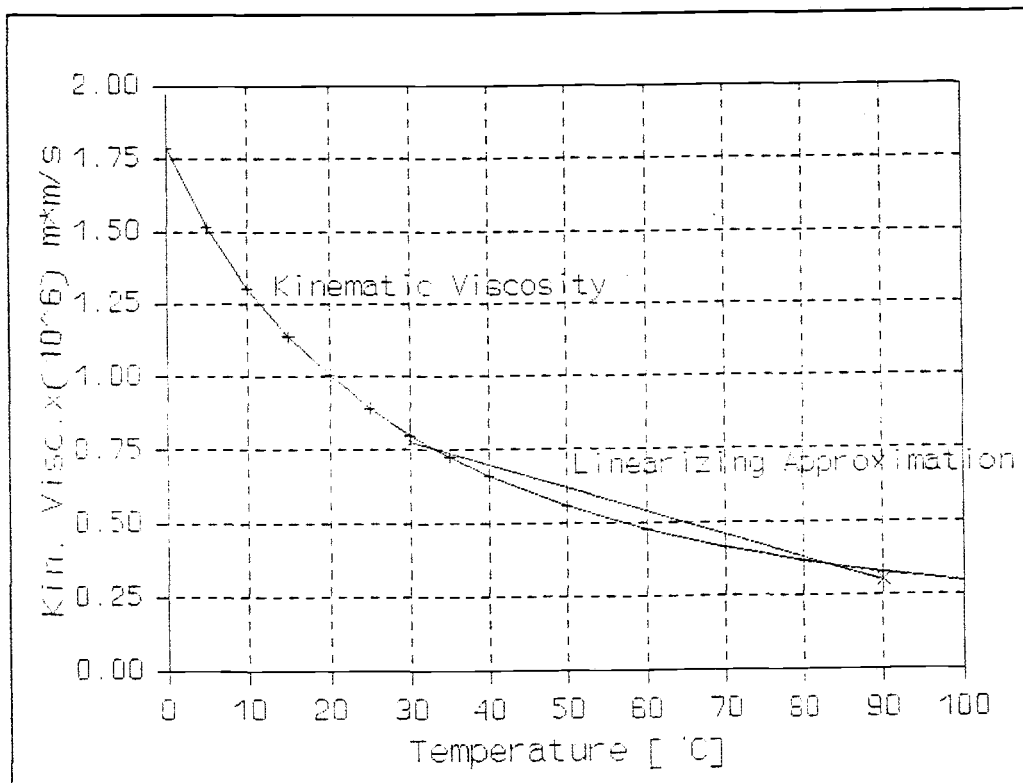


Figure F1  
Kinematic viscosity for water versus temperature and linearizing approximation. (Data taken from Bejan [15])

$$(30^\circ) \approx .8(10^{-6}) \text{ [m}^2/\text{s]}$$

$$(90^\circ) \approx .3(10^{-6}) \text{ [m}^2/\text{s]}$$

If the segment is assumed linear, the average is thus:

$$\bar{v} = \frac{1}{2} ( (30^\circ) + (90^\circ) )$$

$$\bar{v} = .550(10^{-6}) \text{ [m}^2/\text{s]}$$

## 2 AVERAGE VELOCITY AND REYNOLDS NUMBER

For sample 81F9 of Dr. D. Tuckerman's thesis [1]{page 81}, the average velocity and Reynolds number will be calculated.

The width of each microchannel and fin repeating unit was  $100 \mu\text{m}$ ,  $= W_w + W_c$ . Thus, the number of microchannels in a 2 cm wide heat sink is:

$$\# \text{ microchannels} = \frac{2 \text{ [cm]}}{100 \text{ [\mu m]}} = 200 \text{ microchannels.}$$

The flow area for each microchannel is:

$$\begin{aligned} \text{Flow area/microchannel} &= HW_c = (50 \text{ [\mu m]}) (302 \text{ [\mu m]}) \\ &= 15,100 \text{ [(\mu m)}^2\text{]} \end{aligned}$$

The volumetric flowrate for a 2 centimeter wide heat sink was  $8.6 \text{ [cm}^3/\text{s]}$ . Thus the average velocity can now be calculated.

$$\bar{u} = F/A = \frac{(8.6 \text{ [cm}^3/\text{s]}) (1 \text{ [m]}/100 \text{ [cm]})^3}{(15,100(10^{-12}) \text{ [m}^2/\text{channel}]) (200 \text{ [channels]})}$$

$$\bar{u} = 2.85 \text{ [m/s]}$$

The Hydraulic Diameter is calculated as:

$$D_{\text{hydr}} = \frac{4A}{P_{\text{wetted}}} = \frac{4(50 \text{ [\mu m]}) (300 \text{ [\mu m]})}{2(50 + 300) \text{ [\mu m]}} = 85.7 \text{ [\mu m]}$$

Now calculating the Reynolds Number yields:

$$\text{Re} = \frac{D_{\text{hydr}} \bar{u}}{\nu} = \frac{(85.7 \text{ [\mu m]}) (2.85 \text{ [m/s]})}{.550(10^{-6}) \text{ [m}^2/\text{s]}} = 444$$

Since a round number was desired for the calculations, it was decided to use the value of 500 for the Reynolds Number calculations.

## APPENDIX G

### Output from 2DREYN.FOR

The computer code which was developed for this problem produces two output files. The first file contains the velocity and temperature array and is named 2DOUT. The second file contains Nusselt number calculations, integral analysis comparisons and the fin temperature distribution and is called 2DGRAPH. These two output files will be highlighted here and are included in this appendix in 1 and 2 respectively.

The example presented in this appendix is the optimized ninety micrometer wide channel. The height of this channel is eleven hundred and sixty micrometers and the fin width is ninety micrometers. The pressure drop across a 1.4 centimeter length heat sink is 2.8 pounds per square inch.

#### 1 VELOCITY AND TEMPERATURE OUTPUT

The title of this file indicates that the shell of this computer program was written originally for ME573 which was taught at Oregon State University by Dr. D. Trent in the winter of 1989.

##### 1.1 Solution Method.

The solution information contained is the number of computational cells used in each coordinate direction, the cell geometry in each direction, the microchannel geometry and the hydraulic Diameter. Also contained is the solution method which was Point Successive Over Relaxation, the overrelaxation factor  $\omega$ , the maximum number of iterations, the convergence criteria for  $\delta$ -

$\phi^1$ , the heat balance error criterion and the initial velocity.

#### 1.2 Iteration Details for the velocity solution.

For the Point Successive Over Relaxation iteration, the velocity solution is printed out at four monitor cells for every twentieth iteration along with the delta-u criteria. Iteration stops when the delta-u criteria is less than the delta-phi criteria. The monitor points were all chosen in the solid region because the temperature at these points was of interest. Thus the velocity at these four points is zero.

#### 1.3 Steady State Velocity Solution.

The entire steady state velocity array is printed out in groups of ten rows by ten columns each. All of the zero's indicate the solid region in **Figure E1**. Above each column is the y cell number and the y distance. To the left of each column is the z cell number. The column corresponding to  $I=1$  is for the centerline of the fin ( $u=0$ ) and the column corresponding to  $I=41$  is for the centerline of the channel where the velocity profile can be observed.

#### 1.4 Information Calculated From Velocity Array.

The axial pressure gradient in [Pa/m] for the heat sink and the pressure drop across a 1.4 cm heat sink are presented. The average velocity, the base heat flux  $q''$  and the total sum of the heat generation for the entire computational area are presented. The way the problem is modelled is to put positive heat generation in the energy generation area and use negative heat generation to represent the convective term in the energy equation.

---

<sup>1</sup> See the discussion appendix A of the Point Successive Over Relaxation algorithm.

These two computational heat effects exactly balance each other out so the heat generation is effectively zero.

#### 1.5 Temperature Solution Information.

The optimum over relaxation factor is calculated and the same solution information for the velocity solution of 1.1 is presented for the temperature solution. The iteration details correspond to the temperatures at the four monitor points of interest along with the delta-T criteria printed at every fiftieth iteration. The four monitor points are; a) the base of the fin at the corner of the microchannel, b) The center of the fluid channel, c) A point directly above the generation region and d) a point near the base and centerline of the fin. Remember that these monitor temperatures are the computational temperatures which must be "shifted" according to the method of the bulk energy balance of appendix A.

#### 1.6 Temperature Array.

The entire temperature array is printed out in columns of ten. Above each column is the y cell number and y distance. To the left of every row is the z cell number.

#### 1.7 Information Calculated from the Temperature Solution.

Tuckerman's constant Heat transfer coefficient is presented for this geometry along with the conductivity ratio ( $k_w/k$ ) and the conductivity of the fluid. The numerically calculated value of  $y_0$  and the integral analysis prediction along with the value of beta  $\beta$  are presented. The ratio of heat flux up the fin to the total heat flux (i.e. also through the base of the microchannel) is calculated. This is expected to be almost unity for all cases. It is .974 for this case.

Finally, the peak water temperature and silicon temperature at the base of the fin are presented.

## 2 CALCULATED INFORMATION

The information pertaining to the discretization of Figure E1 is presented which involves the cell number of the left and bottom boundaries (which are solid cells) and the number and geometry of the computational cells in each direction. The flow channel height, width and hydraulic diameter are presented. The pressure gradient and pressure drop across a given length of heat sink are presented. The Reynolds number, average velocity, energy generation wall flux, heat generation sum, bulk fluid temperature, Tuckerman's constant  $H$ , the conductivity ratio ( $k_w/k$ ) and fluid conductivity ratio are all presented for this microchannel geometry. The numerical and integral analysis values of  $y_0$  are presented for this value of beta  $\beta$ .

In tabular form for the different values of  $z$  up the fin is presented the heat transfer coefficient calculated using the bulk temperature, the nusselt number the temperature distribution and the integral analysis  $f$  and  $g$  functions which are the nondimensional fin temperature distribution and nondimensional hot spot functions respectively. Finally, the ratio of flux up the fin to the total flux is presented along with the peak fluid temperature and fin base temperature.

TRANSPORT EQUATION SOLUTION ALGORITHM TESTER

```

SOLUTION METHOD          PSOR
NUMBER OF CELLS IN X1-DIRECTION, NMX1 - - - - 42
NUMBER OF CELLS IN X2-DIRECTION, NMX2 - - - - 29
WIDTH OF CELLS IN X1-DIRECTION, DX1 - - - - *****
WIDTH OF CELLS IN X2-DIRECTION, DX2 - - - - *****
OVER-RELAXATION FACTOR , OMEGA - - - - 1.929
MAXIMUM NUMBER ITERATIONS , ITMAX - - - - 5000
DELTA-PHI ERROR CRITERION , ICRIT - - - - 1.000e-05
HEAT BALANCE ERROR CRITERION , QMAX - - - - 0.100
INITIAL VELOCITY , IINIT - - - - 0.
    
```

ITER NO.	DELTA-U	ITERATION DETAILS			
		U( 12, 10)	U( 21, 22)	MONITOR VELOCITY U( 11, 5)	U( 5, 12)
20	0.2350	0.00	0.00	0.00	0.00
40	0.0555	0.00	0.00	0.00	0.00
60	0.0128	0.00	0.00	0.00	0.00
80	0.0038	0.00	0.00	0.00	0.00
100	0.0011	0.00	0.00	0.00	0.00
120	0.0003	0.00	0.00	0.00	0.00
140	0.0001	0.00	0.00	0.00	0.00
160	0.0000	0.00	0.00	0.00	0.00

THE FLOW CHANNEL HEIGHT IS: 1160.000 MICROMETERS  
 THE FLOW CHANNEL WIDTH (complete) IS: 90.000 MICROMETERS  
 THE HYDRAULIC DIAMETER IS: 167.040 MICROMETERS

STEADY STATE VELOCITY ARRAY OUTPUT FOR ITERATION NUMBER: 169

I =		1	2	3	4	5	6	7	8	9	10
X1 = *****		1.1250e-06	3.3750e-06	5.6250e-06	7.8750e-06	1.0125e-05	1.2375e-05	1.4625e-05	1.6875e-05	1.9125e-05	
J= 29	X2=*****	0.	0.	0.	0.	0.	0.	0.	0.	0.	0.
J= 28	X2=*****	0.	0.	0.	0.	0.	0.	0.	0.	0.	0.
J= 27	X2=*****	0.	0.	0.	0.	0.	0.	0.	0.	0.	0.
J= 26	X2=*****	0.	0.	0.	0.	0.	0.	0.	0.	0.	0.
J= 25	X2=*****	0.	0.	0.	0.	0.	0.	0.	0.	0.	0.
J= 24	X2=*****	0.	0.	0.	0.	0.	0.	0.	0.	0.	0.
J= 23	X2=*****	0.	0.	0.	0.	0.	0.	0.	0.	0.	0.
J= 22	X2=*****	0.	0.	0.	0.	0.	0.	0.	0.	0.	0.
J= 21	X2=*****	0.	0.	0.	0.	0.	0.	0.	0.	0.	0.
J= 20	X2=*****	0.	0.	0.	0.	0.	0.	0.	0.	0.	0.
J= 19	X2=*****	0.	0.	0.	0.	0.	0.	0.	0.	0.	0.
J= 18	X2=*****	0.	0.	0.	0.	0.	0.	0.	0.	0.	0.





```

J# 28 X2=***** 1.798e+00 0.
J# 27 X2=***** .422e+00 0.
J# 26 X2=***** .555e+00 0.
J# 25 X2=***** .555e+00 0.
J# 24 X2=***** .555e+00 0.
J# 23 X2=***** .555e+00 0.
J# 22 X2=***** .555e+00 0.
J# 21 X2=***** .555e+00 0.
J# 20 X2=***** .555e+00 0.
J# 19 X2=***** .555e+00 0.
J# 18 X2=***** .555e+00 0.
J# 17 X2=***** .555e+00 0.
J# 16 X2=***** .555e+00 0.
J# 15 X2=***** .555e+00 0.
J# 14 X2=***** .555e+00 0.
J# 13 X2=***** .555e+00 0.
J# 12 X2=***** .555e+00 0.
J# 11 X2=***** .422e+00 0.
J# 10 X2=***** .422e+00 0.
J# 9 X2=***** 1.798e+00 0.
J# 8 X2=***** 0. 0.
J# 7 X2=***** 0. 0.
J# 6 X2=***** 0. 0.
J# 5 X2=***** 0. 0.
J# 4 X2=***** 0. 0.
J# 3 X2=***** 0. 0.
J# 2 X2=***** 0. 0.
J# 1 X2=***** 0. 0.

```

THE PRESSURE GRADIENT IS: -1.38732749582448007439106119d+06 PA/M  
PRESSURE DROP ACROSS A 1.400CM CHIP IS: -2.817PSI

THE REYNOLDS NUMBER IS: 500.00 [UNITLESS]  
THE AVERAGE VELOCITY IS: 1.6463 [METERS/SEC]  
THE ENERGY GENERATION WALL FLUX IS: 1000.000 [W/CM^2]  
THE SUM OF THE HEAT GENERATION IS: 4.922e-28 [WATTS]  
OUTPUT FOR OPTIMUM OMEGA SEARCHING ROUTINE  
FOR THE CASE WHERE THE ASPECT RATIO IS: 1.00000000000000000000000000d+00

ITERATIONS LAMBDA OMEGA  
THE OPTIMUM OMEGA IS: 1.923

SOLUTION METHOD PSOR

```

NUMBER OF CELLS IN X1-DIRECTION, NMX1 - - - - 42
NUMBER OF CELLS IN X2-DIRECTION, NMX2 - - - - 29
WIDTH OF CELLS IN X1-DIRECTION, DX1 - - - - *****
WIDTH OF CELLS IN X2-DIRECTION, DX2 - - - - *****
OVER-RELAXATION FACTOR, OMEGA - - - - 1.923
MAXIMUM NUMBER ITERATIONS, ITMAX - - - - 5000
DELTA-PHI ERROR CRITERION, ICRT - - - - 1.000e-04
HEAT BALANCE ERROR CRITERION, QMAX - - - - 0.100
INITIAL TEMPERATURE, TINIT - - - - 2.5000e+01

```

ITER NO.	DELTA-T	ITERATION DETAILS			
		T( 12, 10)	T( 21, 22)	T( 11, 5)	T( 5, 12)
50	0.0518	24.66	24.43	25.53	24.67



J=	16	X2=	*****	9.0999e+01	9.0999e+01	9.0998e+01	9.0977e+01	9.0966e+01	9.0966e+01	9.0995e+01	9.0944e+01	9.0933e+01	9.0922e+01
J=	15	X2=	*****	9.6077e+01	9.6066e+01	9.6066e+01	9.6055e+01	9.6055e+01	9.6033e+01	9.6022e+01	9.6011e+01	9.6000e+01	9.5999e+01
J=	14	X2=	*****	1.0174e+02									
J=	13	X2=	*****	1.1377e+02									
J=	12	X2=	*****	1.2044e+02	1.2033e+02	1.2022e+02							
J=	11	X2=	*****	1.2755e+02	1.2744e+02	1.2733e+02	1.2722e+02						
J=	10	X2=	*****	1.3499e+02									
J=	9	X2=	*****	1.4255e+02									
J=	8	X2=	*****	1.4700e+02									
J=	7	X2=	*****	1.5100e+02									
J=	6	X2=	*****	1.5499e+02									
J=	5	X2=	*****	1.5888e+02									
J=	4	X2=	*****	1.6144e+02									
J=	3	X2=	*****	1.6277e+02									
J=	2	X2=	*****	1.6277e+02									
J=	1	X2=	*****	1.6277e+02									

I = 21 22 23 24 25 26 27 28 29 30  
 XI = 4.3875e-05 4.6125e-05 4.8375e-05 5.0625e-05 5.2875e-05 5.5125e-05 5.7375e-05 5.9625e-05 6.1875e-05 6.4125e-05

J=	29	X2=	*****	6.128e+01	6.021e+01	5.809e+01	5.600e+01	5.394e+01	5.194e+01	5.000e+01	4.814e+01	4.637e+01	4.469e+01
J=	28	X2=	*****	6.128e+01	6.021e+01	5.809e+01	5.600e+01	5.394e+01	5.194e+01	5.000e+01	4.814e+01	4.637e+01	4.469e+01
J=	27	X2=	*****	6.157e+01	6.026e+01	5.767e+01	5.511e+01	5.259e+01	5.014e+01	4.776e+01	4.548e+01	4.330e+01	4.124e+01
J=	26	X2=	*****	6.224e+01	6.085e+01	5.810e+01	5.538e+01	5.271e+01	5.010e+01	4.757e+01	4.515e+01	4.283e+01	4.065e+01
J=	25	X2=	*****	6.330e+01	6.189e+01	5.910e+01	5.634e+01	5.363e+01	5.098e+01	4.842e+01	4.596e+01	4.361e+01	4.139e+01
J=	24	X2=	*****	6.476e+01	6.335e+01	6.055e+01	5.778e+01	5.506e+01	5.241e+01	4.984e+01	4.737e+01	4.501e+01	4.278e+01
J=	23	X2=	*****	6.663e+01	6.521e+01	6.241e+01	5.964e+01	5.692e+01	5.426e+01	5.169e+01	4.922e+01	4.686e+01	4.463e+01
J=	22	X2=	*****	6.889e+01	6.748e+01	6.467e+01	6.190e+01	5.918e+01	5.652e+01	5.395e+01	5.148e+01	4.912e+01	4.689e+01
J=	21	X2=	*****	7.155e+01	7.014e+01	6.734e+01	6.457e+01	6.184e+01	5.919e+01	5.662e+01	5.414e+01	5.179e+01	4.956e+01
J=	20	X2=	*****	7.462e+01	7.321e+01	7.041e+01	6.763e+01	6.491e+01	6.225e+01	5.968e+01	5.721e+01	5.485e+01	5.262e+01
J=	19	X2=	*****	7.809e+01	7.668e+01	7.387e+01	7.110e+01	6.838e+01	6.572e+01	6.315e+01	6.068e+01	5.832e+01	5.609e+01
J=	18	X2=	*****	8.196e+01	8.055e+01	7.774e+01	7.497e+01	7.225e+01	6.959e+01	6.702e+01	6.455e+01	6.219e+01	5.996e+01
J=	17	X2=	*****	8.623e+01	8.482e+01	8.202e+01	7.924e+01	7.652e+01	7.386e+01	7.129e+01	6.882e+01	6.646e+01	6.423e+01
J=	16	X2=	*****	9.090e+01	8.949e+01	8.669e+01	8.392e+01	8.119e+01	7.854e+01	7.597e+01	7.349e+01	7.114e+01	6.891e+01
J=	15	X2=	*****	9.598e+01	9.457e+01	9.177e+01	8.900e+01	8.627e+01	8.362e+01	8.104e+01	7.857e+01	7.621e+01	7.399e+01
J=	14	X2=	*****	1.015e+02	1.001e+02	9.725e+01	9.448e+01	9.175e+01	8.910e+01	8.653e+01	8.406e+01	8.170e+01	7.947e+01
J=	13	X2=	*****	1.073e+02	1.059e+02	1.031e+02	1.004e+02	9.765e+01	9.499e+01	9.242e+01	8.996e+01	8.760e+01	8.537e+01
J=	12	X2=	*****	1.136e+02	1.122e+02	1.094e+02	1.067e+02	1.040e+02	1.013e+02	9.878e+01	9.632e+01	9.397e+01	9.176e+01
J=	11	X2=	*****	1.203e+02	1.190e+02	1.162e+02	1.135e+02	1.109e+02	1.083e+02	1.058e+02	1.034e+02	1.011e+02	9.891e+01
J=	10	X2=	*****	1.274e+02	1.262e+02	1.233e+02	1.213e+02	1.189e+02	1.165e+02	1.143e+02	1.121e+02	1.100e+02	1.081e+02
J=	9	X2=	*****	1.349e+02	1.342e+02	1.329e+02	1.316e+02	1.303e+02	1.290e+02	1.277e+02	1.265e+02	1.254e+02	1.243e+02
J=	8	X2=	*****	1.431e+02	1.432e+02	1.433e+02	1.434e+02	1.435e+02	1.436e+02	1.437e+02	1.438e+02	1.439e+02	1.440e+02
J=	7	X2=	*****	1.471e+02									
J=	6	X2=	*****	1.510e+02									
J=	5	X2=	*****	1.549e+02									
J=	4	X2=	*****	1.588e+02									
J=	3	X2=	*****	1.614e+02									
J=	2	X2=	*****	1.627e+02									
J=	1	X2=	*****	1.627e+02									

I = 31 32 33 34 35 36 37 38 39 40  
 XI = 6.6375e-05 6.8625e-05 7.0875e-05 7.3125e-05 7.5375e-05 7.7625e-05 7.9875e-05 8.2125e-05 8.4375e-05 8.6625e-05

J=	29	X2=	*****	4.312e+01	4.167e+01	4.034e+01	3.915e+01	3.808e+01	3.716e+01	3.639e+01	3.577e+01	3.530e+01	3.499e+01
J=	28	X2=	*****	4.312e+01	4.167e+01	4.034e+01	3.915e+01	3.808e+01	3.716e+01	3.639e+01	3.577e+01	3.530e+01	3.499e+01
J=	27	X2=	*****	4.331e+01	4.175e+01	4.034e+01	3.915e+01	3.811e+01	3.718e+01	3.640e+01	3.577e+01	3.530e+01	3.499e+01
J=	26	X2=	*****	4.360e+01	4.170e+01	4.034e+01	3.915e+01	3.811e+01	3.718e+01	3.640e+01	3.577e+01	3.530e+01	3.499e+01
J=	25	X2=	*****	4.391e+01	4.179e+01	4.034e+01	3.915e+01	3.811e+01	3.718e+01	3.640e+01	3.577e+01	3.530e+01	3.499e+01
J=	24	X2=	*****	4.407e+01	4.176e+01	4.034e+01	3.915e+01	3.811e+01	3.718e+01	3.640e+01	3.577e+01	3.530e+01	3.499e+01
J=	23	X2=	*****	4.454e+01	4.161e+01	4.034e+01	3.915e+01	3.811e+01	3.718e+01	3.640e+01	3.577e+01	3.530e+01	3.499e+01



GRAPH FILE FOR TEMPERATURE RESULTS

The left water boundary is at: 21  
 The bottom water boundary is at: 8  
 The maximum horizontal cells is: 42  
 The maximum vertical cells is: 29  
 Delta x horizontal is: 2.25000e-06  
 Delta x vertical is: 5.80000e-05

THE FLOW CHANNEL HEIGHT IS: 1160.000 MICROMETERS  
 THE FLOW CHANNEL WIDTH (complete) IS: 90.000 MICROMETERS  
 THE HYDRAULIC DIAMETER IS: 167.040 MICROMETERS  
 THE PRESSURE GRADIENT IS: -1.38732749582448007439106119d+06 PA/M  
 PRESSURE DROP ACROSS A 1.400CM CHIP IS: -2.817PSI  
 THE REYNOLDS NUMBER IS: 500.00 [UNITLESS]  
 THE AVERAGE VELOCITY IS: 1.6463 [METERS/SEC]  
 THE ENERGY GENERATION WALL FLUX IS: 1000.000 [W/CM^2]  
 THE SUM OF THE HEAT GENERATION IS: 4.922e-28 [WATTS]  
 THE BULK FLUID TEMPERATURE IS: 60.068 [DEGREES C]  
 TUCKERMAHS (constant) H IS: 32538.88 [W/M^2K]

THE CONDUCTIVITY RATIO IS: 224.242  
 THE CONDUCTIVITY OF WATER IS: 0.6600 [W/MK]  
 THE VALUE OF Y<sub>0</sub> IS: 0.51621 [UNITLESS]  
 THE INTEGRAL ANALYSIS Y<sub>0</sub> IS: 0.46157 [UNITLESS]  
 THE VALUE OF BETA IS: 1.2824 [UNITLESS]

Cell #	z [meters]	z/h [1]	h(z) [W/m <sup>2</sup> k]	f(z) [1]	g(z) [1]
1	*****	0.02500	5234.513	2.06552	0.51790
2	*****	0.07500	10733.743	1.35143	0.95570
3	*****	0.12500	13285.834	1.20873	1.05834
4	*****	0.17500	15263.091	1.14752	1.08082
5	*****	0.22500	17367.912	1.11340	1.08550
6	*****	0.27500	19853.994	1.09157	1.08643
7	*****	0.32500	22887.774	1.07637	1.08662
8	*****	0.37500	26657.285	1.06514	1.08666
9	*****	0.42500	31420.472	1.05648	1.08667
10	*****	0.47500	37552.319	1.04957	1.08667
11	*****	0.52500	45616.307	1.04393	1.08667
12	*****	0.57500	56486.442	1.03921	1.08668
13	*****	0.62500	71565.105	1.03519	1.08667
14	*****	0.67500	93183.107	1.03173	1.08665
15	*****	0.72500	125338.559	1.02869	1.08650
16	*****	0.77500	174970.769	1.02600	1.08576
17	*****	0.82500	253359.451	1.02359	1.08225
18	*****	0.87500	372148.896	1.02142	1.06663
19	*****	0.92500	506417.442	1.01949	1.00490
20	*****	0.97500	512948.458	1.01799	0.82135

# of cell in z dir.	z/h	NU(z)
1	2.50000e-02	1.325
2	7.50000e-02	2.717
3	1.25000e-01	3.363
4	1.75000e-01	3.863
5	2.25000e-01	4.396

6	2.75000e-01	5.025
7	3.25000e-01	5.793
8	3.75000e-01	6.747
9	4.25000e-01	7.952
10	4.75000e-01	9.504
11	5.25000e-01	11.545
12	5.75000e-01	14.296
13	6.25000e-01	18.112
14	6.75000e-01	23.584
15	7.25000e-01	31.722
16	7.75000e-01	44.284
17	8.25000e-01	64.123
18	8.75000e-01	94.188
19	9.25000e-01	128.170
20	9.75000e-01	129.823

THE RATIO OF FLUX UP THE FIN TO TOTAL FLUX IS: 0.97398 [UNITLESS]  
 THE PEAK WATER TEMPERATURE IS: 134.245 [DEGREES C]  
 THE PEAK SILICON TEMP. IS: 154.898 [DEGREES C]

Cell #	z[meters]	T(z) [C]
1	5.80000e-05	162.714
2	1.16000e-04	161.410
3	1.74000e-04	158.802
4	2.32000e-04	154.887
5	2.90000e-04	150.956
6	3.48000e-04	146.919
7	4.06000e-04	142.274
8	4.64000e-04	134.927
9	5.22000e-04	127.518
10	5.80000e-04	120.439
11	6.38000e-04	113.750
12	6.96000e-04	107.462
13	7.54000e-04	101.578
14	8.12000e-04	96.098
15	8.70000e-04	91.020
16	9.28000e-04	86.346
17	9.86000e-04	82.074
18	1.04400e-03	78.205
19	1.10200e-03	74.737
20	1.16000e-03	71.671
21	1.21800e-03	69.006
22	1.27600e-03	66.742
23	1.33400e-03	64.879
24	1.39200e-03	63.415
25	1.45000e-03	62.350
26	1.50800e-03	61.677
27	1.56600e-03	61.369

THE RATIO OF FLUX UP THE FIN TO TOTAL FLUX IS: 0.97398 [UNITLESS]  
THE PEAK WATER TEMPERATURE IS: 134.245 [DEGREES C]  
THE PEAK SILICON TEMP. IS: 154.898 [DEGREES C]

## APPENDIX H

## Spreadsheet for Parametric Study

The spreadsheet containing the important information from the cases in the parametric study is presented. The important parameters presented are: a) case identification b) aspect ratio  $\alpha$  c) fin to channel width ratio  $W_w/W_c$  d) conductivity ratio  $k_w/k$  e) microchannel width  $W_c$  f) beta  $\beta$  g) maximum water temperature h) fin base temperature i) percentage of the distance up the fin where the fin temperature drops below the bulk fluid temperature (if applicable) j) ratio of fin flux to total flux k) pressure drop across the heat sink l)  $y_0$  calculated numerically m)  $y_0$  calculated from the prediction of the integral analysis n) bulk fluid temperature  $T_{bulk}$  o) hydraulic Diameter  $D_{hydr}$  p) bulk minus inlet fluid temperature  $T_{bulk}-T_{inlet}$  q) fin base temperature minus the bulk fluid temperature  $T_{wall}-T_{bulk}$  r) fin base temperature minus inlet fluid temperature  $T_{wall}-T_{inlet}$ .

General analysis of 2d microchannels Laminar Fully Developed

Case	alpha	Ww/Wc	kw/k	Wchannel [micrometers]	Beta	Twat. max ['C]	Tsi. max ['C]	Tran pt [%]	qfin/qtot	deltaP [psi]	Yzero	Yzero (I.A)	Tmean ['C]	D(hydr)	[1] Tb-Ti ['C]	[2] Tw-Tb ['C]	[1]+[2] ['C]
1a)	5	0.5	224.24	60	4.186	140.305	148.752	-	0.94501	11.7	0.883	0.75192	85.881	100	60.881	54.424	115.305
1d)	7.5	0.5	224.24	60	1.861	120.605	129.498	-	0.95498	10.6	0.575	0.5194	67.795	105.882	42.795	52.81	95.605
1b)	10	0.5	224.24	60	1.047	114.516	124.329	80	0.96157	9.91	0.468	0.4381	58.208	109.091	33.208	56.308	89.516
1e)	12.5	0.5	224.24	60	0.6697	114.681	124.452	63	0.96171	9.66	0.414	0.4003	52.058	111.111	27.058	62.623	89.681
1c)	15	0.5	224.24	60	0.4651	118.144	127.921	55	0.96483	9.51	0.385	0.3798	47.831	112.5	22.831	70.313	93.144
2b)	10	0.5	224.24	30	1.0465	85.309	93.019	88.9	0.9221	80.1	0.4504	0.438	58.208	54.545	33.208	27.101	60.309
1b)	10	0.5	224.24	60	1.047	114.516	124.329	80	0.96157	9.91	0.468	0.4381	58.208	109.091	33.208	56.308	89.516
3b)	10	0.5	224.24	90	1.047	143.124	153.994	83	0.9607	3.1	0.466	0.438	58.208	163.636	33.208	34.916	118.124
1b)	10	0.5	224.24	60	1.047	114.516	124.329	80	0.96157	9.91	0.468	0.4381	58.208	109.091	33.208	56.308	89.516
4b)	10	1	224.24	60	2.13	118.824	126.75	-	0.97123	9.91	0.621	0.546	69.277	109.091	44.277	49.547	93.824
5b)	10	1.5	224.24	60	3.25	130.863	139.229	-	0.97136	9.91	0.773	0.6585	80.347	109.091	55.347	50.516	105.863
1b)	10	0.5	224.24	60	1.047	114.516	124.329	80	0.96157	9.91	0.468	0.4381	58.208	109.091	33.208	56.308	89.516
6b)	10	0.5	448.48	60	2.0929	129.739	139.582	-	0.95235	9.91	0.588	0.543	58.208	109.091	33.208	71.531	104.739
Miscellaneous																	
test1	8	1	224.24	50	3.3286	120.503	130.463	-	0.961	17.9	0.778	0.666	79.117	88.889	54.117	41.386	95.503
2a)	5	0.5	224.24	30	4.1859	112.858	120.684	-	0.94285	93	0.884	0.752	85.881	50	60.881	26.977	87.858